Microtubule-dependent nuclear congression in fission yeast and a novel factor in cellular morphogenesis of fission yeast

Kathleen Scheffler

Université Pierre et Marie Curie

Ecole Doctorale Complexité du Vivant

Unité Compartimentation et Dynamique Cellulaires (Institut Curie/UMR144)

Equipe Architecture du Cytosquelette et Morphogenèse Cellulaire

Microtubule-dependent nuclear congression in fission yeast

and

A novel factor in cellular morphogenesis of fission yeast

Par Kathleen Scheffler

Thèse de doctorat de Biologie

Dirigée par Dr Phong Tran

Présentée et soutenue publiquement le 29 Septembre 2014

Devant un jury composé de :

Vincent GALY (Group leader, UPMC, France)	Président du Jury
Antoine GUICHET (Group leader, Institut Jacques Monod, France)	Rapporteur
Nicolas MINC (Group leader, Institut Jacques Monod, France)	Rapporteur
Michael KNOP (Group leader, ZMBH, Germany)	Examinateur
Phong TRAN (Group leader, Institut Curie, France)	Directeur de thèse

Acknowledgements

First and foremost, I'd like to thank Phong Tran, who offered me this unique experience of performing my PhD studies under his supervision. Thanks to him, I have experienced great challenges and acquired important attributes, such as perseverance and self-confidence that helped me growing scientifically and personally. In particular, I appreciated the independence and his trust he granted me allowing me to develop my own scientific ideas and intensifying my enthusiasm for research.

I would like to thank the members of my thesis committee – the reviewers Antoine Guichet and Nicolas Minc, the examiner Michael Knop and the president Vincent Galy – for kindly accepting to evaluate my work.

I am also very grateful to Anne Paoletti, and my tutors Renata Basto and Franck Perez for the helpful discussions and the time they dedicated to me.

I thank all the people that have awoken my fascination for science in the past, in particular Takashi Toda, who supervised me during my diploma thesis and showed me how exciting it is to address interesting and challenging scientific questions in an inspiring environment.

I also thank all the people that contributed to make the 4th floor of the Institut Curie such an enjoyable and stimulating place. A special "merci", "gracias" and "dankeschön" to my colleagues and friends Imène, Lena, Mercè and Sergio, who always lent me an ear for my scientific and personal problems.

Ich danke auch meinen Freunden und meiner Familie in Deutschland, die mir trotz der großen Entfernung immer zur Seite gestanden haben. Dabei möchte ich sagen, dass mir die Unterstützung und dasVertrauen meiner Eltern den Weg bis hierher geebnet haben. Besonders wertvoll und erholend waren für mich die Tage, die ich mich bei euch zurückziehen konnte, wenn mir mal alles über den Kopf gewachsen war.

Zum Schluss möchte ich Yann-Cédric danken, der mir jeden Tag aufs Neue Kraft und Selbstvertrauen gegeben hat, der immer an mich gelaubt und der mich zurück auf den Boden geholt hat, wenn es mal gar zu schwarz am Horizont war. Vielen Dank, dass du mit mir diesen Weg gegangen bist.

Summary

Part I: MT-dependent nuclear congression in fission yeast

Controlling nuclear positioning is crucial for diverse cellular processes including cell division, cell polarity, cell motility and sexual reproduction. During sexual reproduction, after oocyte fertilization, the male and female pronuclei migrate towards each other in a microtubule (MT)- and motor-dependent manner allowing nuclear fusion. In fission yeast, it has been proposed that two minus end-directed motors, kinesin-14 Klp2 and dynein, drive nuclear congression. However, to date no study has been carried out to investigate the molecular mechanisms underlying this process.

Here, we developed a microfluidic-based technology for long-term imaging of mating cells to capture precise timing of nuclear congression and perform a systematic screen through all MT motors to test their role. We demonstrate that dynein and Klp2 constitute parallel pathways, as nuclear congression is only delayed in respective single mutants, but completely arrested in a double mutant. Measurements of the SPB dynamics at high temporal resolution revealed that, while in wildtype and *klp2Δ*, nuclear movements accelerate over time, lack of dynein results in nuclear migrations at a constant speed, further indicating that these motors play distinct roles. Consistently, they exhibit different localization patterns: Klp2 localizes at MT plus ends, and dynein accumulates at the SPB. Finally, we show that SPB-, but not MT-bound dynein is responsible for generation of pulling forces and that its function in nuclear congression requires the light intermediate chain Dli1, but surprisingly not the dynactin complex. This is in contrast to animal cells, where dynactin appears to be required for virtually all dynein functions, but might suggest that certain dynein functions may be carried out without involvement of dynactin. Furthermore, *dli1*deletion decreases the pool of dynein at both structures, SPBs and MTs, suggesting a rather overall role in stabilizing or helping forming the dynein complex.

In summary, we provide evidence that Klp2 and dynein form two distinct parallel mechanisms underlying nuclear congression in fission yeast. Klp2 probably cross-links and slides anti-parallel MTs, while dynein at the SPB may pull on MTs emanating from the opposite SPB.

Part II: A novel factor in cellular morphogenesis of fission yeast

Cell morphogenesis is a fundamental process that contributes to diverse specialized cell functions and tissue integrity. It largely relies on polarization of cellular growth and subsequently on the area and direction of growth. Since, the complex processes governing cellular morphogenesis appear to be conserved, the unicellular fission yeast *Schizosaccharomyces pombe* has proven to be a useful model system for the identification of morphogenetic pathways. It is well established that MTs deliver spatial cues including Tea1 to the cell tip regions directing the growth machinery at the cell tips and driving linear extension of this rod-shaped organism to maintain a straight growth axis.

Here, we report the characterization of a novel gene, *knk1*, which plays a role in maintenance of a straight growth axis. Cells carrying a deletion of *knk1* display a kink close to cell tips constituting a unique shape phenotype and a new class of shape mutants. Through genetic analysis, we place Knk1 into a novel pathway directing growth independent of MTs and Tea1. Furthermore, Knk1 is dispensable for normal organization and dynamics of the microtubule and actin cytoskeleton.

During interphase, Knk1 localizes at cell tips consistently with a role in morphogenesis. Knk1 belongs to the AAA^+ ATPases that typically assemble into ring-shaped hexamers. Monitoring the subcellular distribution of truncated and mutant versions of Knk1 suggested that cell tip localization is mediated by the N-terminus and enhanced upon ATP binding to the C-terminal ATPase domain, probably because it allows oligomerization and cooperation of several N-termini. Knk1 tip recruitment relies on actin-based processes, but is independent of microtubules and actin cables. Furthermore, Knk1 tip levels are regulated in an unknown manner by Sla2 and Cdc42 independent of Sla2 role in endocytosis. That also suggests a novel link between endocytosis and the cellular polarization machinery in fission yeast.

Finally we discovered that Knk1 shows a fascinating anti-correlated periodic oscillatory behavior between the two cell tips in *sla2* and *cdc42* mutant background, and less clear in wildtype. Knk1 oscillations appear uncoupled from the previously reported Cdc42 oscillations, as both systems oscillate at different periodicities.

Future work will be required to reveal the molecular mechanisms of Knk1 function in morphogenesis, how it is recruited to cell tips and how and why it oscillates.

Table of contents

Acknowledgements 2

Summary 3

Table of contents 5

Figure Index 8

Abbreviations 10

Introduction – Part I: MT-dependent nuclear congression in fission yeast 13

1. Nuclear movements in eukaryotes 14

1.1. The nucleus 14

1.2. Diversity of nuclear positioning 16

1.3. Toolbox for nuclear positioning 18

1.4. Nuclear positioning and related pathologies 19

2. The eukaryotic cytoskeleton 20

2.1. The actin cytoskeleton 20

2.1.1. Actin structures and dynamics 20

2.1.2. Actin-based motors: Myosins 23

2.1.3. Actin-dependent mechanisms of nuclear positioning 23

2.2. Intermediate filaments and their role in nuclear positioning 24

2.3. The microtubule cytoskeleton 25

2.3.1. MT structure and dynamics 25

2.3.2. Regulation of MT dynamics 27

2.3.3. MT nucleation 29

2.3.4. MTOCs – Centrosomes and SPBs 30

2.4. Motor proteins of the microtubule cytoskeleton 33

2.4.1. Kinesins (KIFs) 33

2.4.2. Dynein 36

2.4.2.1. Molecular structure of the dynein motor 36
2.4.2.2. Regulation of dynein function 38
2.5. MT-dependent mechanisms of nuclear positioning 40
3. Nuclear movements in fungi 43
3.1. Overview of fungal nuclear migrations 43
3.2. Fission yeast as a model system 45
3.3. Microtubule organization and nuclear positioning in interphase 48
3.4. Microtubule organization and nuclear horsetail movement during meiotic prophase 50
3.5. The roles of kinesins and dynein in fission yeast 51
3.6. Microscopy of mating fission yeast cells in microfluidic flow chambers 53

Introduction – Part II: A novel factor in cellular morphogenesis of fission yeast 54

4. Morphogenesis of eukaryotic cells 55
4.1. Cell polarity and cell shape 55
4.2. Key processes underlying polarized growth and cellular morphogenesis 56
4.2.1. RhoGTPases 57
4.2.2. Exocytosis 59
4.2.3. Endocytosis 60
4.2.4. Role of microtubules in cortical polarity 63
4.3. Cellular morphogenesis of fission yeast cells 65
4.3.1. Fission yeast as a model system for morphogenesis 65
4.3.2. Cell wall and turgor pressure 67
4.3.3. Cdc42 and other Rho proteins in fission yeast polarized growth 68
4.3.4. Polarized secretion and endocytosis in fission yeast 70
4.3.5. Positioning of growth zones by microtubules in fission yeast 72
4.3.6. Control of cell shape by external manipulation 73
4.3.7. Oscillatory dynamics of Cdc42 in fission yeast 75
5. The AAA+-ATPase protein family 78
5.1. Diverse functions of AAA+-ATPases 78
5.2. Common structure and mechanism of AAA+-ATPases 80

Aim of this work 82

Results – Part I: MT-dependent nuclear congression in fission yeast 84

Results – Part II: A novel factor in cellular morphogenesis of fission yeast 125

Discussion – Part I: MT-dependent nuclear congression in fission yeast 169

Discussion – Part II: A novel factor in cellular morphogenesis of fission yeast 176

Resume 189

1. Introduction 190

1.1. Les mouvements nucléaires 190

1.1.1. Diversité des mouvements nucléaires chez les eucaryotes 190

1.1.2. Les mouvements nucléaires contrôlés par les microtubules 191

1.1.3. La congression nucléaire chez la levure 192

1.2. La morphogenèse cellulaire 194

1.2.1. Les facteurs clefs contrôlant la morphologiE cellulaire chez les eucaryotes 194

1.2.2. La morphogenèse chez *Schizosaccharomyces pombe* 195

2. Résultats 197

2.1. La dynéine et une kinésine-14 contrôlent la congression nucléaire chez la levure *S. pombe* 197

2.2. L'AAA-ATPase oscillatoire Knk1 fonctionne dans une nouvelle voie de morphogenèse chez la levure *S. pombe* 199

3. Conclusion 201

3.1. Congression nucléaire contrôlée par les microtubules chez *S. pombe* 201

3.2. Un nouveau facteur de morphogenèse chez *S. Pombe* 201

References 203

Annexe: *Motor proteins: kinesin can replace myosin* (Comment) 226

FIGURE INDEX

Figure 1.1. Intracellular compartmentalization of an animal cell 14

Figure 1.2. Nuclear envelope organization 15

Figure 1.3. Examples of nuclear positioning 17

Figure 2.1. Actin nucleation and dynamics 22

Figure 2.2. Actin-dependent mechanisms of nuclear movements 24

Figure 2.3. Microtubule structure, dynamic instability and γ-tubulin mediated nucleation 26

Figure 2.4. Centriole and SPB structure 31

Figure 2.5. MT arrays in fission yeast upon structural rearrangements of SPB 32

Figure 2.6. Kinesin structure and stepping model 35

Figure 2.7. Dynein structure and stepping model 37

Figure 2.8. Dynactin structure and its association to dynein 40

Figure 2.9. MT-dependent mechanisms of nuclear movements 41

Figure 3.1. Nuclear distribution in Aspergillus nidulans 44

Figure 3.2. Nuclear migration during mitosis and meiosis in Saccharomyces cerevisiae 45

Figure 3.3. The fission yeast vegetative cell cycle 46

Figure 3.4. The fission yeast meiotic cell cycle 47

Figure 3.5. MT architecture in an interphase fission yeast cell 49

Figure 3.6. Dynein-driven nuclear horsetail movement 51

Figure 3.7. The microfluidic flow chamber 53

Figure 4.1. Diversity of cell shapes 55

Figure 4.2. The RhoGTPase cycle 57

Figure 4.3. Organization of the budding yeast actin cytoskeleton during the cell cycle 59

Figure 4.4. Steps in exocytosis 60

Figure 4.5. Spatial coupling between endocytosis and exocytosis in Aspergillus nidulans 61

Figure 4.6. The endocytic pathway 62

Figure 4.7. Cytoskeletal organization during the cell cycle 65

Figure 4.8. Shape mutants 67

Figure 4.9. Regulators and effectors of Cdc42 in fission yeast 69

Figure 4.10. Polarized secretion in fission yeast 71

Figure 4.11. The MT-Tea1 polarity pathway 73

Figure 4.12. External manipulation of cell shape 74

Figure 4.13. Cdc42 oscillations in fission yeast 77

Figure 5.1. Diverse functions of AAA+ ATPases 79

Figure 5.2. The superfamily of MT severing enzymes 80

Figure 5.3. Oligomeric arrangement of the AAA+ domains 81

Figure 6.1. Supplemental results to Dli1 function in dynein regulation 175

Figure 6.2. Supplemental results to Knk1 function 180

Figure 6.3. Supplemental results to regulation of Knk1 localization 183

Figure 6.4. Supplemental results to oscillatory behavior of Knk1 185

Abbreviations

+TIP	plus end tracking proteins
aa	amino acid
AAA	ATPases associated with diverse cellular activities
ABP	actin-binding protein
ADP	adenosine diphosphate
ANTH	AP180 N-terminal homology
APC	adenomatous polyposis coli
ATP	adenosine triphosphate
B	halfbridge
Bgs	β(1,3)-glucansynthase
CAP-Gly	Cytoskeleton-Associated Proteins GLYcine-rich
CCP	clathrin-coated pit
CH	calponin homology
CLASP	Cytplasmic Linker Associated Protein
CME	Clathrin-mediated endocytosis
CNS	central nervous system
CP	central plaque
DHC	dynein heavy chain
DIC	dynein intermediate chain
DLC	dynein light chain
DLIC	dynein light intermediate chain
DNA	deoxyribonucleic acid
ENTH	epsin N-terminal homology
ER	endoplasmic reticulum
GAP	GTPase-activating protein
GCP	γ-tubulin complex protein
GDI	Rho guanine-nucleotide-dissociation inhibitor
GDP	guanosine diphosphate
GEF	guanine-nucleotide exchange factor

GFP	green fluorescent protein
GTP	guanosine triphosphate
γTuRC	γ-tubulin ring complex
γTuSC	γ-tubulin small complex
IF	intermediate filament
INM	inner nuclear membrane
IP	inner plaque
KASH	Klarsicht, ANC-1, Syne homology
KCBP	kinesin-like calmodulin-binding protein
LatA	Latrunculin A
LINC	Linker of Nucleoskeleton and Cytoskeleton
MAP	microtubule associated protein
MIT	microtubule interacting and trafficking
MOR	morphogenesis Orb6 network
MT	microtubule
MTOC	microtubule organizing center
NE	nuclear envelope
NETO	New End Take Off
NPC	nuclear pore complex
NPF	nucleating-promoting factor
NTP	nucleoside triphosphate
PCM	pericentriolar material
PDMS	polydimethylsiloxane
PIP2	phosphatidylinositol 4,5-biphosphate
PNS	perinuclear space
OP	outer plaque
ONM	outer nuclear membrane
mRFP	monomeric red fluorescent protein
SNARE	soluble N-ethylmaleimide-sensitive factor attachment receptor
SPB	spindle pole body
SRH	second region of homology

SUN	Sad1 and Unc-82
THATCH	talin-HIP1/R/Sla2p actin-tethering C-terminal homology
TM	transmembrane
TOG	Tumor Overexpressed Gene

Introduction Part I –

MT-dependent nuclear congression in fission yeast

1. Nuclear movements in eukaryotes

1.1. The nucleus

The evolution from a prokaryotic to a eukaryotic cell is hallmarked by the process of compartmentalization leading to the emergence of membrane-enclosed organelles within the cell (Figure 1.1). That allowed the spatial and temporal separation of different metabolic activities by locally generating specific microenvironments.

The largest organelle in the cell is the nucleus. It contains most of the cell's hereditary material, the deoxyribonucleic acid (DNA), arranged into chromatin and is principal location of DNA replication and transcription.

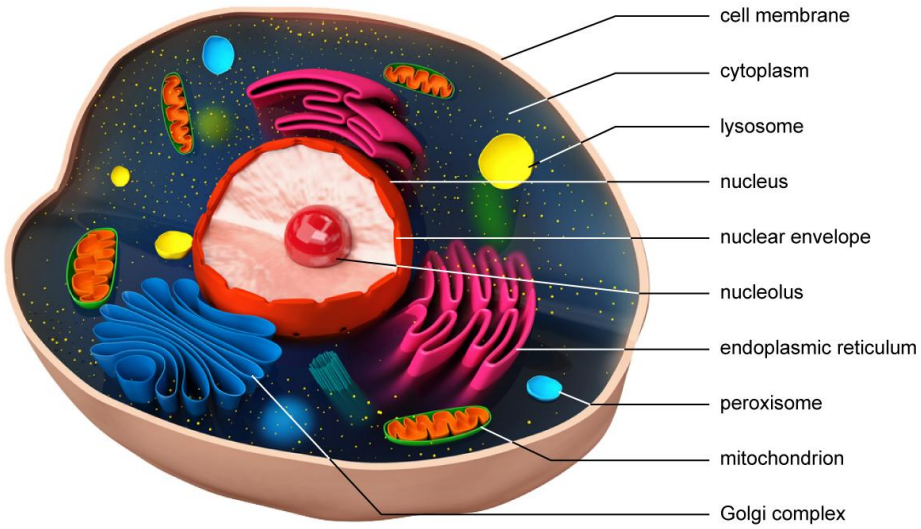

Figure 1.1. Intracellular compartmentalization of an animal cell.
The cytosol (dark blue), endoplasmic reticulum (pink), Golgi apparatus (blue), nucleus (orange), mitochondrion (green/orange) and lysosomes (yellow) are distinct compartments isolated from the rest of the cell by at least one selectively permeable membrane. *(source: http://www.aboutthemcat.org)*

The nucleus is encircled by the nuclear envelope (NE) (Figure 1.2) composed of two membrane leaflets (Callan and Tomlin, 1950) consistent of the outer nuclear membrane (ONM) and inner nuclear membrane (INM) separated by a perinuclear space (PNS) of 30-50nm, and the underlying nucleoskeleton, the lamina (Fawcett, 1966). The double membrane is physically and functionally in continuity with the rough endoplasmic reticulum (ER) via the ONM (Gerace and

Burke, 1988) and is connected at sites of nuclear pore complexes (NPCs) (Gall, 1967, Feldherr et al., 1984), which allow free diffusion of small molecules and mediate the selective exchange of macromolecules between the nucleoplasm and the cytosol (reviewed in (Terry et al., 2007), (Grossman et al., 2012)). The NE also provides anchoring sites for chromosomes in the nucleoplasm and the cytoskeleton at the cytoplasmic side, of which later is required to position the nucleus within the cell (reviewed in (Starr, 2007, Starr and Fridolfsson, 2010, Tapley and Starr, 2013)).

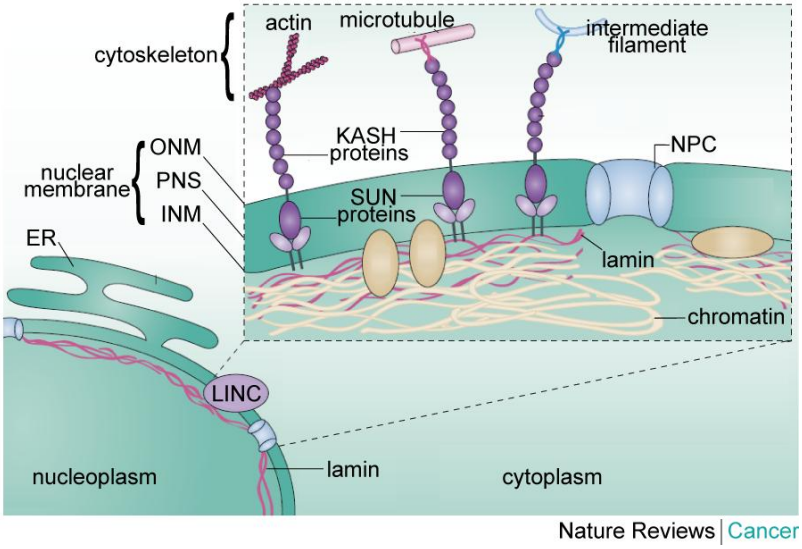

Figure 1.2. Nuclear envelope organization.

The nucleus is surrounded by a double membrane consistent of the outer and inner nuclear membrane (ONM and INM) and separated by the luminal perinuclear space (PNS). ONM is continuous with the endoplasmic reticulum (ER). ONM and INM are connected at sites of nuclear pore complexes (NPCs). The lamina constitutes the nucleoskeleton. Furthermore, the nuclear envelope (NE) is connected to the cytoskeleton by KASH-SUN protein complexes spanning both nuclear membranes. KASH proteins interact with their cytoplasmic domain with cytoskeletal elements including actin, microtubules or intermediate filaments. This protein network linking the nucleoskeleton to the cytoskeleton has been termed LINC complex. *(Chow et al., 2012)*

The nucleus is often depicted in the center of the cell, but in fact its location is controlled by complex mechanisms either to maintain a defined position or to actively move the nucleus towards a specific site. In general, the development of many, if not all, eukaryotes is accompanied by movements of the nucleus dependent on cell cycle stage and differentiation status. Nuclear positioning is crucial for diverse cellular processes including cell division, cell polarity and motility and sexual reproduction. The importance of understanding the mechanisms

regulating nuclear movements is underlined by the fact that failure in proper nuclear positioning has been implicated in human pathologies of the skeletal muscle and the central nervous system (CNS) (Razafsky et al., 2011).

1.2. Diversity of nuclear positioning

To date, nuclear migrations have been observed in many different cell types from yeast to human, and can serve various purposes.

In medially dividing cells of the fission yeast *Schizosaccharomyces pombe* (Figure 1.3A) the nucleus is maintained in the cell center (Tran et al., 2001), as it sets the cell division plane (Chang and Nurse, 1996). In contrast, in the budding yeast *Saccharomyces cerevisiae* (Figure 1.3B) the nucleus takes up an asymmetric position prior to mitosis by translocation into the bud neck ensuring faithful chromosome segregation (reviewed in (Huisman and Segal, 2005)).

In early development of multicellular organisms, following fertilization (Figure 1.3C), male and female pronuclei migrate towards one another and fuse near the middle of the zygote in order to create two equal daughter cells upon division (reviewed in (Reinsch and Gonczy, 1998)).

Also the fly *Drosophila melanogaster* and the nematode *Caenorhabditis elegans* have proven to be very useful systems to uncover mechanisms underlying nuclear positioning that takes place particularly during the development of these organisms. For example, the nuclei of the syncytial *Drosophila* embryo move towards the cortex before they are included in the newly forming cells by invagination of the plasma membrane (Foe and Alberts, 1983, Mazumdar and Mazumdar, 2002). Inversely, in embryonic *C. elegans* hyp7 precursor cells (Figure 1.3D), nuclear migration precedes cell fusion to create a syncytium (Starr et al., 2001, Fridolfsson et al., 2010).

In vertebrates, the nervous system constitutes a particularly interesting tissue for studies of nuclear translocations, as such appear to be critical for several aspects of neuronal development (reviewed in (Baye and Link, 2008)). First, interkinetic nuclear migration is a common feature of pseudostratified columnar epithelial cells forming the neuroepithelium (Figure 1.3E). Here, in a series of events, the nuclei migrate in a cell cycle-dependent manner along the apico-basal axis, which appears to regulate cell fate (Del Bene et al., 2008). On the other hand, upon cell cycle exit, neuronal progenitors must travel to their final destination (Figure

1.3F), which they do in a specific fashion. At first, the leading neurite grows by extension, before the nucleus including soma follows.

Similarly, in most migrating cells (Figure 1.3G), like fibroblasts and astrocytes, the nucleus is translocated in the rear of the cell to not interfere with the events in the protruding front (Gomes et al., 2005, Dupin et al., 2009).

Finally, one of the most striking examples in mammals is represented by the specialized syncytia of the skeletal muscle fibers (Figure 1.3H), where hundreds of nuclei are evenly spaced along the periphery of the cell, while a few are stably anchored beneath the neuromuscular junctions (Bruusgaard et al., 2003).

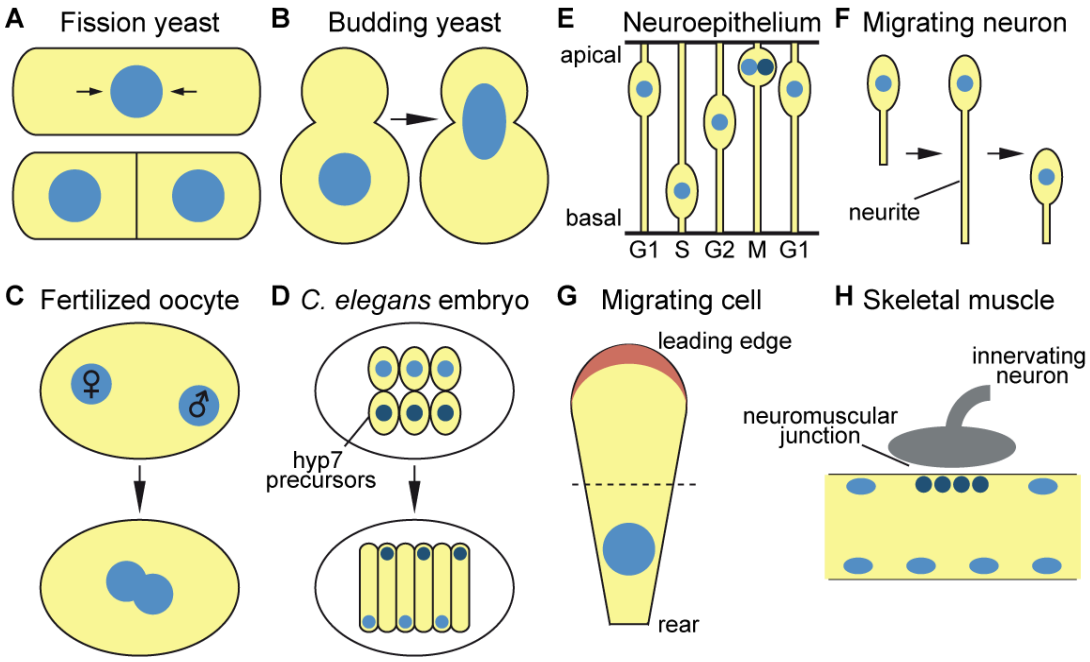

Figure 1.3. Examples of nuclear positioning.

Schematics of model systems used to study nuclear positioning. Nuclei are depicted in blue, differentiated nuclei are in dark blue. (A-C) The nucleus is positioned relative to the future division plane in yeast and fertilized oocytes. (D) Nuclear translocation in embryonic *C. elegans* hyp7 cells prior to syncytium formation. (E) Interkinetic nuclear migration in the vertebrate neuroepithelium. The location of the nucleus is in phase with cell cycle progression. (F) During neuronal translocation, migrating neurons grow by neurite extension until they reach their final destination before the nucleus follows. (G) Rearward nuclear position in migrating cells. Schematic of a migrating cell with the protruding leading edge and contracting tail. Dotted line represents the midpoint between front and rear. (H) Peripheral nuclear positioning in skeletal muscle fibers. In general, nuclei are evenly spaced, except at the neuromuscular junction, where specialized nuclei are clustered. *(Adapted from (Starr, 2009, Burke and Roux, 2009, Dupin and Etienne-Manneville, 2011, Gundersen and Worman, 2013))*

1.3. Toolbox for nuclear positioning

Translocation of the nucleus or its anchoring at specific sites requires two principal elements. First of all, a cytoplasmic force must be generated, which is conducted by the cytoskeleton. To date, all three cytoskeletal elements, actin, microtubules (MTs) and intermediate filaments (IFs), have been implicated in nuclear displacements, either alone or together, depending on the cell type. Their contribution to force generation will be discussed in detail in the next chapters.

In a second step, these forces must then be transferred across the NE via a link that spans both, the INM and the ONM, otherwise pulling forces would simply pull an ER tubule away from the NE without displacement of the nucleus (Allan and Vale, 1994). During the last decade, evidence for the existence of a conserved force-transferring bridge coupling the nucleoskeleton and cytoskeleton has been derived from different organisms, and has been termed LINC complex (reviewed in (Starr, 2007, Starr and Fridolfsson, 2010, Tapley and Starr, 2013, Gundersen and Worman, 2013)) (Figure 1.2). LINC complexes are essentially composed of KASH (Klarsicht, ANC-1, Syne homology) and SUN (Sad1 and Unc-82) proteins that are highly conserved in all eukaryotes (Razafsky and Hodzic, 2009). Initial studies in *C. elegans* showed that mutations in the INM protein Unc-84 interacting with the nuclear lamina (Malone et al., 1999, Lee et al., 2002, McGee et al., 2006) and the ONM protein Unc-83 (Starr et al., 2001) disrupted nuclear migrations during different developmental stages (Starr and Han, 2005) suggesting a force transmission across the NE.

In general, SUN proteins localize to the INM via at least one transmembrane (TM) domain and contain a highly conserved SUN domain at their C-terminus extending into the PNS, where they interact with KASH proteins. The nucleoplasmic N-terminus mediates interaction with the lamina (Crisp et al., 2006, Haque et al., 2006) providing a structural scaffold to sustain cytoplasmic forces (Ji et al., 2007). In organisms like *S. pombe* lacking a lamina, SUN may be linked to chromatin via centromeres (Funabiki et al., 1993, Hou et al., 2012) or telomeres (Chikashige et al., 2006, Ding et al., 2007).

Specificity arises from the more divergent KASH proteins, whose large N-termini extends into the cytoplasm and interacts with a variety of components of the cytoskeletal including actin filaments, MT motor proteins and IFs.

1.4. Nuclear positioning and related pathologies

As demonstrated above, nuclear positioning appears to be fundamental for diverse cellular processes; thus mislocalization of the nucleus, due to mutations in cytoskeletal components, LINC complexes and the lamina, has been implicated in a range of human pathologies. In general, these diseases appear to affect in particular the development of the brain or the function of the skeletal muscle (Razafsky et al., 2011).

One very well known example is Lissencephaly, a severe mental retardation disease that is characterized by a smooth cerebral surface due to an underpopulation by neurons (Lambert de Rouvroit and Goffinet, 2001). Usually, neurons migrate radially out from the neuroepithelium (Figure 1.3F) into the outer layers of the cortex. A failure in neuronal migration is caused by disrupting the mechanisms underlying the subsequent nuclear migration. To date, several distinct mutations impairing the dynein-dependent translocation of the nucleus along MTs have been reported, either by affecting dynein or its regulatory proteins (Shu et al., 2004) (Tsai et al., 2007) or by disrupting the KASH-SUN complex required for dynein recruitment to the NE (Zhang et al., 2009b).

Muscle dystrophies characterized by muscle loss and impaired muscle function are commonly diagnosed through mispositioned myonuclei that are clustered in the center of the myotube instead of being located along the periphery (Folker et al., 2014) (Figure 1.3H). Even though it remains unclear how nuclear positioning impacts on muscle function, it has been shown that the absence of nuclei beneath the neuromuscular junction correlates with dystrophies (Grady et al., 2005) (Zhang et al., 2007). These and other studies have further demonstrated that mutations in proteins located at NE cause the dysfunction of myofibers (Puckelwartz et al., 2009), suggesting that nucleoskeleton-cytoskeleton interactions are critical for muscle formation. Further work will be required to identify the key players for cytoplasmic force production; however both, MTs and actin appear to be required for proper localization of myonuclei (Cadot et al., 2012, Metzger et al., 2012, Puckelwartz et al., 2009).

2. The eukaryotic cytoskeleton

The cytoskeleton fulfills diverse functions such as setting up the cell division apparatus, controlling cell polarity, motility and morphogenesis and provides mechanical strength to the cell. Furthermore, it also allows the directed transport of cargos including molecules, vesicles and organelles in the cell. The cytoskeleton is built up by filamentous polymers that extend throughout the cell. Their properties and their dynamics are controlled and regulated by associated proteins. The eukaryotic cytoskeleton is formed by three distinct classes: actin, microtubules (MTs) and intermediate filaments (IFs).

During nuclear positioning, the cytoskeleton generates forces either directly, or by motor proteins to translocate and anchor the nucleus. The MT cytoskeleton appears to play a major role in many systems, but it has become clear that also actin and IFs contribute to force production, either alone or through cooperation. Finally, nuclear migrations can be achieved by three principal modes – by pulling forces, by pushing forces or by tracking, which describes the transport of the nucleus along the cytoskeleton.

2.1. The actin cytoskeleton

2.1.1. Actin structure and dynamics

Actin, as the most abundant protein in most eukaryotic cells, contributes to many cellular functions such as cellular morphogenesis, cell motility, cell-cell-communication, cytokinesis and intracellular membrane trafficking including secretion and endocytosis (Pollard and Cooper, 2009). The monomeric globular G-actin polymerizes into a right-handed double-stranded helical filament (Holmes, 2009) referred to as F-actin (Figure 2.1), which, through interactions with other actin filaments and accessory proteins, forms an elaborated cytoskeletal network. F-actin assembly is spontaneously initiated *in vitro* by adenosine triphosphate (ATP)-bound G-actin (Straub and Feuer, 1989), but requires *in vivo* additional proteins, actin nucleators, such as the Arp2/3 complex and formins (reviewed in (Pollard, 2007, Campellone and Welch, 2010)). Upon G-actin incorporation, ATP is hydrolyzed to adenosine diphosphate (ADP), which in turn

mediates the dissociation of monomer subunits (Egelman et al., 1982). Thus, actin filaments exhibiting an arrowhead-like structure are highly dynamic with a barbed (+) end, where G-actin is preferentially incorporated, while disassembly dominantly occurs from the pointed (-) end (Kabsch and Vandekerckhove, 1992). The rates of polymerization at the barbed and depolymerization at the pointed end define whether the filament elongates or shrinks. When both processes proceed at similar rates, the filament is an equilibrium state known as treadmilling (Selve and Wegner, 1986). The dynamics of F-actin defined by its nucleation, elongation, disassembly, severing and capping are highly regulated and cross-linking of filaments are mediated by a so-called actin-binding proteins (ABPs, (Pollard et al., 2000, Pollard and Cooper, 2009)). The spatial and temporal regulation of these proteins in turn helps to model actin networks of distinct architecture for different cellular functions (Chhabra and Higgs, 2007). Moreover, rapid growth and shrinkage rates characteristic for actin provide the fast turnover required for driving processes such as cell movement and endocytosis (Pollard and Borisy, 2003).

Briefly, generation of new actin filaments along existing ones is regulated by the Arp2/3 complex mediating the formation of branched filaments required for example in endocytosis (Amann and Pollard, 2001). The Arp2/3 complex consists of seven subunits (Machesky et al., 1994) and its nucleation activity is stimulated by regulatory proteins called nucleating-promoting factors (NPFs) (Welch and Mullins, 2002), to which WASp (Wiskott-Aldrich syndrome protein) belongs (Machesky et al., 1999). Commonly, members of this protein family contain a C-terminal Arp2/3-binding sequence (Machesky and Insall, 1998) and an adjacent actin-binding site either for G-actin (WH2 region, (Vaduva et al., 1997)) or F-actin (ADF-H domain, (Lappalainen et al., 1998)). NPFs in turn are activated or inhibited through a variety of signaling pathways including small Rho GTPases like Cdc42 or phosphatidylinositol 4,5-biphosphates (PIP2s) (Rohatgi et al., 1999, Stradal et al., 2004).

On the other hand, formin-induced actin polymerization generates unbranched filaments (Pruyne et al., 2002) found in actin bundles and the cytokinetic contractile ring. Formins form donut-shaped dimers through an FH2 domain (Xu et al., 2004) and display multiple actin binding sites in their core. Some formins, like mDia, autoinhibit their actin nucleating activity (Alberts, 2001), which is relieved upon binding of small Rho GTPases (Dong et al., 2003, Peng et al., 2003). Through the FH1 domain, they can interact with ABPs, in particular with profilin (Chang et al., 1997). This interaction near the tip of a growing filament is believed to facilitate the

incorporation of new monomers accelerating elongation (Romero et al., 2004). Profilin has been shown to bind to actin monomers to stimulate the exchange from ADP to ATP (Mockrin and Korn, 1980) and, through interaction with formin, to guide them to a growing barbed end (Lu and Pollard, 2001).

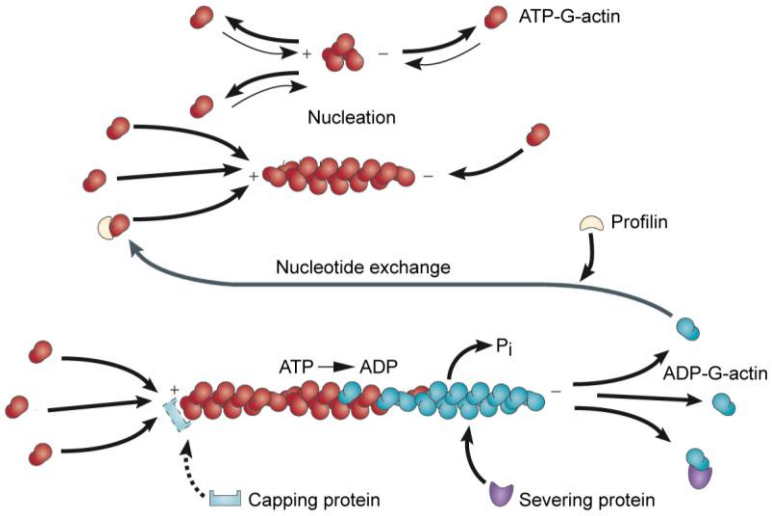

Figure 2.1. Actin nucleation and dynamics.

Actin polymerization from ATP-bound G-actin is initiated spontaneously *in vitro*, but due to unfavorable kinetics (thin arrows), requires nucleators, such as Arp2/3 and formins, *in vivo*. New actin monomers are preferentially incorporated at the barbed (+) end. Hydrolysis of ATP at F-actin destabilizes the filament mediating depolymerization at the pointed (-) end releasing ADP-bound G-actin. Additionally, severing proteins, such as cofilin can cause further disassembly. Profilin facilitates the nucleotide exchange from ADP to ATP at G-actin. Finally, elongation at growing plus ends can be terminated by capping proteins such as gelsolin. *(Nurnberg et al., 2011)*

To regulate the length of filaments, elongation needs to be limited, which occurs through capping of polymerizing barbed ends by capping proteins such as gelsolin (Sun et al., 1999) preventing addition of new actin monomers. Furthermore, disassembly at the pointed ends can be further increased by cofilin and other severing proteins, which bind preferentially to ADP-actin and weaken lateral contacts in the filament (Lappalainen and Drubin, 1997, Bamburg et al., 1999).

Finally, actin filaments are organized into specialized architectures through stabilization, bundling and crosslinking, Stabilization of F-actin is achieved by tropomyosin binding along the length of filaments and protecting them from severing proteins (Wang and Coluccio, 2010). α-

actinin and spectrin, known crosslinkers, contain two actin-binding calponin homology (CH) domains (Stradal et al., 1998, Broderick and Winder, 2002).

Activity of ABPs and their regulators are controlled by extrinsic and intrinsic signaling pathways allowing spatial and temporal regulation of actin structures. Furthermore, many key players in actin dynamics are very well conserved in structure and function from yeast to human.

2.1.2. Actin-based motors: Myosins

The only actin-based motors are myosins that move along actin filaments in an ATP-dependent manner (Krendel and Mooseker, 2005, Hartman and Spudich, 2012). The superfamily of myosins is divergent and, thus, myosins are grouped into 15 to 20 structurally distinct classes. They transport molecules, vesicles and organelles along F-actin and contribute therefore to intracellular membrane trafficking events, cell polarity and locomotion. Furthermore, they can generate contraction forces during cytokinesis and muscle movement. Myosins are essentially composed of one or two heavy chains that interact with light chains. The heavy chains essentially contain three functional domains, head, neck and tail. The head includes the motor domain, which interacts with actin and ATP. The neck functions as a lever during motion and provides a docking site for the light chains. Finally, the tail domain binds subcellular structures such as cargos and mediates dimerization in some myosins. Therefore, they can be classified into single- or two-headed motors. Most myosins move in a plus end directed fashion towards the barbed, while a few, like Myo6, walk towards the pointed end of actin filaments or, like Myo9, can walk in both directions.

2.1.3. Actin-dependent mechanisms of nuclear positioning

Actin was first described to participate in anchoring nuclei at specific sites as reported for Drosophila oogenesis (Robinson and Cooley, 1997). Here, stable actin bundles prevent the drifting of nuclei from the nurse cells into the oocyte during the rapid flow of cytoplasmic material.

Additionally, actin also plays an active role during nuclear movements (Figure 2.2), for example through acto-myosin contractions. During neuronal migration (Figure 1.3F), an acto-

myosin network is created behind the nucleus to push the nucleus forward through contractions (Bellion et al., 2005, Tsai et al., 2007). Alternatively, in migrating cells like fibroblasts, the rearward position of the nucleus (Figure 1.3G) is triggered by an actin retrograde flow and depends on myosin activity (Gomes et al., 2005, Luxton et al., 2010).

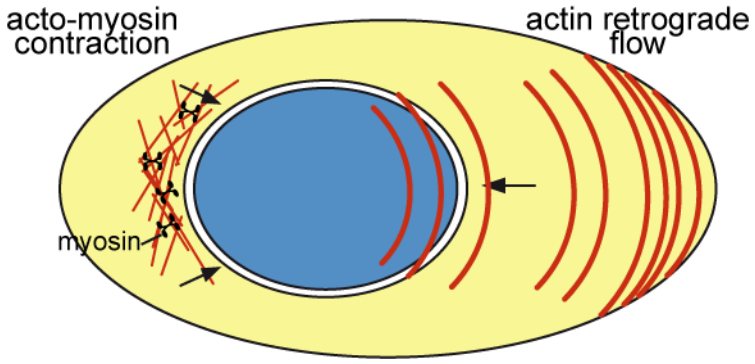

Figure 2.2. Actin-dependent mechanisms of nuclear movements.

The actin cytoskeleton transmits pushing forces to the nucleus through acto-myosin contractions or an actin retrograde flow. Nucleus is depicted in blue, actin filaments and bundles in red. *(Adapted from (Dupin and Etienne-Manneville, 2011))*

2.2. Intermediate filaments and their role in nuclear positioning

IFs constitute a metazoan-specific cytoskeletal system that provides mechanical strength to the cells and helps maintain cell shape (Herrmann et al., 2007). IF proteins are a heterogeneous protein family with little sequence similarity but a similar pattern in their secondary structure (Hanukoglu and Fuchs, 1983). IFs self-assemble into filaments of about 10nm diameter independent of ATP and GTP (Strelkov et al., 2003) and are composed of fibrous proteins that exhibit a central α-helical rod domain flanked by a non-α-helical N-terminal head and C-terminal tail (Herrmann et al., 2007). Recently, it has become clear that IFs do not form a static network but are rather dynamic and motile, which at least in some part is attributed by a crosstalk to motor proteins of the actin and MT cytoskeleton (Helfand et al., 2004).

Nuclear IFs, lamins, build up the lamina (Gruenbaum et al., 2005), which supports nuclear integrity and serves as a scaffold for heterochromatin and protein complexes such as the LINC complexes (Parnaik, 2008). A cytoplasmic IF network, including keratins, desmin and neurofilaments, links cell-cell junctions to the ONM (Herrmann and Aebi, 2004).

The role of IFs in nuclear positioning remains elusive, however evidence suggest a general function for these filaments. Intriguingly, desmin, for example, appears to be required for proper clustering of nuclei beneath the neuromuscular junction and regular spacing for extra-junctional nuclei in myotubes (Ralston et al., 2006) (Figure 1.3H). Furthermore, the pushing forces generated by an actin retrograde flow (Figure 2.2) in migrating astrocytes may be transferred onto the nucleus by IFs in front of the nucleus, a mechanism that has been found in other cell types as well (Dupin et al., 2009).

2.3. The microtubule cytoskeleton

The MT cytoskeleton plays an essential role in the establishment of polarity and cell shape, in the formation of the mitotic apparatus and in intracellular trafficking in co-operation with its motor proteins kinesins and dynein. Furthermore, most processes of nuclear movement appear to be dependent, solely or in combination with other cytoskeletal elements, on the MT cytoskeleton.

2.3.1. Microtubule structure and dynamics

MTs are polymers that are made up of αβ-tubulin heterodimers (Desai and Mitchison, 1997, Nogales and Wang, 2006) (Figure 2.3A). Both subunits exhibiting a globular structure share 40% identity at their amino-acid level (Burns, 1991) and interact through non-covalent bonds (Nogales et al., 1998). The αβ-tubulin dimers assemble uniformly from head-to-tail into linear protofilaments (Amos and Klug, 1974, Downing and Nogales, 1998) that then in turn laterally associate to form a MT, a rigid hollow left-handed helical cylinder. The number of protofilaments built up into a single polymer can vary from 10 to 16 *in vitro* (Desai and Mitchison, 1997), however *in vivo* MTs are organized by the association of 13 protofilaments, with an outer diameter of 25nm, and are capable of growing longer than 20μm (Evans et al., 1985). Usually, within the lattice, lateral contacts are made between two α-tubulins or two β-tubulins of two adjacent protofilaments, known as the B-type lattice, except at the seam where an α- and a β-tubulin of the two neighboring protofilaments interact (Mandelkow et al., 1986, Kikkawa et al., 1994). The assembly of the protofilaments proceeds unidirectionally due to an

intrinsic molecular polarity, with an α-tubulin at the slower-polymerizing minus end and a β-tubulin at the faster polymerizing plus end (Mitchison, 1993, Nogales et al., 1999). Each tubulin unit binds a molecule guanosine triphosphate (GTP) via its N-terminus (Nogales et al., 1998); therefore each dimer is associated with 2 molecules of GTP, one non-hydrolysable GTP at the α-tubulin and one hydrolysable at the β-tubulin (Mitchison, 1993).

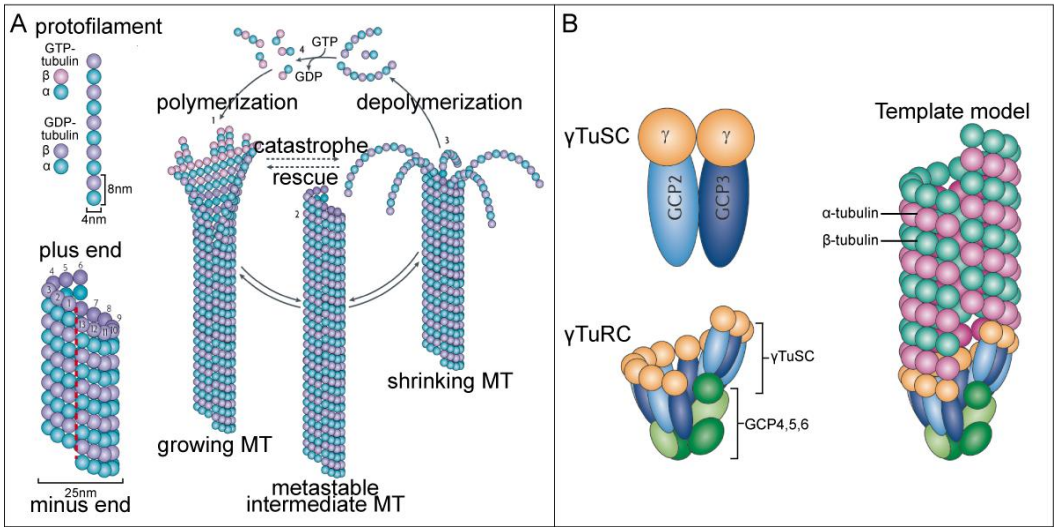

Figure 2.3. Microtubule structure, dynamic instability and γ-tubulin mediated nucleation.

(A) αβ-tubulin heterodimers assemble in a polar fashion head-to-tail fashion into protofilaments and 13 protofilaments associate laterally to form a microtubule (MT) of 25nm diameter. Polymerization and depolymerization are driven by binding, hydrolysis and exchange of GTP bound to β-tubulin. The typical behavior characterized by alternating cycles of polymerization and depolymerization through catastrophe and rescue events is termed "dynamic instability". (B) γTuSCs are assembled into γTuRC that than serve as template presenting a ring of γ-tubulins that makes longitudinal contacts with αβ-tubulin dimers. *((A) (Akhmanova and Steinmetz, 2008), (B) (Kollman et al., 2011))*

As a highly dynamic structure, MTs constantly switches between stages of polymerization and depolymerization referred to as dynamic instability (Mitchison and Kirschner, 1984). Upon incorporation, GTP bound to β-tubulin is hydrolyzed to guanosine diphosphate (GDP). During growth, the rate of tubulin heterodimers added to the MT plus tips exceeds the rate of GTP hydrolysis resulting in the formation of a so-called GTP cap at the plus tip, which allows MT growth to continue (Drechsel and Kirschner, 1994). However, when incorporation rate falls below the rate of GTP hydrolysis, the GTP cap is lost exposing GDP-β-tubulin at the plus tips

and causing instability of the MT that eventually initiates rapid depolymerization in a phenomenon called catastrophe. During the following rapid shrinkage, the MT may switch back to growth, in an event known as rescue, which was believed to occur stochastically. However, recently, it was shown *in vivo* that GTP-β-tubulin was not only accumulating at the plus tips, but also as "GTP islands" along the lattice, probably as remnants from previous cycles of catastrophe, and that these GTP islands might be responsible for rescue events (Dimitrov et al., 2008).

2.3.2. Regulation of MT dynamics

Dynamic instability describes the behavior of MTs to undergo alternating cycles of rescue and catastrophe separated by phases of growth and shrinkage. Prior to catastrophe, it has been shown that MTs also pause without visibly polymerizing or depolymerizing for a certain period called dwell time (Walker et al., 1988). Furthermore, dynamic behavior has been dominantly observed at plus tips, as minus ends are usually capped and anchored at MT organizing centers (MTOCs, discussed in a later chapter).

The parameters of dynamics are highly regulated in the cell by a complex network of proteins combined into the heterogeneous group of MT associated proteins (MAPs), which in turn define the overall properties of single MTs and allow assembly into arrays with different geometry and density. One subgroup is composed of the motor proteins that will be discussed in a later chapter. However, most of the factors interacting with MTs modulate their dynamics and may be divided in a simplified manner into two subgroups: MT stabilizers and destabilizes (van der Vaart et al., 2009). MT stabilizer can act through distinct mechanisms: by suppressing catastrophe, by increasing the probability of rescue or by slowing down shrinkage. Inversely, a destabilization is achieved through promoting catastrophe and suppressing rescue as well as increasing speed of depolymerization. Some MAPs also influence the growth rate, which cannot be easily assigned into these two classifications. Some of these proteins can localize along the MT lattice, while other specifically accumulate at the plus tips, or are found at both locations.

A large group of MAPs includes the structural MAPs (Dehmelt and Halpain, 2005), to which MAP2 and Tau and homologues belong. They bind along the MT lattice and generally stabilize MTs by suppressing catastrophe (Gamblin et al., 1996) (Ichihara et al., 2001, Al-Bassam

et al., 2002). Typically, these proteins have repeating MT-binding regions at the C-terminus (Lewis et al., 1988) allowing association and crosslinking of several tubulin dimers at once (Al-Bassam et al., 2002) increasing overall stability of an MT. Secondly, the highly conserved family of XMAP215/Stu2 (Al-Bassam and Chang, 2011) has been shown to strongly promote rapid MT growth (Gard and Kirschner, 1987, Kawamura and Wasteneys, 2008, Brouhard et al., 2008) by binding to free tubulin dimers through its two or more TOG (Tumor Overexpressed Gene) domains and facilitate the dimer incorporation at the plus tip (Al-Bassam et al., 2006, Brouhard et al., 2008). Another TOG-like domain containing family are CLASPs (Cytplasmic Linker Associated Proteins), which have been reporter as promoting factors of frequency while suppressing catastrophe (Mimori-Kiyosue et al., 2006, Bratman and Chang, 2007), probably through a similar mechanism as XMAP215 proteins (Al-Bassam et al., 2010). Members of these two families belongs to the larger group of microtubule plus end tracking proteins (+TIPs) (Akhmanova and Steinmetz, 2010) that commonly accumulate at growing plus ends (Perez et al., 1999, Mimori-Kiyosue et al., 2000). To date, more than 20 +TIPs have been identified, among which are EB proteins and CLIP-170. EB proteins play a central role in control of MT dynamics, by promoting MT growth and suppressing catastrophe (Tirnauer et al., 2002, Busch and Brunner, 2004). They contain a MT-binding CH domain and an EB homology domain which mediates the recruitment of other proteins exhibiting an SxIP motif (Honnappa et al., 2009), such as the adenomatous polyposis coli (APC) tumor suppressor. Furthermore, CLIP-170 and the dynactin subunit p150, so-called CAP-Gly (Cytoskeleton-Associated Proteins GLYcine-rich) proteins, induce generally rescue events (Arnal et al., 2004, Honnappa et al., 2006). Finally, also some kinesins due to their plus tip tracking behavior are grouped into this class.

The best studied MT destabilizers are the non-motile kinesin-13 motors, such as MCAK, that promote catastrophe and depolymerization by removing the GTP cap at the plus tips (Kinoshita et al., 2006, Howard and Hyman, 2007). Other kinesins that may promote MT depolymerization are the members of the kinesin-8 family (Tischer et al., 2009) or Kar3 of the kinesin-14 family (Sproul et al., 2005). A different type of negative regulator is stathmin that principally sequesters free tubulin dimers to prevent incorporation of new subunits and to slow down polymerization (Belmont and Mitchison, 1996, Jourdain et al., 1997, Steinmetz, 2007). Finally, katanin and spastin belong to the special group of MT severing enzymes that weaken lateral contacts of tubulin units by pulling on C-terminal tubulin tails sticking out of the MT

lattice and thereby initiating catastrophe (Roll-Mecak and Vale, 2008, Roll-Mecak and McNally, 2010).

A last group of MAPs that appears not to directly influence MT dynamics is the family of MAP65/Ase1/PRC1 that has been described to crosslink MTs into antiparallel bundles (Chang-Jie and Sonobe, 1993, Walczak and Shaw, 2010). These crosslinkers contain a MT-binding domain and a domain mediating homodimerization (Schuyler et al., 2003), which in turn allows the simultaneous interaction with two MTs.

In general, the interaction between MAPs containing a rather positively charged MT-binding domain and the negatively charged C-terminal tail of tubulins is based on electrostatic bonds (Rodionov et al., 1990, Lefevre et al., 2011) and can be negatively modulated by posttranslational modifications. Disruption of the MAP-MT association can be achieved either through phosphorylation on MAPs (Cassimeris and Spittle, 2001) or through post-translational modifications like detyrosination, acetylation and polyglutamylation at the tubulin tails (Janke and Bulinski, 2011). For example, the phosphorylation of a serine residue near the SxIP domain interrupts the interaction with EB proteins (Honnappa et al., 2009), and the detyrosination of α-tubulin leads to a decreased recruitment of CLIP-170 to MT plus ends (Peris et al., 2006).

2.3.3. MT nucleation

Although rescue events allow maintaining existing MTs, the cell also creates new MTs *de novo* in a process called nucleation. *In vivo*, MT nucleation dominantly occurs at MTOCs, including centrosomes and non-centrosomal MTOCs (Luders and Stearns, 2007), and requires γ-tubulin as main MT nucleators (Oakley and Oakley, 1989). γ-tubulin assembles together with γ-tubulin complex proteins (GCPs) into a complex called γ-tubulin ring complex (γTuRC) (Moritz et al., 1995, Zheng et al., 1995) (Figure 2.3B). GCPs, some of which contain a highly conserved region, the Grip domain (Gunawardane et al., 2000), are required for the assembly and structural integrity of the γTuRC (Teixido-Travesa et al., 2012). At first, smaller Y-shaped subcomplexes, the γ-tubulin small complexes (γTuSCs), consistent of each one molecule of GCP2 and GCP3 and two molecules γ-tubulin, are formed. Then, several of γTuSCs are arranged into a helix by GCP4-6 (Kollman et al., 2008, Kollman et al., 2010). A long outstanding question was how γTuRC facilitated the polymerization of new MTs. Recent structural studies showing that γTuRC

are assembled into 13-fold MT-like symmetric rings (Moritz et al., 2000, Kollman et al., 2010) have suggested a model, the template model, where γTuRC functions as a template by mimicking the end of an MT and allowing the incorporation of αβ-tubulin dimers at the end (reviewed in (Kollman et al., 2011)).

Another key player is pericentrin, a component of the pericentriolar material (PCM) that recruits γTuRC to centrosomes (Knop and Schiebel, 1997, Zimmerman et al., 2004).

In addition to its role in nucleation, γTuRC appears also important for the capping and stabilization of minus ends (Anders and Sawin, 2011, Wiese and Zheng, 2000) and in control of plus end dynamics (Bouissou et al., 2009).

2.3.4. MTOCs – Centrosomes and SPBs

Nucleation of new MTs is initiated from MTOCs (Luders and Stearns, 2007) that tether MT minus ends and define the spatial MT organization in the cell. In animal cells, the centrosome presents the primary MTOC and plays a critical role in spindle assembly and organization and genomic stability in mitosis, as well as cell polarity in interphase cells (Azimzadeh and Bornens, 2007). Furthermore, in many systems, nuclear migrations are led by the centrosome. In these cases, the centrosome is found associated to the NE, but, in other systems, can be also observed distant from the nucleus.

The centrosome (Figure 2.4A) consists of a pair of centrioles that are surrounded by an electro-dense material, the PCM. The PCM constitutes a matrix assembled by large coiled-coil proteins of the pericentrin family, which serve as a binding platform recruiting other matrix proteins such as γTuRC. Each centriole forms an MT-based cylinder with a highly conserved nine-fold symmetry. Both centrioles are capable of nucleating MTs in their vicinity, but only the mother centriole can also dock cytoplasmic MTs due to its two sets of nine appendages at the distal ends (Paintrand et al., 1992, Piel et al., 2000). The duplication of centrioles is tightly coupled to cell cycle progression to ensure the assembly of a bipolar mitotic spindle (Kuriyama and Borisy, 1981). Briefly, during G1 the two centrioles are separated and a new centriole is assembled at each pre-existing one in S to G2 phase. Prior to mitosis, the two centrosomes recruit PCM proteins, which leads to a burst of MT nucleation activity and the two centrosomes are

separated simultaneously with NE breakdown (reviewed in (Bettencourt-Dias and Glover, 2007)).

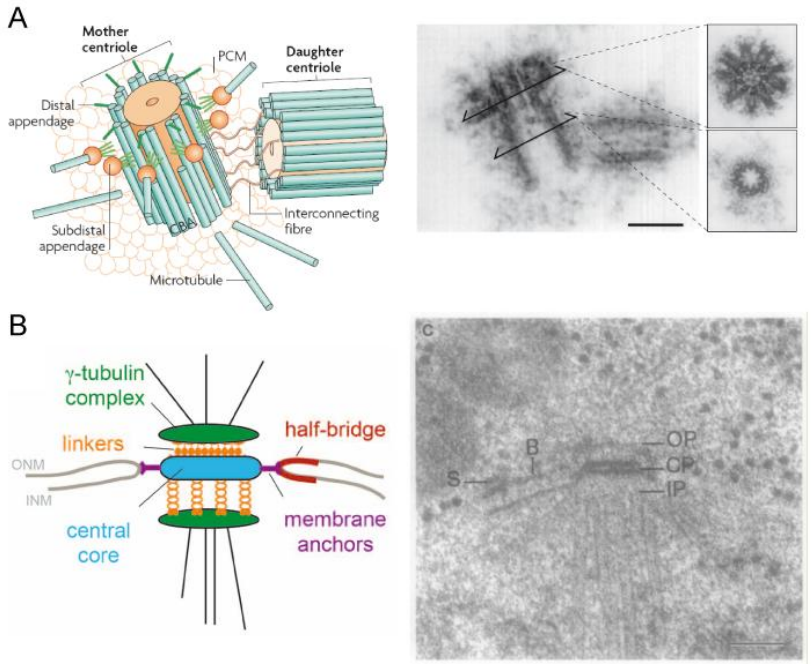

Figure 2.4. Centrosome and SPB structure.

(A) Schematic view of the centrosome illustrating the electron micrograph of the centrosome depicted on the right. MTs form triplets, which then assemble into a barrel-like structure with a nine-fold symmetry. The mother centriole provides a platform for MTs to dock at its distal end. Bar, 0.2µm. (B) Schematic view of the SPB in budding yeast illustrating electron micrograph of the SPB depicted on the right. Organization of the SPB structure into 5 substructures: the outer plaque (OE) with cytoplasmic γ-tubulin, the inner plaque (IP) with nuclear γ-tubulin, both linked to the central plaque (CE, core of the SPB), the halfbridge (B) constituting initiation site for assembly of a new SPB (S, satellite) and membrane anchors tethering the core SPB onto or in the NE. Bar, 0.1µm. *((A) (Bettencourt-Dias and Glover, 2007) (B) (Jaspersen and Ghosh, 2012, Giddings et al., 2001))*

In yeasts that undergo closed mitosis, the major MTOC is the spindle pole body (SPB, Figure 2.4B), the functional equivalent to centrosomes. It can be either embedded in the NE throughout the entire cell cycle, like in budding yeast, or it can sit on the cytoplasmic side of the NE during interphase and becomes inserted exclusively during mitosis as seen in fission yeast (Ding et al., 1997). The SPB has been described as a cylindrical organelle consistent of three plaques: an outer plaque facing the cytoplasm, an inner plaque facing the nucleoplasm or connected to the ONM and a central plaque (Giddings et al., 2001, Jaspersen and Winey, 2004).

While the outer plaque is associated with cytoplasmic MTs that persist throughout interphase in fission yeast, the inner plaque interacts with MTs nucleated inside the nucleus. Furthermore, an electron-dense region extending laterally on the outer side of the SPB has been observed and termed halfbridge. During duplication, the halfbridge is initiation site of the assembly of the new SPB (Adams and Kilmartin, 1999). To date, many components have been identified and located within the SPB structure, but it became apparent that the SPB exhibits a more complex structure with multiple interconnected layers (Jaspersen and Winey, 2004).

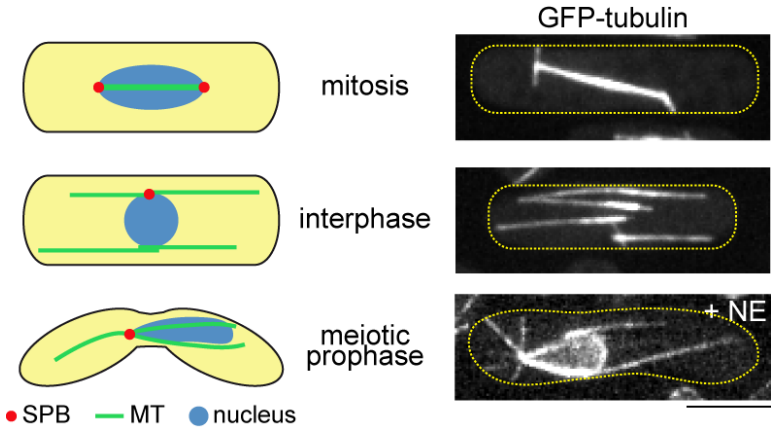

Figure 2.5. MT arrays in fission yeast upon structural rearrangements of the SPB.
A metaphase spindle is formed from overlapping MT arrays nucleated from opposite SPB. In interphase, MT bundles are linearly arranged along long axis of the cell. During meiotic prophase, MTs form a radial array. Microscopic images of cells in respective stages expressing a green marker for tubulin (GFP-Atb2) and additionally for the NE (Cut11-GFP) during meiotic prophase. Bar, 5µm. *(schematic adapted from (Dammermann et al., 2012), images my own studies)*

Like centrosomes, the SPB is major nucleation site of new MTs. It recruits γ-tubulin via pericentrin-related proteins, either to the outer, for example via the fission yeast Mto1 (Sawin et al., 2004), or inner side of SPB, via Pcp1 (Fong et al., 2010). The SPB also determines the spatial organization of the MT arrays within the cells. This is clearly illustrated by the different MT array presented in fission yeast, as it undergoes structural changes at the SPB from interphase to mitosis (Toya et al., 2007, Tallada et al., 2009) (Figure 2.5), as well as during the transition from mitotic to meiotic cell cycle (Tanaka et al., 2005, Ohta et al., 2012). During mitosis, a bipolar spindle is nucleated, where MTs originating from the inner plaque are extending perpendicularly from the SPBs. However, interphase MTs are laterally associated with the SPB and NE forming a

linear array along the long axis of the cell (Hagan, 1998). Finally, upon onset of meiosis, meiotic specific SPB components are recruited that arrange MTs into a radial array resembling centrosomes (Ding et al., 1998, Dammermann et al., 2012). Therefore, SPBs are very important structures for all MT-dependent nuclear migration processes as particular observed during fission yeast karyogamy. They exhibit an additional role as a tether for chromosomes linking chromatin to the cytoskeleton (Funabiki et al., 1993, Chikashige et al., 2006).

2.4. Motor proteins of the microtubule cytoskeleton

Two classes of motor proteins using MTs as tracks are known: dyneins and kinesins. Like actin-dependent myosin motors, they bind and hydrolyze ATP that induces conformational changes in the globular motor domain that are eventually translated into a displacement along the cytoskeletal filament. While the motor domain contains a MT-binding site, additional domains are required to control oligomerization and interaction with other proteins allowing their subcellular targeting (Schliwa and Woehlke, 2003). MT-dependent motors are involved in most of the MT-based cellular functions, such as cell division, vesicle trafficking and organelle transport. Thereby, they walk in a directed fashion along MTs either towards the plus ends, for most kinesins, or towards the minus ends, for dyneins and some kinesins. Some motors have been shown to mediate MT interactions by bundling and sliding and are required for the organization of the MT cytoskeleton, while others positively or negatively influence MT dynamics.

2.4.1. Kinesins (KIFs)

To date, at least 14 distinct kinesin families are described in eukaryotes based on structural features (Lawrence et al., 2004, Hirokawa et al., 2009). The human genome contains 45 KIF genes covering all families (Miki et al., 2001). Kinesins are often composed of two identical heavy chains that can be associated to light chains in metazoan (Vale, 2003) (Figure 2.6A). As mentioned above, kinesin heavy chains exhibit a modular design with a motor domain, a coiled-coil stalk/neck region and a tail domain (Hirokawa et al., 1989). The well conserved motor domain contains the catalytic core for nucleotide binding and hydrolysis and the MT-binding site. On the other hand, the divergent tails determine subcellular localization and cargo specificity,

also through interaction with the light chains (Hirokawa et al., 1989), and regulate overall activity (Coy et al., 1999). The stalk region facilitates dimerization, combining two motor domains, which appears to be crucial for the movement of most kinesins along MTs (Hancock and Howard, 1998).

In most kinesins, grouped as N-kinesins, the motor domain is located close to the N-terminus; however a few kinesins, C- and M-kinesins, possess their motor domain at the C-terminus or in the middle, respectively (Hirokawa et al., 1989) (Figure 2.6B). Furthermore, the location of the motor domain appears to determine the function and directionality of kinesins. N-kinesins typically walk along MTs in a plus end-directed manner, while C-kinesins essentially composed of the kinesin-14 family, are characterized by a minus end-directed motility, like cytoplasmic dynein. M-kinesins comprised of the non-motile kinesin-13 family act as MT depolymerases (Howard and Hyman, 2007).

The molecular mode of movement of most two-headed kinesins is exemplified by the kinesin-1 KIF5A, a conventional kinesin that has been shown to take 8nm-steps along MTs, the distance between adjacent tubulin dimers (Svoboda et al., 1993), and that each step is coupled to hydrolysis of one ATP molecule (Schnitzer and Block, 1997). Furthermore, these motors are processive taking several hundred steps before detaching from MTs, even under load, (Hackney, 1995, Vale et al., 1996). The “hand-over-hand” model (Figure 2.6C) proposes that a kinesin walks through alternating head movements of 16nm (Kaseda et al., 2003, Yildiz et al., 2004), where upon MT release of one head, the other one attaches to the MT allowing a permanent MT-kinesin association and processivity (reviewed in (Gennerich and Vale, 2009)). In detail, the movement of each is head is caused through nucleotide-driven conformational changes, and the cycles of both heads are tightly coupled via the neck/stalk (Rice et al., 1999). Kinesin bound to ADP binds to an MT which triggers ADP release and replacement by ATP in one head (front head) causing a strong association between this head and the MT. Then, ATP hydrolysis generates a power stroke that is translated by the neck into a forward (towards plus end) displacement of the second weakly bound head, the rear head, where it binds in-turn a new tubulin dimer. Interestingly, some monomeric N-kinesins, like the kinesin-3 KIF1A, are also processive. Here, a complete detachment upon ATP hydrolysis may be prevented through electrostatic interactions between motor and the positively charged tubulin tails (Okada and Hirokawa, 2000).

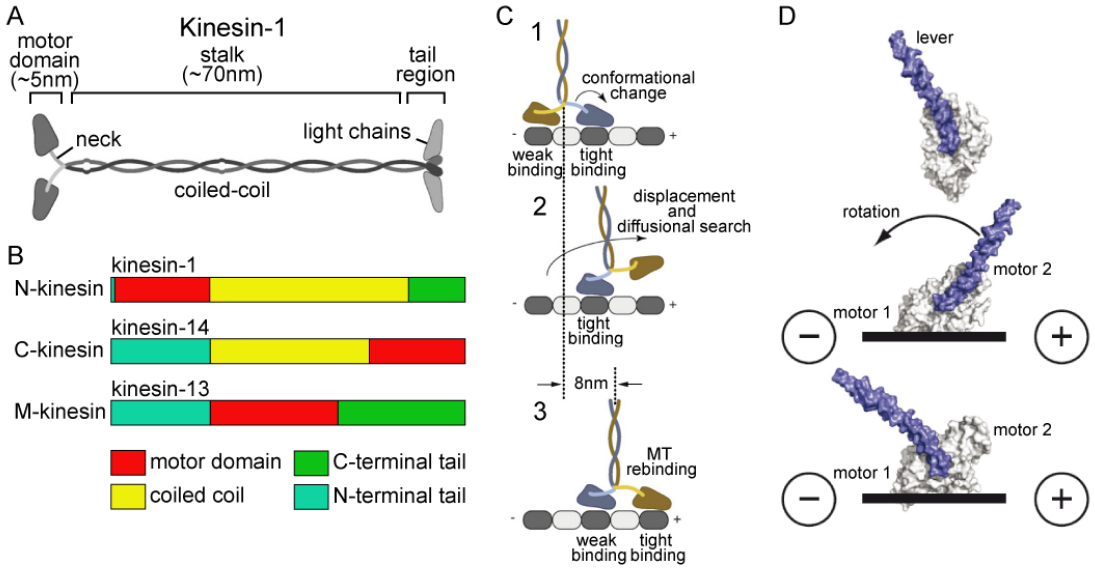

Figure 2.6. Kinesin structure and stepping model.

(A) Schematic representation of kinesin structure exemplified by the conventional kinesin-1. Two heavy chains form a dimer via the coiled-coil region in the stalk. The neck connects the dimerization domain to the N-terminal globular motor domain containing catalytic and MT-binding activity. C-terminal tail mediates cargo- and light chain-binding. (B) Domain structure of N-, C- and M-kinesins. (C) "Hand-over-hand" model for dimeric N-kinesin: A nucleotide-driven conformational change in the front head bound tightly to MT is translated via the neck into a plus end-directed displacement of the weakly bound rear head. (D) Stepping model for kinesin-14, where ATP turnover drives lever motion and plus end-directed displacement of one motor domain. *((A,C) (Gennerich and Vale, 2009); (B) adapted from (Marx et al., 2005); (D) (Cross, 2010))*

However, the minus end-directed C-kinesins, kinesin-14 proteins, show a mode of movement that differs from the "hand-over-hand" model. *Drosophila* Ncd possesses a head that is structurally very similar to N-kinesins and also forms homodimers (Sablin et al., 1998). But it does not only show opposite directionality, but also walks in a non-processive manner taking only one step coupled to hydrolysis of one ATP molecule before release from MTs (deCastro et al., 1999, Foster and Gilbert, 2000). Studies generating chimeric motor proteins, revealed that a region between the catalytic core and the stalk is responsible for the minus end-directed motility (Case et al., 1997, Endow and Waligora, 1998, Sablin, 2000). Additionally, the stalk of C-kinesins exhibits a different architecture than in N-kinesins resembling rather a lever (Figure 2.6D), which is thought to perform a rotation towards the minus end driven by ATP turnover, which simultaneously displaces one motor head towards the MT minus end (Wendt et al., 2002,

Yun et al., 2003). However, it remains unclear whether this rotation is triggered by ATP binding or ADP release (Cross, 2010). The non-processivity may be caused by involvement of only one motor head in MT binding and movement.

Ncd and its homologues, like budding yeast Kar3, *hamster* CHO2 and human *HSET*, have been shown to play fundamental roles in mitosis and meiosis. During mitosis, kinesin-1s4 contribute to the formation of spindle poles and regulation of spindle length (Matuliene et al., 1999, Goshima et al., 2005a, Goshima et al., 2005b, Zhu et al., 2005). In budding yeast, Kar3 is required for the congression of the two haploid nuclei during meiosis (Molk et al., 2006, Gibeaux et al., 2013). Kinesin-14 motors contain two MT-binding domains, one in the head and an additional one in the tail allowing interaction with two MTs at once. In general, these motor proteins cooperate to induce MT bundling and sliding in a parallel or anti-parallel fashion (Karabay and Walker, 1999, Oladipo et al., 2007, Braun et al., 2009, Fink et al., 2009). Furthermore, they might influence MT dynamics, for example depolymerase activity at plus ends has been suggested for Kar3 (Sproul et al., 2005).

2.4.2. Dynein

2.4.2.1. Molecular structure of the dynein motor

Dyneins are consistent of two distinct groups, cytoplasmic and axonemal dynein, of which later is involved in ciliary and flagellar movements (Vallee and Hook, 2003). However, most cellular dynein functions including in intracellular transport, mitosis and cell migration are performed by a single cytoplasmic dynein that was originally identified as MAP1C (Paschal et al., 1987). Dynein also plays a conserved role in spindle and nuclear positioning. In fact, dynein is probably the most important minus end-directed motor in the cell, as it controls a very wide range of different cellular processes.

Like most kinesins, dynein (Figure 2.7A, B) is composed of two heavy chains (DHCs) that are responsible for its motor activity (Sakakibara and Oiwa, 2011). Additionally, it contains a variety of accessory subunits, termed intermediate chains (DICs), light intermediate chains (DLICs) and light chains (DLCs) and interacts with adaptor proteins or protein complexes,

among them the dynactin complex, which allows specific cargo binding and regulation of the motor activity.

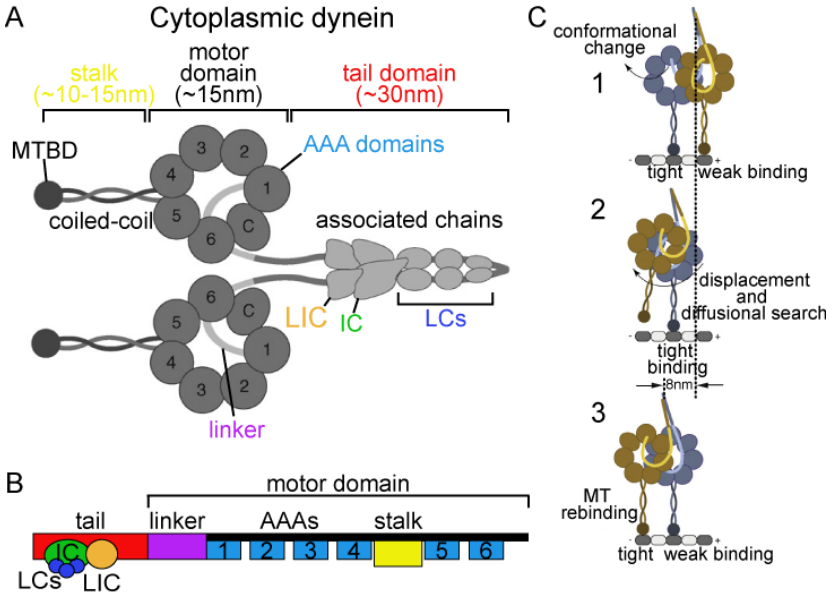

Figure 2.7. Dynein structure and stepping model.

(A) Cartoon representation of dynein composed of two heavy chains and several subunits (intermediate chains ICs, light intermediate chains LICs and light chains LCs) at the tail. The heavy chain contains a catalytic motor domain formed by 6 AAA domains and a coiled-coil stalk with the MT-binding domain (MTBD) at its tip. Tail and motor domain are joined by a linker element. (B) Domain composition of the dynein heavy chain. (C) Possible dynein stepping sequence, similar to "hand-over-hand" model of kinesins, but towards opposite direction. *((A,C) (Gennerich and Vale, 2009); (B) adapted from (Vallee et al., 2012))*

Dynein belongs to the family of AAA ATPases that usually form ring-shaped hexamers by association of the AAA ATPase domains (reviewed in (White and Lauring, 2007)). In the case of dynein, the six ATPases domains are combined in a single DHC polypeptide that is arranged in a ring with a central cavity (Samso et al., 1998, Burgess et al., 2003). The MT-binding site is located on a stalk that extends from the motor domain (Gee et al., 1997). Finally, the N-terminal tail domain forms a large projection, the stem, which mediates homodimerization, serves as a docking platform for the accessory subunits and binds to cargos (Habura et al., 1999). Mutagenesis studies revealed that only four out of the six ATPase domains are capable of ATP binding and hydrolysis, thereby only AAA1 and AA3 appear absolutely essential for dynein motility (Reck-Peterson and Vale, 2004). Compared to kinesins, the stepping mode of dynein is

less understood, because its stepping behaviour and directionality are more irregular (Reck-Peterson et al., 2006, Gennerich et al., 2007). Similarly to kinesins, for processivity the coordination of the two motor domains is required (Shima et al., 2006) leading to the proposal that dynein may also walk in a "hand-over-hand"-like fashion (Reck-Peterson et al., 2006, Toba et al., 2006) (Figure 2.7C), where ATP turnover induces confirmation changes, a rotation of the motor domain (front) tightly bound to MTs that is then translated into a forward displacement of the second motor domain (rear) via the linker (Gennerich and Vale, 2009). Simultaneously, the front head is released from the MT (Gibbons et al., 2005, Kon et al., 2009).

The DHCs interact directly with 2 DICs and 2 DLICs, which bind distinct but overlapping regions in the tail (Tynan et al., 2000a), and indirectly with DLCs, via DICs. These non-catalytic subunits are thought to control cargo binding and subcellular dynein localization, but are not required for dynein motility *in vitro* (Reck-Peterson et al., 2006). For example, in mammals DLIC1 targets dynein to pericentrin to organize the mitotic spindle (Purohit et al., 1999, Tynan et al., 2000b), while DLIC2-dependent interaction between dynein and the polarity protein Par3 is essential for centrosome orientation in migrating cells (Schmoranzer et al., 2009). However, there may be some redundancy, as both DLICs localize to kinetochores and centrosomes (Tan et al., 2011) consistent with a role in mitosis as reported in *C. elegans* (Yoder and Han, 2001). However, in other systems, the role of DLICs is more controversial. In Drosophila and Aspergillus, the DLIC is the not required for targeting the dynein complex, but for its formation or stability (Mische et al., 2008, Zhang et al., 2009a). On the other hand, DICs are thought to be important for the association with the dynactin complex (Vaughan and Vallee, 1995). LICs are assumed to reflect similar roles, but also appear to have dynein-independent functions (Vallee and Hook, 2003).

2.4.2.2. Regulation of dynein function

Additional adaptor proteins participate in dynein recruitment to subcellular sites of action and, in the case of the dynactin and LIS1/NudE complex in regulation of motor activity (Vallee et al., 2012, Kardon and Vale, 2009).

Dynactin is a large multiprotein complex (Figure 2.8A) that is required for most dynein functions. It was discovered as an activator of the minus end-directed motility *in vitro* (Schroer

and Sheetz, 1991). The central scaffold is formed by a 40nm long filament of actin-related protein Arp1 decorated at its barbed end with capping protein, which in turn interacts with the p150 subunit extending as a 24nm long sidearm from the short filament. p150 binds to MTs and +TIPs EB1 and CLIP170 via the N-terminal CAP-Gly (Culver-Hanlon et al., 2006) and to dynein via DICs. Therefore, in some organisms like Aspergillus, the dynactin complex is required for dynein plus tip localization, which appears to drive nuclear migration (Xiang et al., 2000). In metazoan, plus tip loading of dynein is less clear, but it may be correlated to initiation of vesicle transport (Vaughan et al., 2002) (Figure 2.8B). Furthermore, dynactin is implicated in cargo binding, as it targets dynein to the surfaces of vesicles and other membrane-surrounded organelles either via interaction between the Arp1-filament and spectrin covering most cellular membranes (Holleran et al., 2001) or p150-mediated interaction with GTPases and GTPase-interacting proteins (Kardon and Vale, 2009). Finally, it is believed that it stimulates dynein motility by providing an additional MT-binding domain to the dynein motor, thereby increasing its processivity (King and Schroer, 2000). However, more recent studies showed that the stimulating affect was independent of the CAP-Gly domain of p150 suggesting another mechanism that remains elusive (Kardon et al., 2009).

Other dynein adaptors are the LIS1/NudE complex, Bicaudal D, the RZZ complex and Spindly. Briefly, Lis1 and NudE homologues are required for plus tip localization of dynein in budding yeast to properly positioning the spindle during mitosis (Lee et al., 2003) (Figure 1.3B). In metazoan, these proteins recruit to various subcellular locations including kinetochores, centrosomes, NE and cortical regions. Most prominent example, is the nuclear movement observed in migrating neurons (Figure 1.3F), where Lis1/NudE are essential for dynein-dependent coupling between centrosome and nucleus (Tanaka et al., 2004). However, future work will be required to reveal how these proteins are targeted to these diverse cellular structures. Furthermore, it was suggested that LIS1 regulates dynein activity (Mesngon et al., 2006), however, its mechanism is not understood. The metazoan-specific Bicaudal D appears to be dominantly involved in dynein-based transport of mRNAs like during Drosophila oogenesis and embryo development (Bullock and Ish-Horowicz, 2001), while the RZZ (ROD-ZW10-Zwilch) complex and spindly dock dynein to kinetochores during prometaphase facilitating kinetochores capture (Li et al., 2007, Griffis et al., 2007).

In summary, dynein function and localization is regulated through a complex network of varying subunits and adaptors allowing dynein to fulfill diverse functions.

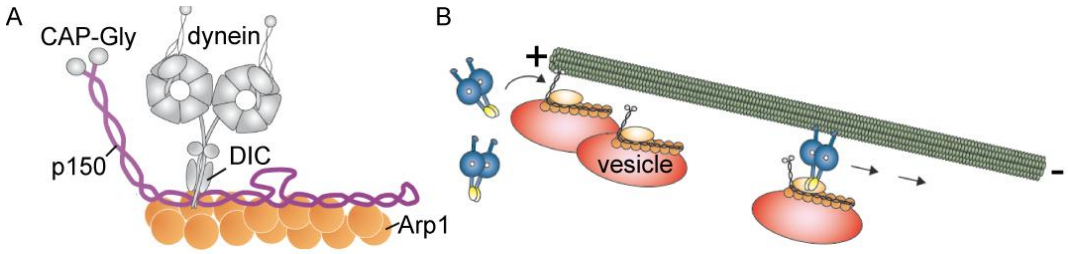

Figure 2.8. Dynactin structure and its association to dynein.

(A) Carton representation of the dynactin complex interacting with dynein. (B) Dynactin-associated vesicles decorating MT plus ends, which may facilitate the capture of vesicles and other membranous organelles for dynein-dependent minus end-directed transport. *(Vallee et al., 2012)*

2.5. MT-dependent mechanisms of nuclear positioning

MTs and its associated motor proteins play a prominent role in nuclear positioning (reviewed in (Reinsch and Gonczy, 1998)). In many cases, the nucleus is tightly associated to MTOCs, often centrosome or SPB, and forces to displace the nucleus are generated along MTs emanating from these MTOCs. Alternatively, when the nucleus is not associated to an MTOC, it is laterally transported along MTs.

In the MTOC-dependent mode, nuclear migration can be driven by two major types – pushing or pulling forces. Pushing forces can be simply generated by MT polymerization towards a fixed object, such as the cortex. Thereby, the MTOC (and nucleus) tethered to MT minus ends will be displaced away from the cortex. Such mechanism has been found in rod-shaped fission yeast cells (Figure 1.3A), where interphase MTs connected to the NE via MTOCs grow with their dynamic plus ends towards the cell poles resulting in a balance of pushing forces maintaining the nucleus in the cell middle (Tran et al., 2001). Similarly, in fertilized eggs, the male pronuclei are pushed towards the cell center by a growing MT aster. However, the pushing forces exerted by growing MTs are limited to relative short distances, as longer MTs will buckle under compression. Alternatively, minus end-directed MT motors, mostly dynein, anchored at specialized cortical sites may generate pulling forces. Most prominent example is represented by the positioning of the spindle during budding yeast mitosis (Figure 1.3B). The nuclear movement

into the neck is driven by astral MTs that laterally slide along the cortex, which is caused by cortically-anchored dynein that pulls the MTs and the associated nucleus in a minus end-directed fashion (Adames and Cooper, 2000). The mode of cortical dynein exerting pulling forces appears a well conserved and wide-spread mechanism found in *C. elegans* embryos and epithelial cells to position the mitotic spindle (Busson et al., 1998, Nguyen-Ngoc et al., 2007), during Drosophila oogenesis (Dujardin and Vallee, 2002) and in interphase and migrating cells to position the centrosome (Burakov et al., 2003, Schmoranzer et al., 2009) and has been demonstrated *in vitro* (Laan et al., 2012).

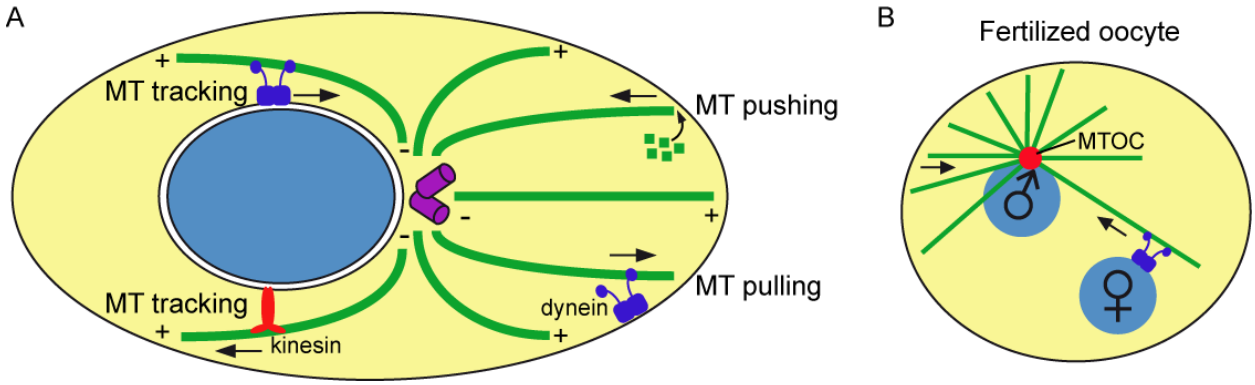

Figure 2.9. MT-dependent mechanisms of nuclear movements.

(A) The MT cytoskeleton transmits pushing forces by MT growth towards the cortex. Pulling forces are generated by cortical dynein. Both mechanisms require the attachment of the centrosome to the NE. The third mode, tracking, is performed by motors at the nuclear surface. (B) Pronuclei migration in fertilized oocytes. Male pronuclei are pushed towards the center by a growing MT aster emanating from the MTOC. The female pronucleus is transported along these MTs in a dynein-dependent manner. *(Adapted from (Dupin and Etienne-Manneville, 2011) and (Reinsch and Gonczy, 1998))*

The MTOC-independent mode of nuclear positioning - tracking along MTs - is applied by the female pronuclei in fertilized eggs. These nuclei laterally engage with MTs nucleated by the male pronuclei and are transported along MTs towards the cell center by motor proteins. The motors are directly recruited to the NE via their interaction with LINC complexes (reviewed in }(Starr and Fridolfsson, 2010)) and can move in a plus or minus end-directed manner. In fact, the female pronuclei have been shown to translocate along MTs towards the minus ends via dynein (Reinsch and Karsenti, 1997). In *C. elegans* hyp7 cells (Figure 1.3D), the KASH protein Unc-83 recruits two opposite motors, kinesin-1 and dynein, to the NE, where these motors have distinct

role to drive nuclear migration (Fridolfsson et al., 2010). Here, kinesin-1 generates the major force to move the nuclei forward, and dynein mediates short backwards movements to bypass cellular roadblocks (Fridolfsson and Starr, 2010). Similarly, during interkinetic nuclear migration (Figure 1.3E) characterized by migrations of the nuclei along the apico-basal axis in neuronal precursor cells, kinesins, in this case, kinesin-3, and dynein cooperate to transport the nuclei towards the basal or apical side, respectively (Tsai et al., 2010). Finally, also developing muscle cells (Figure 1.3H) appear to require both, dynein and kinesin, to position myonuclei correctly along the periphery. Immediately after fusion of myoblasts, the nuclei are first translocated towards the center of the myotubes, which is driven by dynein anchored to the NE and pulling on MTs emanating from neighboring nuclei (Cadot et al., 2012). Subsequently, kinesin-1 is proposed to bring these nuclei towards the cell periphery, as its depletion results in abnormal aggregation of nuclei in the cell middle (Wilson and Holzbaur, 2012).

Finally, dynein possess a second role at the NE by maintaining the connection of the MTOC at the NE, which in turn is essential to drive MTOC-dependent processes of nuclear positioning. Studies in *C. elegans* revealed that dynein anchored to the cytoplasmic domain of KASH proteins walks towards the minus ends of centrosomal MTs pulling the centrosome towards the NE (Malone et al., 2003). Recently, it has been demonstrated that also kinesins can perform a similar function in keratinocytes (Schneider et al., 2011), however the mechanism remains elusive. An extreme case of dynein-dependent centrosome anchorage at the NE is illustrated by the neuronal migration (Figure 1.3F), where first the leading process extends, then the centrosome follows and finally the nucleus. In detail, the nucleus is transported towards minus ends anchored at the centrosome by the dynein/LIS1 complex, which is further assisted by acto-myosin contraction behind the nucleus (Shu et al., 2004, Tsai et al., 2007).

The mechanisms to control nuclear positioning are very diverse and complex and in many systems still not fully understood. Therefore, studies in simpler organisms have helped to shed light on the molecular details and future work may help to uncover novel principles.

3. Nuclear movements in fungi

Tremendous advances in the field of nuclear positioning have been made through studies in fungi. Due to high conservation of the cytoskeleton machinery, these simple genetically tractable organisms have greatly contributed to our conceptual understanding underlying nuclear movements. In particular, the role of dynein, its interactors and its mode of action have been first uncovered and mechanistically described in these systems, but subsequently found in higher organisms.

3.1. Overview of fungal nuclear migrations

Among the most studied fungi are the filamentous fungus *Aspergillus nidulans*, the budding yeast *Saccharomyces cerevisiae* and the fission yeast *Schizoaccharomyces pombe.* One common feature of all these species is that nuclear movements are led by MTOCs, usually the SPB, that connect MTs to the NE.

The filamentous fungus *Aspergillus nidulans* contains multinucleated hyphal segments, in which the nuclei are positioned, evenly spaced, along the length of hypha (Xiang and Fischer, 2004) (Figure 3.1A). During vegetative growth, these nuclei move in a coordinated manner with the growing tips, thereby maintaining regular distances. MTs are nucleated from the SPBs and radiate in all directions in this organism. The isolation and characterization of mutants defective in nuclear distribution identified major components of the dynein-related pathway, which were found to be conserved in human. Most prominent example is LIS1/NudF and NudE that were described in *Aspergillus* mimicking the deletion phenotype of dynein (Willins et al., 1997), which later impacted on the studies related to the disease Lissencephaly (Xiang et al., 1995), establishing a regulatory role of the LIS1/NudE complex on dynein function and activity. In *Asoergillus*, dynein localizes to MT plus tips. Even though not completely solved, but the characterization of a cortical protein required for nuclear positioning led to the suggestion that dynein functions by sliding MT along the cortex (Fischer and Timberlake, 1995, Veith et al., 2005) (Figure 3.1B). However, a second dynein-dependent mechanism may be operating along the internuclear MTs to maintain the even spacing.

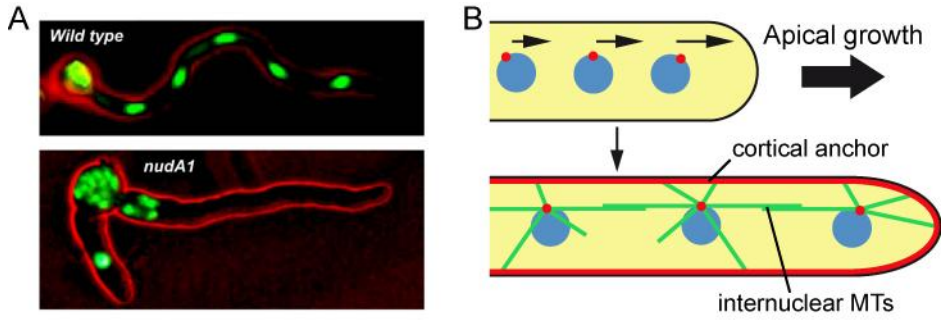

Figure 3.1. Nuclear distribution in *Aspergillus nidulans.*

(A) Nuclear distribution in wildtype and dynein mutant (*nudA1*). Overlay of phase contrast images to visualize cell borders (colored in red) and fluorescent image to visualize nuclei labeled with GFP (green). (B) Schematic of nuclear distribution and MT organization during apical growth. Cytoplasmic MTs either form antiparallel internuclear bundles between adjacent nuclei or make contact with the cortex. *((A) (Xiang and Fischer, 2004); (B) adapted from (Yamamoto and Hiraoka, 2003, Veith et al., 2005))*

In budding yeast, the nucleus migrates first to the mother-bud neck prior to mitosis and then, in a second step, into the bud neck during anaphase (Adames and Cooper, 2000, Pearson and Bloom, 2004) (Figure 3.2A). These two distinct, but partially overlapping redundant mechanisms are mediated by astral MTs (Palmer et al., 1992). At first, MTs anchored to the SPB are captured at the cell cortex by Kar9 (APC homologue) that localizes to MT plus tips in a Bim1/EB dependent manner and interacts with cortical actin at the bud site (Miller and Rose, 1998, Miller et al., 1999, Korinek et al., 2000). Upon MT depolymerization, the nucleus is pulled towards the bud site. In the subsequent movement into the bud neck, dynein slides MT laterally along the cortex of the mother and daughter cell resulting in an oscillatory behavior of the nucleus within the neck.

On the other hand, during meiosis the two haploid nuclei of mating cells migrate towards each other to allow nuclear fusion. Nuclear congression in budding yeast is independent on dynein but relies on the action of another minus end-directed motor, the kinesin-14 Kar3 (Meluh and Rose, 1990, Molk et al., 2006). Prior to cell fusion, the nucleus is oriented and guided to the shmoo tip, as MT plus ends are transported along actin cables emanating from the shmoo tip, which requires the activity of Bim1, Kar9 and the myosin Myo2 (Korinek et al., 2000, Yin et al., 2000, Hwang et al., 2003). Then, the MT plus tips are attached at the cortex; during phases of polymerization by Bim1 and depolymerization by Kar3 and Bik1 (CLIP170 homologue) (Maddox et al., 2003, Zaichick et al., 2009). This model suggests that Kar3 acts as an anchor for

MTs and prevents shrinkage supported by the detection of MTs detached from the cortex that shorten back to the SPB. Finally after cell fusion, MTs rapidly interact, which requires again the activity of Bik1 and Kar3 (Berlin et al., 1990, Meluh and Rose, 1990). An early model suggested that Kar3 located at MT plus tips crosslinks and slides antiparallel MTs emanating from opposite SPB pulling the two nuclei together (Rose, 1996) (Figure 3.2B). This model predicts long MT overlaps and plus tips located near SPBs. However, newer studies failed to confirm these predictions and proposed a model, where Kar3 rather links plus ends with a minimum of MT-MT sliding (Molk et al., 2006). Furthermore, Kar3 may initiate MT depolymerization drawing both nuclei together. Interestingly, a very recent electron microscopic analysis suggests a novel model, where Kar3 anchored to the SPB, but not along MTs, interacts with MTs from the opposite nucleus driving nuclear congression (Gibeaux et al., 2013).

Also fission yeast has proven to be a very useful tool to investigate different aspects of nuclear positioning, which will be illustrated in the next chapters and are subject of this work.

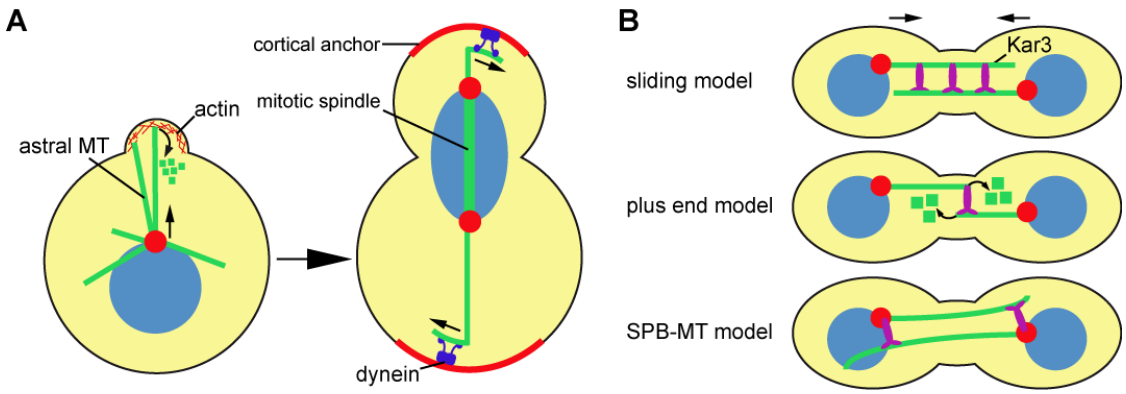

Figure 3.2. Nuclear migration during mitosis and meiosis in *Saccharomyces cerevisiae*.
(A) Spindle orientation during mitosis driven by cortical capture of MT, either by Kar9-mediated interaction with actin or by dynein. (B) Models for how Kar3 drives nuclear congression. *(Adapted from (Huisman and Segal, 2005), (Molk and Bloom, 2006) and (Gibeaux et al., 2013))*

3.2. Fission yeast as a model system

The fission yeast *Schizosaccharomyces pombe* is a unicellular eukaryote and belongs to the ascomycete fungi. Originally, it was isolated by the German biologist Paul Lindner in 1893 from a millet beer imported from East Africa.

To date, fission yeast serves as an excellent eukaryotic model, as many fundamental cellular functions bear similarity at molecular level to higher eukaryotes combined with its genetic tractability. In particular, the basis of the cell cycle, a molecular clock driving alternating rounds of growth, replication and division, was initially described in *S. pombe* by Paul Nurse and his collaborators, for which he was awarded the Nobel Prize with Lee Hartwell and Tim Hunt in 2006.

Fission yeast preferentially lives in a haploid state and its genome contains 5123 genes (Wood et al., 2002) (www.pombase.org) on three large chromosomes. Fission yeast forms rod-shaped cells (Figure 3.3) of about 4µm in diameter with a rigid cell wall and grow from 7 to 14µm length by linear tip extension. Like other eukaryotes, its cell cycle is divided into four sequential phases, G1, S (DNA replication), G2 and M (mitosis) phase and one round takes about three hours at 25°C. In an exponentially growing culture, it spends three quarters of its time in G2, while G1 phase is almost not noticeable. After completion of chromosome segregation in mitosis, cytokinesis and septation divide the cells in two. As S phase takes place concomitantly with septation, the two daughter cells generated from the medial fission are early G2 phase and already contain two copies of genetic material.

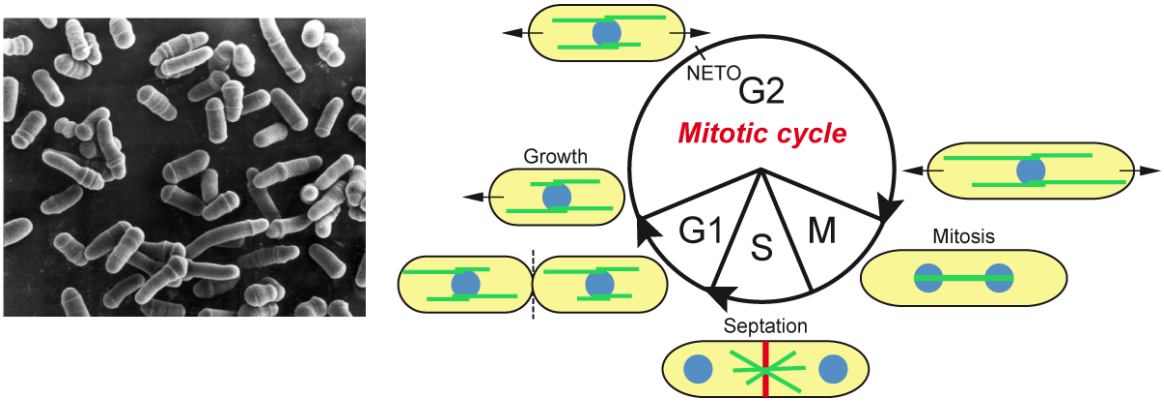

Figure 3.3. The fission yeast vegetative cell cycle.

Left, electron microscopic image of fission yeast cells. Left, vegetative cell cycle of haploid fission yeast cells. Nuclei (blue), MTs (green) and septum (red). *(Image from (Hayles and Nurse, 2001))*

Early immunofluorescence studies on fixed cells and, more recently, real-time imaging of the MTs labeled by green fluorescent protein (GFP) combined with advanced technology in microscopy with higher resolution allowed the visualization of the MT cytoskeleton throughout

the entire vegetative cell cycle (Hagan, 1998, Tran et al., 1999) as well as during meiosis (Ding et al., 1998).

During interphase, MTs extend through the cytoplasm in a linear array. Upon mitotic entry, cytoplasmic MTs disappear and the mitotic spindle is assembled in the nucleus. Chromosomes are equally segregated, the spindle disassembles and a radial MT array, termed post-anaphase array, is nucleated from the cell middle before it transforms again into the interphase array.

Under nitrogen starvation, haploid fission yeast cells exit the mitotic cell cycle and enter stationary phase (Harigaya and Yamamoto, 2007). If cells of opposite mating types, called h^+ and h^-, are present, cells enter the meiotic cell cycle (Figure 3.4). Thereby two neighboring cells grow towards each other by forming an extension, the shmoo, representing the site of cell fusion. During nuclear congression and fusion, a process called karyogamy, a diploid zygote is produced that is capable of growing and dividing in a vegetative manner under favorable conditions. However, this state is very instable, and usually, after nuclear fusion, diploid zygotes will undergo two consecutive rounds of nuclear division, meiosis I and II, which will results in four haploid nuclei that are encapsulated in a specialized spore wall. Under rich conditions, the spore can germinate and re-enter the vegetative cell cycle again.

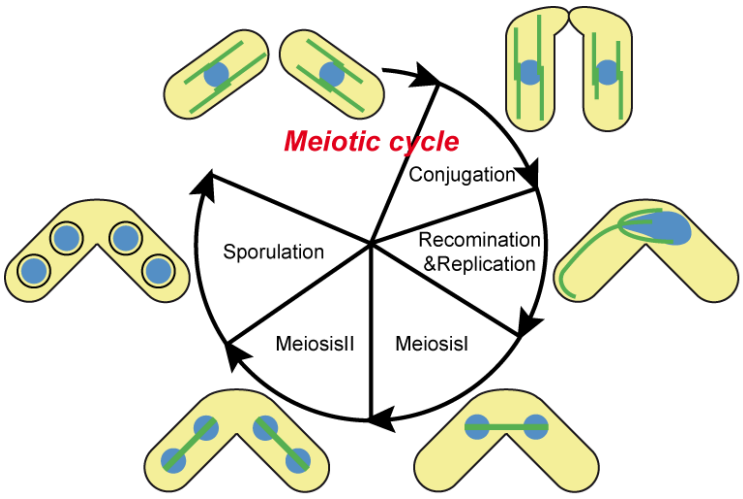

Figure 3.4. The fission yeast meiotic cell cycle.

Haploid fission yeasts enter meiotic cell cycle upon nitrogen starvation. Nuclei (blue) and MTs (green). A *S. pombe*-specific phase is the nuclear horsetail movement during meiotic prophase prior to Meiosis I.

During meiotic prophase, spanning the period from cell fusion to the onset of meiosis I, the cytoplasmic MT array undergoes dramatic changes forming a radial array emanating exclusively from the SPB (Ding et al., 1998). This is important for an unique type of nuclear migration that occurs in fission yeast – the nuclear horsetail movement, where the diploid nucleus migrates forth and back along the cell axis for about two hours prior to meiosis I (Chikashige et al., 1994). Typically, the nucleus adopts an elongated shape. This oscillatory behavior of the nucleus is believed to facilitate pairing and recombination of homologue chromosomes (Ding et al., 2004). Both, studies in interphase and during meiotic prophase, have uncovered MT-guided processes of nuclear positioning explained in the next chapters.

3.3. Microtubule organization and nuclear positioning in interphase

Interphase MTs are organized in 3 to 4 bundles oriented along the long axis of the cell (Drummond and Cross, 2000) (Figure 3.5). These bundles contain MTs in an antiparallel configuration, thereby the less dynamic minus ends are dominantly found within a narrow overlap zone of a bundle close to the cell middle and are tethered to the NE through multiple interphase MTOCs (iMTOCs) comprised by the SPB and additional MTOCs (Tran et al., 2001). While the composition of the SPB has been largely revealed, the composition and assembly of the additional iMTOCs is still mysterious (Sawin and Tran, 2006). The MT nucleating γ-tubulin complex is recruited to iMTOCs and activated by the pericentrin-related protein Mto1 (Sawin et al., 2004, Lynch et al., 2014). *mto1Δ* cells are incapable of nucleating new MTs and contains only one abnormally long bundle inherited from the previous generation.

The dynamic plus ends extend towards opposite cell poles, switching between stages of polymerization and depolymerization. They maintain contact with the cortex for one to two minutes before catastrophe is initiated, preferentially at the distal ends. This behavior appears crucial for cellular morphogenesis in fission yeast and is explained in a later chapter. Like in other eukaryotes, the dynamics are regulated by +TIPs. Key player and major suppressor of catastrophe is Mal3, the EB1 homologue. Cells lacking Mal3 are phenotypically characterized by very short MTs (Beinhauer et al., 1997) that initiate catastrophe before reaching the cell cortex (Busch and Brunner, 2004). Mal3 is also required for plus tip localization of Tip1, CLIP170 homologue, which like Mal3 is implicated in suppression of catastrophe. Even though less severe

than *mal3Δ*, its deletion also results in shorter MTs. Interestingly, while catastrophe events most likely occur at the far cell tips in wildtype cells, shrinkage is initiated immediately upon contact with the cortex in *tip1Δ* cells, even when contact has been made close to the cell middle (Brunner and Nurse, 2000). This suggests a role for Tip1 in protecting plus tips from premature catastrophe upon touching the cortex.

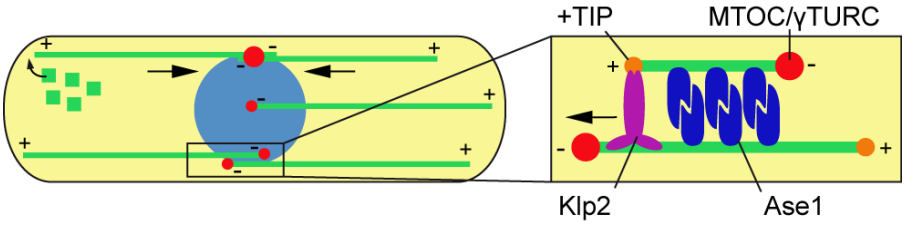

Figure 3.5. MT architecture in an interphase fission yeast cell.

(A) Schematic representing MT architecture. Depicted are MTs (green), nucleus (blue) and iMTOCs associated with the NE (red) including the SPB as major MTOC and additional MTOCs. Minus ends are focused in the cell center, while plus ends extends towards opposite cell tips. A balance of MT polymerization-generated pushing forces maintains the nucleus in the cell middle. (B) Model of formation of antiparallel MT bundles by the kinesin-14 Klp2 and MT bundler Ase1. *(Adapted from (Sawin and Tran, 2006))*

The antiparallel and symmetric linear interphase array "self-organizes" through the action of MAPs, in particular the MT bundler Ase1 (MAP65 homologue) and the kinesin-14 Klp2 (Carazo-Salas and Nurse, 2006, Daga et al., 2006) (Figure 3.5). In *ase1Δ* cells, iMTs are disorganized into single MTs instead of bundles (Loiodice et al., 2005). On the other hand, in *klp2Δ* cells, the overlap zones are unfocused and MT minus ends can be found more often away from the cell middle suggesting that Klp2 slides newly nucleated MTs towards minus ends (Carazo-Salas et al., 2005, Janson et al., 2007).

Finally, why do MTs self-organize these linear arrays? Indeed, it has been shown that particular organization of the MT cytoskeleton can generate opposing pushing forces by MT polymerization, thereby maintaining the nucleus in the cell middle, which in turn sets the cell division plane (Tran et al., 2001).

3.4. Microtubule organization and nuclear horsetail movement during meiotic prophase

During meiosis, first two haploid cells fuse followed by nuclear congression and fusion. In fission yeast meiotic prophase, the diploid nucleus subsequently undergoes nuclear horsetail movement driven by dynein, and MTs that are arranged into a radial array that is emanating from one MTOC, the rMTOC, constituted by the SPB (Ding et al., 1998).

In general, the composition of the SPB changes dramatically from mitotic to meiotic cell cycle characterized by the recruitment of new meiosis-specific proteins and the removal of others (Ohta et al., 2012). While the significance of most of these changes still needs to be determined, electron tomographic studies showed that the rMTOC exhibits some similarity to mammalian centrosomes in that the cytoplasmic side of the SPB is surrounded by an electron-dense area which anchors MTs (Dammermann et al., 2012). The formation of the rMTOC depends on Hrs1, a meiosis-specific SPB component, enriched in the amorphous structure (Saito et al., 2005, Tanaka et al., 2005, Funaya et al., 2012). Hrs1 interacts with components of γTURC as well as with the KASH protein Kms1 suggesting that it may act as a structural scaffold bridging MT minus ends to the SPB (Funaya et al., 2012).

Dynein (Dhc1) accumulates at the SPB and along the length of MTs extending towards the cell periphery (Yamamoto et al., 1999) and interacts simultaneously with the cortical protein Num1 (Saito et al., 2006, Yamashita and Yamamoto, 2006), which stimulates dynein activity (Ananthanarayanan et al., 2013) and generates pulling forces (Yamamoto et al., 2001) (Figure 3.6). Unidirectional pulling forces rely on the asymmetric distribution of motor proteins that are more numerous along the longer leading MTs in front of the migrating nucleus (Vogel et al., 2009).

For proper dynein function, it needs to associate with the intermediate light chain Dic1 and the light intermediate chain Dli1 and to interact with the dynactin complex, as cells lacking Dic1, Dli1 or Ssm4, the Glued homologue and part of the dynactin complex, fail to undergo proper nuclear oscillations through disruption of dynein localization at MTs (Niccoli et al., 2004, Fujita et al., 2010). In detail, dynein is no longer found along MTs, but still recruited to the SPB in *ssm4Δ* and *dic1Δ* zygotes, where the interaction between dynein and dynactin is interrupted. In *dli1Δ* zygotes, dynein localization is globally decreased; however its role in dynein regulation is currently unknown. Interestingly, most of these factors are meiotically upregulated and it has

been shown that some of these meiosis-specific transcripts can be selectively eliminated during the vegetative cell cycle (Harigaya et al., 2006, Ohtaka et al., 2007).

In addition to its role in nuclear horsetail movement, dynein may perform further meiosis-related functions such as the clustering of telomeres at the SPBs (Yoshida et al., 2013). Here, a novel type of MTOCs, the telocentrosome induced by the SUN-KASH complex, colocalizes with telomeres and aggregation of these MTOCs at the NE depends in part on dynein, which interacts with cytoplasmic MTS nucleated from these sites. Furthermore, it has been proposed that dynein participates together with Klp2 in nuclear congression as *dhc1Δ klp2Δ* zygotes more often contained unfused nuclei (Troxell et al., 2001).

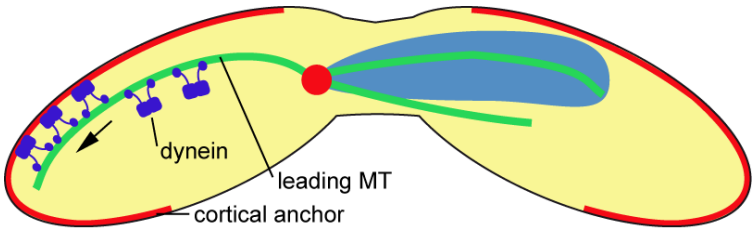

Figure 3.6. Dynein-driven nuclear horsetail movement.

Dynein localizes to MTs and interacts with the cortical protein Num1, which in turn activates dynein motility. Dynein generates pulling forces to move the nucleus towards the cell pole. Once nucleus has reached the cell pole, the cycle is repeated towards the opposite site.

3.5. The roles of kinesins and dynein in fission yeast

Fission yeast contains nine kinesins and one dynein heavy chain. As discussed above, dynein is a meiotically upregulated gene, which is in particular essential for meiotic processes. However, a mitotic role for dynein has been suggested by participating in chromosome biorientation and by focusing and anchoring spindle MTs at the poles (Courtheoux et al., 2007) (Grishchuk et al., 2007), even though the exact mechanism is not understood.

Klp2 contains two MT-binding domains (Braun et al., 2009), is loaded onto MTs by Mal3 (Mana-Capelli et al., 2012) and has been well characterized as a MT slider in interphase (Janson et al., 2007). During mitosis, Klp2 localizes to kinetochores where it may facilitate chromosome capture by two mechanisms: 1. end-on pulling and 2. lateral sliding (Gachet et al., 2008). This and another study provide evidence that Klp2 may also increase the depolymerization rate at plus

tips of MTs (Grishchuk and McIntosh, 2006) similarly to *Sc*Kar3. During meiosis, it may cooperate with dynein to drive nuclear congression (Troxell et al., 2001).

Fission yeast contains another member of the kinesin-14 family, Pkl1. In contrast to Klp2, Pkl1 localizes to SPBs and inside the nucleus (Rodriguez et al., 2008) and it is implicated in spindle pole organization shown by electron microscopy (Grishchuk et al., 2007) and may regulate the γTuRC by disrupting the γTuSC (Olmsted et al., 2013).

All remaining kinesins exhibit a plus end-directed motility. The only essential kinesins is Cut7, a member of the kinesin-5 family and homologue to Eg5, which localizes to spindle poles and midzone and is required for bipolar spindle formation early in mitosis (Hagan and Yanagida, 1992, Fu et al., 2009). In contrast, the kinesin-6 Klp9 plays an important role during anaphase B by sliding antiparallel MTs facilitating the separation of the spindle poles (Fu et al., 2009).

Klp5 and Klp6, two members of the kinesin-8 family, function as heterodimers and localize to MTs in interphase and to kinetochores and spindle in mitosis (West et al., 2001, Garcia et al., 2002). Originally, deletion of those kinesins led to longer hyperstable MTs and chromosome segregation defects. Subsequent studies showed that Klp5/6 promote catastrophe in a length-dependent manner by accumulation of the kinesins at growing MTs (Tischer et al., 2009).

Another kinesin, kinesin-7 Tea2 also influences MT dynamics, but by suppressing catastrophe (Browning et al., 2003, Busch et al., 2004). Its deletion mimics the *tip1Δ* phenotype, and indeed Tea2 belongs to +TIPs and transports Tip1 along MTs towards the plus ends.

Finally, the function of the two remaining kinesins, kinesin-1 Klp3 and kinesin-3 Klp8 remains mysterious. Klp3/Krp1 is found along MTs and required for proper Golgi membrane distribution (Brazer et al., 2000) as well as during cytokinesis (Jeong et al., 2002) and polarized growth (Rhee et al., 2005). Klp8 has been found at the contractile acto-myosin ring, but its deletion does not cause any obvious cytokinetic defects (Moseley et al., 2009).

Future work will reveal how these motor proteins functions in these diverse processes. Moreover, it will be interesting to test how they cooperate to control specific cellular aspects.

3.6. Microscopy of mating fission yeast cells in microfluidic flow chambers

Under nitrogen starvation and presence of opposite mating types, fission yeast cells enter the meiotic cell cycle. In contrast to budding yeast, where initiation of mating is rather efficient, mating in fission yeast occurs only after long incubation periods in nitrogen poor medium with a random initiation time and at a low frequency. For long term live cell imaging, cells have to be maintained in liquid medium for many hours. We developed a protocol using the microfluidic technology to optimize mating efficiency and imaging quality of mating fission yeast cells.

We created microfabricated microfluidic flow chambers that were previously used to externally manipulate cell shape (Terenna et al., 2008). µm-scaled channels of desired dimensions are fabricated based on a combination of soft lithography and microfluidic technology (Figure 3.7). Briefly, the design for the chambers is laser-etched into a thin layer of chromium on a quartz plate, which serves as a photo-mask. Next, a negative photo-resist is spin-coated onto a silicon wafer. The features are then transferred from the photo-mask onto the photo-resist layer by exposure and cross-linking with UV light. The wafer can now be used as a master mold, on which repeated replication of molds can be made by casting from polydimethylsiloxane (PDMS). Finally, chambers are assembled by peeling off the PDMS replica from the mold, introducing inlet and outlet holes, and bonding the replica to a microscope glass cover slip after surface treatment using a plasma cleaner. For microscopy, cells of opposite mating types are starved for several hours and then syringe-pumped into the channels and incubated another several hours again before imaging (Figure 3.7).

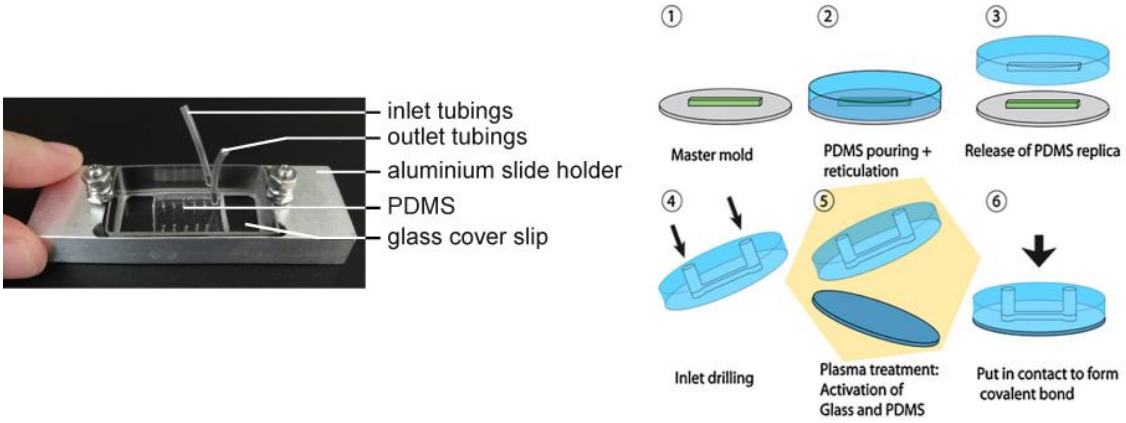

Figure 3.7. The microfluidic flow chamber.

Left, microfluidic channels for long-term imaging of mating cells. Right, fabrication procedure for a single layer microfluidic device. *(Velve-Casquillas et al., 2010)*

Introduction Part II –

A novel factor in cellular morphogenesis of fission yeast

4. Morphogenesis of eukaryotic cells

4.1. Cell polarity and cell shape

In the previous chapters, I have described in detail how cells move their nuclei away from the cell center resulting in an internal asymmetry within the cell. In fact, since the discovery of centrosomes, it has been proposed that the nucleus and the centrosome align along the front-back axis, which is especially conspicuous in different migrating cells (Luxton and Gundersen, 2011) (Figure 1.3). Here, the nucleus is positioned towards the rear, while the centrosome lies between the nucleus and the leading edge. On the one hand, this large organelle does not spatially interfere with the rapid processes happening at the migrating front, where actin is concentrated and moves the cell forward. It also ensures that centrosome-nucleated MTs dominantly extend towards the front directing the transport of vesicles to the leading edge. Therefore, the establishment of the nucleus-centrosome axis can be considered as a hallmark of cell polarity in migrating cells.

Cell polarity is defined by an asymmetric organization of cellular components and structures. It is established and maintained by the asymmetrical distribution of polarity cues and cytoskeletal rearrangement (Li and Gundersen, 2008).

Polarity can also determine the site and orientation of growth zones. Polarized growth essentially controls cell shape. Cell morphology appears critical for functions of specialized cells and the integrity of tissues. Some animal cells indeed adopt extreme shapes in order to be able to fulfill their assigned functions (Figure 4.1).

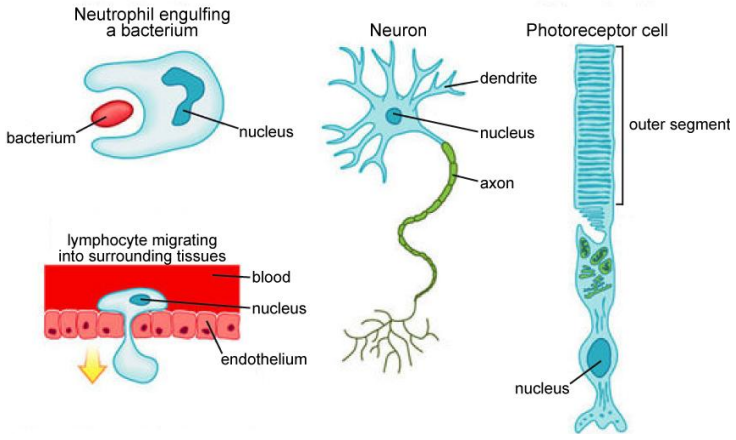

Figure 4.1. Diversity of cell shapes.

Animal cells can adopt many different shapes and sizes to carry out different functions in the body. *(source: http://www.sciencelearn.org.nz)*

For example, neurons constituting the core components of the CNS are characterized by a relative small soma with several long projections of two different types: dendrites to receive and the axon to propagate information (Alberts, 2008). Neurons serve as transmitters of electrochemical signals allowing the communication over long distances. In fact, photoreceptors as specialized neurons are able to detect light and transmit signals from the eye to the brain. Most peculiar feature is a long protrusion at one end formed from a highly modified cilium, the outer segment, which contains stacked membrane shelves, into which the light-absorbing molecule rhodopsin is embedded. While these cells are required to permanently maintain their morphology, others need to dynamically change their shape in order to migrate or squeeze through tight passages. Cells of the immune system such as the lymphocytes migrate through tissues in search of pathogens. Neutrophiles undergo changes in shape during phagocytosis of bacteria. Also, fibroblasts that secret collagen and help building the extracellular matrix migrate to damaged places in the tissue and support wound healing.

Simpler organisms like fungi have been used to study diverse aspects of polarized growth. In filamentous fungi or the rod-shaped fission yeast, cells grow by linear tip extension (Hayles and Nurse, 2001, Fischer et al., 2008). In contrast, budding yeast cells first grow isotropically, but break symmetry to select a site for bud emergence or during formation of a mating projection in response to pheromones (Arkowitz and Bassilana, 2011).

Although cell shapes are diverse, the core components of polarized growth and cellular morphogenesis are astonishingly similar from yeast to human (Nelson, 2003).

4.2. Key processes underlying polarized growth and cellular morphogenesis

Polarization of growth is induced by internal and external cues that generate cellular asymmetry. Changes in the cytoskeletal organization mediate asymmetric distribution of cellular components controlling cellular growth. Positive feedback signaling allows the maintenance of the polarized zones (Pruyne et al., 2004, St Johnston and Ahringer, 2010).

In many organisms, small GTPases play a major role in the control of most processes underlying growth, such as the dynamics and architecture of actin networks or secretion. The translocation of vesicles from or towards the membrane can be carried out along MTs or the actin cytoskeleton. The particular fast dynamics of assembly and disassembly of actin filaments

provide the force for membrane internalization, while, in particular, MTs have been implicated in the delivery of spatial cues for maintaining polarity.

4.2.1. RhoGTPases – inducers of polarized growth and regulators of the actin cytoskeleton

RhoGTPases are a conserved family of proteins that control diverse processes of cell polarity from yeast to human and, in particular, have been implicated in regulating the actin cytoskeleton (Heasman and Ridley, 2008, Perez and Rincon, 2010). They belong to the Ras superfamily of small G-proteins and can bind and hydrolyze GTP. RhoGTPases are effective growth regulators as they function as molecular switches, with an inactive GDP-bound and an active GTP-bound state, during which these proteins can interact with a wide range of effectors (Figure 4.2). They have an intrinsic GTPase activity that can be enhanced upon binding to a GTPase-activating protein (GAP), which therefore leads to the inactivation of the Rho protein. On the other hand, the exchange from GDP to GTP is stimulated by a guanine-nucleotide exchange factor (GEF). A third family of regulators is constituted by Rho guanine-nucleotide-dissociation inhibitors (RhoGDIs) that maintain the inactive state of Rho proteins by inhibiting the release of GDP and by extracting them from the membrane preventing their re-activation by GEFs. Finally, the spatial control of the activation status of RhoGTPases generates asymmetry required for polarized growth.

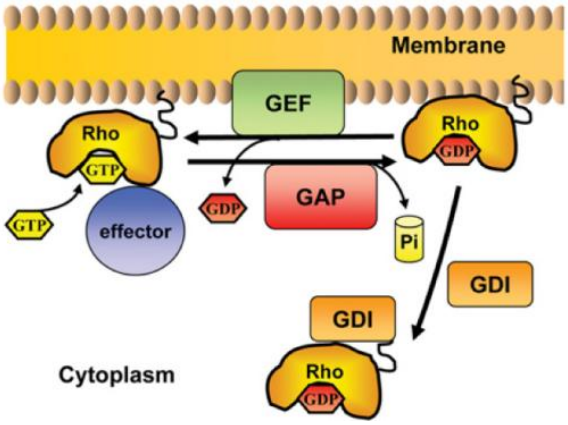

Figure 4.2. The RhoGTPase cycle.

Inactive RhoGTPases bound to GDP are activated upon exchange of GDP to GTP, which is promoted by GEFs. Hydrolysis of GTP to GDP is enhanced by GAPs and renders Rho proteins inactive. GDIs block release of GDP and extract Rho proteins from the membrane inhibiting re-activation. *(Perez and Rincon, 2010)*

To date 20 members of the Rho GTPases have been identified in mammals, while there are six of them in yeast. In particular, one member has been intensively studied, Cdc42, which, especially in yeast, appears to be key regulator of polarization and growth. It plays essential roles in epithelial and migratory polarity, as well as during the development of *C. elegans* and *Drosophila melanogaster*. To the actin-related downstream targets of Cdc42 belong formins to generate linear actin filaments for vesicle movement (Kuhn and Geyer, 2014), the actin-severing protein cofilin, which appears to play a role in axon growth (Chen et al., 2006), and the NPF WASp to stimulate Arp2/3-mediated assembly of a branched actin network for example required for internalization of endocytic vesicles (Ridley, 2006). Its mechanisms in promoting polarized growth has been fully explored in budding yeast, where Cdc42 accumulates at the presumptive bud site (Pruyne et al., 2004). Once activated by its GEF Cdc24, Cdc42 directly or indirectly leads to the activation of the formin Bni1 to stimulate actin cable assembly and the activation of type I myosins, stimulatorss of the Arp2/3 activity, to polarize actin patches as sites of endocytosis. Furthermore, it regulates the localization of the exocyst component Sec3 to the membrane mediating polarized secretion. The function of Cdc42 and other Rho proteins in fission yeast, subject of this study, will be explored in a later chapter.

It has been known for long time that the actin cytoskeleton is crucial for maintaining cell shape. In animal cells lacking a cell wall, a thin layer of cross-linked actin filaments beneath the plasma membrane provides structural stability and stiffness (Salbreux et al., 2012). Additionally, myosin-mediated contractility of this cortical actin network allows rapid shape changes.

One important role of actin during growth is the translocation of secretory vesicles towards the membrane. In organisms, like budding and fission yeast, actin cables constitute the only tracks to deliver exocytic vesicles to growth zones in a myosin-dependent manner. Actin cables are composed of polar linear bundles of parallel actin filaments that are nucleated from the growth site by formins (Mishra et al., 2014) (Figure 4.3). However, in larger cells, MTs usually perform the long-range transport carrying vesicles close to the periphery, where they then associate with the actin cytoskeleton to bring vesicles in close proximity with the plasma membrane, where exocytosis takes place (Porat-Shliom et al., 2013) (Figure 4.4).

Finally, also internalization of endocytic vesicles occurs dominantly in areas of growth. Here, a branched actin network forms around invaginations of the membrane, which are called actin patches in yeast (Figure 4.3).

In summary, the actin cytoskeleton regulated by RhoGTPases performs important functions during polarized growth, in particular exo- and endocytosis, two processes, which orchestrate the remodeling of the membrane.

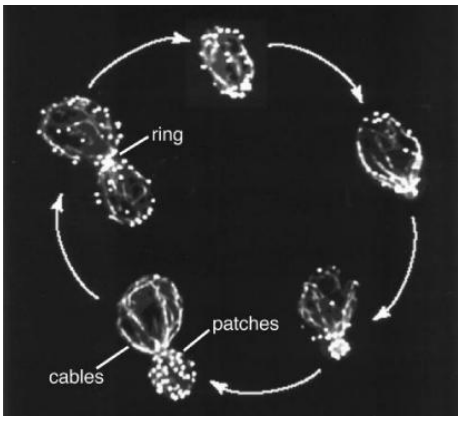

Figure 4.3. Organization of the budding yeast actin cytoskeleton during the cell cycle.

Budding yeast cells contain three different structures built by F-actin: cortical actin patches, polarized actin cables and a cytokinetic actin ring. *(Moseley and Goode, 2006)*

4.2.2. Exocytosis

Secretion controls the release of molecules into the extracellular space and results in the addition of new membrane material, which essentially leads to growth of the cell. By restricting secretion to specific sites, growth is polarized and takes place exclusively at these sites.

Polarized secretion relies on the directed transport of exocytic vesicles and their local tethering and fusion with the plasma membrane. As described above, the delivery is performed mainly along linear actin filaments that are nucleated in a polarized manner due to the activity of RhoGTPases.

The fusion of secretory vesicles with the plasma membrane (Figure 4.4) is catalyzed by SNARE (soluble N-ethylmaleimide-sensitive factor attachment receptor) proteins (Sudhof and Rothman, 2009) that are present in both membranes, of the vesicle and the target membrane. The

pairing of these SNARE proteins docks the vesicle to the membrane and eventually induces lipid fusion.

The initial interaction between vesicle and plasma membrane is mediated by the exocyst complex, an evolutionary conserved protein complex composed of eight subunits, which functions as a tether for exocytic vesicles (He and Guo, 2009 1543). In yeast, two components, Sec3 and Exo70 are localized to the cortex at the bud tip independently of actin cables, but are separately regulated by RhoGTPases, while the other components are associated with the exocytic vesicle and therefore rely on actin cables for their delivery. It is believed that, once a vesicle arrives, the exocyst complex is fully assembled and may now tether the vesicle to the plasma membrane. Interaction between subunits of the exocyst complex and SNAREs have been reported in yeast (Sivaram et al., 2005) and the brain (Hsu et al., 1996) and may facilitate the assembly of the SNARE complex.

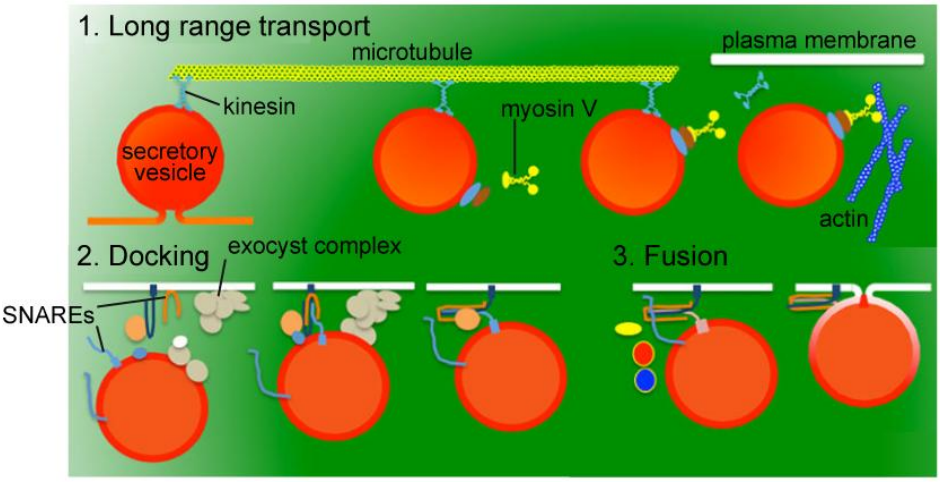

Figure 4.4. Steps in exocytosis.

Exocytic vesicles are translocated towards the cell periphery along MTs in a motor-dependent manner. At the cell periphery, vesicles are transferred onto actin filaments via myosins. In an initial step, vesicles are tethered to the membrane by the exocyst facilitating the formation of the SNARE complex, which finally induces membrane fusion. *(Adapted from (Porat-Shliom et al., 2013))*

4.2.3. Endocytosis

Endocytosis describes the process of internalization of extracellular material and membrane proteins by invagination of the plasma membrane eventually resulting in the formation

of endocytic vesicles, endosomes, that are designated for degradation as lysosomes or can be recycled back to the plasma membrane. Thereby, they control the recycling of receptor proteins and other membrane-bound proteins and lipids.

More recent work in yeast and filamentous fungi has revealed the importance of endocytosis to maintain polarized zones, which has been subsequently shown for other systems such as migrating or epithelial cells. In fact, cortical proteins, such as Cdc42, rapidly diffuse along or away from the plasma membrane, which, in theory, would counteract the stabilization of an asymmetric accumulation of polarity cues (Wedlich-Soldner et al., 2004, Li and Gundersen, 2008). It has been elegantly demonstrated that endocytosis maintains polarized localization patterns of membrane proteins by removing and recycling "escaped" molecules, like SNARE proteins (Valdez-Taubas and Pelham, 2003) and Cdc42 (Marco et al., 2007). The role of endocytosis in cell morphology has been also highlighted during the hyphal growth of *Aspergillus nidulans* that elongates by linear tip extension (Shaw et al., 2011). The hyphoid shape appears to be created by a balance between exo- and endocytic processes, whereby a subapical collar of endocytosis is able to preserve a zone of exocytosis at the growing apex, which in turn directs growth.

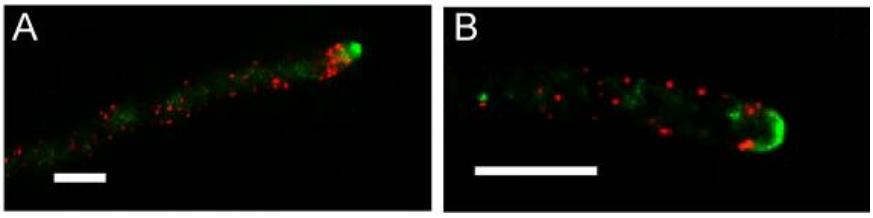

Figure 4.5. Spatial coupling between endocytosis and exocytosis in *Aspergillus nidulans*.

Images of a hyphal tip cell expressing ABPA-mRFP (actin-binding protein A) as a marker of actin patches forming a collar around the hypha behind the apex and GFP-SYNA (SNARE protein) as a marker of exocytic activity, which appears concentrated at the apex of the hypha. Represented as a maximum projection of a 3D stack (A) or as a single optical section (B). Bars, 5µm. *(Taheri-Talesh et al., 2008)*

One conserved type of an endocytic pathway is constituted by the Clathrin-mediated endocytosis (CME) that is found in yeast and mammals (Boettner et al., 2012). The complex process of CME is coordinated by a well orchestrated chain of events including the recruitment, activity and disassembly of approximately 60 proteins (Weinberg and Drubin, 2012). Most of our understanding has derived from tremendous work in budding yeast by identifying and characterizing many endocytic factors and their timely and spatial order of recruitment.

Additionally, findings in mammalian and *in vitro* systems have greatly helped to shed light on this evolutionarily conserved process. However, the role of actin in different systems still remains controversial, as studies in yeasts demonstrate an absolute requirement for actin, while in mammalian cells, actin polymerization supports invagination under normal conditions, but endocytosis still proceeds, even when actin dynamics are inhibited (Kaksonen et al., 2006).

An endocytic event is characterized by three distinct phases (Figure 4.6). At first, during the immobile phase, cortical actin patches at the plasma membrane are assembled into a clathrin-coated pit (CCP) by so-called endocytic coat factors. Typically during CME, clathrin forms a cage around the budding vesicle. Next, additional proteins including NPFs are recruited that promote Arp2/3-dependent actin polymerization during the second slow mobile phase. This actin burst drives the invagination of the membrane, and the tip of the newly forming endosome moves slowly cell inwards. Finally, membrane-deforming proteins arrive to prepare vesicle scission. Once released, the endocytic coat is disassembled, and now the vesicle migrates rapidly deep into the cell as observed during the third fast mobile phase.

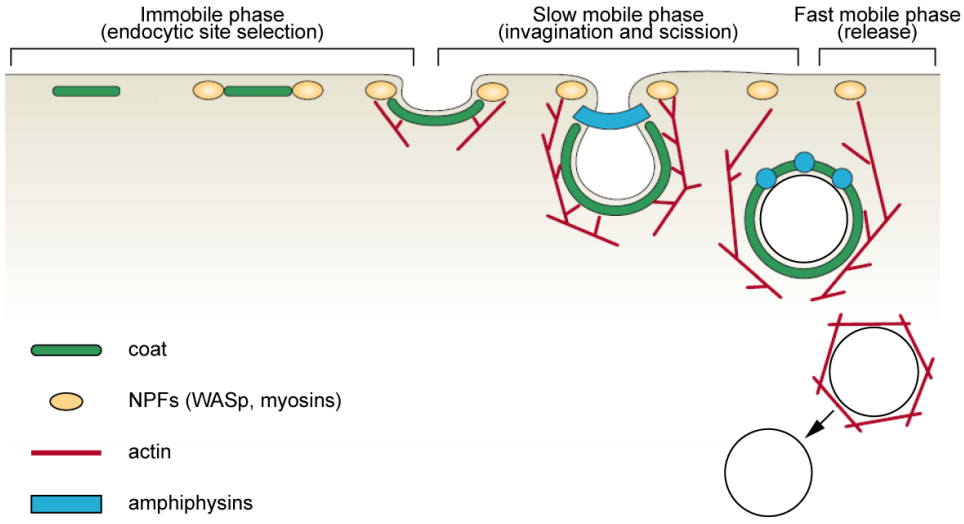

Figure 4.6. The endocytic pathway.

Early factors assembling the coat are recruited during the immobile phase. Arrival of the NPFs Las17/WASp and myosins stimulates Arp2/3-mediated actin polymerization driving membrane invagination during the slow mobile phase. The vesicle scission apparatus is formed at the narrowing neck to promote scission. After release, coat and actin are disassembled and the vesicle moves rapidly inwards. *(Adapted from (Kaksonen et al., 2006))*

During early stages of endocytosis, coat proteins accumulate at one specific place along the plasma membrane. It is still mysterious how exactly the recruitment of these early factors is initiated and how these sites are selected. Potentially, certain lipids, like PIP2s, may play a role here, but future work will be required to address this question. One of the first proteins to arrive, beside clathrin, are Ede1 (Eps15 in mammals) and the F-Bar protein Syp1 (FCHo1/2). Their roles are also not fully understood. While cells deleted for *syp1*, show a symmetrical distribution of actin patches, lack of Ede1 reduces the number of actin patches. Both appear important for effectively initiating endocytosis at the proper places, but there may be additional unknown factors that function in parallel in recruiting later components. Next, cargos start accumulating at these sites and further coat proteins arrive, among them Sla2 (Hip1) that binds PIP2s in the membrane via its ANTH (AP180 N-terminal homology) and actin via its THATCH (talin-HIP1/R/Sla2p actin-tethering C-terminal homology) domain.

The transition from the immobile to the slow mobile phase is marked by the recruitment and activity of NPFs such as Las17/WASp and myosins (*Sc*Myo3/5) that in turn strongly stimulate Arp2/3 activity resulting in an actin burst. The branched actin network around the CCPs is tethered to the membrane and promotes the invagination of the membrane forming an extended tubule with a clathrin-coated tip. Sla2 plays an essential role in maintaining the connection between the actin cytoskeleton and the membrane. Deletion of *sla2* does not prevent the assembly of the CCPs nor actin polymerization, but actin filaments are waving of the membrane as long "comet tails" unable to drive invagination (Kaksonen et al., 2003).

In yeast, final scission is achieved by the collaboration of N- and F-Bar proteins, like amhpiphysins that are capable of deforming the membrane and the actin network itself together with myosin motors concentrated at the base of the pits. Furthermore, scission may be also facilitated by a line tension generated by lipid phase separation. In metazoan, the GTPase dynamin plays a critical role in this process (Mettlen et al., 2009). Immediately, after scission the coat is dissembled and the actin network broken down by actin-severing proteins including cofilin.

4.2.4. Role of microtubules in cortical polarity

Despite their contribution to directed vesicle trafficking in larger cells, MTs also play a common role in the establishment or maintenance of the position of cortical polarity, but are not required for induction of polarity *per se* (Siegrist and Doe, 2007). In fact, MTs have been shown in different systems including fission yeast and migrating fibroblast, to deliver positional markers to polarized sites at the cortex and, by interaction with components of the actin cytoskeleton, to create positive feedback loops to reinforce these sites.

Most simple example illustrating this function for MTs is the rod-shaped fission yeast. Linear MT bundles running along the long axis of the cells and extending with their plus tips towards the cell tips carry a protein complex composed of Tea1/4 in a +TIP-dependent manner (Chang and Martin, 2009). Once at the cortex, the complex is anchored to the membrane, where it activates the formin For3 to promote actin cable assembly and cell growth (more details will be given in a later chapter). However, it remains elusive, whether MTs can interact with the actin cytoskeleton to generate positive feedback loops. Rather, the shape of cells may dictate the organization of MTs creating a feedback loop (Terenna et al., 2008, Minc et al., 2009b).

As described earlier, in migrating fibroblasts, the centrosome is positioned between the rearward nucleus and the leading edge (Luxton and Gundersen, 2011); hence MTs extend especially towards the leading edge. Similarly to fission yeast, MT plus tips carry a positional marker, IQGAP, to the front cortex, where this protein interacts with the small GTPase Rac1 leading to a local increase of active Rac1 levels. Active Rac1 stimulates cell migration and, in a positive feedback loop, inhibits MT destabilizing stathmin resulting in stabilization of MTs at this site. Additionally, MTs are used as tracks to deliver secretory vesicles, particularly to the front, to promote cell migration.

Finally, also neuronal growth requires MTs to position the site of growth within the growth cone, the structure guiding the extension of the neuron (Siegrist and Doe, 2007). It has been shown that loss of MTs does not block growth cone extension, but rather leads to a "wandering" of the growth cone.

In summary, the mechanisms and core components utilized by cells to create diverse shapes are conserved, but their interactions and regulations may vary between systems. The

generation of cell shape through integration of all components will be illustrated on the basis of the rod-shaped cells of fission yeast in the next chapter.

4.3. Cellular morphogenesis of fission yeast cells

4.3.1. Fission yeast as a model system for morphogenesis

The unicellular fission yeast *Schizosaccharomyces pombe* has proven to be a powerful tool to study different aspects of cellular morphogenesis. It forms cells of highly reproducible shape and size surrounded by a cell wall. Fission yeast cells are rod-shaped, of about 4µm in diameter and 7-14µm in length. They grow by linear tip extension through polarization of growth at the tips and divide medially to produce two daughter cells of equal length. Growth is spatially and temporally coordinated with the cell cycle (Mitchison and Nurse, 1985) (Figure 4.7). Immediately after cell division, cells start growing in a monopolar fashion, that is, from only one end, the "old" end, inherited from the previous cell cycle. Then, at a specific time point during G2 in a process called NETO (New End Take Off), cells also initiate growth at the second "new" end and extend in a bipolar manner. During mitosis, growth is arrested at the cell tips and the growth machinery is re-directed towards the cell division site to drive cytokinesis and cell separation. Upon completion of cell division, growth is once again initiated at the "old" ends of the daughter cells.

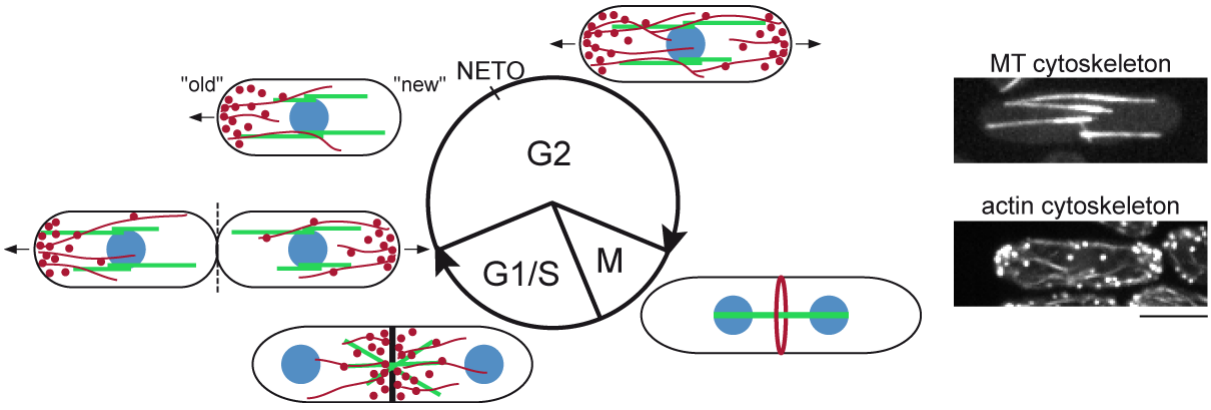

Figure 4.7. Cytoskeletal organization during the cell cycle.

Active sites of growth are marked by actin cables and actin patches (dark red). MTs (green) are arranged into a linear array. During division, the growth machinery is directed to the cell division site. Microscopic images show cells

expressing MT marker GFP-Atb2 or actin marker GFP-CHD. *(Adapted from (Chang and Martin, 2009), images from my own studies)*

The two cytoskeletons, actin and MTs, play distinct roles in fission yeast morphogenesis. During interphase, actin is found in two different structures located at growing cell tips – actin cables and actin patches (Kovar et al., 2011) (Figure 4.7). The actin patches represent endocytic activity, while long actin cables deliver secretory vesicles to the growing tips, where new cell membranes are added and new cell wall material is synthesized. Furthermore, the exocyst complex is located here in an actin cable-independent manner to ensure polarized secretion. During mitosis, actin is arranged into a medial contractile ring responsible for cytokinesis. Simultaneously with ring constriction, the septum, an ingressing cell wall-based structure facilitating cytokinesis, is formed through endo- and exocytic processes re-directed to the medial division plane (Sipiczki, 2007). Finally, the septum is partially dissolved and the two daughter cells are separated. As proteins regulating growth are often involved in septum formation, many shape mutants also display defects in cytokinesis.

On the other hand, MTs are organized into 3-4 bundles of antiparallel MTs oriented along the long axis of the cell (Sawin and Tran, 2006) (Figure 4.7). MT minus ends are anchored to the NE via iMTOCs and their plus ends extend to the cell tips. Once MTs reach the cortex, they maintain contact for 1-2 minutes before catastrophe is initiated, preferentially at the distal ends. MTs are not essential for polarized growth *per se*, but define the position of growth zones by delivering spatial cues. These markers also serve as a memory for "arrested" growth sites to allow re-initiation of growth later on these sites again.

An additional little explored factor of cellular morphogenesis in fission yeast and other organisms is the contribution of membrane domains that may provide a specific docking platform for polarization and growth markers independent of the actin and MT cytoskeleton (Wachtler and Balasubramanian, 2006). Here, lipids of different types are spatially separated within the membrane forming "lipid rafts" (reviewed in (Sonnino and Prinetti, 2013)). However, in fission yeast their exact contribution remains elusive. Staining with the sterol dye filipin reveals that sterols are indeed organized into large domain coinciding with growth zones (Wachtler et al., 2003). Their role in directing growth is not clear. Other lipids, in particular PIP2s that are highly abundant in most biological membranes, impact on the localization, for example, of the exocyst complex (Bendezu et al., 2012).

As wildtype *S.* pombe cells are highly reproducible in shape and size, mutants of altered morphology were identified and characterized in the past (Verde et al., 1995, Chang and Martin, 2009). In fact, it has become apparent that defects in different components of the growth and polarization machinery lead to distinct characteristic shape changes (Figure 4.8).

Major regulator of polarized growth is the RhoGTPase Cdc42. Without Cdc42 activity or aberrant spatial regulation of Cdc42, cells grow isotropically and become roundish due to a loss of polarity. On the other hand, mutants affecting actin-based structures usually partially fail to polarize growth at the cell tips, resulting in plump cells. In contrast, interfering with MT-related functions leads to the loss of a straight axis, resulting in bent or T-shaped cells.

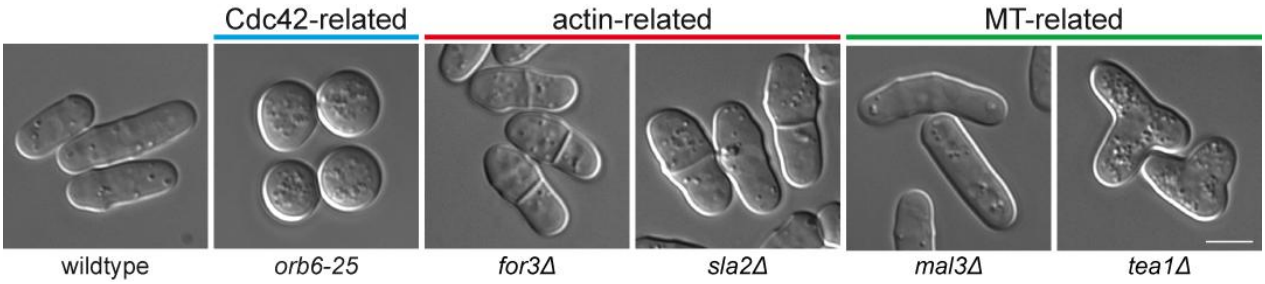

Figure 4.8. Shape mutants.

Wildtype forms rod-shaped straight cells. Cdc42-related defects result in roundish cells, in contrast to plump partially unpolarized actin-related mutants and bent or T-shaped mutants of MTs or the Tea1 pathway. *(Images from my own studies)*

4.3.2. Cell wall and turgor pressure

One characteristic feature of fungal cells is the cell wall that surrounds the plasma membrane. It forms a thick highly impermeable layer of carbohydrates and glycoproteins and serves as a protective barrier against a wide range of environmental conditions (Ishiguro, 1998). The cell wall also constitutes a rigid layer with high mechanical strength hindering cellular growth. More recent work has demonstrated that high turgor pressure in the cells may be the primary force to drive cell extension (Minc et al., 2009a). However, as turgor pressure exerts outward forces in all directions, cells must spatially restrict cell wall elasticity to the cell tips. Therefore, incorporation of new material by secretion of cell wall biosynthetic enzymes is limited

to the cell tips. Coordination of synthesis and degradation of cell wall by Rho proteins are essential to ensure cell integrity and to prevent cell lysis (Perez and Rincon, 2010).

The major component of the fission yeast cell wall is the β(1,3)-glucan that is synthesized by the β(1,3)-glucansynthase (Bgs), an enzymatic protein complex composed of a regulatory and a catalytic subunit (Ishiguro, 1998). In fission yeast, the GTPase Rho1 is the regulatory subunit, which can associate with four different catalytic subunits called Bgs1-4. Bgs2 is only expressed during meiosis, while the other three have distinct roles during the vegetative cell cycle. In particular, Bgs1 and Bgs4 appear to be essential to maintain cell integrity during polarized growth (Garcia et al., 2006).

During cytokinesis, glucansynthases build the septum that is composed of an inner primary septum and the two flanking secondary septa (Sipiczki, 2007). Later will be part of the cell wall of the newly formed daughters, but the primary septum is dissolved by glucanases to allow physical cell separation.

The importance of the turgor pressure in growth has been recently shown. When lowering the internal turgor pressure, but not when disrupting actin cables, forces pushing the cell wall outwards were significantly decreased demonstrating that tip extension was dominantly achieved by outward forces generated by the high intracellular pressure (Minc et al., 2009a). But these forces oppose other cellular processes such as cytokinesis (Proctor et al., 2012) and endocytosis (Basu et al., 2014). Therefore, septum assembly and actin polymerization around newly forming vesicles, respectively, may provide additional forces to drive these processes in fungal cells.

4.3.3. Cdc42 and other Rho proteins in fission yeast polarized growth

The small GTPase Cdc42 constitutes the core of the polarization machinery in fission yeast (Figure 4.9). The spatial regulation of Cdc42 activity is achieved by its two GEFs Scd1 and Gef1 and its GAP Rga4 (Perez and Rincon, 2010). Scd1 and Gef1 have partially overlapping and distinct functions, whereby Scd1 is mainly required for polarized growth and Gef1 also for the polarity switch during NETO. Both proteins are located at the cell tips and are regulated, in the case of Scd1, by the small GTPase Ras1 and, in the case of Gef1, by the NDR kinase Orb6 (Das et al., 2009) and the Bar protein Hob3 (Coll et al., 2007). In fact, Orb6 constitutes the most downstream effector of a signaling network called MOR (morphogenesis Orb6 network) spatially

regulating Cdc42 (Gupta and McCollum, 2011). In contrast, the GAP Rga4 localizes along the cell sides and is excluded from the cell tips to prevent Cdc42 activity at the cell sides. Its deletion results in broader cells (Das et al., 2007).

One major function of Cdc42 is to activate and recruit the formin For3 and stimulate actin cable assembly (Martin et al., 2007). Usually, For3 exists in an auto-inhibited state by intramolecular interaction. Cdc42 together with the polarisome component Bud6 relieves auto-inhibition. Additionally, the interaction between Cdc42 and For3 may be helped by the essential protein Pob1 (Rincon et al., 2009).

In addition, Cdc42 impacts on polarized secretion by controlling the recruitment of the exocyst complex to the cell tips (Bendezu and Martin, 2011, Estravis et al., 2011). In detail, it is required to localize the exocyst subunit Sec3 in a PIP2-dependent manner and potentially also Exo70 (Bendezu et al., 2012). Thereby, Cdc42 may function in parallel to Rho3 (Rincon et al., 2009, Estravis et al., 2011, Nakano et al., 2011).

Another downstream effector of Cdc42 includes the kinase Orb2/Shk1 (Ottilie et al., 1995). Their interaction is bridged by the scaffold protein Scd2. Even though not fully understood, it appears that Orb2 is involved in endocytosis by regulating the activity of the myosin Myo1 (Attanapola et al., 2009). Therefore, Cdc42 might be also linked to endocytic uptake. A newly proposed role for Cdc42 is endosomal recycling, as altered Cdc42 activity appears to reduce levels of certain but not all Bgs proteins (Estravis et al., 2011, Estravis et al., 2012).

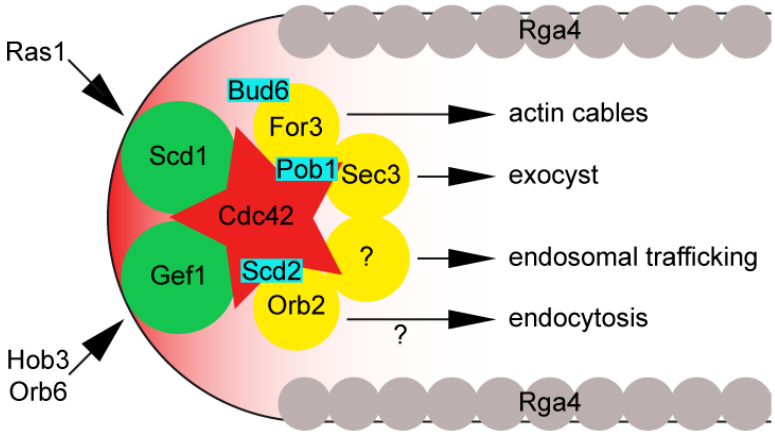

Figure 4.9. Regulators and effectors of Cdc42 in fission yeast.

Active, GTP-bound Cdc42 (red) concentrates at growing cell tips. Its localization and activity are regulated by its GEFs (green) and by its GAP (grey). Depicted are Cdc42 effectors (yellow) and collaborators (blue). *(Adapted from (Rincon et al., 2014))*

In summary, Cdc42 coordinates multiple events of polarized growth at the cell tips. There are still many open questions concerning its own regulation and the role of its downstream effectors. An additional layer of complexity comes from the fact that Cdc42 displays an oscillatory behavior between the cell tips. Features and possible roles of these Cdc42 oscillations will be discussed later.

Besides Cdc42, there are five other RhoGTPases, Rho1-5. Rho1 as the regulatory subunit of the Bgs enzyme and Rho2 control cell integrity (Perez and Rincon, 2010). Rho5 may function similarly to Rho1, but is not essential (Rincon et al., 2006). Rho3 and Rho4 are implicated in secretion, whereby Rho4 appears exclusively required for cytokinesis, while Rho3 also for polarized growth.

4.3.4. Polarized secretion and endocytosis in fission yeast

Polarized secretion is achieved by two independent pathways – the actin-based delivery of secretory vesicles and the PIP2-dependent asymmetric localization of the exocyst complex (Bendezu and Martin, 2011) (Figure 4.10). Disruption of the transport along actin cables or interfering with the exocyst function alone does not abolish polarized growth as mutants of either pathway maintain at least a certain degree of polarized secretion. However, when both pathways are affected, cells start growing isotropically.

Actin cables composed of short parallel actin filaments are nucleated by the formin For3 that in turn is activated and recruited by Cdc42 and Bud6 (Feierbach and Chang, 2001, Martin et al., 2007). Translocation along actin cables is mediated by the myosin V Myo52 (Motegi et al., 2001, Win et al., 2001).

The localization of the exocyst complex also relies on Cdc42 and PIP2s but is largely independent of actin cables (Bendezu and Martin, 2011). Mutants of the exocyst complex were identified by their strong defects in cytokinesis (Wang et al., 2002). Similarly to budding yeast, Sec3 and Exo70 are recruited to the plasma membrane, while other subunits are loaded onto

vesicles and transported along actin cables (He and Guo, 2009). Exo70 and the recently identified Sec3 are proposed to function in parallel but may be partially redundant to achieve proper localization of the exocyst complex (Bendezu et al., 2012). In contrast to budding yeast, all components including Sec3 and Exo70 may be assembled at vesicles before arriving at the plasma membrane under wildtype conditions. Finally, the GTPase Rho3 also displays secretion defects and may be required for exocyst regulation independently of Cdc42 (Estravis et al., 2011).

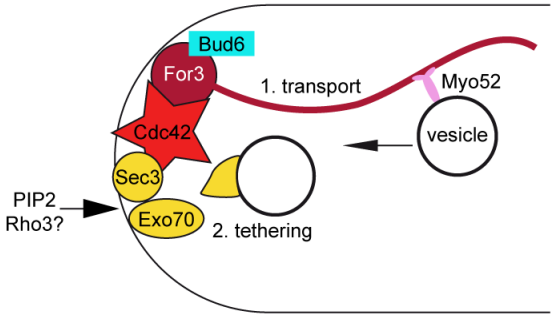

Figure 4.10. Polarized secretion in fission yeast.

Actin cables nucleated by For3 and asymmetric localization of the exocyst complex constitute two independent pathways regulating cell shape in fission yeast.

Actin patches representing endocytic activity dominantly assemble at growing tips in interphase cells (Gachet and Hyams, 2005) suggesting that endocytosis may participate in polarized growth in fission yeast. Cells lacking the early endocytic factor Sla2 required for efficient internalization display an aberrant morphology with shorter and fatter cells (Iwaki et al., 2004, Castagnetti et al., 2005). However, how this process impacts on fission yeast morphogenesis has not been investigated. One could suggest that it may serve a similar purpose, like in budding yeast or *Aspergillus*, to uptake diffused membrane proteins to maintain a polarized zone and to recycle proteins and lipids.

To date, not many cargos, besides Bgs1 (Estravis et al., 2012) and the SNARE Syb1, (Basu and Chang, 2011) have been identified in fission yeast, but may include receptors, transporters and SNAREs. Like in budding yeast, Arp2/3 complex-mediated actin polymerization is required for internalization, probably to overcome the high turgor pressure (Basu et al., 2014). Homologues of virtually all actin patch components from budding yeast are present in fission yeast and assemble into patches with a similar timing (Sirotkin et al., 2010). After recruitment of

early coat proteins including clathrin to promote initial membrane invagination, other later coat proteins, or adaptors, arrive. Among them Sla2, whose localization to actin patches is independent of actin, but may bind to actin via its THATCH-like domain (Castagnetti et al., 2005). Next, NPFs, in particular Pan1, Wsp1 (WASp) and Myo1 (myosin I) are recruited and stimulate Arp2/3 activity resulting in an actin burst (Lee et al., 2000). They share overlapping functions, but all three proteins are required for full activity of Arp2/3, as endocytosis in respective single mutants is blocked (Attanapola et al., 2009, Basu and Chang, 2011). For scission, several F-Bar proteins accumulate at the neck to drive membrane deformation. Interestingly, two F-Bar proteins, Cdc15 and Bzz1, simultaneously impact on Myo1 and Wsp1 activity that remain at the base of the invaginating tubule and might contribute to membrane scission through actin polymerization (Arasada and Pollard, 2011). Upon internalization, the branched actin network rapidly disassembles probably through actin-severing cofilin (Kovar et al., 2011). Released vesicles have been observed to move undirected or directed along actin cables cell inwards (Pelham and Chang, 2001).

4.3.5. Positioning of growth zones by microtubules in fission yeast

MTs contribute to cell shape by defining the position of growth zones at the distal ends of cell tips. Here, the arrangement of MTs into linear arrays and proper plus end dynamics are crucial (further details given in 3.3). Mutant cells of the MT cytoskeleton still grow in a polarized manner but at aberrant positions resulting in bent or T-shapes (Chang and Martin, 2009). In particular, MTs are important to re-initiate growth at arrested growth sites, for example during NETO or after recovery from starvation (Sawin and Snaith, 2004) suggesting that MTs maintain a memory of previous growth zones. To date, we know that MTs carry spatial cues, the so-called Tea1/Tea4 complex, at their growing plus ends to the cell tips (Chang and Martin, 2009) (Figure 4.11). This transport is dependent on Mal3 (EB1), Tip1 (CLIP170) and the kinesin Tea2 (Browning et al., 2000, Brunner and Nurse, 2000, Browning et al., 2003, Busch et al., 2004). Once MT ends reach the cortex, the complex is released and anchored to the plasma membrane via the prenylated membrane protein Mod5 (Snaith et al., 2005) and via Tea3 during NETO (Arellano et al., 2002), whereby the role of Tea3 remains rather mysterious. Interestingly, accumulation of the membrane anchors at the cell tips is promoted by Tea1 in a positive feedback

loop. At the cortex, Tea4 interacts with For3 to mediate its recruitment (Martin et al., 2005). Furthermore, Bud6 may also interact with Tea1 and Tea4 in a large complex called polarisome and helps stimulating For3 activity (Feierbach et al., 2004).

Mutants displaying defects in MT organization, like *mal3Δ* cells with short MTs that do not reach cell ends (Beinhauer et al., 1997, Busch and Brunner, 2004) or *mto1Δ* cells with a reduced number of cytoplasmic MTs (Sawin et al., 2004), are bent as Tea1 is asymmetrically deposited or is dispersed along the cortex (Brunner and Nurse, 2000, Janson et al., 2005). The loss of Tea1 or Tea4 leads to similar morphological changes to MT mutants (Mata and Nurse, 1997) (Martin et al., 2005). Furthermore, these mutants are often NETO-defective and grow exclusively only from one tip indicating that these factors are involved in the transition from mono- to bipolar growth, probably by recruiting For3 and initiating actin cable assembly at the non-growing pole. However, how this process is coordinated is still not clear and may involve a complex network of many factors such as already known and novel growth promoting factors and kinases (Koyano et al., 2010).

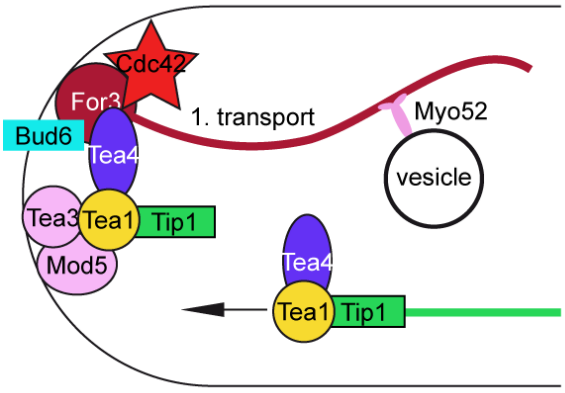

Figure 4.11. The MT-Tea1 polarity pathway.

The Tea1-Tea4 complex is transported to cell tips at the growing plus ends of MTs. Tea3 and Mod5 anchor Tea1, and Tea4 recruits For3 for actin cable assembly. *(Adapted from (Chang and Martin, 2009))*

4.3.6. Control of cell shape by external manipulation

In many systems, MTs help determining the position of a polarity site that has been induced by Rho proteins and the actin cytoskeleton. Often, positive feedback loops are generated between the MTs and actin-related factors. Migrating fibroblasts display a typical example of

such a feedback loop (see section 4.2.4), where MTs extending to the leading front deposit IQGAP and GEFs to locally increase Rac1 activity levels stimulating actin polymerization and inhibiting stathmin activity, which leads to a stabilization of MTs in this region (Siegrist and Doe, 2007).

Such feedback mechanisms involving communication between the actin and MT cytoskeleton have not been identified in fission yeast, but might exist. However, the cell shape itself may dictate the organization of the MT cytoskeleton to ensure delivery of the Tea1-Tea4 complex to the cell tip and thereby reinforcing the linear rod shape. When round unpolarized mutant *orb6*^{ts} cells with a disorganized MT cytoskeleton and dispersed localization of polarity factors were forced to adopt wildtype morphology by pushing them into straight channels, MTs aligned with the long axis of the cell and polarity factors such as Tea1 and actin accumulated at the cell tips (Terenna et al., 2008) (Figure 4.12A).

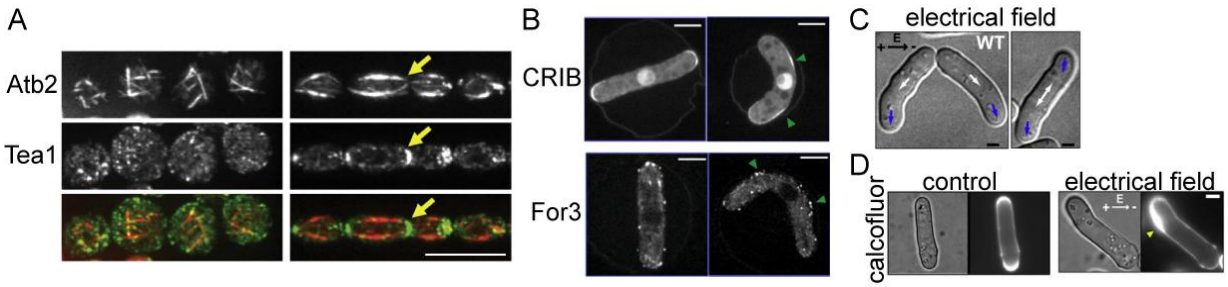

Figure 4.12. External manipulation of cell shape.

(A) orb6^{ts} cells expressing mCherry-Atb2 (MTs) and Tea1-GFP are forced to adopt a linear rod shape in microfluidic channels thereby re-establishing polarity and MT organization *(Terenna et al., 2008)*. Bar, 10µm. (B) Localization of active Cdc42 (CRIB-GFP) and For3 along cell sides, when cells are forces into bent channels *(Minc et al., 2009b)*. Bar, 5µm. (C) Growth is redirected orthogonally to an electrical field resulting in a bent or "kinked" shape. (D) Cell wall staining with calcofluor reveals an anodal accumulation of cell wall material *(Minc and Chang, 2010)*.

Additionally, using microfluidic technology to manipulate cell shape, a similar study revealed a novel yet uncharacterized MT-based polarization pathway independent of Tea1. Originally straight cells were forced into a bent configuration and MTs were unable to reach the cell ends but instead contacted the cell sides resulting in the accumulation of polarity factors, like Bud6, For3 and Cdc42, at ectopic sites along the cell sides (Minc et al., 2009b) (Figure 4.12B). However, deletion of *tea1* did not abolish the ectopic recruitment of these proteins; instead it was dependent on Mal3 and Moe1, which has been shown to interact with Mal3 and Scd1 (Chen et

al., 1999, Chen et al., 2000) suggesting that Moe1 at the cortex may recruit Scd1, which in turn will increase local Cdc42 activity levels at these sites. Even though the contribution of this pathway to wildtype morphogenesis is not clear, one could imagine that it may be used in the absence of Tea1 promoting growth at the cell sides leading to the bent *tea1Δ* cell shape (Chang and Martin, 2009).

Also electrical signals in form of an exogenous electrical field influence cell shape and result in the reorientation of tip growth orthogonally to the field (Minc and Chang, 2010) (Figure 4.12C). Cells in an electrical field adopt a bent or rather "kinked" morphology. This study identified the ATPase Pma1, an integral membrane protein that functions as a proton pump and regulates the intracellular pH, to be important for this behavior. Cells with inhibited Pma1 activity still responded to the electrical field, but directed growth in the opposite direction. Pma1 localizes along cell sides and creates a pH gradient with more acidic growing tips. This gradient may impact on growth factors such as For3 and Cdc42 during normal growth. An electrical field may alter the local proton influx and thereby influence cell shape. Additional, this study showed that some cell tip proteins migrated within the plasma membrane, when an electrical field was applied. In particular, cell wall synthesizing Bgs proteins that contain a large negatively charged extracellular domain accumulated aberrantly at one side of the cell pole independently of Cdc42 or For3, which probably promotes the reorientation of growth (Figure 4.12D). That suggests that external manipulation of the morphology can cause uncoupling of pathways controlling cell shape and may help us to widen our understanding of the processes linked to cell morphogenesis.

4.3.7. Oscillatory dynamics of Cdc42 in fission yeast

Oscillations of Cdc42 were first observed in budding yeast. Here, Cdc42 clusters competing for Cdc42 travel in waves along the cortex prior to symmetry breaking and eventually stabilize into a single cluster due to a positive "winner-takes-it-all" feedback mechanism (reviewed in (Arkowitz and Bassilana, 2011)). Also, negative feedback loops must be operating to inactivate or disperse Cdc42, which is proposed to improve the robustness of symmetry breaking (Howell et al., 2012).

In contrast to budding yeast, fission yeast polarizes growth at two sites concurrently. Recently, active Cdc42 (labeled by CRIB-GFP) was shown to oscillate between the two poles in

an anti-correlated manner with a regular periodicity of about 5 minutes (Das et al., 2012) (Figure 4.13). These oscillations were symmetric in bipolar cells, that is, levels of Cdc42 at each pole were similar, and asymmetric in monopolar cells, where the growing tip exhibited higher amounts of Cdc42. Based upon a mathematical model, Cdc42 oscillations are predicted to be achieved, first, by an accumulation of Cdc42 at one pole via positive feedback and then by the removal of Cdc42 due delayed negative feedback mechanisms. Furthermore, anti-correlated oscillations indicate that the two cell tips compete for Cdc42 suggesting the existence of regulatory factors limiting the amount of "available" Cdc42. Positive feedback mechanisms have been well characterized in budding yeast and include the scaffold protein Bem1, the GEF Cdc24 and a PAK kinase (Arkowitz and Bassilana, 2011). Bem1 controls localization of Cdc42 and its GEF to cortical sites, which impacts positively on activity and localization of the PAK kinase. PAK kinase and Bem1 interact and more Cdc24 is recruited, thus promoting further local activation of Cdc42. Fission yeast counterparts, Cdc42, GEF Scd1, scaffold Scd2 and PAK kinase Orb2, also interact with each other suggesting a similar mechanism underlying Cdc42 accumulation at one tip. However, the nature of the negative feedback loop remains elusive in both systems. Based upon the observation that reduced Orb2 activity leads to asymmetric Cdc42 oscillations, Orb2 is also proposed to be involved in negative feedback signaling (Das et al., 2012). It may do so by phosphorylating itself or the scaffold protein Scd2 leading to a decrease in active Cdc42. Alternatively, negative regulators such as GAPs might exist, but deletion of *rga4*, the only known Cdc42 GAP in fission yeast, does not affect Cdc42 oscillations.

Besides the lack of understanding of the mechanisms controlling periodic oscillation, it is also not clear how this behavior impacts on Cdc42 function. One model predicts that it may be the driving force during transition from mono- to bipolar growth at NETO, which is characterized by a switch from asymmetric to symmetric oscillations (Das and Verde, 2013) (Figure 4.13). In small cells, Cdc42 regulatory factors such as GEFs are limited so that, when proteins involved accumulate at the growing tip, the cytoplasmic pool is rapidly depleted. Cell expansion may coincide with production of GEFs and promote symmetric oscillations. A second proposed function for Cdc42 oscillations may be the more accurate control over the cell diameter. This idea is supported by the fact that increase of Gef1 leading to a partial stabilization of Cdc42 by dampening the periodic falls resulted in a wider diameter (Das and Verde, 2013). Thus, periodically recruiting and removing Cdc42 may prevent a broadening of growth zones.

In general, oscillations of biological systems are believed to provide flexibility to adapt to changing intracellular conditions such as cell expansion. Whether the oscillatory dynamics of Cdc42 are indeed required for its function remains to be addressed in the future. For instance, the bacterial Min system contributes to the position of the cytokinetic Z-ring by preventing its formation away from the cell middle (reviewed in (Lutkenhaus, 2007)). However, while this system oscillates in some, it does not do so in all bacteria suggesting that oscillations are not necessarily required for function of these proteins.

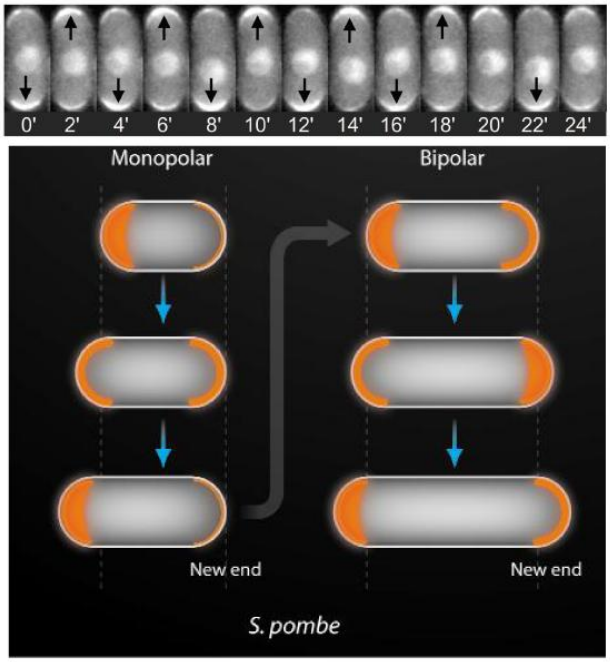

Figure 4.13. Cdc42 oscillations in fission yeast.

Top, oscillation of active Cdc42 (CRIB-GFP) at cell tips in a bipolar cell at 2min intervals. Bottom, switch from asymmetric to symmetric oscillation during NETO. Blue arrows indicate cell growth. *(Das et al., 2012, Bendezu and Martin, 2012)*

Finally, Cdc42 also shows a dynamic "wandering" along the cortex in response to mating hormones (Bendezu and Martin, 2013). Upon increase of pheromone levels, Cdc42 is stabilized into a single spot and directs exocytosis and polarized growth. Therefore, Cdc42 exploration during mating may facilitate reorientation of growth towards a pheromone gradient emanating from a mating partner.

5. The AAA$^+$-ATPase protein family

5.1. Diverse functions of AAA$^+$-ATPases

ATPases, and in more general NTPases, are very important in all pro- and eukaryotic cells (Ogura and Wilkinson, 2001). They use chemical energy in form of nucleoside triphosphate (NTP) to perform biological functions. The most common type of NTPases are the Walker-type NTPases, which are characterized by two conserved motifs required for NTP binding and hydrolysis, the Walker A (or P-loop) and the Walker B motif.

AAA$^+$ proteins (ATPases associated with diverse cellular activities) constitute a subgroup of Walker-type NTPases. Members of this protein family contain a 200-250aa long AAA$^+$ domain. The AAA$^+$ family includes the classical AAA proteins containing an additional feature, the SRH (second region of homology) motif, but newer members lacking this region have been added based upon structural similarities to classical AAA ATPases (Neuwald et al., 1999).

AAA$^+$ ATPases are involved in diverse cellular processes including membrane fusion and trafficking, proteolysis and DNA replication (Figure 5.1). Many AAA$^+$ proteins serve as chaperones or perform chaperone-like functions, whereby they assist in the non-covalent association of proteins, for example between proteases and proteins designated for degradation. Chaperones bind to misfolded and mistranslated proteins, induce their unfolding, and subsequently feed these proteins into the degradation machinery. Indeed, AAA$^+$ proteins have been identified as a regulatory subunit of the 26s proteasome.

During membrane fusion events, AAA$^+$ proteins associate with SNARE complexes to mediate their dissociation after fusion has been completed. This allows the recycling of SNARE proteins and facilitates the next round of membrane fusion. This function is carried out by Sec18/NSF at the plasma membrane during vesicle secretion and by Cdc48/p97 during organelle membrane fusion events within the cell to reconstitute the ER and the Golgi apparatus.

Furthermore, AAA$^+$ ATPases are also involved in peroxisome biogenesis and DNA replication. Moreover, the motor protein dynein belongs to this protein family and carries six AAA domains within a single polypeptide chain.

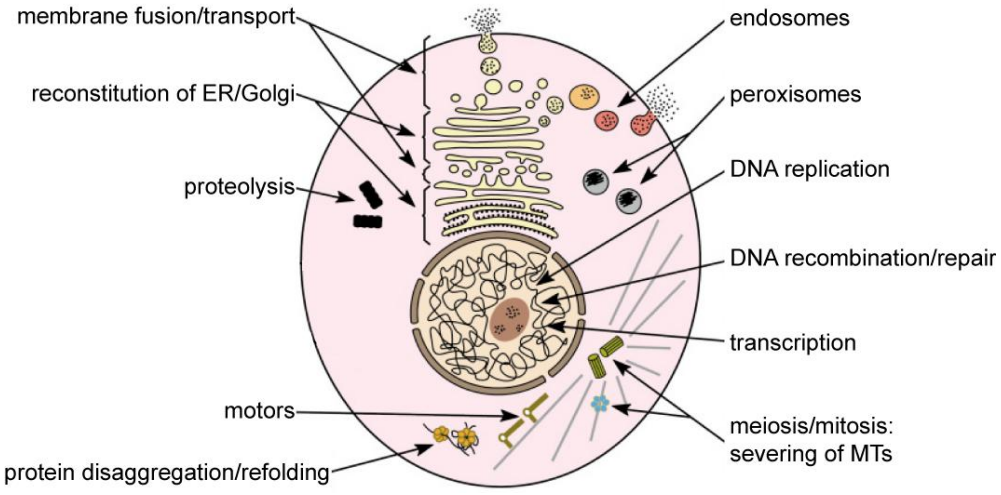

Figure 5.1. Diverse functions of AAA$^+$ ATPases.

Schematic of a eukaryotic cell. Biological processes, in which AAA$^+$ ATPases are involved, are depicted. *(Adapted from (Ogura and Wilkinson, 2001))*

A special group of AAA$^+$ ATPases is constituted by the MT-severing enzymes katanin, spastin and fidgetin that generate internal breaks in the MT leading to catastrophic breakdown of the polymer (Roll-Mecak and McNally, 2010) (Figure 5.2). These proteins associate with MTs via their MIT (microtubule interacting and trafficking) domain and pull on the C-terminal tails of tubulins sticking out of the lattice partially unfolding tubulin units or destabilizing lateral contacts between tubulin units. First reports on MT-severing derived from *C. elegans*, where katanin-mediated MT-severing is required for formation of a bipolar meiotic spindle. In plants, the cortical parallel MT array responsible for cellulose deposition and thereby cell shape is generated by katanin that releases newly nucleated MTs at branch points and allows their arrangement into a parallel array. Finally, work in *Drosophila* and *Chlamydomonas* established the importance of these proteins in mitosis and cilia biogenesis.

Another member of this subgroup is VPS4, which, in contrast, does not sever MTs but is involved in the disassembly of the ESCRTIII complexes that regulate membrane deformation and fission events. Interestingly, Vps4 uses its MIT domain to interact with components of this complex, but not with MTs. Together, Vps4 and ESCRTIII drive the formation of vesicles packed with TM proteins in the lumen of endosomes. These endosomes fuse with lysosomes and release the internal vesicles into the hydrolytic lumen, where degradation takes place.

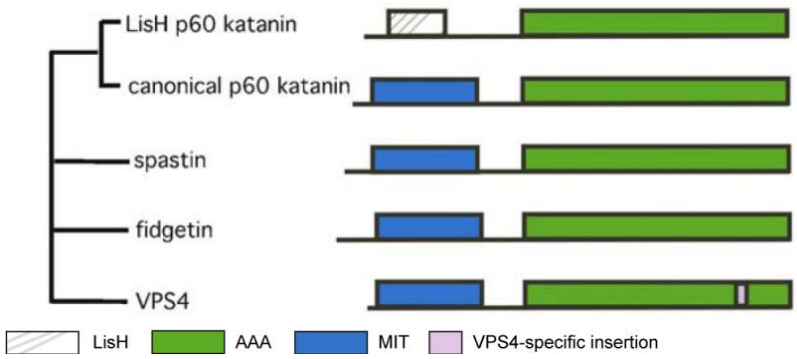

Figure 5.2. The superfamily of MT-severing enzymes.

Schematic representation of the domains found in the family of MT-severing enzymes. The LisH domain mediates dimerization. The MIT domain allows interaction with MTs or ESCRT proteins. The AAA domain is responsible for ATPase activity. The role of the VPS4-specific insertion (or Vps4 oligomerization domain) is currently not clear (Vajjhala et al., 2008). *(Roll-Mecak and McNally, 2010)*

5.2. Common structure and mechanism of AAA$^+$-ATPases

Electron microscopic observations and crystallographic studies revealed that, despite their functional diversity, AAA$^+$ ATPases exhibit a common mechanism to transform chemical energy into mechanical work. AAA$^+$ enzymes typically assemble into ring-shaped hexamers with a central cavity or pore (Hanson and Whiteheart, 2005, Wendler et al., 2012) (Figure 5.3). Substrate proteins can bind on the surface of the pore, where they are re- or unfolded. ATP binding and hydrolysis at the AAA$^+$ domains induce conformational changes in the ATPase oligomer that are than translated to remodel substrates. The Walker A and B motif are required for ATP turnover. Site-directed mutagenesis of different AAA$^+$ proteins demonstrated that the Walker A motif is involved in both steps, the binding and hydrolysis of ATP, as mutations in the Walker A sequence abolish ATP binding and therefore ATPase activity. Additionally, this often leads to dissociation of the hexameric complexes. On the other hand, mutagenesis of the Walker B revealed that this motif is only crucial for ATPase activity. AAA$^+$ proteins mutagenized in the Walker B sequence are capable of binding of ATP and oligomer assembly, but inhibit hydrolysis, which blocks the release of substrates from the hexamers. Other structural features within the AAA$^+$ domains allow tighter association between subunits, mediate substrate specificity and further regulate the ATP turnover.

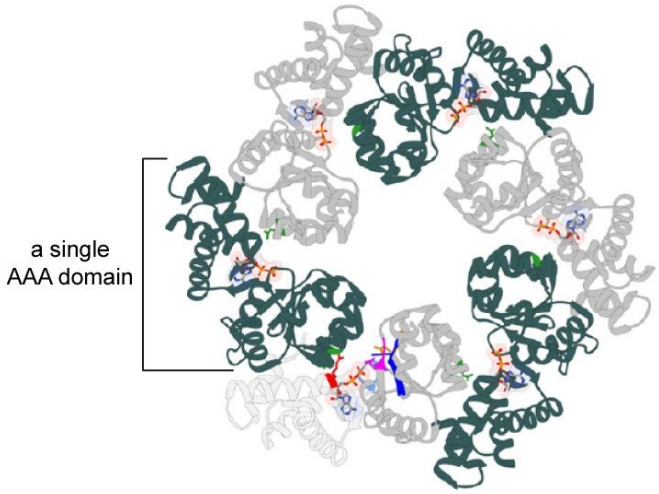

Figure 5.3. Oligomeric arrangement of the AAA$^+$ domains.

The AAA$^+$ modules are assembled into hexamers as revealed from crystal structures of many AAA$^+$ proteins. Neighboring subunits are colored alternating in green and grey. *(Wendler et al., 2012)*

To date, there are about 80 AAA$^+$ ATPases known in human, and about 50 in yeast. Many AAA$^+$ proteins found in mammals have functional counterparts in yeast, which suggests that characterization of function and mechanisms of AAA$^+$ ATPases in yeast may help us to clarify the diverse functions for AAA proteins in human.

Aim of this work

Part I: MT-dependent nuclear congression in fission yeast

In contrast to budding yeast, the forces driving nuclear congression, the period when the two haploid nuclei migrate together prior to nuclear fusion, are not well characterized in fission yeast. It has been elucidated how dynein simultaneously interacts with the cortex and MTs to generate pulling forces during nuclear horsetail movement. However, dynein is additionally enriched at the SPB. One could imagine that it accumulates at MT minus ends due to its minus end-directed motility, but dynein may potentially play also an important role at the SPB during meiotic prophase.

Immunofluorescence of fixed cells with nuclear labeling demonstrated that deletion of two minus end-directed motors, dynein and the kinesin-14 Klp2, results in a higher frequency of zygotes with unfused nuclei, some of which exhibited an elongated shape typically for horsetail phase suggesting that these cells had progressed in meiosis without completing nuclear fusion (Troxell et al., 2001). Recent studies showed that nuclear congression was dramatically affected in *mal3Δ* cells with perturbed MT dynamics and that cells were able to enter meiosis I without completing nuclear congression and fusion (Yamashita et al., 2013, Polakova et al., 2014). Together this led us to the proposal that Klp2 and dynein generate cooperatively the forces underlying nuclear congression, which is different to budding yeast, where only one motor, Kar3, is essential. However, as no real time imaging has been performed, it is currently not known, how these two motors contribute to nuclear congression, whether they work in the same or in parallel pathways and whether other kinesins or mechanisms participate. Therefore, we developed a microfluidic-based technology for long term imaging of mating cells to capture precise timing of nuclear congression and to perform a systematic screen through all MT-dependent motors to test their role and to identify the mechanisms underlying this process.

Part II: A novel factor in cellular morphogenesis of fission yeast

Schizosaccharomyces pombe contains 5123 genes (www.pombase.org), of which about 41% have been experimentally characterized. The role of many uncharacterized genes has been proposed based upon sequence homology to other systems. However, whether these predictions coincide with the biological gene functions in the cell has to be determined in the future.

Fission yeast has been widely used as a model system to study different morphological processes. Work over decades has identified major components of growth and polarity. However, the discovery of new pathways and the gaps in our understanding of how these pathways are regulated and linked provokes the necessity for identification of novel factors that may be missing links.

We therefore performed a screen to discovery novel genes involved in fission yeast morphogenesis. Using the genome-wide library of haploid fission yeast deletion mutants, we focused our attention onto yet unknown genes whose role inferred from homology were predicted to relate to MTs.

We discovered that deletion of the gene *SPBC947.01* (named hereafter *knk1*) caused a novel shape phenotype marked by the formation of kinks at the cell tips. Interestingly, its gene product belongs to the conserved and important family of AAA^+ ATPases and was announced as fidgetin-like suggesting that its involvement in MT-severing.

In this study, I characterized the unique shape defect created by deletion of *knk1* and relate it to known pathways of morphogenesis.

Results Part I –

MT-dependent nuclear congression in fission yeast

In this chapter, the results obtained in this study concerning the identification of MT-dependent mechanisms of nuclear congression are presented in form of an article entitled: *Kinesin-14 and dynein drive fission yeast nuclear congression in parallel pathways*. This article is currently in preparation to be submitted to Developmental Cell.

Kinesin-14 and dynein drive fission yeast nuclear congression in parallel pathways

Kathleen Scheffler[1], Rafael Minnes[2], Anne Paoletti[1], Vincent Fraisier[1] and Phong T. Tran[1,2]

[1]Institut Curie, CNRS-UMR144, Paris 75005, France

[2]University of Pennsylvania, Cell & Developmental Biology, Philadelphia PA 19104, USA

Correspondence: phong.tran@curie.fr

Running title:

Klp2 and dynein drive nuclear congression

Summary

The microtubule cytoskeleton and associated motors play a central role in nuclear migrations, which are crucial for diverse cellular processes including cell division, polarity and sexual reproduction. To mediate bi-directionality, dynein and plus end-directed kinesins accumulate at the nuclear surface and move nuclei laterally along MTs. Here, we report the cooperation of two minus end-directed motors to translocate nuclei during fission yeast karyogamy via parallel mechanisms. We developed a microfluidic-based technology for long-term imaging of mating cells to capture precise timing of nuclear congression and perform a systematic screen through all microtubule motors. We find that kinesin-14s at plus ends may cross-link and slide antiparallel MTs, while dynein at the SPB pulls on MTs. Surprisingly, dynactin is dispensable for this process suggesting dynactin is not crucial for fission yeast dynein activity. In summary, our work suggests that collaboration of dynein with kinesin-14s in parallel pathways increases efficiency and accuracy of nuclear positioning events.

Introduction

The development of many, if not all, eukaryotes is accompanied by movements of the nucleus depending on cell cycle stage and differentiation state. Controlling the nuclear position is crucial for diverse cellular processes including cell division, cell polarity and motility and sexual reproduction.

The microtubule (MT) cytoskeleton and its associated motor proteins, kinesins and dynein, play a central role during nuclear positioning in many systems (Reinsch and Gonczy, 1998). Pulling forces exerted by the minus end-directed motor dynein anchored to the cortex constitutes a prominent mode to ensure proper positioning of mitotic spindles, centrosomes and nuclei from yeast to human (Burakov et al., 2003; McNally, 2013; Roberts et al., 2013; Schmoranzer et al., 2009). In other cases, dynein or kinesins accumulate directly at the nuclear envelope to move nuclei laterally along MTs like in *C. elegans* hypodermal cells (Fridolfsson and Starr, 2010) or during interkinetic nuclear migration (Tsai et al., 2010).

Recent work demonstrated that the fission yeast *Schizosaccharomyces pombe* is likewise a valuable model system to study diverse aspects of nuclear movements. The nucleus is tightly associated to MTs at multiple sites along the nuclear envelope including the SPB (spindle pole body, yeast equivalent to centrosomes) in interphase, while MT plus tips dynamically grow and shrink in the cytoplasm allowing contact to cellular structures such as the cell cortex or other MTs (Drummond and Cross, 2000; Tran et al., 2001). Organization of interphase MT bundles partly depends on Klp2, a member of the minus end-directed kinesin-14 family (Carazo-Salas et al., 2005), which mediates sliding of MTs of opposite polarity along each other (Braun et al., 2009; Janson et al., 2007). A role for Klp2 in pulling nuclei together has been shown at the end of mitosis, where a misregulation of Klp2 leads to an aberrant clustering of nuclei in the cell middle (Mana-Capelli et al., 2012).

Another minus end-directed motor, dynein, is responsible for dramatic oscillations of the nucleus during meiotic prophase, known as horsetail nuclear movement (Chikashige et al., 1994; Yamamoto et al., 1999), which is driven by pulling forces generated through simultaneous interaction with microtubules and the cortical anchor protein Num1 (Saito et al., 2006; Vogel et al., 2009; Yamamoto et al., 2001; Yamashita and Yamamoto, 2006).

Dynein forms a multiprotein complex consistent of two heavy chains and several subunits, the intermediate, light intermediate and light chains, and interacts with additional adaptor proteins such as the dynactin complex. These interactions are thought to target dynein to subcellular structures and cargos and regulate its motor activity (Kardon and Vale, 2009; Roberts et al., 2013; Vallee et al., 2012). Especially, the dynactin complex is essential for almost all dynein

functions in mammals by increasing its processivity along MTs (King and Schroer, 2000). In fission yeast, the intermediate chain Dic1, the light intermediate chain Dli1 and the dynactin component Ssm4, homologue of Glued, are absolutely required to generate dynein-dependent pulling forces during horsetail nuclear movement as cells lacking any of these factors fail to undergo proper nuclear oscillations through disruption of dynein localization to MTs (Fujita et al., 2010; Niccoli et al., 2004).
Additionally, dynein may play multiple roles during meiotic prophase as it has been shown that dynein also helps clustering telomeres at the SPB via interaction with cytoplasmic MTs nucleated from a novel type of MTOC, the telocentrosomes (Goto et al., 2001; Yoshida et al., 2013).

During sexual reproduction, after oocyte fertilization, the male and female pronuclei migrate towards each other allowing nuclear fusion in a MT-dependent manner (Reinsch and Gonczy, 1998). In budding yeast, nuclear congression, the phase when the haploid nuclei move towards each other after cell fusion to form a diploid zygote, requires the kinesin-14 Kar3 (Molk et al., 2006). Due to its localization to MTs (Meluh and Rose, 1990), it was proposed that Kar3 might mediate interaction of MTs from opposite SPBs, either by sliding overlapping anti-parallel MTs or by cross-linking depolymerizing MT plus tips, pulling the two nuclei together (Molk and Bloom, 2006). However, it has been recently demonstrated that rather SPB-anchored Kar3 exerts lateral forces on MTs from the opposite SPB generating pulling forces (Gibeaux et al., 2013).

In fission yeast, nuclear congression proceeds in a MT-dependent manner (Polakova et al., 2014; Yamashita et al., 2013). Earlier studies revealed that, upon depletion of Klp2 and dynein, zygotes contained often two nuclei, compared to only one in wildtype, who appeared to undergo nuclear horsetail movement suggesting that the process of nuclear congression or fusion was impaired in these mutants (Troxell et al., 2001). However, to date, no study has been carried out to investigate the mechanisms underlying nuclear congression in detail.
Here, we developed a microfluidic-based technology for long-term imaging of mating cells to capture precise timing of nuclear congression and perform a systematic screen through all MT-dependent motors to test their role in this process. In contrast to budding yeast, we demonstrate that nuclear congression is mediated by two minus end-directed motors, dynein and Klp2. We provide evidence that these motors work in parallel mechanisms at distinct subcellular structures and hypothesize that, while Klp2 might mediate MT interactions at plus tips and along MT lattice, dynein may functions at the SPB, together promoting efficient nuclear congression.

Results

Klp2 and dynein mediate nuclear congression

We used fabricated µm-scaled channels based on a combination of soft-lithography and microfluidics technology (Velve-Casquillas et al., 2010) permitting long-term imaging of mating cells (Fig. S1A, B) both expressing Cut11-GFP (West et al., 1998) and, in one of the mating partners, GFP-Atb2 (Ding et al., 1998) to visualize simultaneously the nuclear envelope and microtubules (Fig. 1A). Nuclear congression was defined as the time upon cell fusion marked by diffusion of cytoplasmic GFP-labeled tubulin until nuclear contact was established and was achieved in average within 28.6min in wildtype zygotes (Fig. 1A, S1C).

To identify all the motors involved in nuclear congression, we systematically deleted or inactivated the 9 kinesins and the single dynein (deletion of the heavy chain) of the fission yeast genome. In summary, nuclear congression was significantly delayed in *klp2Δ*, *dhc1Δ* and *tea2Δ* zygotes (Fig. 1B). *klp2Δ* zygotes (Fig. 1D) exhibited the greatest delay of almost 20min (47.6min), while the delay in *dhc1Δ* zygotes (Fig. 1E) was the mildest with 5min (33.7min) compared to wildtype suggesting that Klp2 generates stronger forces than dynein. Noteworthy, *dhc1* deletion produced also a slowing down of the nuclear fusion process after nuclear contact has been achieved suggesting that dynein might particularly function at late stages of this process (Fig. S1D). Despite a delay, nuclear congression was always successfully completed in all single mutants (Fig. 1G, S1E), indicating that parallel mechanisms are operating. Therefore, we also tested double mutants of *klp2Δ* combined with deletion of the other motor proteins (Fig. 1C, S1E). Strikingly, the *klp2Δ dhc1Δ* mutant failed almost completely to bring their nuclei together (Fig. 1F, G) confirming the observations made by Troxell et al. (2001). This suggested that these two motors directly contribute to force generation required for nuclear congression in a parallel manner or, alternatively, might be involved in the organization of the MT array specific for meiotic prophase. When more closely examined, we observed that, before and immediately after cell fusion, cells mainly contained linear MT bundles attached at multiple sites to the nucleus as typically seen during interphase (Fig. 1A, -5 to 10min). Eventually, MTs were organized into a radial array exclusively nucleated from the SPB (Saito et al., 2004; Tanaka et al., 2005) and a bright bundle between the two nuclei was often observed, probably created by overlapping anti-parallel MTs emanating from opposite SPBs (Fig. 1A, yellow arrowhead). This MT bundle was still established in absence of one or both motors (Fig. 1D-F, yellow arrowhead) demonstrating that the failure in nuclear congression in *klp2Δ dhc1Δ* zygotes was probably not produced due to an aberrant MT array, but rather due to a lack of MT-dependent forces.

In addition, the depletion of the plus end-directed kinesin Tea2 exhibited a delay of 13min (41.6min) compared to wildtype, but unlike *klp2Δ dhc1Δ,* did not show synergistic defects in a *klp2Δ* or *dhc1Δ* background. These results imply that Tea2 only plays an indirect role, most likely due to its function in the control of MT dynamics as a +TIP by transporting Tip1, the CLIP170 homologue, towards MT plus tips (Busch et al., 2004). Consistently, *tip1Δ* zygotes characterized by shorter MTs as well (Brunner and Nurse, 2000) mimicked the *tea2Δ* phenotype and exhibited a similar delay of 13.3min (41.9min) (Fig. S1F) suggesting that proper MT dynamics facilitate the process, but neither Tea2 nor Tip1 is essential for nuclear congression.

Distinct roles for Klp2 and dynein in nuclear congression

Next, we examined the dynamics of nuclear congression in wildtype and mutant zygotes in more detail by monitoring the migration of the SPB marker Sfi1-GFP (Almonacid et al., 2011) at 1min intervals before and after cell fusion until SPBs were juxtaposed (hereafter referred to as SPB fusion). Distances of the two SPBs measured from kymographs are presented as a function over time (Fig. 2A). In wildtype cells, nuclei usually started moving immediately upon cell fusion (t_0), slowly at the beginning, but migration was speeded up as nuclear congression proceeded (Fig. 2B, dark green graph). In approximation, this graph may be described as a second degree polynomial function (black graph), which, in other words, demonstrates that the velocities of the two approaching nuclei was accelerated in a roughly linear manner (light green graph). This behavior observed for individual wildtype zygotes could be confirmed by plotting the median curve obtained by a population (n=25) to describe the SPB distances (Fig. 2C, S2A) and the velocities (Fig. 2H green curve, Fig. 2SB) over time.

We performed the same analysis in *klp2Δ* zygotes, where nuclear congression depends solely on dynein. Despite a delay, the two nuclei migrated towards each other in a similar fashion like wildtype, slowly at the beginning but with an accelerating speed over time, as shown for an individual cell (Fig. 2D) or as a median graph for all monitored examples (Fig. 2G, red curve; S2C). Consistently, velocities clearly increased, but at a lower rate compared to wildtype (Fig. 2D, H, S2C) caused by the absence of Klp2-generated forces.

The behavior of the approaching nuclei was most strikingly altered in *dhc1Δ* zygotes, where nuclear congression was only driven by Klp2. Remarkably, in about half of the observed events, distances of the two SPBs decreased in a linear fashion upon cell fusion as shown for an individual zygote (Fig. 2E) or plotted as a median graph for this subset (12/25 cells) of *dhc1Δ* zygotes (Fig. 2G, orange curve, S2D). When described as a second degree polynomial function, the resulting velocities were only mildly increasing compared to wildtype and *klp2Δ* zygotes (Fig.

2H, S2D). It should be noted that the SPB distances over time may be more accurately described by a linear regression, as, in fact, the speed of the moving nuclei appeared approximately constant for this mutant. However, to be consistent in our analysis, we used the same approximation method as for wildtype and *klp2Δ* resulting in an artifactual mild increase of the *dhc1Δ* velocities.

Furthermore, the remaining 13 *dhc1Δ* zygotes displayed a particularity during nuclear congression. Here, an initial phase with no directed nuclear movement preceded the migration of the nuclei towards each other (Fig. 2F). When nuclei congressed, they appeared to do so with a constant speed. However, as the period between cell fusion and initiation of nuclear congression varied between cells, a median curve did not accurately represent the behavior of individual cells (Fig. S2E). Furthermore, as the SPB distances over time could not be described by neither a linear nor polynomial function (Fig. 2F, black line), we depicted the SPB distances and velocities over time only for the first *dhc1Δ* subset of mating cells representing typical features of *dhc1Δ* nuclear congression in comparison to wildtype and *klp2Δ* (Fig. 2G, H).

Taken together, these observations suggest that nuclear congression proceeds differently in *klp2Δ* and *dhc1Δ* zygotes. While in wildtype and *klp2Δ* zygotes, where dynein participates in force generation, the nuclei approach each other with accelerating velocities, depletion of dynein results in nuclear migrations at constant speeds indicating that Klp2 exerts forces onto nuclei in a constant fashion and that contribution of dynein increases during this process. Therefore, we propose that these two motors function in distinct, but parallel pathways.

Additionally, we confirmed that double *klp2Δ dhc1Δ* mutant (n=10) failed to congress their nuclei as well as their SPBs (Fig. S2H, I). Remarkably, some nuclei managed to migrate towards each other to some extent without completing nuclear congression. We hypothesized that this observation may be a result of pushing forces exerted by growing MTs against the cortex (Tran et al., 2001). Therefore, we tested also a triple *klp2Δ dhc1Δ tea2Δ* mutant that exhibits aberrant MT dynamics. Indeed the nuclear migrations towards each other were slightly dampened (Fig. S2H, J), further indicating that proper MT dynamics support efficient nuclear congression, but alone are not capable of bringing nuclei together.

Klp2 localization at MT plus tips and along MTs

To better understand their distinct roles, we visualized Klp2 and dynein in mating cells. Consistent with their differing phenotypes, they also showed distinct localization patterns during nuclear congression.

GFP-tagged Klp2 has been observed at plus tips of cytoplasmic MTs during interphase in vegetative cells (Janson et al., 2007). Similarly during karyogamy, we detected Klp2 in a punctuated manner at plus tips of MTs and more weakly along the lattice of all MTs (Fig. 3A), but not only along bridging MTs between the two nuclei, which appears somewhat different to Klp2 localization during telophase in cytokinetic mutants, when nuclei clustering occurs (Mana-Capelli et al., 2012). These observations suggest that Klp2 contributes to nuclear congression by mediating interactions between MTs either by sliding antiparallel MTs, as demonstrated during interphase (Carazo-Salas et al., 2005) (Janson et al., 2007), or by cross-linking depolymerizing MT plus tips.

Klp2 localization to the MT plus ends seemed unaffected in mating *dhc1Δ* cells (Fig. S3A), indicating further that both motors function in independent pathways.

Recently, it was found that SPB-anchored Kar3, Klp2 homologue in budding yeast, exerts pulling forces laterally on MTs emanating from the opposite SPB (Gibeaux et al., 2013). We therefore examined whether Klp2 was also recruited to the SPB in fission yeast. Due to the complex cytoplasmic MT arrays assembled in this organism, with MTs and MT plus tips extending towards the SPB of the mating partner in wildtype cells, we imaged Klp2-GFP in cells depleted for the +TIP Mal3 (EB1 homologue) that is characterized by short MTs (Beinhauer et al., 1997) and fails to load Klp2 onto MTs (Mana-Capelli et al., 2012). In *mal3Δ* cells, Klp2 was greatly absent from the short MTs, however we found that a residual staining in close proximity to the nucleus could be observed in non-mating cells (Fig. S3A, yellow arrowheads), which might be caused by weak Mal3-independent binding to MTs and accumulation at MT minus ends due its minus end-directed motility. Surprisingly, Klp2 appeared to localize as a single dot at the nuclear envelope in mating cells, which might suggest its recruitment to the SPB. Alternatively, Klp2 might accumulate exclusively at the SPB during karyogamy as it represents the only anchor point for MT minus ends (Saito et al., 2004; Tanaka et al., 2005). However, the SPB-located Klp2 pool appeared minor compared to the MT-bound one. We therefore propose that Klp2 dominantly generates forces by cross-linking antiparallel MTs to pull nuclei together.

Dynein recruitment to SPB during nuclear congression

To study the localization of dynein, we imaged the meiotically upregulated dynein heavy chain (Miki et al., 2002) tagged to 3xGFP (Fujita et al., 2010) (hereafter referred to as dynein). While no dynein was detected in non-mating cells, it localized to one or both SPBs in 89.2% of cells with congressing nuclei as shown in cells co-expressing either the nuclear envelope protein Cut11-mCherry and mCherry-Atb2 (Fig. 3B) or SPB marker Sfi1-RFP (Fig. 3C), which is in

contrast to the phase of nuclear horsetail movement, where dynein is greatly found along MTs (Yamamoto et al., 1999). Noteworthy, in some cells (21.1%) dynein could be seen as multiple dots which may represent its co-recruitment to the SPB and telocentrosomes (Yoshida et al., 2013) (Fig. S3B, yellow arrowheads), but rarely (6.9%) along the MT bundle bridging the two nuclei (Fig. S3B, magenta arrowhead).

A time-lapse study revealed that dynein was only being recruited to the SPB upon cell mating (Fig. 3D), which in consistency with the increasing forces exerted by dynein as shown by monitoring Sfi1-GFP dynamics. It was initially detected at SPBs in average 31.2min prior to SPB fusion (Fig. 3F) and then gradually increased in intensity until SPB fusion (Fig. 3E, G). We proposed that the SPB intensities of dynein should be recruited to higher levels at the time point of SPB fusion in mating cells exhibiting a slowed down nuclear congression, like *klp2Δ* cells with a 20min delay. Consistently, in *klp2Δ* cells, where overall dynein localization pattern was not altered (Fig. S3B), dynein was detected 18min earlier (Fig. 3F, S3C, D) and its levels at SPBs were in average 1.9-fold increased at 15min before SPB fusion and 1.6-fold upon SPB fusion (Fig. 3G) compared to wildtype. SPB levels of dynein, which could be confidently detected and measured at 15min prior to SPB fusion in wildtype cells, were similar to levels at -30/35min in *klp2Δ* cells, demonstrating that increased dynein intensities at respective time points in *klp2Δ* cells were caused due to a nuclear congression delay extending the period of dynein recruitment (Fig. 3G).

Taken together, we show that Klp2 is mainly recruited to MTs and MT plus tips, while dynein appears dominantly at SPBs during nuclear congression, further demonstrating their involvement in parallel but distinct mechanisms to pull nuclei together.

SPB-bound dynein drives nuclear congression and requires Dli1 for proper function

During nuclear congression, dynein could be rarely seen at MTs, but dominantly at SPBs. A previous study showed that the N-terminus of Dhc1 lacking the motor domain (Dhc1(1-1266)) was sufficient for its recruitment to the SPB (Yoshida et al., 2013) (Fig. 4C), demonstrating that its SPB localization was not purely due to an accumulation close to MT minus ends via its minus end-directed motility. However, this truncated version of Dhc1 was not functional in nuclear congression as it mimicked the *dhc1Δ* phenotype in single and *klp2Δ* double mutants (Fig. 4A, B), implying that dynein indeed requires its motor domain to generate forces capable of pulling nuclei together.

During nuclear horsetail movement, dynein localizes along MTs and interacts with the cortex to generate pulling forces. Its dominant recruitment to the SPB during nuclear congression

suggests that dynein functions in a different manner. Consistent with this hypothesis, lack of the cortical anchor Num1 did not affect nuclear congression in a single or *klp2Δ* double mutant (Fig. 4A, B). As next we tested the role of the dynactin complex, by deletion of the component *ssm4*, the Glued homologue. Surprisingly, in *ssm4Δ* single as well as in *klp2Δ ssm4Δ* double mutant zygotes nuclear congression proceeded like in wildtype or *klp2Δ* single mutants respectively (Fig. 4A, B), suggesting that the dynactin complex was not required for this specific dynein function in fission yeast. As previously reported, dynein was absent from MTs throughout meiotic prophase in *ssm4Δ* cells, but was still recruited to SPBs in mating cells (Niccoli et al., 2004) (Fig. 4D). In fact, dynein was detected in the majority of cells (84%) prior to SPB fusion (Fig. 4E) and reached almost wildtype levels at the time point of SPB fusion (Fig. 4F). Similar defects were observed in *dic1Δ* zygotes (Fig. S4A-C), which is proposed to link the dynein to the dynactin complex (Vaughan and Vallee, 1995). Together, that suggested that, firstly, dynein localization along MTs is not required for its function and secondly, that, even though essential for nuclear horsetail movement, neither the dynactin complex nor Dic1 are necessary for dynein-dependent force generation during nuclear congression.

Remarkably, the depletion of the light intermediate chain Dli1 resulted in a delay of 4.7min (33.3min) compared to wildtype mimicking *dhc1* deletion (Fig. 4A). Furthermore, 79% of a double *klp2Δ dli1Δ* mutant failed to successfully complete nuclear congression, while the remaining 21% exhibited a great delay (Fig. 4A, B). However, a double *dhc1Δ dli1Δ* mutant only mimicked the phenotype of the single mutants (Fig. 4A), demonstrating that Dli1 functions in the dynein-dependent pathway. Compared to *ssm4Δ* and *dic1Δ* zygotes, dynein was not only absent from MTs, but also from SPBs in mating *dli1Δ* and *klp2Δ dli1Δ* cells (Fig. 4D, S4D), which is in agreement with a previous report (Fujita et al., 2010). In fact, dynein was never observed at SPBs prior to SPB fusion and in 46% of cells not even after (Fig. 4E).

In summary, Dli1 appears to play an essential role in dynein localization and function in meiotic prophase by allowing its recruitment to MTs and SPBs, while the dynactin complex and Dic1 are dispensable. In particular, dynein localization to the SPB seems crucial for its role in nuclear congression possibly by generating pulling forces along MTs emanating from the nucleus of the mating partner. As *dli1* deletion leads to greatly decreased levels at both subcellular structures, we propose that Dli1 might not function by targeting dynein to these sites, but rather by facilitating the formation or by stabilization of the dynein complex.

Discussion

Here, we demonstrate that two minus end-directed motors, the kinesin-14 Klp2 and dynein, are required to efficiently drive nuclear congression in fission yeast. To our knowledge, this is the first report of two minus end-directed motors cooperating to translocate nuclei by distinct mechanisms. Our observations propose following model (Fig. 5): Klp2 localizes dominantly to plus ends and cross-links and slides MTs emanating from the opposite SPB in an antiparallel manner. Dynein accumulates at SPBs and probably pulls on MTs nucleated by the mating partner.

Our work provides a first detailed description of nuclear congression in live fission yeast cells and confirms the observations made by Troxell at al. (2001). In summary, Klp2 and dynein are major force generators and alone are sufficient to drive nuclear congression. But a double mutant completely fails to bring nuclei together demonstrating that each gene becomes essential in absence of the other. The observation that deletion of *klp2* causes a greater delay than *dhc1* demonstrates that Klp2 pathway contributes more forces.

Additionally, we find that proper control of MT dynamics may enhance efficiency of nuclear congression as *tea2* deletion causes a delay of 10 to 15min in wildtype, *klp2Δ* and *dhc1Δ* zygotes. Shorter MTs are less likely to meet and be cross-linked by Klp2 or to reach the opposite SPB and be caught by dynein. Furthermore, we show that movement of the nuclei towards each other, without reaching each other, in a *klp2Δ dhc1Δ* zygote are dampened upon *tea2* deletion suggesting that MTs extending towards the cortex also exert forces able to push nuclei, as shown for interphase cells (Tran et al., 2001). Thus, shorter MTs in *tea2Δ* and *tip1Δ* cells can push nuclei only smaller distances away from the cortex. However, these motor-independent forces are clearly not sufficient to drive nuclear congression.

Klp2, like other members of the kinesin-14 family, contains two MT-binding domains, one in the motor domain and one additional in the tail, allowing to interact with two MTs at once and to cross-link them (Braun et al., 2009). We confirm its Mal3-dependent localization to MT plus tips during meiosis.

In general, kinesin-14s are implicated in MT sliding, and accordingly, Klp2 has been shown to slide newly nucleated MTs towards minus ends concentrated in the overlap zone of the bundle (Janson et al., 2007). It is therefore likely that Klp2 generates pulling forces during nuclear congression in a similar manner; by sliding antiparallel MTs relative to each as suggested for nuclei clustering at the end of mitosis in mutants defective in septation (Mana-Capelli et al., 2012). Alternatively, Klp2 might cross-link shrinking plus tips and potentially induce

depolymerization. Klp2 at kinetochores appears to operate via such a mechanism during mitosis; by provoking shortening of kinetochores fibers to facilitate retrieval of lost chromosomes to spindle poles (Gachet et al., 2008; Grishchuk and McIntosh, 2006). At the moment, based upon the detection of a bright MT bundle between the two nuclei, we favor the first hypothesis of Klp2 sliding MTs relative to each other to produce pull nuclei together.

In our model, the large dynein complex anchored at the SPB may interact with MTs emanating from the SPB of the mating partner pulling the two nuclei together, as it has been now demonstrated for Kar3 by electron microscopy (Gibeaux et al., 2013). We show that dynein starts to accumulate at SPBs about 30min prior to SPB fusion, approximately at the time of cell fusion, and increases in intensity during nuclear congression suggesting that dynein-dependent pulling forces may also amplify, which was confirmed by measuring SPB dynamics showing that, specifically in wildtype and *klp2Δ* zygotes, where dynein contributes to force generation, nuclear movements appear to accelerate. Moreover, when nuclear congression is delayed, like in *klp2Δ* zygotes, dynein levels further increase and it can even be observed along MTs, indicating that dynein levels might continuously rise even after completion of nuclear congression. That suggests a model, where dynein first localizes to the SPB and, when present in sufficient quantities, also to MTs allowing the progression through horsetail movement. This behavior could be regulated by dynein itself possessing a higher affinity for SPB-specific components than for MTs or by presence of regulatory proteins such as dynactin enhancing affinity to MTs.
Surprisingly, dynactin is dispensable for dynein-dependent nuclear congression in fission yeast. This is in sharp contrast to mammals, where dynactin appears to be required for virtually all activities carried out by dynein. It remains elusive why fission yeast dynein does not require dynactin for all its functions, but possibly it is not crucial for dynein activity, but only helps recruiting dynein to MTs.
On the other hand, we discovered that the light intermediate chain Dli1 is crucial for dynein function during nuclear congression and horsetail movement, as its deletion greatly reduces dynein levels at SPBs and MTs (Fujita et al., 2010). We propose that Dli1 might globally affect dynein levels and not serve to target dynein to specific structures. Dli1 may do so by controlling the stabilization of Dhc1, by facilitating dimerization of Dhc1 or by mediating interaction with other proteins allowing its recruitment to SPBs and MTs.
In summary, fission yeast karyogamy represents a good model illustrating how different subcellular localizations of dynein achieve diversity in function. Here, within a relative short period of time, dynein is recruited to the SPB driving nuclear congression, to telocentrosomes

contributing to telomere clustering (Yoshida et al., 2013) and to MTs and the cortex promoting nuclear horsetail movement.

To our knowledge, the study presented here might be the first report of two minus end-directed motors acting in concert. In mammals, most minus end-directed translocations of organelles including nuclei and vesicles are executed by dynein. Cooperation between kinesins, primarily plus end directed, and dynein in nuclear positioning has been reported for several systems and provide bi-directionality of nuclear movements. Hence, our work suggests that also collaboration of dynein with kinesin-14s in parallel pathways may increase efficiency and accuracy of nuclear positioning events.

In *dhc1Δ* zygotes, where nuclear congression solely depends on Klp2 lacking forces generated at the SPBs, this process proceeds only with a slight delay, until nuclear contact is established. Considering that light microscopy can resolve distances of 200nm and higher, then one could imagine that two nuclei “touching” each other, are in fact still separated by a space below 200nm. Interestingly, *dhc1Δ* zygotes seem to exhibit an extended time between nuclear contact and completion of nuclear fusion (Fig. S1D), suggesting that SPB-bound motors bring nuclei more efficiently together on the last “nanometers” than when bound to MT plus ends. Interestingly, about 50% of zygotes lacking dynein initiate nuclear congression immediately upon cell fusion, while the remaining 50% exhibited an initial phase without directed nuclear migrations. These observations suggest to us that dynein may additionally support interactions between antiparallel MTs required for initiation of nuclear congression. Our preliminary data suggests that this specific role of dynein may become more important in mating cells with more complex geometries adopting S- or U-shape (Fig. S2G). We hypothesize that in simpler geometries, like straight or L-shapes, plus ends might be more likely to meet and be cross-linked by Klp2, but the presence of a large motor complex at the SPB may help catching MTs from the mating partner, when Klp2 fails.

All together, the distinct properties as well as specific localization pattern of motor proteins allow differential roles for minus end-directed motors in the same process of nuclear positioning.

Experimental procedures

Strains and media

Standard fission yeast media and techniques were used as described (Moreno et al., 1991). Strains used in this study are listed in Table S1.

The microfluidic flow chamber

For long term imaging of mating cells, we used microfabricated microfluidic flow chambers previously constructed and described from our lab (Terenna et al., 2008). Briefly, the design for the flow chamber was drawn using the computer-assisted design software L-Edit (www.tanner.com/EDA). The design was then laser-etched into a thin layer of chromium on a quartz plate, which served as a photo-mask (www.microtronicsinc.com). Next, SU8 negative photo-resist was spin-coated onto a silicon wafer (www.microchem.com). The features were then transferred from the photo-mask onto the photo-resist layer by exposure and cross-linking with UV light (365nm) for 20s. The photo-resist was developed with SU8 developer and cleaned with isopropyl alcohol and nitrogen gas. The wafer was then able to serve as a master mold on which repeated replication of molds could be made by casting from polydimethylsiloxane (PDMS) (www.dowcorning.com). Chambers were assembled by peeling off a PDMS replica from a mold, introducing inlet and outlet holes, and bonding the replica to a microscope glass cover slip after surface treatment using a plasma cleaner (www.harrricksci.com).

Live-cell microscopy of mating cells

Under nitrogen starvation and presence of opposite mating types, cells enter the meiotic cycle. Mating occurs only after long incubation in nitrogen poor medium at random initiation time and at a low frequency. However, with the here described technique, the protocol was optimized to obtain a good number of mating cells during long term imaging.

Cells of both mating types were separately grown in nitrogen-poor maltose extract (ME) medium at 25°C overnight. Next, cells were mixed in an equal cell number and were manually injected into a microfluidic chamber. When h90 were imaged, for example to visualize Klp2-GFP and Dhc1-3xGFP, cells were grown in rich YE5S medium overnight, before transferred to ME medium and injected into chambers, as these strains initiate mating more quickly. After injection, devices were incubated 6-8h at 25°C before imaging.

Imaging was usually carried out at 25°C and only for cut7-24 strains (Fig. 1C, D) at 37°C. In this case, cells were shifted to the restrictive temperature 30min before imaging.

For imaging, we used the Yokogawa spinning disc confocal head mounted on a Nikon Eclipse Ti inverted microscope (www.nikoninstruments.com), equipped with Nikon PlanApo 100X/1.45 NA objective lens, a PIFOC objective stepper and a Hamamatsu cooled back-thinned HQ2 CCD camera (Roper) as previously described [8]. Usually 3D optical sections were taken; those are represented and were analyzed as maximal projections.

In detail, to image cells expressing Cut11-GFP GFP-Atb2 (Fig. 1, 4A, B, S1, S4B, C) , 6 planes spaced 0.8µm, or expressing either Sfi1-GFP mCherry-Atb2 (Fig. 2, S2) or Klp2-GFP Cut11-mCherry mCherry-Atb2 (Fig. 3A, S3A) or Dhc1-3xGFP Cut11-mCherry mCherry-Atb2 or Dhc1-3xGFP Sfi1-RFP (Fig. 3B-G, 4C-F, S3B-D, S4A, D), 5 planes spaced 1µm were acquired.

For measuring nuclear congression time, cells were imaged 12h at 5min intervals (Fig. 1, 4A, B, S1, S4B, C) as well as for capturing time points of detection and measuring intensity levels of Dhc1-3xGFP at SPBs (Fig. 3D-G, 4E, F, S3D). In later case, cells coexpressing Dhc1-3xGFP and Cut11-mCherry or Sfi1-RFP were imaged.

To monitor Sfi1-GFP dynamics, images were acquired at 1min intervals for a period of 8h (Fig. 2, S2).

Data Analysis

Images were acquired and processed with MetaMorph 7.7 (www.MolecularDevices.com).

Nuclear congression was defined as the period between cell fusion (marked by cytoplasmic diffusion of mCherry- or GFP-tagged Atb2 carried by only one mating partner) and when nuclei were juxtaposed that means in contact with each other (Fig 1B, C, 4A, S1F, S4D). Data were plotted as box plots generated with Kaleidagraph 4.0 (www.synergy.com). Each box encloses 50% of the data with the median value displayed as a line. The top and bottom of each box mark the minimum and maximum values within the data set that fall within an acceptable range. Any value outside of this range, called an outlier, is displayed as an individual point. Statistical analyses of data were performed using the Student’s t-test for comparison between means in Microsoft Excel 2010.

For Sfi1-GFP dynamics, traced lines were drawn along longitudinal axis in zygotes accordingly to their shape to create kymographs (Fig. 2, S2). Distances were measured and plotted in diagrams generated by Microsoft Excel 2010 as a function over time. A second degree polynomial equation was calculated to create a linear function representing the velocities over time. For each cell, SPB distances were normalized to the average SPB distance calculated from first 10 time points prior to cell fusion. Velocities were individually adjusted to the average

value of velocity at t_0 for each strain. Presented are median curves and upper and lower quartiles.

Dhc1-3xGFP intensities at the SPB were measured as integrated intensity on maximal projections of 3D stacks (Fig. 3E, G, 4F, S3D) and corrected for cytoplasmic background.

Author Contributions

KS designed and performed experiments, analyzed data and wrote paper. AP and TP edited paper.

Acknowledgements

We thank the lab of A. Yamamoto (Shizuoka University) for generously providing reagents. We thank Sergio Rincon and Imene Bouhlel for helpful technical advice and discussion. KS is supported by a PhD fellowship from Complexité du Vivant-UPMC and Fondation ARC. This work is supported by grants from the ANR, INCa, and ARC.

References

Almonacid, M., Celton-Morizur, S., Jakubowski, J.L., Dingli, F., Loew, D., Mayeux, A., Chen, J.S., Gould, K.L., Clifford, D.M., and Paoletti, A. (2011). Temporal control of contractile ring assembly by Plo1 regulation of myosin II recruitment by Mid1/anillin. Curr Biol *21*, 473-479.

Beinhauer, J.D., Hagan, I.M., Hegemann, J.H., and Fleig, U. (1997). Mal3, the fission yeast homologue of the human APC-interacting protein EB-1 is required for microtubule integrity and the maintenance of cell form. J Cell Biol *139*, 717-728.

Braun, M., Drummond, D.R., Cross, R.A., and McAinsh, A.D. (2009). The kinesin-14 Klp2 organizes microtubules into parallel bundles by an ATP-dependent sorting mechanism. Nat Cell Biol *11*, 724-730.

Brunner, D., and Nurse, P. (2000). CLIP170-like tip1p spatially organizes microtubular dynamics in fission yeast. Cell *102*, 695-704.

Burakov, A., Nadezhdina, E., Slepchenko, B., and Rodionov, V. (2003). Centrosome positioning in interphase cells. J Cell Biol *162*, 963-969.

Busch, K.E., Hayles, J., Nurse, P., and Brunner, D. (2004). Tea2p kinesin is involved in spatial microtubule organization by transporting tip1p on microtubules. Dev Cell *6*, 831-843.

Carazo-Salas, R.E., Antony, C., and Nurse, P. (2005). The kinesin Klp2 mediates polarization of interphase microtubules in fission yeast. Science *309*, 297-300.

Chikashige, Y., Ding, D.Q., Funabiki, H., Haraguchi, T., Mashiko, S., Yanagida, M., and Hiraoka, Y. (1994). Telomere-led premeiotic chromosome movement in fission yeast. Science *264*, 270-273.

Ding, D.Q., Chikashige, Y., Haraguchi, T., and Hiraoka, Y. (1998). Oscillatory nuclear movement in fission yeast meiotic prophase is driven by astral microtubules, as revealed by continuous observation of chromosomes and microtubules in living cells. J Cell Sci *111 (Pt 6)*, 701-712.

Drummond, D.R., and Cross, R.A. (2000). Dynamics of interphase microtubules in Schizosaccharomyces pombe. Curr Biol *10*, 766-775.

Fridolfsson, H.N., and Starr, D.A. (2010). Kinesin-1 and dynein at the nuclear envelope mediate the bidirectional migrations of nuclei. J Cell Biol *191*, 115-128.

Fujita, I., Yamashita, A., and Yamamoto, M. (2010). Contribution of dynein light intermediate and intermediate chains to subcellular localization of the dynein-dynactin motor complex in Schizosaccharomyces pombe. Genes Cells *15*, 359-372.

Gachet, Y., Reyes, C., Courtheoux, T., Goldstone, S., Gay, G., Serrurier, C., and Tournier, S. (2008). Sister kinetochore recapture in fission yeast occurs by two distinct mechanisms, both requiring Dam1 and Klp2. Mol Biol Cell *19*, 1646-1662.

Gibeaux, R., Politi, A.Z., Nedelec, F., Antony, C., and Knop, M. (2013). Spindle pole body-anchored Kar3 drives the nucleus along microtubules from another nucleus in preparation for nuclear fusion during yeast karyogamy. Genes Dev *27*, 335-349.

Goto, B., Okazaki, K., and Niwa, O. (2001). Cytoplasmic microtubular system implicated in de novo formation of a Rabl-like orientation of chromosomes in fission yeast. J Cell Sci *114*, 2427-2435.

Grishchuk, E.L., and McIntosh, J.R. (2006). Microtubule depolymerization can drive poleward chromosome motion in fission yeast. EMBO J *25*, 4888-4896.

Janson, M.E., Loughlin, R., Loiodice, I., Fu, C., Brunner, D., Nedelec, F.J., and Tran, P.T. (2007). Crosslinkers and motors organize dynamic microtubules to form stable bipolar arrays in fission yeast. Cell *128*, 357-368.

Kardon, J.R., and Vale, R.D. (2009). Regulators of the cytoplasmic dynein motor. Nat Rev Mol Cell Biol *10*, 854-865.

King, S.J., and Schroer, T.A. (2000). Dynactin increases the processivity of the cytoplasmic dynein motor. Nat Cell Biol *2*, 20-24.

Mana-Capelli, S., McLean, J.R., Chen, C.T., Gould, K.L., and McCollum, D. (2012). The kinesin-14 Klp2 is negatively regulated by the SIN for proper spindle elongation and telophase nuclear positioning. Mol Biol Cell *23*, 4592-4600.

McNally, F.J. (2013). Mechanisms of spindle positioning. J Cell Biol *200*, 131-140.

Meluh, P.B., and Rose, M.D. (1990). KAR3, a kinesin-related gene required for yeast nuclear fusion. Cell *60*, 1029-1041.

Miki, F., Okazaki, K., Shimanuki, M., Yamamoto, A., Hiraoka, Y., and Niwa, O. (2002). The 14-kDa dynein light chain-family protein Dlc1 is required for regular oscillatory nuclear movement and efficient recombination during meiotic prophase in fission yeast. Mol Biol Cell *13*, 930-946.

Molk, J.N., and Bloom, K. (2006). Microtubule dynamics in the budding yeast mating pathway. J Cell Sci *119*, 3485-3490.

Molk, J.N., Salmon, E.D., and Bloom, K. (2006). Nuclear congression is driven by cytoplasmic microtubule plus end interactions in S. cerevisiae. J Cell Biol *172*, 27-39.

Moreno, S., Klar, A., and Nurse, P. (1991). Molecular genetic analysis of fission yeast Schizosaccharomyces pombe. Methods Enzymol *194*, 795-823.

Niccoli, T., Yamashita, A., Nurse, P., and Yamamoto, M. (2004). The p150-Glued Ssm4p regulates microtubular dynamics and nuclear movement in fission yeast. J Cell Sci *117*, 5543-5556.

Polakova, S., Benko, Z., Zhang, L., and Gregan, J. (2014). Mal3, the Schizosaccharomyces pombe homolog of EB1, is required for karyogamy and for promoting oscillatory nuclear movement during meiosis. Cell Cycle *13*, 72-77.

Reinsch, S., and Gonczy, P. (1998). Mechanisms of nuclear positioning. J Cell Sci *111 (Pt 16)*, 2283-2295.

Roberts, A.J., Kon, T., Knight, P.J., Sutoh, K., and Burgess, S.A. (2013). Functions and mechanics of dynein motor proteins. Nat Rev Mol Cell Biol *14*, 713-726.

Saito, T.T., Okuzaki, D., and Nojima, H. (2006). Mcp5, a meiotic cell cortex protein, is required for nuclear movement mediated by dynein and microtubules in fission yeast. J Cell Biol *173*, 27-33.

Saito, T.T., Tougan, T., Kasama, T., Okuzaki, D., and Nojima, H. (2004). Mcp7, a meiosis-specific coiled-coil protein of fission yeast, associates with Meu13 and is required for meiotic recombination. Nucleic Acids Res *32*, 3325-3339.

Schmoranzer, J., Fawcett, J.P., Segura, M., Tan, S., Vallee, R.B., Pawson, T., and Gundersen, G.G. (2009). Par3 and dynein associate to regulate local microtubule dynamics and centrosome orientation during migration. Curr Biol *19*, 1065-1074.

Tanaka, K., Kohda, T., Yamashita, A., Nonaka, N., and Yamamoto, M. (2005). Hrs1p/Mcp6p on the meiotic SPB organizes astral microtubule arrays for oscillatory nuclear movement. Curr Biol *15*, 1479-1486.

Terenna, C.R., Makushok, T., Velve-Casquillas, G., Baigl, D., Chen, Y., Bornens, M., Paoletti, A., Piel, M., and Tran, P.T. (2008). Physical mechanisms redirecting cell polarity and cell shape in fission yeast. Curr Biol *18*, 1748-1753.

Tran, P.T., Marsh, L., Doye, V., Inoue, S., and Chang, F. (2001). A mechanism for nuclear positioning in fission yeast based on microtubule pushing. J Cell Biol *153*, 397-411.

Troxell, C.L., Sweezy, M.A., West, R.R., Reed, K.D., Carson, B.D., Pidoux, A.L., Cande, W.Z., and McIntosh, J.R. (2001). pkl1(+)and klp2(+): Two kinesins of the Kar3 subfamily in fission yeast perform different functions in both mitosis and meiosis. Mol Biol Cell *12*, 3476-3488.

Tsai, J.W., Lian, W.N., Kemal, S., Kriegstein, A.R., and Vallee, R.B. (2010). Kinesin 3 and cytoplasmic dynein mediate interkinetic nuclear migration in neural stem cells. Nat Neurosci *13*, 1463-1471.

Vallee, R.B., McKenney, R.J., and Ori-McKenney, K.M. (2012). Multiple modes of cytoplasmic dynein regulation. Nat Cell Biol *14*, 224-230.

Vaughan, K.T., and Vallee, R.B. (1995). Cytoplasmic dynein binds dynactin through a direct interaction between the intermediate chains and p150Glued. J Cell Biol *131*, 1507-1516.

Velve-Casquillas, G., Le Berre, M., Piel, M., and Tran, P.T. (2010). Microfluidic tools for cell biological research. Nano Today *5*, 28-47.

Vogel, S.K., Pavin, N., Maghelli, N., Julicher, F., and Tolic-Norrelykke, I.M. (2009). Self-organization of dynein motors generates meiotic nuclear oscillations. PLoS Biol *7*, e1000087.

West, R.R., Vaisberg, E.V., Ding, R., Nurse, P., and McIntosh, J.R. (1998). cut11(+): A gene required for cell cycle-dependent spindle pole body anchoring in the nuclear envelope and bipolar spindle formation in Schizosaccharomyces pombe. Mol Biol Cell *9*, 2839-2855.

Yamamoto, A., Tsutsumi, C., Kojima, H., Oiwa, K., and Hiraoka, Y. (2001). Dynamic behavior of microtubules during dynein-dependent nuclear migrations of meiotic prophase in fission yeast. Mol Biol Cell *12*, 3933-3946.

Yamamoto, A., West, R.R., McIntosh, J.R., and Hiraoka, Y. (1999). A cytoplasmic dynein heavy chain is required for oscillatory nuclear movement of meiotic prophase and efficient meiotic recombination in fission yeast. J Cell Biol *145*, 1233-1249.

Yamashita, A., Fujita, Y., and Yamamoto, M. (2013). Proper microtubule structure is vital for timely progression through meiosis in fission yeast. PLoS One *8*, e65082.

Yamashita, A., and Yamamoto, M. (2006). Fission yeast Num1p is a cortical factor anchoring dynein and is essential for the horse-tail nuclear movement during meiotic prophase. Genetics *173*, 1187-1196.

Yoshida, M., Katsuyama, S., Tateho, K., Nakamura, H., Miyoshi, J., Ohba, T., Matsuhara, H., Miki, F., Okazaki, K., Haraguchi, T.*, et al.* (2013). Microtubule-organizing center formation at telomeres induces meiotic telomere clustering. J Cell Biol *200*, 385-395.

Figure legends

Figure 1. Klp2 and dynein mediate nuclear congression in a parallel manner

(A) Time-lapse images recorded by spinning disk confocal microscopy of cells expressing Cut11-GFP (nuclear envelope) and unilaterally GFP-Atb2 (MTs) in wildtype cells at 25°C undergoing nuclear congression. Images are presented as maximum projections of 3D stacks. Dotted lines represent cell outlines. Yellow arrowhead highlights MT bundle formed between two nuclei. Nuclear congression was defined as the duration between cell fusion (t_0) and contact between nuclei. **(B)** Time of nuclear congression in wildtype and single motor mutants at 25°C or 36°C. Mean values for strains tested at 25°C: wildtype (28.6±7.3min, n=104), *klp2Δ* (47.6±12.8min, $p<10^{-22}$, n=84), *klp3Δ* (31.1±9.8min, p=0.06, n=76), *tea2Δ* (41.6±14.9min, $p<10^{-11}$, n=94), *klp5Δ* (27.5±8.8min, p=0.38, n=84), *klp6Δ* (29.1±7.5min, p=0.63, n=78), *klp8Δ* (28.8±8.8min, p=0.89, n=60), *klp9Δ* (27.4±9.4min, p=0.39, n=69), *pkl1Δ* (27.2±7.9min, p=0.24, n=75) and *dhc1Δ* (33.7±9.4min, $p<10^{-4}$, n=87). Mean values for strains tested at 36°C: wildtype (25.8±10.9min, n=54), *cut7-24* (23.9±10.4min, p=0.29, n=89) and *klp2Δ* (41.8±22.4min, $p<10^{-4}$, n=44). **(C)** Time of nuclear congression *klp2Δ* double motor mutants at 25°C or 36°C. Mean values for strains tested at 25°C (p-value against *klp2Δ*): *klp2Δ klp3Δ* (44.9±12.7min, p=2, n=75), *klp2Δ tea2Δ* (54.2±15.9min, p=0.015, n=49), *klp2Δ klp5Δ* (44.2±10.2min, p=0.07, n=73), *klp2Δ klp6Δ* (43.8±12.9min, p=0.07, n=69), *klp2Δ klp8Δ* (49.9±11.8min, p=0,26, n=58), *klp2Δ klp9Δ* (46.7±13.1min, p=0.68, n=74), *klp2Δ pkl1Δ* (45.5±12.8min, p=0.31, n=74), *klp2Δ dhc1Δ* (155±14.1min, n=2) and) and *dhc1Δ tea2Δ* (37.8±13.5min, n=67). Mean values for strains tested at 36°C: *klp2Δ cut7-24* (45.6±13.8min, p=0.33, n=60). **(D-F**) Time-lapse images of mating cells expressing Cut11-GFP and unilaterally GFP-Atb2 in *klp2Δ* (D)*, dhc1Δ* (E) or *klp2Δ dhc1Δ* (F) strains at 25°C. **(G)** Percentage of zygotes completing nuclear congression in wildtype (100%, n=104), *klp2Δ* (100%, n=84), *dhc1Δ* (100%, n=87) and *klp2Δ dhc1Δ* (2.4%, n=85). Bars, 5µm.

Figure 2. Klp2 constantly generates pulling forces, while dynein contribution increases during nuclear congression

(A) Top, overlay of differential interference contrast (DIC) and fluorescence images of the SPB marker Sfi1-GFP shown for an individual zygote at 10min prior to cell fusion (defined by cytoplasmic diffusion of mCherry-Atb2) until completion of nuclear congression at 26min after cell fusion. Sfi1-GFP images were taken as 3D stacks at 1min intervals. Bottom, kymograph representing Sfi1-GFP dynamics from -10min until SPBs are juxtaposed. Dotted line indicates moment of cell fusion (t_0). **(B)** SPB distance (dark green) and velocity (light green) over time from example shown in (A). Velocity obtained as a differential function of a second degree

polynomial (black line) of SPB distances. **(C)** SPB distances over time normalized for each cell to average SPB distance prior to cell fusion calculated from first 10 time points. Individual cells are depicted as light green trajectories (n=25). Median is represented as a thick line and upper and lower quartiles as dotted lines. **(D)** Left, kymograph of Sfi1-GFP dynamics in a *klp2Δ* zygote. Right, SPB distances (dark red) and velocity (light red) over time. Black line represents second degree polynomial function as approximation for SPB distance. **(E)** Sfi1-GFP dynamics in a subset of *dhc1Δ* zygotes (12/25 cells) depicted as kymograph, top, or as a function over time, bottom. **(F)** Sfi1-GFP dynamics in a second subset of *dhc1Δ* zygotes (13/25 cells). Initial period without directed nuclear movement is highlighted. It should be noted that a second degree polynomial function does not accurately represents Sfi1-GFP dynamics in these cells. **(G, H)** Median curves of normalized SPB distances (G) or velocities adjusted to average velocity at t_0. (H) over time in wildtype, *klp2Δ* and a subset of *dhc1Δ* zygotes. Bars, 5µm.

Figure 3. Distinct localization pattern of Klp2 and dynein during nuclear congression

(A) Cellular distribution of Klp2-GFP in mating cells co-expressing Cut11-mCherry and mCherry-Atb2 at 25°C. Images are represented as maximum z-projection of 3D stacks. Dotted lines represent outlines of cells in different stages of meiotic prophase. **(B**) Cellular distribution of dynein (Dhc1-3xGFP) in mating cells co-expressing Cut11-mCherry and mCherry-Atb2 at 25°C. **(C**) Colocalization of Dhc1-3xGFP and Sfi1-RFP. Dhc1-3xGFP dot is greater in diameter than Sfi1-RFP dot suggesting that dynein is recruited to entire SPB structure. Bar, 5µm. Bar of magnified image, 1µm. **(D**) Timelapse images of Dhc1-3xGFP in mating cells co-expressing Cut11-mCherry spanning time point of initial detection of dynein (-35min) in one cell until SPB fusion (t=0). **(E)** SPB intensities of Dhc1-3xGFP in individual cells depicted in (D) over time until completion of nuclear congression (t_0). **(F)** Median time of initial detection of dynein in mating cells prior to SPB fusion in wildtype and *klp2Δ* zygotes. Mean values for wildtype (31.2±29.2min) and *klp2Δ* (49.2±28.1min, $p<10^{-5}$) for n=100 SPBs. **(G)** Mean SPB intensities of Dhc1-3xGFP averaged for a cell population (n=100 SPBs) from 15min (for wildtype) or 35min (for *klp2Δ*) prior to SPB fusion. Error Bars: s.d. Dotted line highlights similar dynein level between wildtype and *klp2Δ* zygotes. Bar, 5µm if not stated otherwise.

Figure 4. Dynein functions at the SPB during nuclear congression independent of the dynactin complex

(A) Time of nuclear congression in wildtype and dynein-related single and *klp2Δ* double *klp2Δ* mutants at 25°C. Mean values (p-values against wildtype or *klp2Δ* respectively): wildtype (28.6±7.3min, n=104), *klp2Δ* (47.6±12.8min, $p<10^{-22}$, n=84), *dhc1Δ* (33.7±9.4min, $p<10^{-4}$, n=87), *num1Δ* (30.9±9.2min, p=0.09, n=58), *klp2Δ num1Δ* (48.1±15.9min, p=0.85, n=42), *dhc1(1-1266)*

(34.8±9.9min, $p<10^{-4}$, n=56), *ssm4Δ* (28.9±8.9min, p=0.78, n=65), *klp2Δ ssm4Δ* (44.5±13.7min, p=0.12, n=96), *dli1Δ* (33.3±10.7min, p=0.003, n=60), *klp2Δ dli1Δ* (118.8±65.3min, $p<10^{-6}$, n=33/101) and *klp2Δ dhc1Δ* (34.5±7.2min, n=64). **(B)** Percentage of zygotes completing nuclear congression in wildtype (100%, n=104), *klp2Δ dhc1Δ* (2.4%, n=85), *klp2Δ num1Δ* (100%, n=42), *klp2Δ dhc1(1-1266)* (1.8%, n=56), *klp2Δ ssm4Δ* (100%, n=96) and *klp2Δ dli1Δ* (20.8%, n=101). **(C, D)** Cellular distribution of Dhc1-3xGFP in mating *dhc1(1-1266)* (C) and wildtype, *ssm4Δ* and *dli1Δ* (D) cells co-expressing Cut11-mCherry and mCherry-Atb2 at 25°C. Images are represented as maximum z-projection of 3D stacks. Dotted lines represent outlines of cells in different stages of meiotic prophase. **(E)** Frequency of time points when dynein was detected at SPBs relative to SPB fusion in wildtype, *ssm4Δ* and *dli1Δ* zygotes (n=50 cells). **(F)** SPB intensities of Dhc1-3xGFPat the time point of SPB fusion averaged for a cell population of wildtype, *ssm4Δ* and *dli1Δ* zygotes (n=50SPBs). Bars, 5µm.

Figure 5. Model for nuclear congression in fission yeast

Upon fusion of two haploid cells, MTs dominantly nucleated at SPBs extend into the cytoplasm of the mating partner. Kinesin-14 Klp2 at MT plus ends cross-links MTs in an anti-parallel fashion. Two models for kinesin-14-dependent generation of pulling forces are proposed: 1. Klp2 slides anti-parallel MTs or 2. Klp2 induces depolymerization and cross-links shrinking plus ends. During nuclear congression, dynein accumulates at the SPB (represented by increasing size) resulting in acceleration of nuclear migrations. SPB-bound dynein may exert pulling forces on MTs emanating from the opposite SPB. These parallel mechanisms ensure nuclear congression in fission yeast and illustrate distinct roles for two minus end-directed motor proteins in the same process.

Figure 1. Scheffler et al.

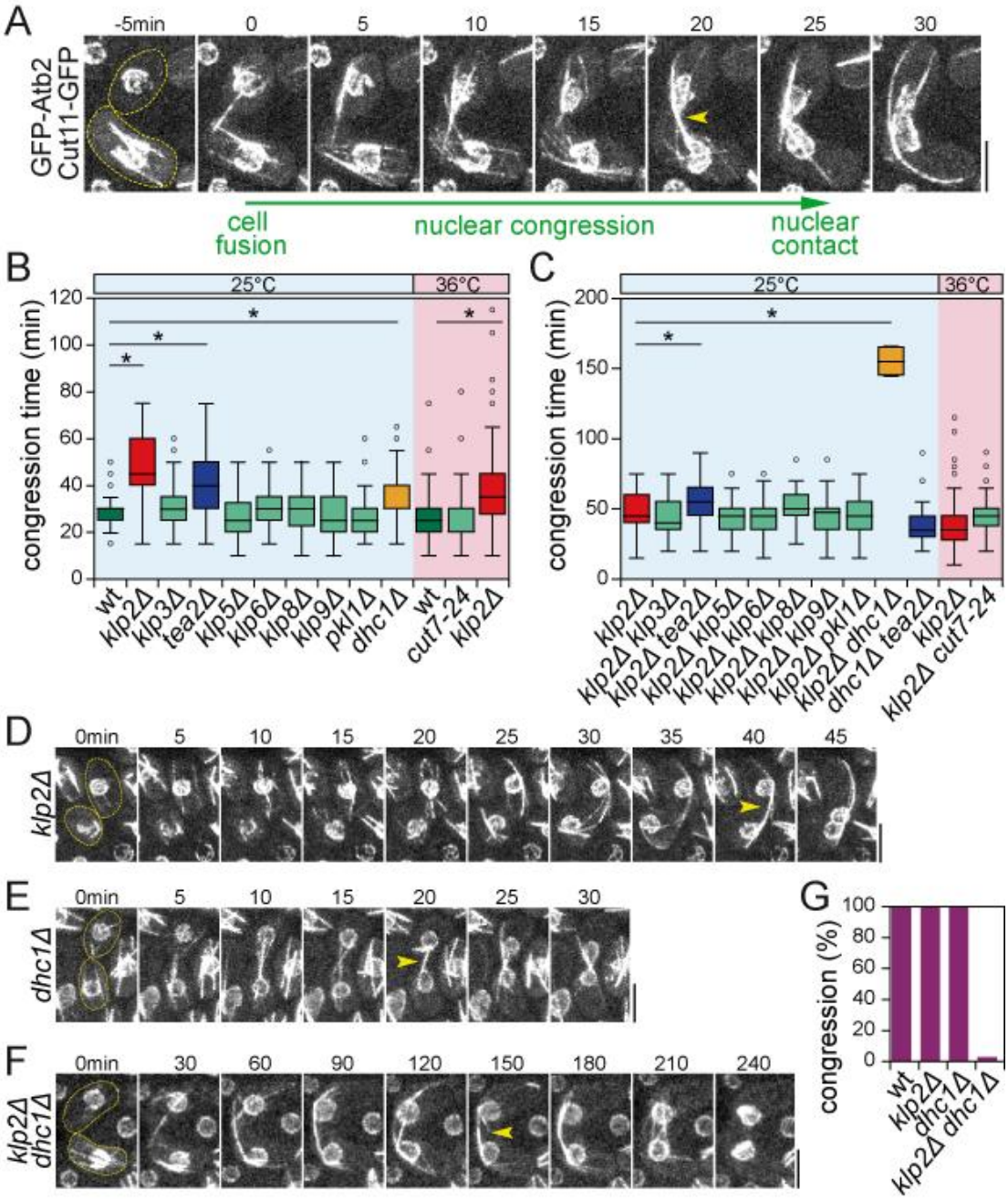

Figure 2. Scheffler et al.

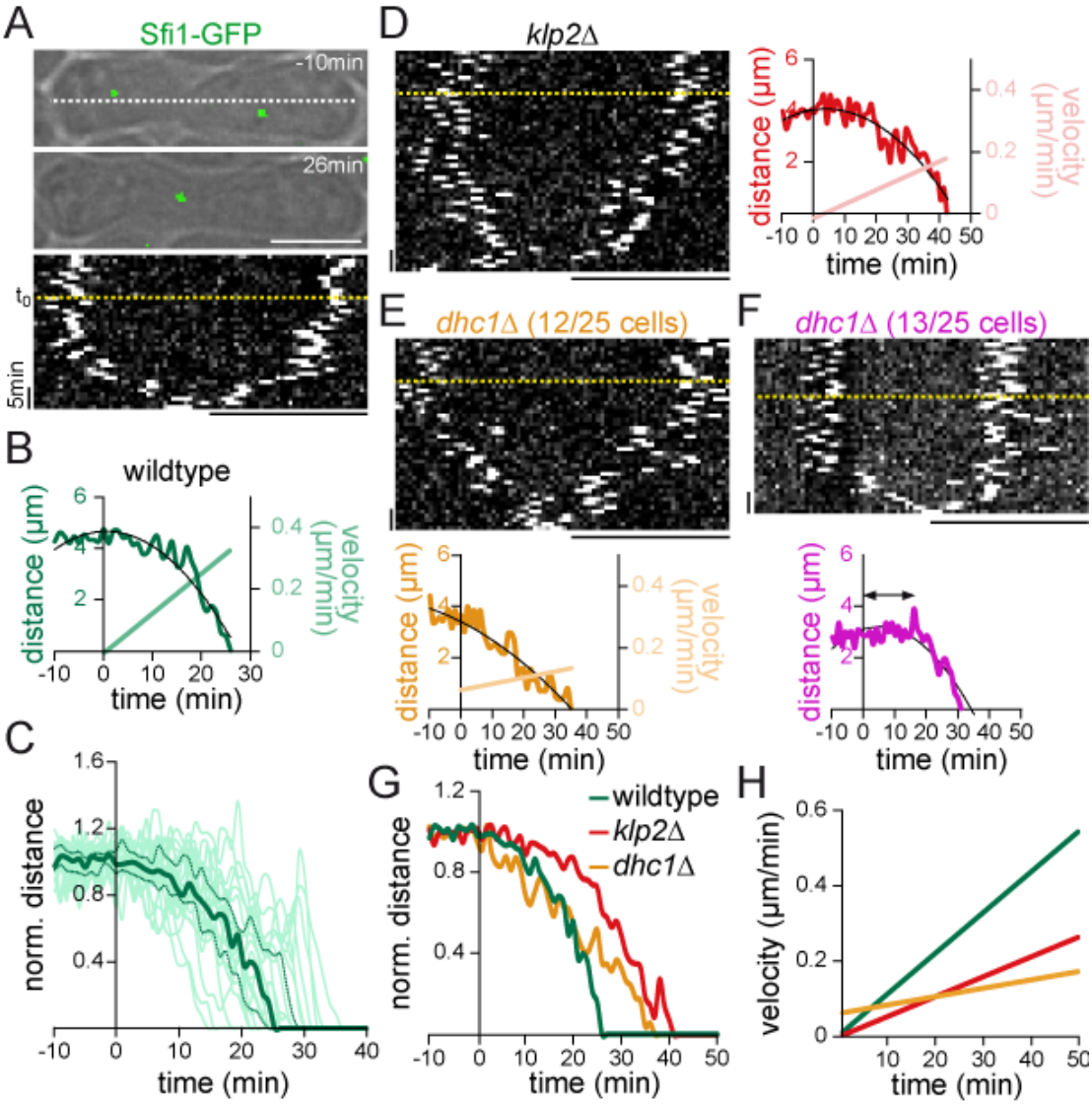

Figure 3. Scheffler et al.

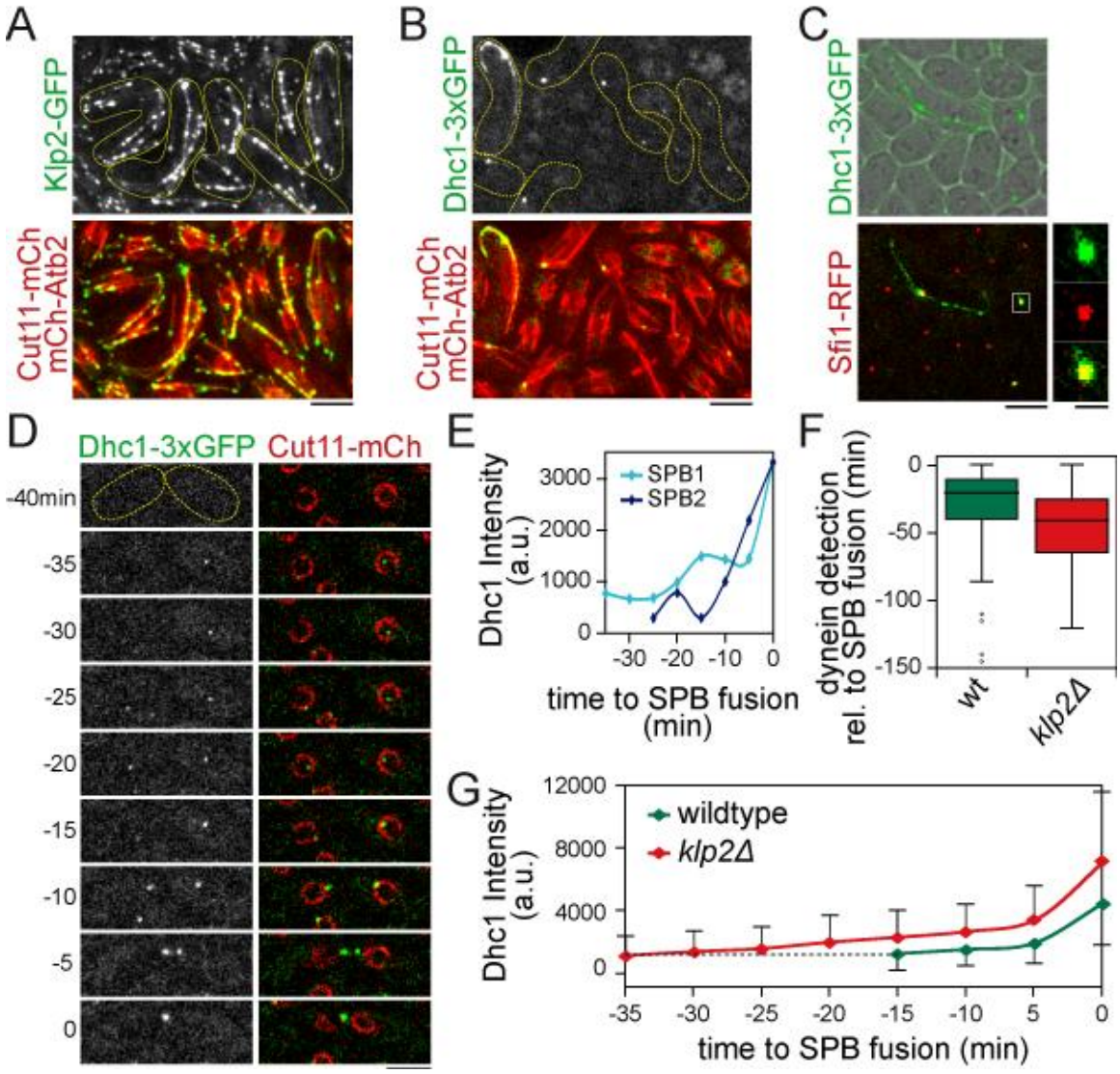

Figure 4. Scheffler et al.

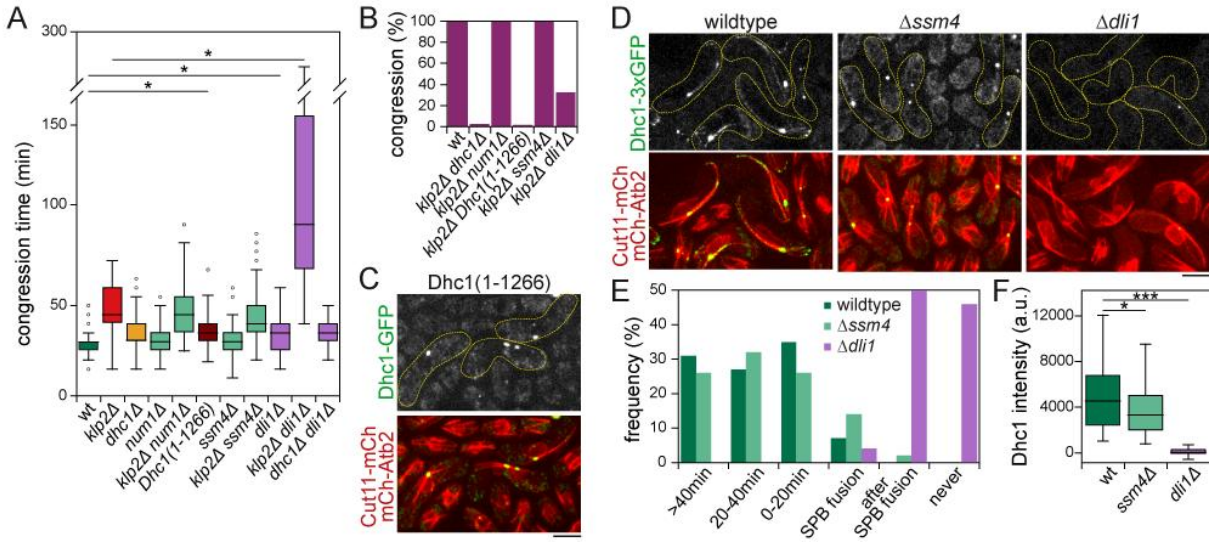

Figure 5. Scheffler et al.

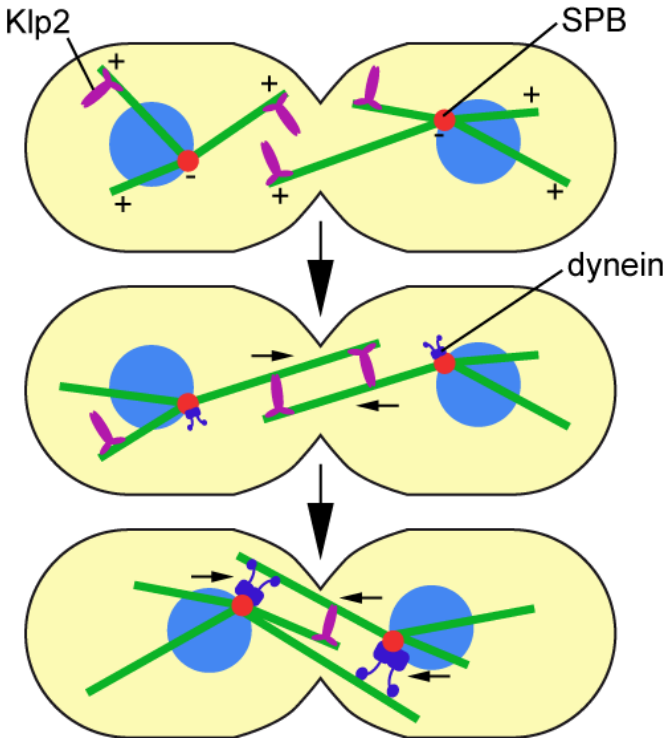

Inventory of Supplemental information

Figure S1: Complement to Figure 1.

Figure S2: Complement to Figure 2.

Figure S3. Complement to Figure 3.

Figure S4. Complement to Figure 4.

Figure Legends

Table S1. List of strains used in this study.

Supplemental References

Figure S1. Scheffler et al.

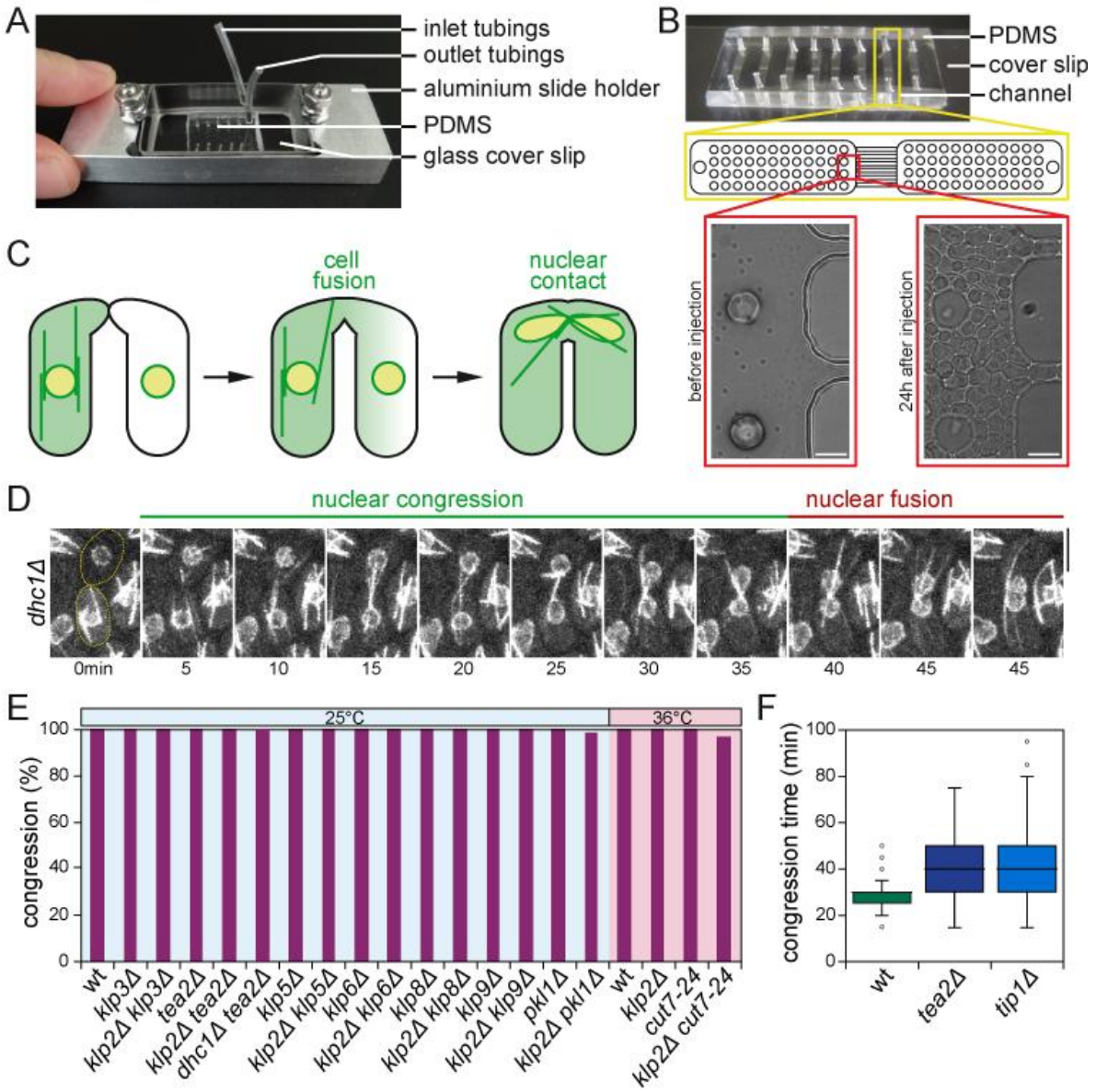

Figure S2. Scheffler et al.

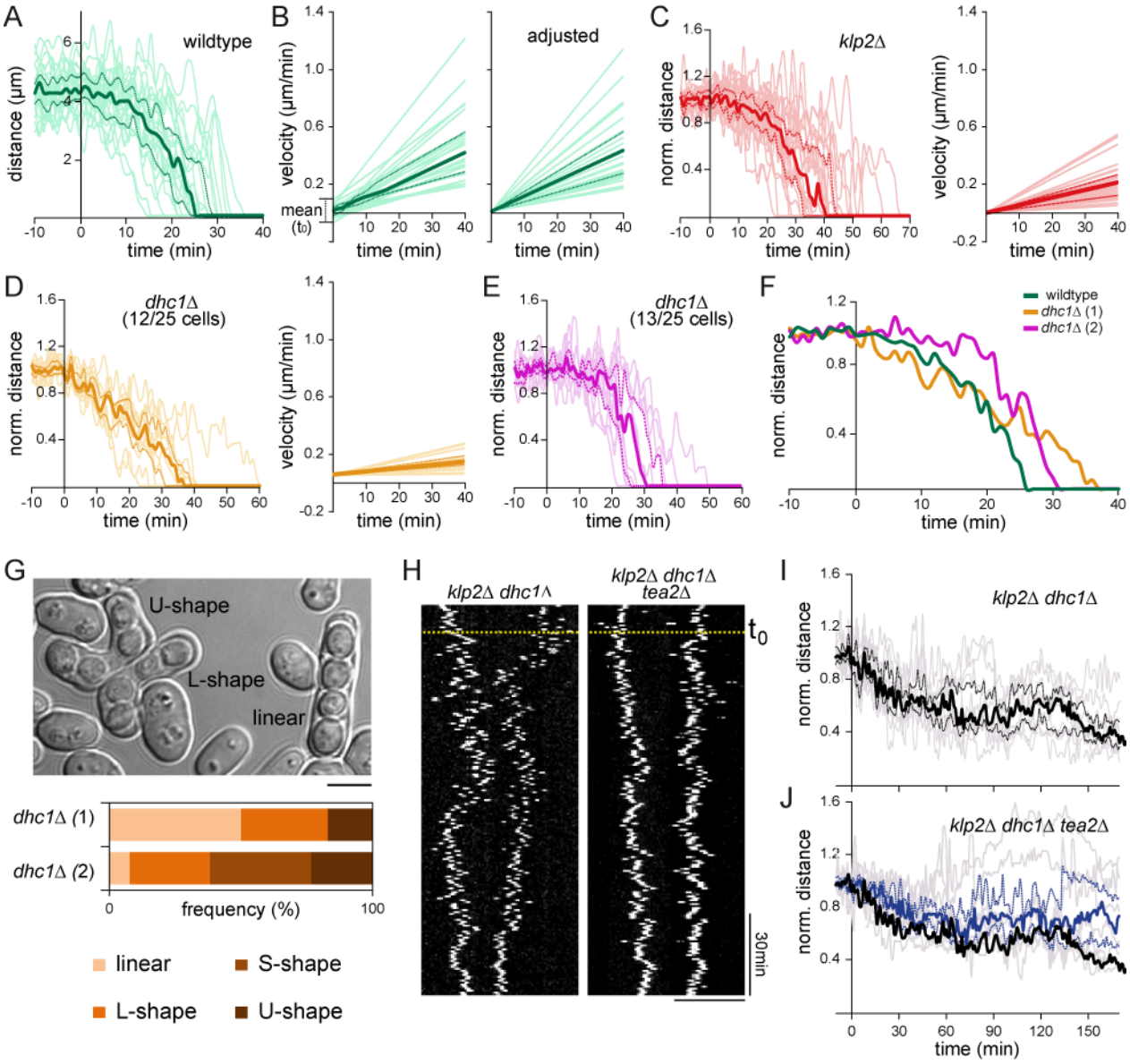

Figure S3. Scheffler et al.

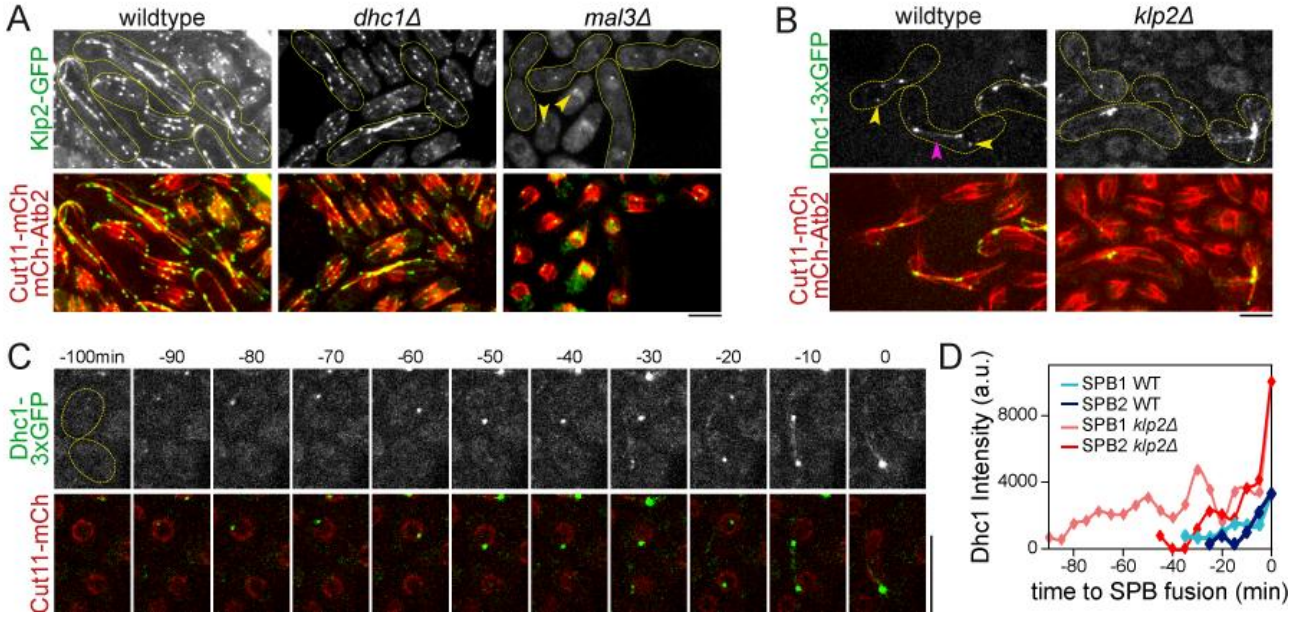

Figure S4. Scheffler et al.

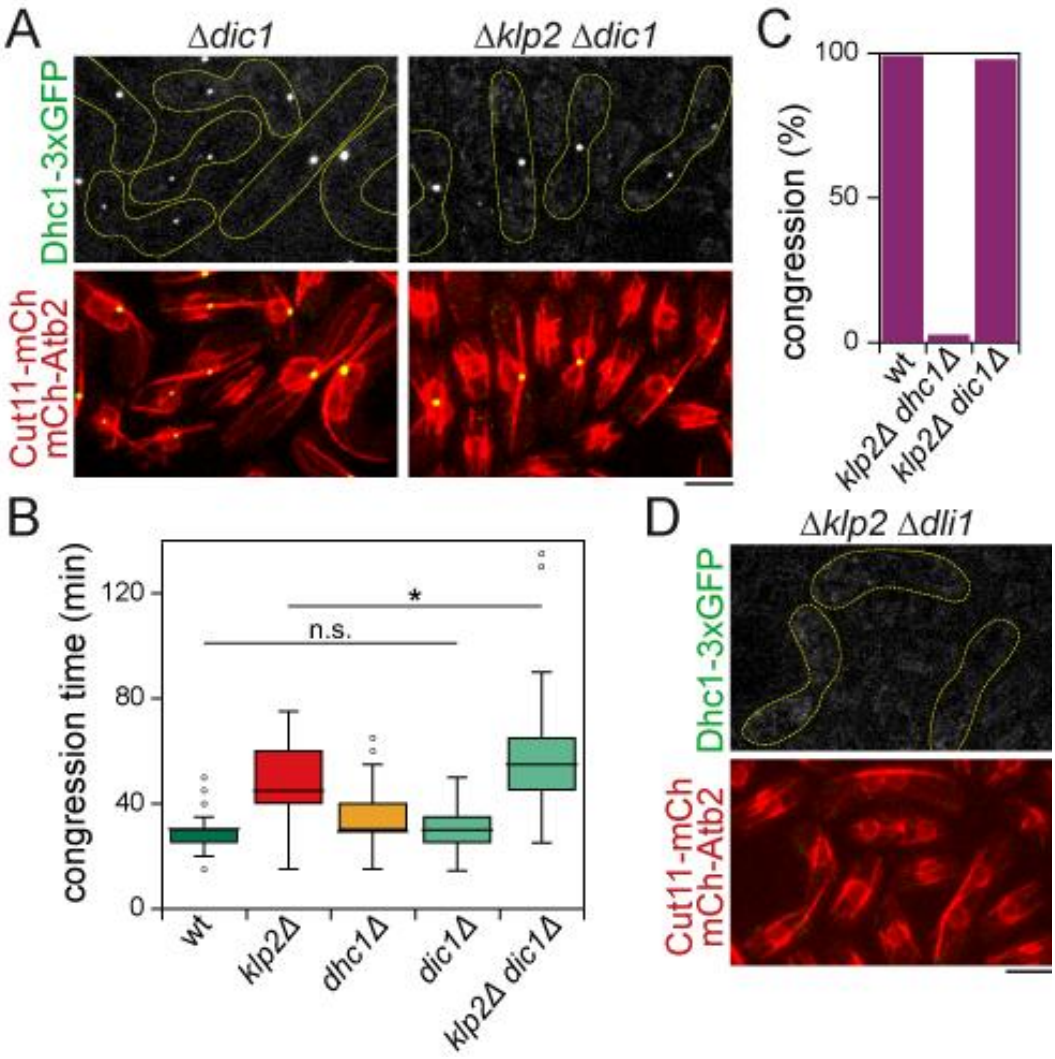

Supplemental

Figure S1.

(A) Microfluidic channels for long-term imaging of mating cells. Shown is a typical cell chamber made by bonding a polydimethylsiloxane (PDMS) replica onto a glass cover slip inserted into an aluminum slide holder. Cells can be syringe-pumped into chamber through inlet. Inlet and outlet tubings serve as reservoirs for liquid medium required for long-term imaging. **(B)** PDMS replica contains straight microfluidic channels hindering cells from entering and leading to an accumulation of cells at the front where mating occurs. **(C)** Schematic representing early steps of karyogamy from cell fusion marked by cytoplasmic exchange between mating cells until completion of nuclear congression. **(D)** Time-lapse images of mating *dhc1Δ* cells expressing Cut11-GFP and unilaterally GFP-Atb2 25°C as shown in Fig. 1E. Further time points after establishment of nuclear contact are depicted to illustrate delayed nuclear fusion process. Bar, 5µm. **(E)** Percentage of zygotes completing nuclear congression in motor mutants at 25°C and 36°C. In most strains, nuclear congression is completed with 100% success, except for *klp2Δ pkl1Δ* (98.6%) and *klp2Δ cut7-24* (96.7%). n≥44. **(F)** Time of nuclear congression in wildtype (28.6±7.3min, n=104), *tea2Δ* (41.6±14.9min, $p<10^{-11}$, n=94) and *tip1Δ* (41.9±16.7min, $p=<10^{-8}$, n=80).

Figure S2.

(A) SPB distances over time in individual cells depicted as light green trajectories (n=25), but not normalized in comparison to Fig. 1C. Median is represented as a thick line and upper and lower quartiles as dotted lines. **(B)** Velocities obtained as differential functions of a second degree polynomial of SPB distances. Median is represented as a thick line and upper and lower quartiles as dotted lines. Left, original data sets. Right, velocity graphs individually adjusted to the average value of velocity at t_0. **(C)** Left, SPB distances over time normalized to average SPB distance prior to cell fusion in individual *klp2Δ* cells depicted as light red trajectories (n=25). Right, velocities (adjusted) in *klp2Δ* cells. **(D, E)** Normalized SPB distances over time for first (D, left) and second (E) subset of *dhc1Δ* zygotes as well as velocities for first subset of *dhc1Δ* zygotes (D, right). Number of events is indicated. **(F)** Median curves of normalized SPB distances over time in wildtype and first and second subset of *dhc1Δ* zygotes. **(G)** Top, DIC images illustrating the varying shapes of mating cells. Bottom, frequency of different zygote shapes in both subsets of the *dhc1Δ* mutant. **(H-J)** Sfi1-GFP dynamics in *klp2Δ dhc1Δ* double (H, I) and *klp2Δ dhc1Δ tea2Δ* triple (H, J) mutant zygotes. Median SPB distances were calculated from 10 cells. Bars, 5µm

Figure S3.

(A) Cellular distribution of Klp2-GFP in mating wildtype, *dhc1Δ* and *mal3Δ* cells co-expressing Cut11-mCherry and mCherry-Atb2 at 25°C. Images are represented as maximum z-projection of 3D stacks.

Dotted lines represent outlines of cells in different stages of meiotic prophase**. (B**) Cellular distribution of dynein (Dhc1-3xGFP) in mating wildtype and *klp2Δ* cells co-expressing Cut11-mCherry and mCherry-Atb2 at 25°C. Yellow arrowheads highlight multiple dots of dynein along nuclear envelope through co-recruitment to SPB and telocentrosomes. Magenta arrowhead highlights rarely detected localization of dynein along MTs during nuclear congression. **(C**) Time-lapse images of Dhc1-3xGFP in mating *klp2Δ* cells co-expressing Cut11-mCherry spanning time point of initial detection of dynein (-90min) in one cell until SPB fusion (t=0). **(D)** SPB intensities of Dhc1-3xGFP in individual cells depicted in Fig. 3D for wildtype and (D) for *klp2Δ* over time until completion of SPB fusion (t=0).

Figure S4.

(A) Cellular distribution of Dhc1-3xGFP in mating *dic1Δ* and *klp2Δ dic1Δ* cells co-expressing Cut11-mCherry and mCherry-Atb2 at 25°C. Images are represented as maximum z-projection of 3D stacks. Dotted lines represent outlines of cells in different stages of meiotic prophase. **(B)** Time of nuclear congression (p-values against wildtype or *klp2Δ* respectively) in wildtype (28.6±7.3min, n=104), *klp2Δ* (47.6±12.8min, $p<10^{-22}$, n=84), *dhc1Δ* (33.7±9.4min, $p<10^{-4}$, n=87), *dic1Δ* (29.7±8.6min, p=0.35, n=72) and *klp2Δ dic1Δ* (55.7±21.2min, p=0.008, n=65). **(C)** Percentage of zygotes completing nuclear congression in wildtype (100%, n=104), *klp2Δ dhc1Δ* (2.4%, n=85), and *klp2Δ dic1Δ* (98.5%, n=66). **(D)** Cellular distribution of Dhc1-3xGFP in mating *klp2Δ dli1Δ* cells co-expressing Cut11-mCherry and mCherry-Atb2 at 25°C.

Table S1. List of *S. pombe* strains used in this study.

Strain	*Genotype*	Source
	Figure 1	
TP913	*h- ade6-M210 leu1-32 ura4-D18 cut11-GFP::Nat^R*	lab collection (West et al., 1998)
TP914	*h+ ade6-M210 leu1-32 ura4-D18 cut11-GFP::Nat^R GFP-atb2::KanMX6*	this work
TP1074	*h- ade6-M210 leu1-32 ura4-D18 klp2Δ::KanMX6 cut11-GFP::Nat^R*	this work (Troxell et al., 2001)
TP1075	*h+ ade6-M210 leu1-32 ura4-D18 klp2Δ::KanMX6 cut11-GFP::Nat^R GFP-atb2::KanMX6*	this work
TP1540	*h- ade6-M210 leu1-32 ura4-D18 klp3Δ::Nat^R cut11-GFP::Nat^R*	this work (lab collection)
TP1541	*h+ ade6-M210 leu1-32 ura4-D18 klp3Δ::Nat^R cut11-GFP::Nat^R GFP-atb2::KanMX6*	this work
TP1550	*h+ ade6-M210 leu1-32 ura4-D18 tea2Δ::his3+ cut11-GFP::Nat^R*	this work (Browning et al., 2000)
TP1551	*h- ade6-M216 leu1-32 ura4-D18 tea2Δ::his3+ cut11-GFP::Nat^R GFP-atb2::KanMX6*	this work
TP1542	*h- ade6-M210 leu1-32 ura4-D18 klp5Δ::ura4+ cut11-GFP::Nat^R*	this work (West et al., 2001)
TP1543	*h+ ade6-M210 leu1-32 ura4-D18 klp5Δ::ura4+ cut11-GFP::Nat^R GFP-atb2::KanMX6*	this work
TP1544	*h- ade6-M210 leu1-32 ura4-D18 klp6Δ::ura4+ cut11-GFP::Nat^R*	this work (West et al., 2001)
TP1545	*h+ ade6-M216 leu1-32 ura4-D18 klp6Δ::ura4+ cut11-GFP::Nat^R GFP-atb2::KanMX6*	this work
TP915	*h- ade6-M210 leu1-32 ura4-D18 klp8Δ ::Nat^R cut11-GFP::KanMX6*	this work (Fu et al., 2009)
TP916	*h+ ade6-M210 leu1-32 ura4-D18 klp8Δ ::Nat^R cut11-GFP::KanMX6 GFP-atb2::KanMX6*	this work
TP1548	*h+ ade6-M210 leu1-32 ura4-D18 klp9Δ::ura4+ cut11-GFP::Nat^R*	this work (Fu et al., 2009)
TP1549	*h+ ade6-M216 leu1-32 ura4-D18 klp9Δ::ura4+ cut11-GFP::Nat^R*	this work
TP1670	*h- ade6-M210 leu1-32 ura4-D18 pkl1Δ::KanMX6 cut11-GFP::Nat^R*	this work (Syrovatkina et al., 2013)
TP1672	*h+ ade6-M216 leu1-32 ura4-D18 pkl1Δ::KanMX6 cut11-GFP::Nat^R GFP-atb2::KanMX6*	this work
TP1538	*h+ ade6-M210 leu1-32 ura4-D18 dhc1Δ::KanMX6 cut11-GFP::Nat^R*	this work (Fu et al., 2009)
TP1539	*h- ade6-M216 leu1-32 ura4-D18 dhc1Δ::KanMX6 cut11-GFP::Nat^R GFP-atb2::KanMX6*	this work
TP1577	*h+ ade6-M210 leu1-32 ura4-D18 cut7-24 cut11-GFP::Nat^R*	this work (Samejima et al., 1993)
TP1578	*h+ leu1-32 ura4-D18 cut7-24 cut11-GFP::Nat^R GFP-atb2::KanMX6*	this work
TP1621	*h- ade6-M210 leu1-32 ura4-D18 klp2Δ::Hph^R klp3Δ::Nat^R cut11-GFP::Nat^R*	this work
TP1622	*h+ ade-M210 6 leu1-32 ura4-D18 klp2Δ::Hph^R klp3Δ::Nat^R cut11-GFP::Nat^R GFP-atb2::KanMX6*	this work
TP1651	*h+ ade6-M210 leu1-32 ura4-D18 klp2Δ::Hph^R tea2Δ::his3+ cut11-GFP::Nat^R*	this work
TP1681	*h- ade6-M210 leu1-32 ura4-D18 klp2Δ::Hph^R tea2Δ::his3+ cut11-GFP::Nat^R GFP-atb2::KanMX6*	this work
TP1623	*h- ade6-M210 leu1-32 ura4-D18 klp2Δ::Hph^R klp5Δ::ura4+ cut11-GFP::Nat^R*	this work
TP1624	*h+ ade6-M210 leu1-32 ura4-D18 klp2Δ::Hph^R klp5Δ::ura4+ cut11-GFP::Nat^R GFP-atb2::KanMX6*	this work
TP1625	*h- ade6-M210 leu1-32 ura4-D18 klp2Δ::Hph^R klp6Δ::ura4+ cut11-GFP::Nat^R*	this work
TP1626	*h+ ade6-M210 leu1-32 ura4-D18 klp2Δ::Hph^R klp6Δ::ura4+ cut11-GFP::Nat^R GFP-*	this work

	atb2::KanMX6	
TP1085	*h- ade6-M210 leu1-32 ura4-D18 klp2Δ::KanMX6 klp8Δ::Nat^R cut11-GFP:: KanMX6*	this work
TP1087	*h+ ade6-M210 leu1-32 ura4-D18 klp2Δ::KanMX6 klp8Δ::Nat^R cut11-GFP:: KanMX6 GFP-atb2::KanMX6*	this work
TP1649	*h- ade6-M210 leu1-32 ura4-D18 klp2Δ::Hph^R klp9Δ::ura4+ cut11-GFP::Nat^R*	this work
TP1680	*h+ ade6-M210 leu1-32 ura4-D18 klp2Δ::Hph^R klp9Δ::ura4+ cut11-GFP::Nat^R GFP-atb2::KanMX6*	this work
TP1703	*h+ ade6-M210 leu1-32 ura4-D18 klp2Δ::Hph^R pkl1Δ::KanMX6 cut11-GFP::Nat^R*	this work
TP1732	*h- leu1-32 ura4-D18 klp2Δ::Hph^R pkl1Δ::KanMX6 cut11-GFP::Nat^R GFP-atb2::KanMX6*	this work
TP1661	*h+ ade6-M210 leu1-32 ura4-D18 klp2Δ::Hph^R dhc1Δ::KanMX6 cut11-GFP::Nat^R*	this work
TP1663	*h- ade6-M216 leu1-32 ura4-D18 klp2Δ::Hph^R dhc1Δ::KanMX6 cut11-GFP::Nat^R GFP-atb2::KanMX6*	this work
TP2264	*h+ ade6-M210 leu1-32 ura4-D18 tea2Δ::his3+ dhc1Δ::KanMX6 cut11-GFP::Nat^R*	this work
TP2233	*h- ade6-M216 leu1-32 ura4-D18 tea2Δ::his3+ dhc1Δ::KanMX6 cut11-GFP::Nat^R GFP-atb2::KanMX6*	this work
TP1655	*h+ ade6-M210 leu1-32 ura4-D18 klp2Δ::Hph^R cut7-24 cut11-GFP::Nat^R*	this work
TP1697	*h- ade6-M210 leu1-32 ura4-D18 klp2Δ::Hph^R cut7-24 cut11-GFP::Nat^R GFP-atb2::KanMX6*	this work
	Figure 2	
TP1974	*h+ ade6-M216 leu1-32 ura4-D18 sfi1-GFP::KanMX6*	this work (Almonacid et al., 2011)
AP3932	*h- leu1-32 ura4-D18 sfi1-GFP::KanMX6 mCherry-atb2::Hph^R*	Lab collection
TP1975	*h- ade6-M216 leu1-32 ura4-D18 klp2Δ::ura4+ sfi1-GFP::KanMX6*	this work
TP1976	*h+ ade6-M216 leu1-32 ura4-D18 klp2Δ::ura4+ sfi1-GFP::KanMX6 mCherry-atb2::Hph^R*	this work
TP1977	*h- ade6-M216 leu1-32 ura4-D18 dhc1Δ::ura4+ sfi1-GFP::KanMX6*	this work
TP1978	*h+ ade6-M216 leu1-32 ura4-D18 dhc1Δ::ura4+ sfi1-GFP::KanMX6 mCherry-atb2::Hph^R*	this work
	Figure 3	
TP1667	*h90 ade6-M216 leu1-32 ura4-D18 klp2-GFP::ura4+ cut11-mCherry::KanMX6 mCherry-atb2::Hph^R*	this work (Troxell et al., 2001)
TP1760	*h90 ade6-M210 leu1-32 ura4-D18 dhc1-3xGFP::KanMX6 cut11-mCherry::Hph^R mCherry-atb2::Hph^R*	this work (Fujita et al., 2010)
TP1926	*h90 ade6-M210 leu1-32 ura4-D18 dhc1-3xGFP::Nat^R sfi1-mRFP::KanMX6*	this work
TP2247	*h90 ade6-M216 leu1-32 ura4-D18 dhc1-3xGFP::Nat^R cut11-mCherry::Hph^R*	this work
TP2215	*h90 ade6-M210 leu1-32 ura4-D18 klp2Δ::ura4+ dhc1-3xGFP::KanMX6 cut11-mCherry::Nat^R*	this work
	Figure 4	
TP1738	*h+ ade6-M216 leu1-32 ura4-D18 num1Δ::KanMX6 cut11-GFP::ura4+*	this work, BIONEER deletion collection
TP1737	*h- ade6-M210 leu1-32 ura4-D18 num1Δ::KanMX6 cut11-GFP::ura4+ GFP-atb2::Nat^R*	this work
TP1888	*h+ ade6-M210 leu1-32 ura4-D18 klp2Δ::Hph^R num1Δ::KanMX6 cut11-GFP::ura4+*	this work
TP1859	*h- leu1-32 ura4-D18 klp2Δ::Hph^R num1Δ::KanMX6 cut11-GFP::ura4+ GFP-atb2::Nat^R*	this work
TP2375	*h+ ade6-M210 leu1-32 ura4-D18 dhc1(1-1266)-GFP::leu1+ cut11-GFP::Nat^R*	this work (Yoshida et al., 2013)

TP2376	*h- leu1-32 ura4-D18 dhc1(1-1266)-GFP::leu1+ cut11-GFP::Nat^R GFP-atb2::KanMX6*	this work
TP2377	*h- leu1-32 ura4-D18 klp2Δ::Hph^R dhc1(1-1266)-GFP::leu1+ cut11-GFP::Nat^R*	this work
TP2389	*h+ leu1-32 ura4-D18 klp2Δ::Hph^R dhc1(1-1266)-GFP::leu1+ cut11-GFP::Nat^R GFP-atb2::KanMX6*	this work
TP1795	*h- ade6-M210 leu1-32 ura4-D18 ssm4Δ::KanMX6 cut11-GFP::ura4+*	this work, BIONEER deletion collection
TP1741	*h+ ade6-M210 leu1-32 ura4-D18 ssm4Δ::KanMX6 cut11-GFP::ura4+ GFP-atb2::Nat^R*	this work
TP1796	*h- leu1-32 ura4-D18 klp2Δ::Hph^R ssm4Δ::KanMX6 cut11-GFP::ura4+*	this work
TP1797	*h- leu1-32 ura4-D18 klp2Δ::Hph^R ssm4Δ::KanMX6 cut11-GFP::ura4+ GFP-atb2::Nat^R*	this work
TP1722	*h+ ade6-M216 leu1-32 ura4-D18 dli1Δ::KanMX6 cut11-GFP::Nat^R*	this work, BIONEER deletion collection
TP1723	*h- ade6-M210 leu1-32 ura4-D18 dli1Δ::KanMX6 cut11-GFP::Nat^R GFP-atb2::KanMX6*	this work
TP1860	*h+ ade6-M210 leu1-32 ura4-D18 klp2Δ::Hph^R dli1Δ::KanMX6 cut11-GFP::ura4+*	this work
TP1878	*h- leu1-32 ura4-D18 klp2Δ::Hph^R dli1Δ::KanMX6 cut11-GFP::ura4+ GFP-atb2::Nat^R*	this work
TP2074	*h+ ade6-M216 leu1-32 ura4-D18 dhc1Δ::KanMX6 dli1Δ::ura4+ cut11-GFP::Nat^R*	this work
TP2034	*h- ade6-M216 leu1-32 ura4-D18 dhc1Δ::KanMX6 dli1Δ::ura4+ cut11-GFP::Nat^R GFP-atb2::KanMX6*	this work
TP2286	*h90 leu1-32 ura4-D18 dhc1(1-1266)-GFP::leu1+ sad1-DsRed::leu1+ cut11-mCherry::Hph^R mCherry-atb2::Hph^R*	this work
TP2102	*h90 ade6-M210 leu1-32 ura4-D18 ssm4Δ::KanMX6 dhc1-3xGFP::Nat^R cut11-mCherry::Nat^R mCherry-atb2::Hph^R*	this work
TP1963	*h90 ade6-M210 leu1-32 ura4-D18 dli1Δ::KanMX6 dhc1-3xGFP::Nat^R cut11-mCherry::Hph^R mCherry-atb2::Hph^R*	this work
TP2216	*h90 ade6-M210 leu1-32 ura4-D18 ssm4Δ::KanMX6 dhc1-3xGFP::Nat^R cut11-mCherry::Nat^R*	this work
TP2292	*h90 ade6-M216 leu1-32 ura4-D18 dli1Δ::KanMX6 dhc1-3xGFP::Nat^R sfi1-mRFP::ura4+*	this work
	Figure S1	
TP1559	*h- ade6-M210 leu1-32 ura4-D18 tip1Δ::KanMX6 cut11-GFP::Nat^R*	this work (Brunner and Nurse, 2000)
TP1560	*h+ ade-M216 leu1-32 ura4-D18 tip1Δ::KanMX6 cut11-GFP::Nat^R GFP-atb2::KanMX6*	this work
	Figure S2	
TP1991	*h+ ade6-M216 leu1-32 ura4-D18 klp2Δ::Hph^R dhc1Δ::ura4+ sfi1-GFP::KanMX6*	this work
TP1992	*h- ade6-M210 leu1-32 ura4-D18 klp2Δ::Hph^R dhc1Δ::ura4+ sfi1-GFP::KanMX6 mCherry-atb2::Hph^R*	this work
TP2383	*h- ade6-M216 leu1-32 ura4-D18 klp2Δ::Hph^R dhc1Δ::ura4+ tea2Δ::his3+ sfi1-GFP::KanMX6*	this work
TP2374	*h+ ade6-M210 leu1-32 ura4-D18 klp2Δ::Hph^R dhc1Δ::ura4+ tea2Δ::his3+ sfi1-GFP::KanMX6 mCherry-atb2::Hph^R*	this work
	Figure S3	
TP2318	*h90 ade6-M216 leu1-32 ura4-D18 mal3Δ::KanMX6 klp2-GFP::ura4+ cut11-mCherry::Nat^R mCherry-atb2::Hph^R*	this work
	Figure S4	
TP1963	*h90 ade6-M210 leu1-32 ura4-D18 dic1Δ::KanMX6 dhc1-3xGFP::Nat^R cut11-mCherry::Hph^R mCherry-atb2::Hph^R*	this work, BIONEER deletion collection
TP2026	*h90 ade6-M216 leu1-32 ura4-D18 klp2Δ::ura4+ dic1Δ::KanMX6 dhc1-3xGFP::Nat^R*	this work

	cut11-mCherry::Hph^R mCherry-atb2::Hph^R	
TP1724	*h- ade6-M210 leu1-32 ura4-D18 dic1Δ::KanMX6 cut11-GFP::Nat^R*	this work
TP1725	*h+ ade6-M210 leu1-32 ura4-D18 dic1Δ::KanMX6 cut11-GFP::Nat^R GFP-atb2::KanMX6*	this work
TP1799	*h- ade6-M210 leu1-32 ura4-D18 klp2Δ::Hph^R dic1Δ::KanMX6 cut11-GFP::ura4+*	this work
TP1800	*h+ leu1-32 ura4-D18 klp2Δ::Hph^R dic1Δ::KanMX6 cut11-GFP::ura4+ GFP-atb2::Nat^R*	this work
TP2025	*h90 ade6-M210 leu1-32 ura4-D18 klp2Δ::ura4+ dli1Δ::KanMX6 dhc1-3xGFP::Nat^R cut11-mCherry::Hph^R mCherry-atb2::Hph^R*	this work

Supplemental References

Almonacid, M., Celton-Morizur, S., Jakubowski, J.L., Dingli, F., Loew, D., Mayeux, A., Chen, J.S., Gould, K.L., Clifford, D.M., and Paoletti, A. (2011). Temporal control of contractile ring assembly by Plo1 regulation of myosin II recruitment by Mid1/anillin. Curr Biol *21*, 473-479.

Browning, H., Hayles, J., Mata, J., Aveline, L., Nurse, P., and McIntosh, J.R. (2000). Tea2p is a kinesin-like protein required to generate polarized growth in fission yeast. J Cell Biol *151*, 15-28.

Brunner, D., and Nurse, P. (2000). CLIP170-like tip1p spatially organizes microtubular dynamics in fission yeast. Cell *102*, 695-704.

Fu, C., Ward, J.J., Loiodice, I., Velve-Casquillas, G., Nedelec, F.J., and Tran, P.T. (2009). Phospho-regulated interaction between kinesin-6 Klp9p and microtubule bundler Ase1p promotes spindle elongation. Dev Cell *17*, 257-267.

Fujita, I., Yamashita, A., and Yamamoto, M. (2010). Contribution of dynein light intermediate and intermediate chains to subcellular localization of the dynein-dynactin motor complex in Schizosaccharomyces pombe. Genes Cells *15*, 359-372.

Samejima, I., Matsumoto, T., Nakaseko, Y., Beach, D., and Yanagida, M. (1993). Identification of seven new cut genes involved in Schizosaccharomyces pombe mitosis. J Cell Sci *105 (Pt 1)*, 135-143.

Syrovatkina, V., Fu, C., and Tran, P.T. (2013). Antagonistic spindle motors and MAPs regulate metaphase spindle length and chromosome segregation. Curr Biol *23*, 2423-2429.

Troxell, C.L., Sweezy, M.A., West, R.R., Reed, K.D., Carson, B.D., Pidoux, A.L., Cande, W.Z., and McIntosh, J.R. (2001). pkl1(+)and klp2(+): Two kinesins of the Kar3 subfamily in fission yeast perform different functions in both mitosis and meiosis. Mol Biol Cell *12*, 3476-3488.

West, R.R., Malmstrom, T., Troxell, C.L., and McIntosh, J.R. (2001). Two related kinesins, klp5+ and klp6+, foster microtubule disassembly and are required for meiosis in fission yeast. Mol Biol Cell *12*, 3919-3932.

West, R.R., Vaisberg, E.V., Ding, R., Nurse, P., and McIntosh, J.R. (1998). cut11(+): A gene required for cell cycle-dependent spindle pole body anchoring in the nuclear envelope and bipolar spindle formation in Schizosaccharomyces pombe. Mol Biol Cell *9*, 2839-2855.

Yoshida, M., Katsuyama, S., Tateho, K., Nakamura, H., Miyoshi, J., Ohba, T., Matsuhara, H., Miki, F., Okazaki, K., Haraguchi, T.*, et al.* (2013). Microtubule-organizing center formation at telomeres induces meiotic telomere clustering. J Cell Biol *200*, 385-395.

Results Part II –

A novel factor in cellular morphogenesis of fission yeast

In this chapter, the results obtained in this study concerning the characterization of the novel AAA^+ ATPase Knk1are presented in form of an article entitled: *The oscillatory AAA+ ATPase Knk1 constitutes a novel morphogenetic pathway in fission yeast*. This article is currently under review in PNAS.

The oscillatory AAA$^+$ ATPase Knk1 constitutes a novel morphogenetic pathway in fission yeast

Kathleen Scheffler [a], Pierre Recouvreux [b], Anne Paoletti [a] and Phong T. Tran [a,c]

[a] Institut Curie, CNRS-UMR144, Paris 75005, France

[b] Institut de Biologie du développement de Marseille, CNRS-UMR7288, Marseille 13009, France

[c] University of Pennsylvania, Cell & Developmental Biology, Philadelphia PA 19104, USA

Correspondence: phong.tran@curie.fr

KS designed and performed experiments. KS and PR analyzed data. KS wrote, AP and PTT edited paper.

Short title:

Oscillatory Knk1 maintains straight growth

Abstract

Cellular morphogenesis largely relies on cell polarization by the cytoskeleton. In the fission yeast *Schizosaccharomyces pombe*, it is well established that microtubules (MTs) deliver the spatial cue Tea1 to the tip regions, to direct the growth machinery at the cell tips driving the linear extension of the rod-shaped organism to maintain a straight long axis. Here, we report the characterization of the novel AAA^+ ATPase Knk1, whose deletion causes a unique morphological defect characterized by formation of kinks close to cell tips. Through genetic analysis, we place Knk1 into a novel pathway controlling cell shape independently of MTs and Tea1. Knk1 localizes at cell tips. Its localization is mediated by Knk1 N-terminus and enhanced upon ATP binding to the C-terminal ATPase domain. Furthermore, Knk1 tip recruitment is regulated by Sla2 and Cdc42 independently of Sla2 role in endocytosis. Finally, we discovered that Knk1 shows a fascinating anti-correlated oscillatory behavior between the two cell tips that appears uncoupled from Cdc42 dynamics as both systems oscillate at different frequencies.

Significance

We describe a novel pathway controlling fission yeast cell morphogenesis depending on Knk1, a member of the conserved AAA^+ ATPases family regulating important cellular processes in all organisms and often function in unfolding, degradation or dissociation of multimeric complexes. *knk1* deletion founds a new class of morphogenesis mutants exhibiting sudden changes in directional growth. Knk1 performs oscillations between the two cell ends that seem uncoupled from the reported Cdc42 oscillations. We conclude that at least two oscillatory systems may co-exist in fission yeast to control cell morphogenesis. We thus propose that oscillatory properties could represent a key feature of morphogenetic factors to control the growth machinery in a dynamic manner and achieve an accurate definition of cell shape.

Introduction

In unicellular and multicellular organisms, cells adopt very specific shapes to ensure their functional and structural integrity of tissues and organs. Since, the complex processes governing cell morphogenesis appear to be evolutionary conserved (1), the unicellular fission yeast *Schizosaccharomyces pombe* has proven to be a very useful model system for the identification of morphogenetic pathways through the characterization of distinct classes of shape mutants (Fig. 1*A*), (2)). Wildtype fission yeast forms rod shaped cells of 4µm in diameter that grow linearly from the cell tips and divide medially. After division, growth resumes in a monopolar fashion before switching to a bipolar growth during NETO (New End Take Off) (3).

As in other eukaryotic cells, morphogenesis and polarization are regulated by both, the microtubule (MT) and actin cytoskeletons, and defects in these respective cytoskeletons lead to characteristic shape changes. Mutants affecting actin-based structures usually partially fail to polarize growth at cell tips, resulting in plump cells; in contrast interfering with MT-related functions leads to the loss of a straight axis of growth, resulting in bent or T-shaped cells (Fig. 1*A*).

In interphase, actin forms two distinct structures concentrated at cell tips, actin cables delivering, via myosin V, secretory vesicles for addition of new cell wall and membrane material and actin patches representing sites of endocytosis (4). Briefly, the activity of the small GTPase Cdc42, constituting the core of the polarization machinery, is confined to the cell poles (5). Otherwise cells become roundish due to isotropic growth as observed upon inactivation of the NDR kinase Orb6 (6). Cdc42 activates the formin For3 responsible for actin cable nucleation (7). *for3Δ* cells lacking actin cables partially lose their polarized state, and become bulbous or swollen. Disruption in the endocytic pathway like in the *sla2Δ* mutant, results in a similar shape phenotype (8, 9). Endocytosis is initiated by accumulation of Clathrin and early adaptor proteins concentrating locally at the plasma membrane prior to a local burst of Arp2/3-dependent actin polymerization driving ingression of the endocytic pit until scission (10, 11). The molecular mechanisms driving endocytosis have been intensively studied in yeast, where it is believed to maintain polarized pattern of cortical proteins by removing and recycling molecules diffused away from the center of the polar zone (12). Work in filamentous fungi has proposed that a sub-apical collar of endocytic patches is required to maintain the hyphoid shape (13).

MTs contribute to cell shape by marking cell tips as sites of growth through depositing the landmark Tea1 protein complex (2, 14). Interphase MTs organized in 3-5 bundles parallel to the

cell long axis, are anchored to the nucleus with their minus ends. Their plus ends show dynamic behavior extending towards cell poles and contacting the cortex for about 50-80s. Simultaneously, the Tea1 protein complex is carried at plus ends of MTs in a Mal3/EB1-dependent manner towards the cell tips, where Tea1 indirectly contributes, in turn, to the activation of For3 (15). Upon loss of Tea1, cells fail to maintain a straight axis and become bent. Similarly, an aberrant MT cytoskeleton leads to bent cells due to Tea1 complex mis-positioning. For example, the deletion of Mal3, which results in very short MTs that do not reach cell ends (16, 17), or of the MT nucleator Mto1, which reduces the number of MT bundles, both cause a bent shape (18).

In this study, we describe a novel gene, *knk1*, which plays a role in morphogenesis, and founds a new class of shape mutants. Knk1 belongs to the AAA^+ superfamily of ATPases that are found in all organisms and implicated in various cellular processes, such as protein degradation and membrane trafficking (19). Despite their diversity in function, they share a common core mechanism by assembling into ring-shaped hexamers.
Interestingly, this novel member of the AAA^+ ATPases, Knk1, shows a fascinating oscillatory behavior between the two cell tips.

Results

knk1Δ displays a novel kinked shape phenotype

We identified *knk1* (kink; encoded by SPBC947.01) in a visual screen for new shape mutants using the genome-wide library of haploid fission yeast deletion mutants (20). Intriguingly, cells carrying a deletion of *knk1* displayed a kink close to cell tips (Fig. 1*A*, *B*).

Kinks were typically observed in ~10% of cells at 25°C and up to ~20% of cells after 3h at 36°C (Fig. 1*C*), usually at only one pole, but rarely at both (~4% of kinked cells at 36°C). While wildtype cells always displayed a straight long axis, kinked mutant cells were characterized by an angle θ between the tip growth axis and the otherwise straight long cell axis (Fig. 1*D*). The average angle of kinks was 26.8°±8.7° at 36°C (Fig. 1*E*).

To understand the origin of the *knk1Δ* shape defect, we imaged cells during interphase (Fig. S1*A*). We observed that the appearance of a kink was caused by a unique and sudden event of a directional change of tip growth.

Overexpression of Knk1-YFP in *knk1Δ* cells led to a gradual disappearance of kinks, demonstrating that Knk1 expression was not able to correct established kinks, but rather prevented the formation of new kinks (Fig. S1*B*). Old kinks were "lost" during several rounds of division.

The kinked phenotype clearly differed from the bent cells of a *tea1Δ* mutant displaying gradual bending or from T-shapes with a medial outgrowth perpendicular to the main long axis (Fig. 1*D*). Moreover, Knk1 was dispensable for the initiation of bipolar growth during NETO, in sharp contrast to the *tea1Δ* mutant (Fig. S1*C*) (21).

We conclude that the kink phenotype defines a novel class of shape mutants in fission yeast suggesting that Knk1 may have a novel role in cell morphogenesis by orientating growth.

Aggravation of kinked phenotype by MT defects

The *knk1Δ* phenotype appeared distinct from those produced by defects in the MT or actin cytoskeletons. Accordingly, MT and F-actin networks labeled with GFP-Atb2 and GFP-CHD respectively appeared indistinguishable from wildtype networks (Fig. S2*A*-*B*). We observed no significant changes in MT dynamics, fully demonstrating that Knk1 is not involved in MT regulation and that kinks are not a consequence of an altered MT behavior (Fig. 2*A*).

Next, we tested for genetic interactions between *knk1Δ* and mutants of the MT/Tea1 network. While *tea1Δ* cells are bent (15.5%) (22) and *knk1Δ* kinked (7.2%), the double mutant showed an addition of the two phenotypes with 10.2% kinked and 16.7% bent cells (Fig. 2*B*, *C*),

demonstrating that Knk1 and Tea1 control cell shape through independent pathways. Interestingly, when *knk1* deletion was combined to mutants affecting the MT cytoskeleton, we observed synergistic shape defects (Fig. 2*B*). For instance, *mal3Δ* alone produced mainly bent cells (14.9%), but the double *mal3Δ knk1Δ* mutant showed a dramatic increase in frequency of kinked cells (28.7%) (Fig. 2*B*-*C*). Additionally, the kink angle was enhanced from 25.6° in *knk1Δ* mutant to 38.3° in *mal3Δ knk1Δ* mutant (Fig. 2*D*, *E*), but remained unchanged in *tea1Δ knk1Δ* mutant (27.3°). A synergistic phenotype was also observed in *knk1Δ* double mutants with *mto1Δ* (Fig. 2*B*, *C, E)*, which produces fewer MTs, and *tip1Δ* (CLIP170; Fig. S2*E*), which produces unstable MTs (23), but not with *klp5Δ klp6Δ* that has more stable MTs (Fig. S2*E*) (24).

It has been shown that mto1 dysfunction upon *mto2* deletion leads to an asymmetric deposition of Tea1 at cell tips (25) and that the loss of Tip1 leads to a dispersed distribution of Tea1 on the cortex (23). Therefore, we tested whether the enhanced kinked phenotype observed in *mto1Δ knk1Δ* and *mal3Δ knk1Δ* double mutants was mediated by mis-positioned Tea1. Accordingly, a *mal3Δ knk1Δ tea1Δ* triple deletion mutant showed a frequency and angle of kinks similar to *knk1Δ* cells, despite an increased number of bent and branched cells, demonstrating that the synergic shape defect of *knk1Δ* MT double mutants relies on Tea1 (Fig. 2*B*, *C*, *E*).

These data suggest that altered MT dynamics result in deposition of Tea1 at aberrant locations leading to a bent shape in *knk1*$^{+}$ and aggravated kinks in *knk1Δ* cells. However, Tea1 distribution was unaffected in *knk1Δ,* suggesting that Knk1 did not impact on Tea1 localization (Fig. S2*D*).

In summary, Knk1 appears to constitute a novel pathway controlling cell shape in a MT- and Tea1-independent manner. Synergy between *knk1Δ* and MT mutants may arise from a particular sensitivity of MT mutants to other shape defects that, in turn, may be even enhanced by mis-positioned Tea1.

Knk1 localizes to cell tips

To understand Knk1 function, we analyzed its intracellular distribution by expressing Knk1 tagged with two copies of GFP from its endogenous locus under control of its own promoter. The fusion protein was functional as cells expressing Knk1-2xGFP were morphologically indistinguishable from wildtype cells.

Knk1 showed a cell cycle-dependent localization pattern (Fig. 3*A*). In interphase, Knk1 was detected at one tip in short pre-NETO cells, and at one (~25%) or both tips in longer post-NETO cells. During mitosis, concomitant to formation of acto-myosin cytokinetic ring, Knk1 dissociated

from cell tips and appeared as patches at the medial cortex before condensing into a ring that constricted as cell division proceeded. Remarkably, the contractile ring constituted by Knk1 resided immediately outside of the acto-myosin ring (Fig. S3*A*), as described for Cdc42 GEFs (26). Knk1 dissociated from the cortex upon cell separation and reappeared subsequently at old cell ends.

Knk1 N-terminus mediates tip recruitment, and is enhanced by the ATPase domain

Knk1 belongs to the AAA^+ superfamily of ATPases that typically assemble into ring-shaped hexamers through interactions between ATPase domains (27). This protein family shows high conservation within the ATPase domain located at the C-terminus, but is quite divergent in other regions. Accordingly, based on sequence analysis, Knk1 was similar to AAA^+ ATPases from fungi to human including human MT-severing enzymes fidgetin and spastin (Fig. 3*B*). Knk1 also contains a putative C-terminal helix found in the endocytic trafficking-related Vps4 protein, but its function remains unclear (28). In contrast, the N-terminus of Knk1 exhibited no resemblance to other proteins.

First, to test how N- and C-terminus contributed to Knk1 function and localization, we expressed truncated versions of Knk1 fused to 2xGFP from *knk1* endogenous locus in replacement of full length Knk1 (Fig. 3*C*). Protein levels were similar to wildtype for Knk1N and increased 6-fold for Knk1C (Fig. S3*C*). Cells expressing Knk1N or Knk1C pheno-copied *knk1* deletion (Fig. S3*B*), demonstrating that both regions were required for Knk1 function.

Knk1C was exclusively cytoplasmic, demonstrating that the ATPase domain needs to be tethered to cell tips for proper function. Interestingly, Knk1N was weakly localized to cell tips or septum region in ~20% of cells (Fig. 3*D*, *E*), indicating that tip recruitment is mediated by the N-terminus, but that recruitment efficiency is enhanced by the ATPase domain, presumably by formation of hexameric complexes.

To test this hypothesis, we created mutant versions of Knk1 by site-directed mutagenesis in the two very well conserved Walker motifs of the ATPase domain (Fig. 3*C*) (29). The Walker A motif constitutes the ATP binding site. Mutating this site abolishes ATP binding and often leads to dissociation of the hexameric complexes, while the Walker B motif allows ATP binding and hexameric assembly, but inhibits ATP hydrolysis.

Protein levels of these mutants were comparable to wildtype Knk1 (Fig. S3*C*). Both mutant *knk1* alleles produced kinked cells (Fig. S3*B*), demonstrating that a fully active ATPase is required for correct cell morphogenesis.

Consistent with our hypothesis that Knk1 oligomerization enhances tip binding of the N-terminus, Knk1(G419A), mutated in the Walker A motif, showed a weak tip signal similarly to Knk1N (Fig. 3*D*, *E*). In contrast, the Walker B mutant, Knk1(D478A E479A), was recruited to cell tips like wildtype Knk1 (Fig. 3*D*, *E*), implying that ATP hydrolysis is not required for Knk1 localization.
Taken together, these data indicate that Knk1 acts as an ATPase and its localization to cell tips is essential for its role in cell morphogenesis. Furthermore, tip recruitment is controlled by the N-terminus and enhanced upon binding of ATP, possibly through formation of Knk1 hexamers, which may allow the cooperation of several N-termini.

Knk1 cell tip localization is independent of MTs and actin cables

Next, we examined whether Knk1 recruitment to cell tips was dependent on the actin or MT cytoskeleton. When cells were treated with 50µg/mL MBC to depolymerize MTs, Knk1 localization was not affected (Fig. 4*A*). Similar results were obtained in mutants of the MT-Tea1 pathway *mal3Δ* or *tea1Δ (*Fig. S2*C*).
In contrast, Knk1 was no longer detected at cell tips upon treatment with 100µM Latrunculin A (LatA), an inhibitor of F-actin, (Fig. 4*B*), leading to disassembly of F-actin patches marked by Crn1-GFP (Fig. 4*B*). Interestingly, while Crn1 patches were restored 20min after washout of LatA, Knk1 tip localization was restored only after 90min, suggesting that Knk1 localization was not simply controlled by presence of F-actin but rather by F-actin-based processes that are required for establishment and maintenance of Knk1 at cell tips.
Importantly, Knk1 levels at cell tips were comparable to wildtype in a *for3Δ* mutant that lacks F-actin cables (Fig. 4*C*, *E*) (30), demonstrating that Knk1 tip localization relies on F-actin patches rather than on F-actin cables.

Sla2 and Cdc42 regulate Knk1 localization independent of endocytosis

Since F-actin patches correspond to sites of endocytosis, we next tested the impact of endocytosis defects on Knk1 distribution. Sla2 is an early coat protein in the endocytic machinery preceding the local burst of Arp2/3-dependent actin polymerization driving ingression of the endocytic pit (10, 11). We used the *sla2Δ* mutant, in which endocytosis is blocked prior to membrane ingression due to uncoupling of membrane and actin dynamics (31). Interestingly, in this mutant, Knk1 reached 2- to 3-fold higher levels at cell tips compared to wildtype cells (Fig. 4*C*, *E*), while global protein levels were not altered as shown by western blot (Fig. S4*B*). Line scans along the long axis confirmed increased tip but lowered cytoplasmic levels (Fig. 4*D*), demonstrating that Knk1 was more bound to cell tips.

The observed accumulation at tips in the *sla2Δ* mutant suggested that Knk1 may be internalized by endocytosis. We therefore tested Knk1 distribution in two other endocytic mutants, *myo1Δ* (class I Myosin) and *wsp1Δ* (Wasp homologue) mutants, both of which fail to activate F-actin nucleation by Arp2/3 (32-34). Surprisingly, Knk1 tip levels were not significantly increased in either mutant (Fig. 4*C*, *E*, S4*A*), demonstrating that Knk1 is not retrieved from tips by endocytosis and excluding that its accumulation in *sla2Δ* cells is due to endocytosis defects. Consistently, co-staining of Sla2-TagRFP and Knk1-2xGFP revealed only partial overlap (Fig. S4*C*). As demonstrated by line scan along cell tip (asterisk), while Sla2 formed patches at the tip that moved inwards (arrow), Knk1 stained tips more uniformly and was never detected in patches distant from the cell tip cortex, suggesting Knk1 is not directly associated with F-actin patches.

We next wondered whether Knk1 might function in endocytosis, which can be monitored by the uptake of the lipophilic dye FM4-64. *sla2Δ* as control, but not *knk1Δ* cells showed a significant disruption in FM4-64 uptake (Fig. S4*D*). Thus, Knk1 is neither cargo of endocytosis nor required for proper endocytosis.

As mentioned above, Knk1 formed a contractile ring (Fig. S3*A*), similar to Cdc42 GEFs (26). We therefore wondered whether Cdc42 activity might impact on Knk1 distribution. To test this, we used the temperature-sensitive allele *cdc42-L160S* (35-37) that exhibits no defects in early steps of endocytosis, but reduced intensity of active Cdc42 at cell tips monitored by CRIB-GFP (38) at 25°C. Intriguingly, Knk1 accumulated to high levels at tips in these conditions (Fig. 4*C*, *E*), similar to *sla2Δ*. However, Sla2 distribution along cell tips in *cdc42-L160S* cells was increased compared to wildtype (Fig. S4*E*), demonstrating that increased Knk1 tip intensity was not simply caused by absence of Sla2. Furthermore, a double *sla2Δ cdc42-L160S* mutant showed no significant difference compared to a single *sla2Δ* mutant (Fig. 4*C*, *E*), indicating that Sla2 and Cdc42 function in the same pathway to regulate Knk1 recruitment to cell tips in a novel endocytosis independent manner.

Knk1 exhibits novel oscillatory dynamics at cell tips

When we visualized Knk1-2xGFP in *sla2Δ* cells at 1min interval, we observed that Knk1 was highly dynamic at cell tips, continuously undergoing cycles of binding and detachment (Fig. 5*A, B*). Strikingly, the behavior of the two cell tips appeared anti-correlated, which was confirmed using a cross correlation function (cross correlation coefficient r = -0.39±0.24). Furthermore, in ~60% of cells, these oscillations appeared periodic with an average periodicity of 13.9min (frequency = 0.072min^{-1}) obtained by Fast Fourier Transform (FFT) analysis on all cells and all

recorded intervals whether or not the oscillatory behavior was detected by eye (Fig. 5*C*). A similar periodicity of 13.5min was detected when FFT was performed for a subgroup of cells exhibiting oscillations noticeable by eye (Fig. S5*A*), demonstrating the robustness of the FFT analysis.

When we followed tip intensities of Knk1-2xGFP in wildtype cells, no striking oscillatory behavior could be observed by eye (Fig. S5*B*, *C*). One possible explanation could be that dynamics of tip-bound Knk1 might not be reliably measured due to strong cytoplasmic intensity and fluctuations. No specific frequency could be observed by FFT analysis (Fig. S5*D*). Nevertheless, Knk1 often showed anti-correlated fluctuations (Fig. S5*C*, marked by arrows) with a cross-correlation coefficient r = -0.16±0.25, in contrast to uncorrelated fluctuations seen for Tea1-GFP with r = 0.04±0.34. This indicates that the two cell tips compete for Knk1 and that the detachment of Knk1 from one tip allows the accumulation of Knk1 at the second competing tip.

A recent study evidenced anti-correlated oscillations of Cdc42 at cell tips, e.g. using CRIB-GFP as a reporter for active Cdc42, with an average period of 5min (39). To determine whether Knk1 and Cdc42 dynamics were linked, we thus analyzed the dynamics of Knk1 in the *cdc42-L160S* mutant. Knk1 oscillated with a period of ~14.8min in an anti-correlated fashion (r= -0.3±0.31) (Fig. 5*D-F*), similar to oscillations seen in *sla2Δ*. CRIB-GFP dynamics could not be determined in this mutant, as levels were dramatically decreased (35). However, the detection of Knk1 oscillation, despite a reduction of active Cdc42 in cell tips, strongly suggests that Knk1 oscillations are not driven by Cdc42 dynamics.

Conversely, we also tested whether Cdc42 oscillations were influenced by the deletion of *knk1*. In wildtype cells, CRIB-GFP oscillations had an average periodicity at 5.3min (Fig. 5*G*), consistent with a previous report (39). CRIB-GFP distribution and oscillation were unaffected in *knk1Δ* cells with an average period of 4.8min (Fig. 5*G*, S5*E*). Finally, we studied CRIB dynamics in *sla2Δ* cells, where Knk1 exhibited anti-correlated oscillations at 13.9min intervals (Fig. 5*C*). Levels of CRIB-GFP were lowered (Fig. S5*E*), which rendered the detection of oscillatory intervals and precise periods more difficult. Nevertheless, a peak at a frequency of ~0.18min^{-1} could be detected, which is similar to wildtype and *knk1Δ* cells (Fig. 5*G*), implying that Knk1 and Cdc42 oscillated at different frequencies in *sla2Δ*, and presumably in wildtype cells.

In summary, these results demonstrate that Knk1-2xGFP shows anti-correlated fluctuations in wildtype and periodic oscillations in *sla2Δ* and *cdc42-L160S* mutant strains. We further show that *knk1* deletion does not interfere with Cdc42 oscillations. Finally, the different frequencies in oscillatory behavior detected for both proteins in *sla2Δ* mutant might suggest the existence of at least two separated oscillatory systems in fission yeast.

Discussion

We identified Knk1 in a screen for new shape mutants. Intriguingly, its deletion caused a unique "kinked" shape defect. Knk1 is an AAA^+ ATPase that showed similarity to MT severing enzymes. However, despite the phenotypic resemblance between the kink and bent cell shapes observed for MT and *tea1Δ* mutants, Knk1 did not play a role in regulation of the MT cytoskeleton. Furthermore, a *knk1Δ tea1Δ* strain showed additive defects. We also show that the aggravation of the kinked phenotype in frequency and angle observed in combination of *knk1Δ* with MT mutants like *mal3Δ* was mediated by Tea1 as the triple mutant *knk1Δ mal3Δ tea1Δ* resembled the double mutant *knk1Δ tea1Δ*. We hypothesize that mis-positioned Tea1 along the cell cortex, exemplified in *mto2Δ (25)* and *tip1Δ (23)*, renders MT mutants more sensitive to the kink morphological defects which leads to a dramatic enhancement of the kinked phenotype. These data confirm that Knk1 functions in a MT/Tea1-independent pathway controlling morphogenesis.

Consistent with its role in morphogenesis, Knk1 was localized to cell tips and the septum region. Remarkably, tip intensity was enhanced in a *sla2Δ* mutant. We showed that this effect was independent of Sla2 role in endocytosis as other endocytic mutants like *myo1Δ* exhibited wildtype Knk1 tip levels. In agreement with this hypothesis, a mutant allele of *cdc42*, *cdc42-L160S* that appears functional in early endocytic steps (36 5) displayed a similar accumulation of Knk1. Furthermore, the double mutant *sla2Δ cdc42-L160S* showed no significant increase compared to the *sla2Δ* single mutant, indicating that Cdc42 and Sla2 act in the same pathway. No direct link between these proteins has been reported in fission yeast, but in budding yeast the Cdc42 system is known to interact with the key endocytic proteins epsins that function cooperatively with Sla2 to couple plasma membrane and actin cytoskeleton dynamics in early steps of endocytosis (40). Mutants in the epsin ENTH (epsin N-terminal homology) domain displayed polarity defects due to decreased levels of active Cdc42, while endocytosis was unaffected. Since our study in fission yeast also suggests a link between the early endocytic adaptor protein Sla2 and Cdc42 in Knk1 localization, there may be a conserved connection between endocytic processes and Cdc42 pathway linking endocytosis and cell polarization machinery to regulate downstream growth factors. Nevertheless, the exact mechanisms regulating Knk1 localization remain elusive at this point.

We showed that Knk1 is recruited to cell tips via its N-terminus. Surprisingly, we could not identify any known membrane binding domains or motifs in this part of the protein suggesting that Knk1 does not bind lipids in classical ways or binds indirectly via other polarity factors. However, we failed to identify such factors during our studies. Furthermore, we provide evidence that efficient Knk1 tip recruitment is achieved upon Knk1 hexamer assembly suggesting the

cooperation of several N-termini mediating tip binding. Alternatively, ATP binding at the Walker A motif might lead to conformational changes in the N-terminus.

We detected a remarkable oscillatory behavior for Knk1 in *sla2Δ* and *cdc42-L160S* mutants, which appeared, at least in *sla2Δ* cells, uncoupled from Cdc42 oscillations (39). Thus, our work suggests the co-existence of two separated oscillatory system with distinct periodicities, for Cdc42 at 5min and Knk1 at 15min, implying that oscillation may be a common mechanism of growth factors controlling cell shapes.

In the case of Knk1, anti-correlated, but not clearly periodic Knk1 fluctuations were detected in wildtype cells. Here, when measuring Knk1 dynamics at cell tips, we often failed to reliably distinguish the tip from the cytoplasmic signal. We therefore hypothesize that Knk1 oscillation might also occur at specific periods in wildtype cells; although we cannot exclude that the periodic oscillations might be triggered by cellular alterations in *sla2Δ* and *cdc42-L160S*, for example by limiting the amount of available Knk1 resulting in the competition of the two cell tips for Knk1. Sla2 and Cdc42 might do so, either by allowing more Knk1 to bind at one cell tip or by limiting regulatory factors that modify Knk1 to allow cell tip binding, as it has been proposed for Cdc42 and its GEFs (39). In fact, the enhanced Knk1 levels in *sla2Δ* and *cdc42-L160S* cells indicate that Cdc42 and Sla2 might be part of the negative feedback mechanism leading to cell tip detachment of Knk1. Under wildtype conditions, such striking anti-correlated periodic oscillations might not be observed as regulatory proteins might usually be present in sufficient quantities or as the levels of Knk1 binding to cell tips might be strictly regulated, which means that the two cell tips do not compete for Knk1.

Furthermore, it remains to be addressed whether Knk1 oscillatory behavior is required for its function in morphogenesis. In the case of Cdc42, it has been proposed that its oscillatory dynamics control the transition from mono- to bipolar growth or the cell diameter more reliably than a stably bound protein (41). The bacterial Min system required for medial positioning of the Z-ring undergoes oscillatory dynamics in some, but not all bacteria suggesting that oscillations might not be necessarily required for protein function (42).

At this point, we can only speculate on how Knk1 may influence cell shape. AAA^+ ATPases are implicated in various cellular processes (19) e.g. membrane trafficking. However, we did not detect any endocytic (via FM4-64 uptake) or exocytic defects (via secretion of acid phosphatase, Fig. S6*A*), suggesting that Knk1 was not essential for these processes.

The kinks seen in *knk1Δ* are reminiscent of the behavior of fission yeast subjected to an electrical field, where cell growth is reoriented orthogonally to the field (43). This report shows that Bgs glucan synthase proteins were abnormally accumulated at one side of cell tips, leading

to asymmetric cell wall synthesis. *knk1Δ* phenotype might be caused by a similar asymmetrical distribution of certain polarity factors. However, when stained with the cell wall marker Calcolfluor or RFP-Bgs4 no apparent cell wall asymmetry was observed (Fig. S6*B*), suggesting Knk1 does not impact on cell wall synthesis.

Alternatively, Knk1 might regulate the turnover of some cell tip proteins via protein folding/unfolding, degradation or protein complex disassembly, as many AAA^+ proteins are implicated in such processes (19). Potentially, by periodically removing components of the cell growth machinery, Knk1 might prevent the amplification of random deflection in growth direction, otherwise stabilized by positive feedback loops reinforcing the growth machinery locally (44).

Our study suggests that oscillatory properties represent a key feature to control cell shape. A first description of oscillatory dynamics emerged from studies in bacteria (42), where the MinCDE system undergoes oscillations to prevent division away from the cell middle. Remarkably, these oscillations are driven by the activity of the ATPase MinD. Future work may uncover that oscillatory dynamics may commonly utilized among ATPases or other NTPases to control various cellular processes.

Experimental procedures

Detailed descriptions are available in the Supplemental.

Acknowledgements

We thank the labs of J.-C. Ribas (University of Salamanca), P. Perez (University of Salamanca), T. Pollard (Yale University) and the Japan National BioResource Project for generously providing reagents. We thank Sergio Rincon and Li Wang for helpful technical advice and discussion. KS is supported by a PhD fellowship from Complexité du Vivant-UPMC and Fondation ARC. PR is supported by CNRS. This work is supported by grants from the ANR, INCa, and ARC.

References

1. Nelson WJ (2003) Adaptation of core mechanisms to generate cell polarity. *Nature* 422(6933):766-774.
2. Chang F & Martin SG (2009) Shaping fission yeast with microtubules. *Cold Spring Harb Perspect Biol* 1(1):a001347.
3. Mitchison JM & Nurse P (1985) Growth in cell length in the fission yeast Schizosaccharomyces pombe. *J Cell Sci* 75:357-376.
4. Mishra M, Huang J, & Balasubramanian MK (2014) The yeast actin cytoskeleton. *FEMS Microbiol Rev* 38(2):213-227.
5. Perez P & Rincon SA (2010) Rho GTPases: regulation of cell polarity and growth in yeasts. *Biochem J* 426(3):243-253.
6. Das M, Wiley DJ, Chen X, Shah K, & Verde F (2009) The conserved NDR kinase Orb6 controls polarized cell growth by spatial regulation of the small GTPase Cdc42. *Curr Biol* 19(15):1314-1319.
7. Martin SG, Rincon SA, Basu R, Perez P, & Chang F (2007) Regulation of the formin for3p by cdc42p and bud6p. *Mol Biol Cell* 18(10):4155-4167.
8. Iwaki T, Tanaka N, Takagi H, Giga-Hama Y, & Takegawa K (2004) Characterization of end4+, a gene required for endocytosis in Schizosaccharomyces pombe. *Yeast* 21(10):867-881.
9. Castagnetti S, Behrens R, & Nurse P (2005) End4/Sla2 is involved in establishment of a new growth zone in Schizosaccharomyces pombe. *J Cell Sci* 118(Pt 9):1843-1850.
10. Weinberg J & Drubin DG (2012) Clathrin-mediated endocytosis in budding yeast. *Trends Cell Biol* 22(1):1-13.
11. Boettner DR, Chi RJ, & Lemmon SK (2012) Lessons from yeast for clathrin-mediated endocytosis. *Nat Cell Biol* 14(1):2-10.
12. Valdez-Taubas J & Pelham HR (2003) Slow diffusion of proteins in the yeast plasma membrane allows polarity to be maintained by endocytic cycling. *Curr Biol* 13(18):1636-1640.

13. Shaw BD, Chung DW, Wang CL, Quintanilla LA, & Upadhyay S (2011) A role for endocytic recycling in hyphal growth. *Fungal Biol* 115(6):541-546.
14. Huisman SM & Brunner D (2011) Cell polarity in fission yeast: a matter of confining, positioning, and switching growth zones. *Semin Cell Dev Biol* 22(8):799-805.
15. Martin SG, McDonald WH, Yates JR, 3rd, & Chang F (2005) Tea4p links microtubule plus ends with the formin for3p in the establishment of cell polarity. *Dev Cell* 8(4):479-491.
16. Beinhauer JD, Hagan IM, Hegemann JH, & Fleig U (1997) Mal3, the fission yeast homologue of the human APC-interacting protein EB-1 is required for microtubule integrity and the maintenance of cell form. *J Cell Biol* 139(3):717-728.
17. Busch KE & Brunner D (2004) The microtubule plus end-tracking proteins mal3p and tip1p cooperate for cell-end targeting of interphase microtubules. *Curr Biol* 14(7):548-559.
18. Samejima I, Lourenco PC, Snaith HA, & Sawin KE (2005) Fission yeast mto2p regulates microtubule nucleation by the centrosomin-related protein mto1p. *Mol Biol Cell* 16(6):3040-3051.
19. White SR & Lauring B (2007) AAA+ ATPases: achieving diversity of function with conserved machinery. *Traffic* 8(12):1657-1667.
20. Kim DU, *et al.* (2010) Analysis of a genome-wide set of gene deletions in the fission yeast Schizosaccharomyces pombe. *Nat Biotechnol* 28(6):617-623.
21. Glynn JM, Lustig RJ, Berlin A, & Chang F (2001) Role of bud6p and tea1p in the interaction between actin and microtubules for the establishment of cell polarity in fission yeast. *Curr Biol* 11(11):836-845.
22. Mata J & Nurse P (1997) tea1 and the microtubular cytoskeleton are important for generating global spatial order within the fission yeast cell. *Cell* 89(6):939-949.
23. Brunner D & Nurse P (2000) CLIP170-like tip1p spatially organizes microtubular dynamics in fission yeast. *Cell* 102(5):695-704.
24. Unsworth A, Masuda H, Dhut S, & Toda T (2008) Fission yeast kinesin-8 Klp5 and Klp6 are interdependent for mitotic nuclear retention and required for proper microtubule dynamics. *Mol Biol Cell* 19(12):5104-5115.
25. Janson ME, Setty TG, Paoletti A, & Tran PT (2005) Efficient formation of bipolar microtubule bundles requires microtubule-bound gamma-tubulin complexes. *J Cell Biol* 169(2):297-308.
26. Hirota K, Tanaka K, Ohta K, & Yamamoto M (2003) Gef1p and Scd1p, the Two GDP-GTP exchange factors for Cdc42p, form a ring structure that shrinks during cytokinesis in Schizosaccharomyces pombe. *Mol Biol Cell* 14(9):3617-3627.
27. Hanson PI & Whiteheart SW (2005) AAA+ proteins: have engine, will work. *Nat Rev Mol Cell Biol* 6(7):519-529.
28. Vajjhala PR, *et al.* (2008) The Vps4 C-terminal helix is a critical determinant for assembly and ATPase activity and has elements conserved in other members of the meiotic clade of AAA ATPases. *FEBS J* 275(7):1427-1449.
29. Wendler P, Ciniawsky S, Kock M, & Kube S (2012) Structure and function of the AAA+ nucleotide binding pocket. *Biochim Biophys Acta* 1823(1):2-14.
30. Feierbach B & Chang F (2001) Roles of the fission yeast formin for3p in cell polarity, actin cable formation and symmetric cell division. *Curr Biol* 11(21):1656-1665.
31. Skruzny M, *et al.* (2012) Molecular basis for coupling the plasma membrane to the actin cytoskeleton during clathrin-mediated endocytosis. *Proc Natl Acad Sci U S A* 109(38):E2533-2542.

32. Lee WL, Bezanilla M, & Pollard TD (2000) Fission yeast myosin-I, Myo1p, stimulates actin assembly by Arp2/3 complex and shares functions with WASp. *J Cell Biol* 151(4):789-800.
33. Codlin S, Haines RL, & Mole SE (2008) btn1 affects endocytosis, polarization of sterol-rich membrane domains and polarized growth in Schizosaccharomyces pombe. *Traffic* 9(6):936-950.
34. Sirotkin V, Beltzner CC, Marchand JB, & Pollard TD (2005) Interactions of WASp, myosin-I, and verprolin with Arp2/3 complex during actin patch assembly in fission yeast. *J Cell Biol* 170(4):637-648.
35. Rincon SA, *et al.* (2009) Pob1 participates in the Cdc42 regulation of fission yeast actin cytoskeleton. *Mol Biol Cell* 20(20):4390-4399.
36. Estravis M, Rincon SA, Santos B, & Perez P (2011) Cdc42 regulates multiple membrane traffic events in fission yeast. *Traffic* 12(12):1744-1758.
37. Estravis M, Rincon S, & Perez P (2012) Cdc42 regulation of polarized traffic in fission yeast. *Commun Integr Biol* 5(4):370-373.
38. Tatebe H, Nakano K, Maximo R, & Shiozaki K (2008) Pom1 DYRK regulates localization of the Rga4 GAP to ensure bipolar activation of Cdc42 in fission yeast. *Curr Biol* 18(5):322-330.
39. Das M, *et al.* (2012) Oscillatory dynamics of Cdc42 GTPase in the control of polarized growth. *Science* 337(6091):239-243.
40. Aguilar RC, *et al.* (2006) Epsin N-terminal homology domains perform an essential function regulating Cdc42 through binding Cdc42 GTPase-activating proteins. *Proc Natl Acad Sci U S A* 103(11):4116-4121.
41. Das M & Verde F (2013) Role of Cdc42 dynamics in the control of fission yeast cell polarization. *Biochem Soc Trans* 41(6):1745-1749.
42. Lutkenhaus J (2007) Assembly dynamics of the bacterial MinCDE system and spatial regulation of the Z ring. *Annu Rev Biochem* 76:539-562.
43. Minc N & Chang F (2010) Electrical control of cell polarization in the fission yeast Schizosaccharomyces pombe. *Curr Biol* 20(8):710-716.
44. Slaughter BD, Smith SE, & Li R (2009) Symmetry breaking in the life cycle of the budding yeast. *Cold Spring Harb Perspect Biol* 1(3):a003384.

Figure Legends

Figure 1. *knk1Δ* has a novel kinked shape phenotype. (A) Differential interference contrast (DIC) images of shape mutants showing the normal rod shape of wildtype cells and the aberrant round (*orb6-25*), plump (*for3Δ and sla2Δ*), bent (*mal3Δ* and *mto1Δ*), T-shaped (*tea1Δ*) and kinked (*knk1Δ*) shapes of morphology mutants. Most strains were grown at 25°C. *orb6-25* cells were imaged after 7h growth at 36°C. *tea1Δ* cells were grown for 3d to stationary phase and imaged 3h after transfer into fresh medium. **(B)** Kinked cell morphology in a *cdc25-22 knk1Δ* strain after 3h at 36°C. **(C)** Percentage of wildtype and *knk1Δ* cells displaying kinks at 25°C or after 3h at 36°C. Bars represent means from 3 independent experiments (n>300 cells per experiment). Error bars: standard deviation (s.d.). (**D)** Schematic highlighting the characteristics of a bent, T-shaped or kinked morphology. θ is the angle between the growth direction (defined tip orientation) and cell long axis. **(E)** Distribution of angles θ in *knk1Δ* cells after 3h at 36°C (n=427). Dotted line indicates mean angle of 26.8°±8.7°. Bars, 5µm.

Figure 2. *knk1* deletion is synergistic with defects in MT-dependent polarity pathways. (A) MT dynamic parameters in wildtype and *knk1Δ* cells (mean ± s.d.; n=50 for each value). **(B)** Percentage of kinked and bent cells in wildtype and mutants at 25°C. Bars represent means from 3 independent experiments (n>300 cells per experiment). Errors bars: s.d. **(C)** DIC images of *knk1Δ* mutants. Green asterisks mark bent cells, red asterisks kinked. Bar, 5µm. **(D)** Distribution of angles θ in *knk1Δ* (n=261) and *knk1Δ mal3Δ* mutants (n=320) at 25°C. Dotted lines indicate mean angles. **(E)** Angles θ in: *knk1Δ* (25.6°±7.7°), *knk1Δ tea1Δ* (27.3°±9.8°, p=0.01), *knk1Δ mal3Δ* (38.3°±13.6°, $p<10^{-37}$), *knk1Δ mto1Δ* (42.2°±18.2°, $p<10^{-29}$), *knk1Δ mal3Δ tea1Δ* (31.4°±11.8°, $p<10^{-8}$) and *knk1Δ mto1Δ tea1Δ* (28.0°±9.9°, p=0.01). (n≥197).

Figure 3. **Knk1N mediates tip binding that is enhanced by the ATPase domain. (A)** Timelapse images of Knk1-2xGFP expressed from endogenous promoter by spinning disk confocal microscopy in a strain co-expressing mCherry-Atb2 (tubulin) and Rlc1-mCherry (acto-myosin ring) through cell cycle. Cells were grown at 25°C. Knk1-2xGFP is presented as single medial z-section, mCherry-Atb2 Rlc1-mCherry as maximum projection of 3D stacks. **(B)** Schematic representation of homology between Knk1 and related AAA^+ proteins. Numbers indicate length of proteins in amino acids (a.a.). Region with high similarity is highlighted with identity (%) and is limited to the ATPase domain (AAA^+). Other domains depicted: MIT (MT interacting-trafficking domain) and Vps4_C (Vps4 oligomerisation domain). **(C)** Schematic of truncated and mutated constructs of Knk1 expressed from *knk1* endogenous locus and tagged with 2xGFP. **(D)** Localization of Knk1 constructs at 25°C. Images recorded as single medial z-

sections. Knk1C was scaled differently due increased protein levels. **(E)** Subcellular distribution of wildtype and Knk1 constructs (n=300). Bars correspond to percentage of cells showing a distinct signal at cell tips or septum, and without a specific cortical signal (cytoplasm). Bars, 5µm.

Figure 4. Sla2 and Cdc42 regulate Knk1 cell tip localization. (A, B) Cells expressing Knk1-2xGFP mCherry-Atb2 (A) or Knk1-2xGFP (yellow asterisks) or Crn1-GFP (actin patch, blue asterisk) (B) were treated with 50µg/mL MBC (A) or 100µM LatA (B) for 20min. Drug was washed out and images recorded at indicated time points. Knk1-2xGFP is presented as single z-section, mCherry-Atb2 as maximum z-projection of 3D stacks. **(C)** Knk1 localization in wildtype and mutant strains. Images recorded as single z-section. **(D)** Line scan of Knk1-2xGFP fluorescence intensity along the long axis of 12 individual wildtype and *sla2Δ* cells of comparable length, intensities were over full cell width at each point along the cell axis. **(E)** Knk1 intensity averaged over individual tips: wildtype (70.4±46.9 arbitrary unit, a.u.), *for3Δ* (73.9±70.3, p=0.68), *sla2Δ* (150.3±119.9, $p<10^{-8}$), *myo1Δ* (71.6±59.5, p=0.87), *cdc42-160S* (142.4±119.9, $p<10^{-6}$) and *sla2Δ cdc24-L160S* (197.7±225.3, $p<10^{-6}$ to wildtype, p=0.07 to *sla2Δ*). (n=100). Bars, 5µm.

Figure 5. Oscillations and fluctuations of Knk1-2xGFP at cell tips. (A, D) Timelapse images of Knk1-2xGFP in a *sla2Δ* (A) and *cdc42-L160S* (D) strain at 25°C. Images recorded as single medial z-sections showing Knk1 distribution. **(B, E)** Knk1-2xGFP tip intensities at 1min intervals in the same *sla2Δ* (B) and *cdc42-L160S* (E) cells shown in (A) and (D). The period is defined as the average time span between two subsequent maxima of intensity (amplitude). Periodicity = 1/frequency min^{-1}. **(C, F)** Frequency spectrum of Knk1-2xGFP tip intensities analyzed by Fast Fourier Transform analysis using all recorded intervals in *sla2Δ* (C) (n=25) and *cdc42-L160S* (F) (n=21). Red line represents a Gaussian function of intervals of frequencies with higher amplitudes indicating average frequencies of $0.072min^{-1}$ for *sla2Δ* (C) and $0.068min^{-1}$ for *cdc42-L160S* (E). **(G)** Frequency spectrum of CRIB-GFP in selected intervals (with periodic anti-correlated dynamics detected by eye) in wildtype (n=14; $0.19min^{-1}$), *knk1Δ* (n=13, $0.21min^{-1}$) and *sla2Δ* (n=8, n.d.). Arrow indicates potential frequency at $0.18min^{-1}$. Bars, 5µm.

Figure 1. Scheffler et al.

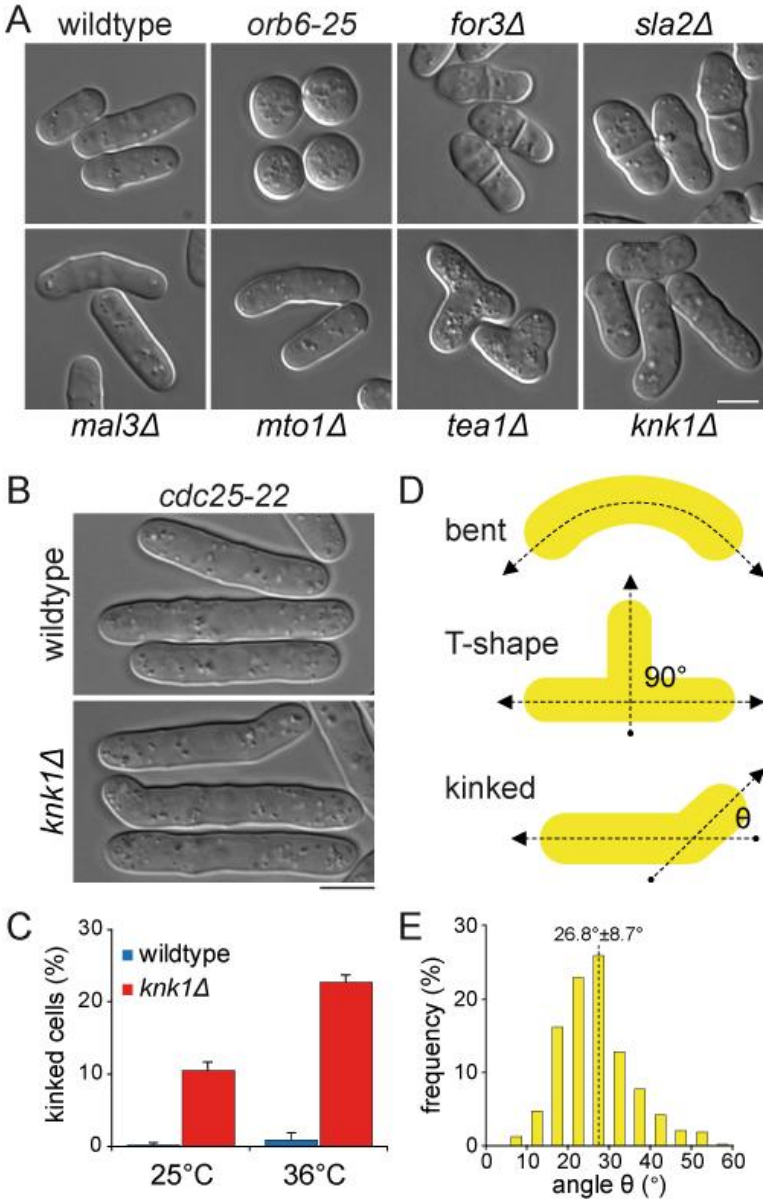

Figure 2. Scheffler et al.

A

strain	Growth Rate (µm/min)	Shrinkage Rate (µm/min)	Catastrophe (events/min)	Rescue (events/min)	Dwell Time (s)
wildtype	2.27±0.58	8.25±2.31	0.35±0.14	0.84±0.65	68.8±35.8
knk1Δ	2.34±0.68	8.78±2.81	0.35±0.13	0.73±0.47	63.5±37.0
p-Value	0.55	0.3	0.82	0.18	0.43

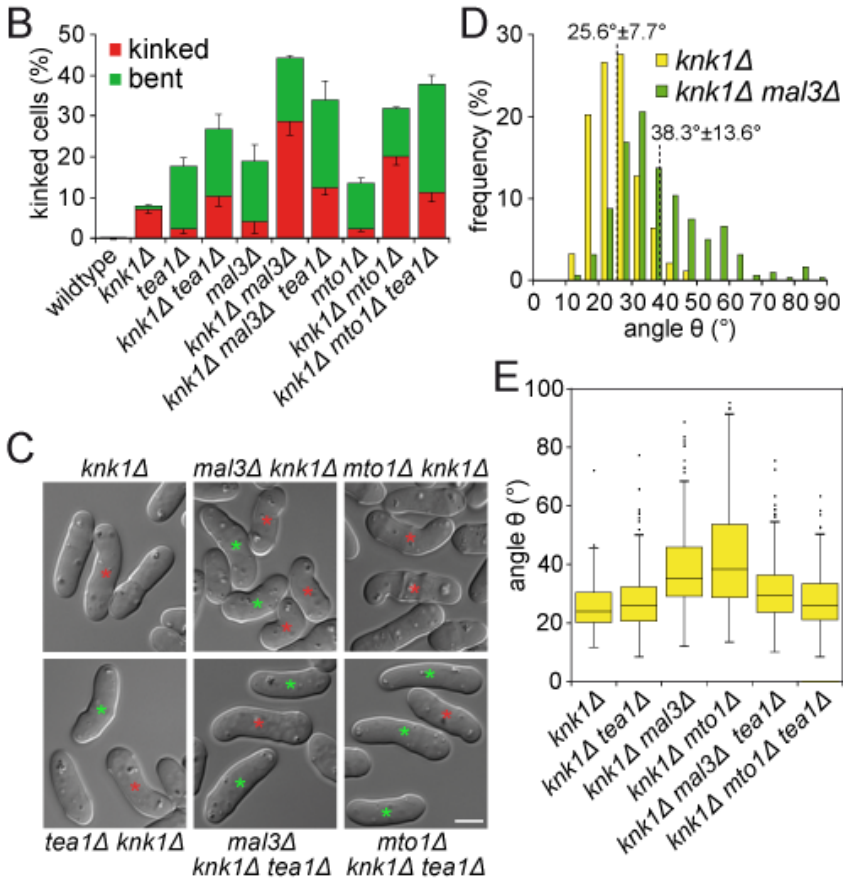

Figure 3. Scheffler et al.

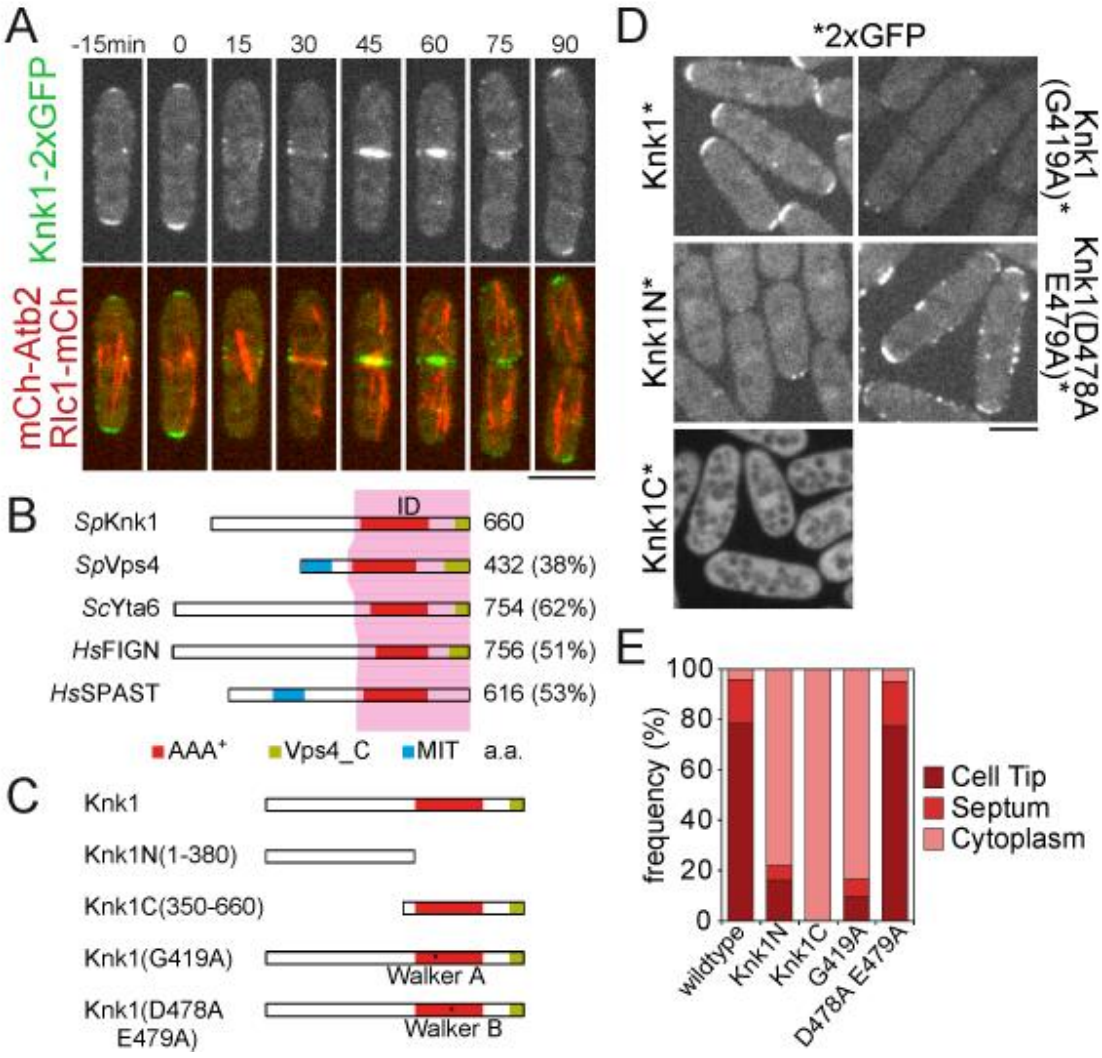

Figure 4. Scheffler et al.

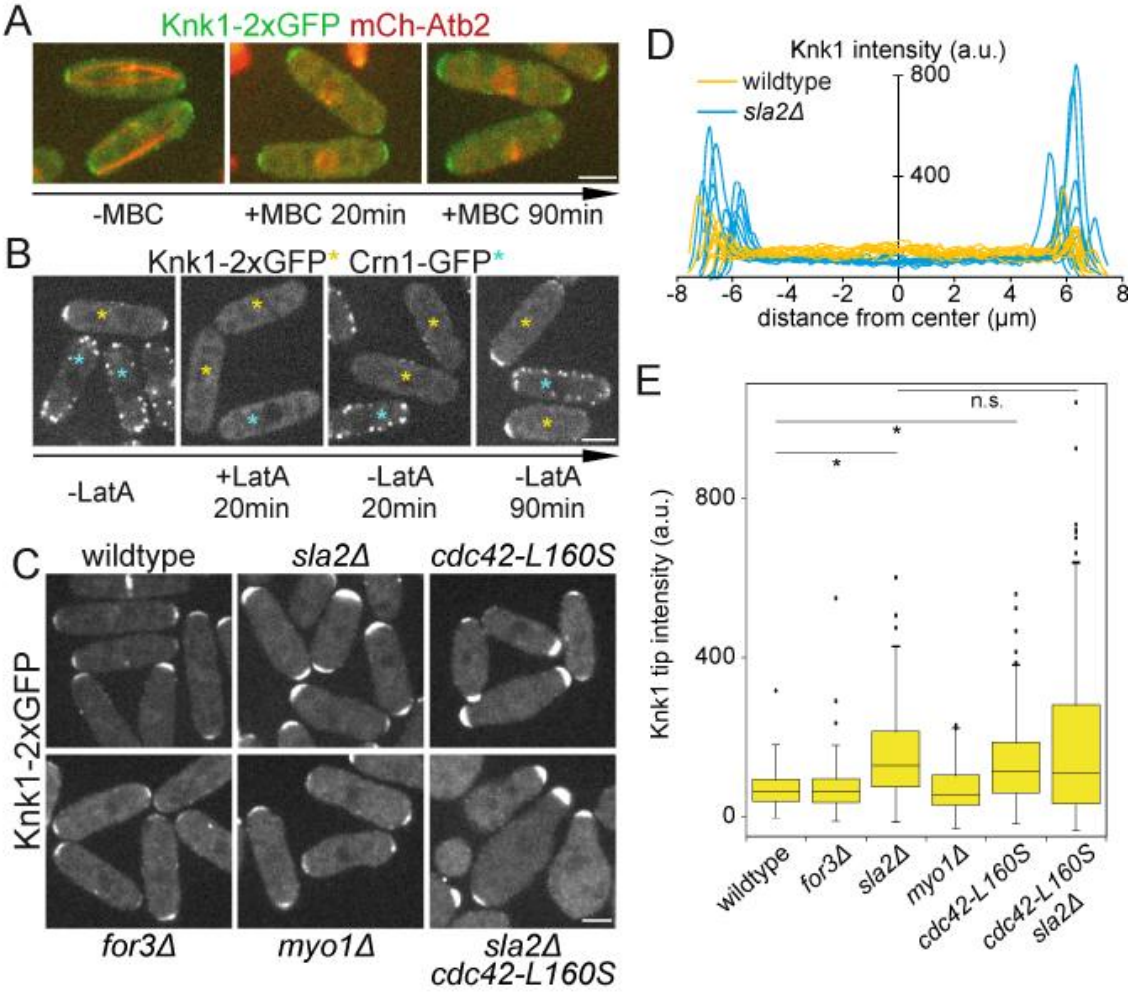

Figure 5. Scheffler et al.

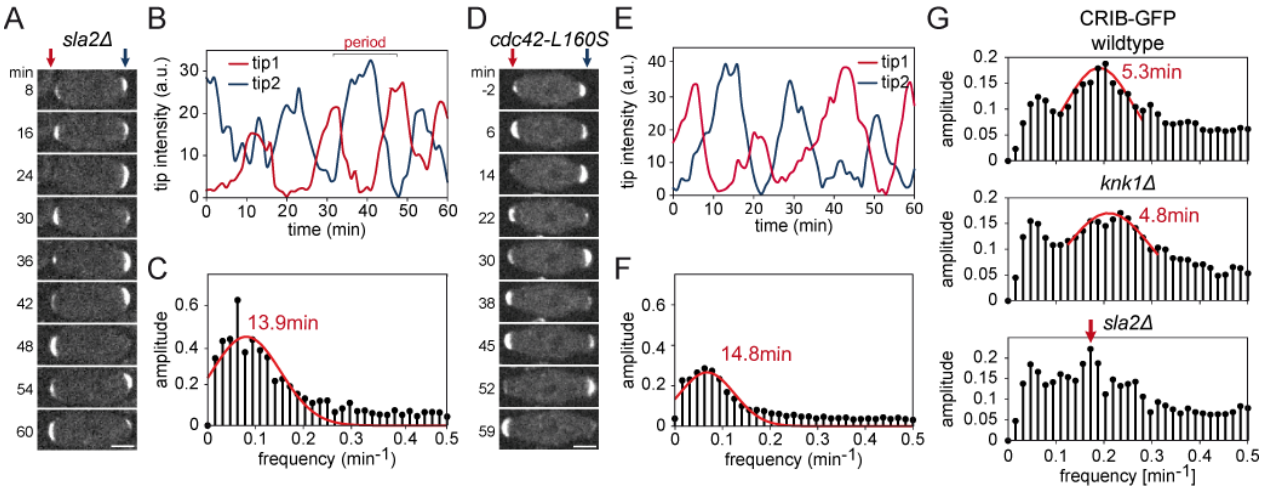

Inventory of Supplemental information

Figure S1: Complement to characterization of *knk1Δ* phenotype shown in Figure 1.

Figure S2: Complement to genetic interactions between MT mutants and *knk1Δ* shown in Figure 2.

Figure S3. Complement to localization of wildtype and mutant Knk1 proteins shown in Figure 3.

Figure S4. Complement to regulation of localization of Knk1 by Sla2 and Cdc42 shown in Figure 4.

Figure S5. Complement to oscillatory behavior of Knk1-2xGFP shown in Figure 5.

Figure S6. Complement to discussion concerning possible functions of Knk1.

Figure Legends

Experimental Procedures: Detailed information for all experiments described in this study.

Table S1. List of strains used in this study.

Table S2. Quantification of Knk1-2xGFP and CRIB-GFP dynamics in wildtype and indicated mutants.

References

Figure S1. Scheffler et al.

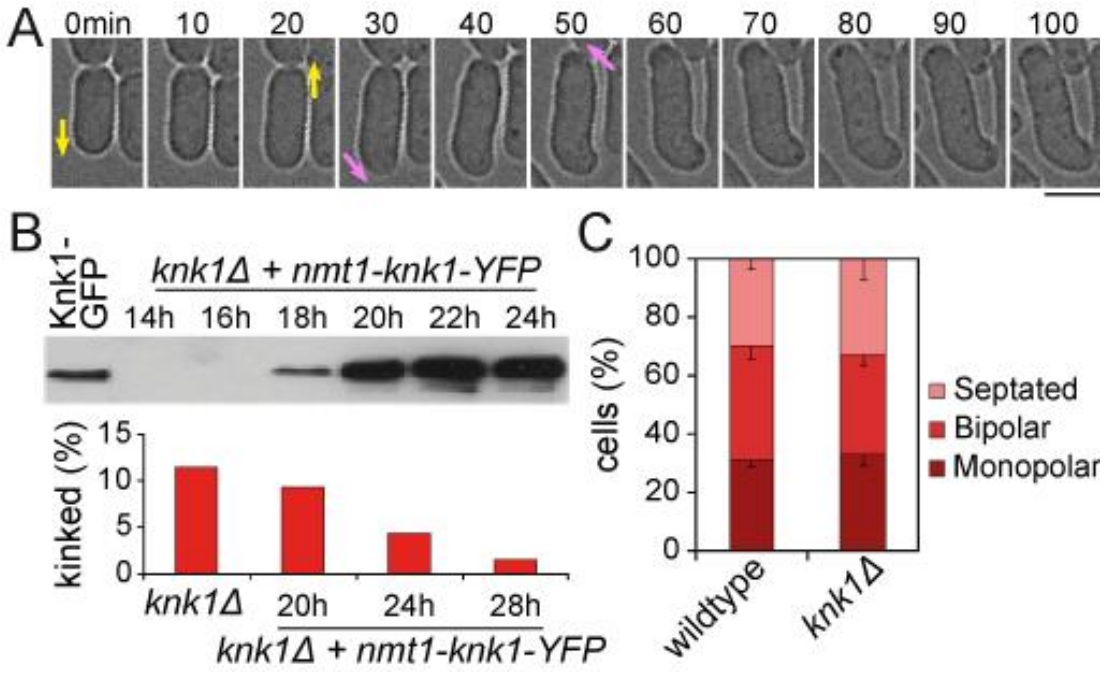

Figure S2. Scheffler et al.

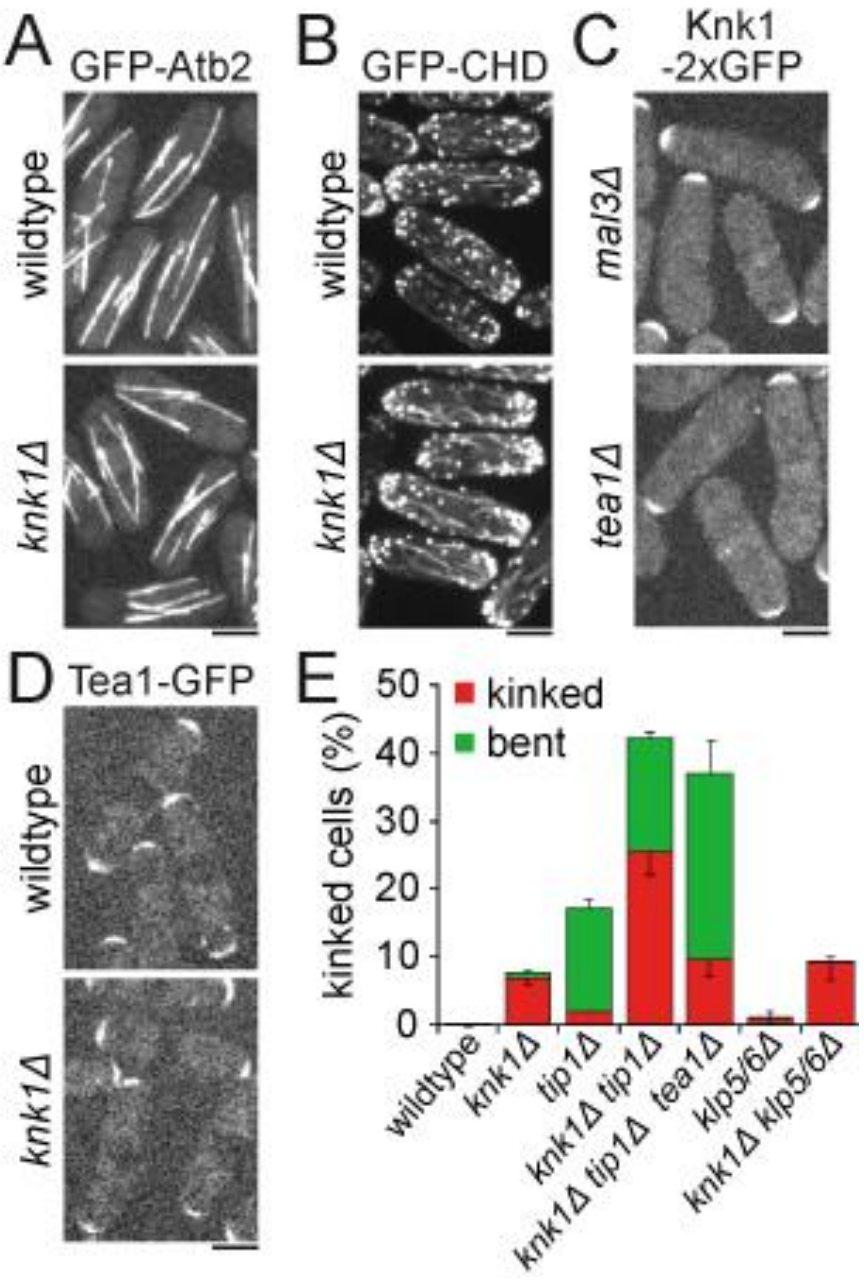

Figure S3. Scheffler et al.

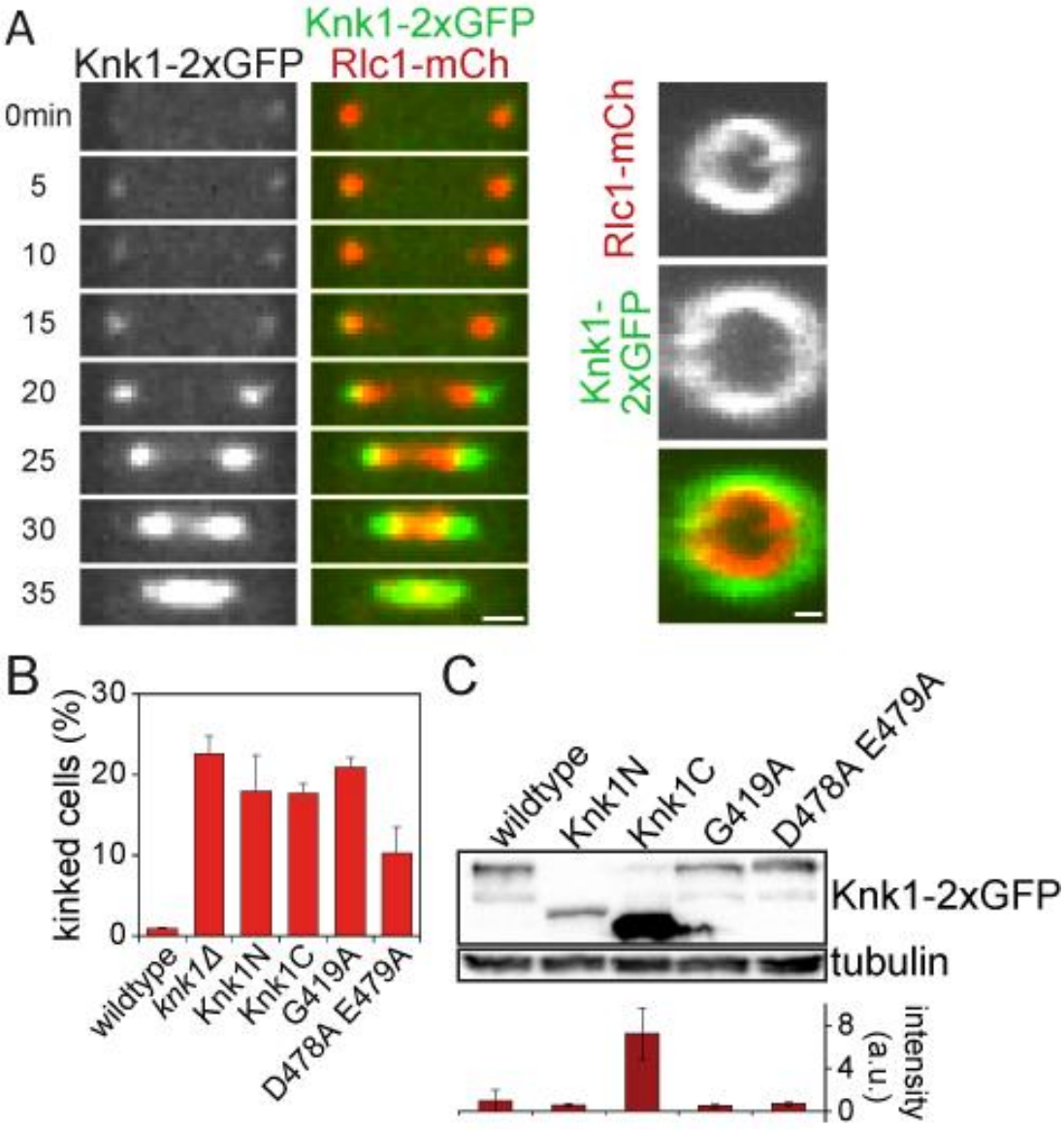

Figure S4. Scheffler et al.

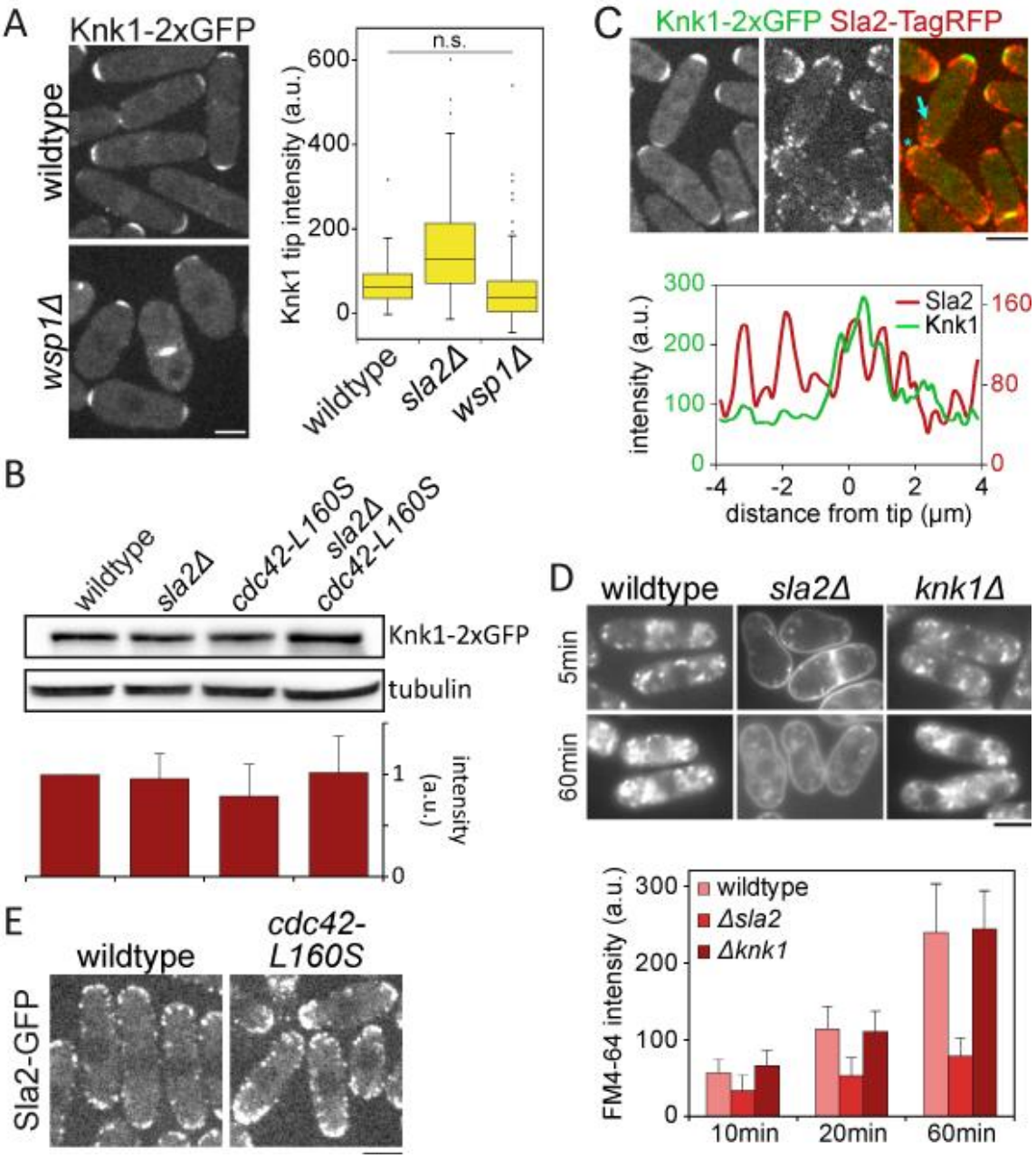

Figure S5. Scheffler et al.

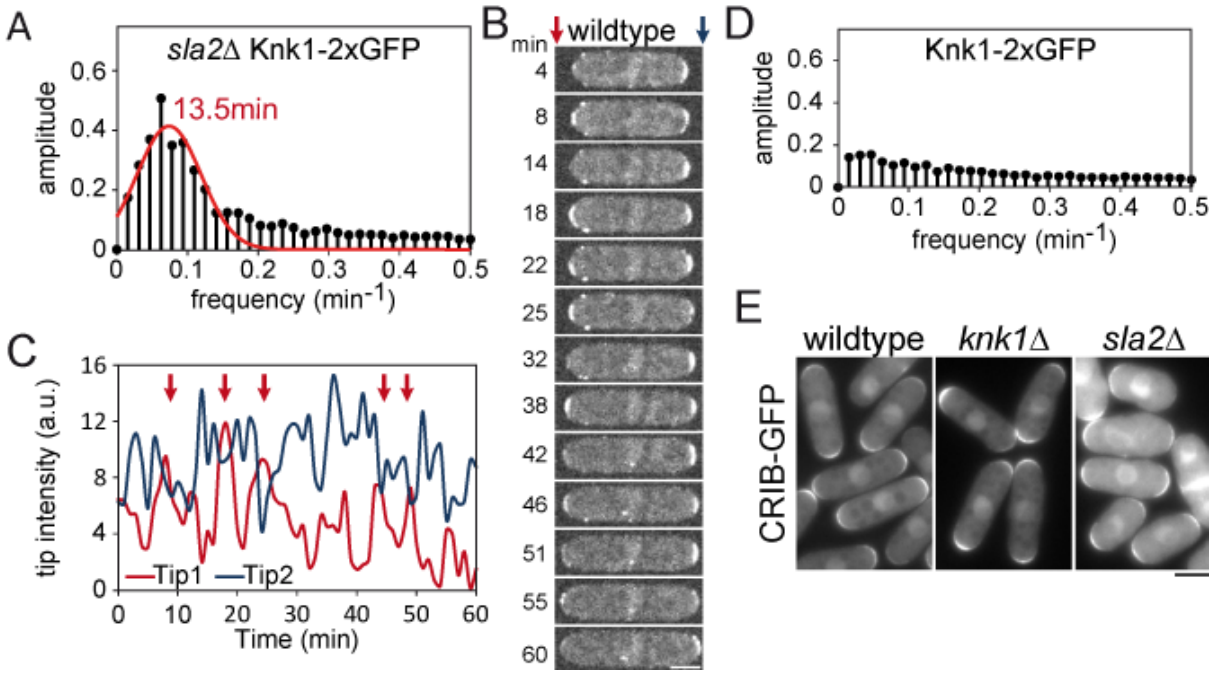

Figure S6. Scheffler et al.

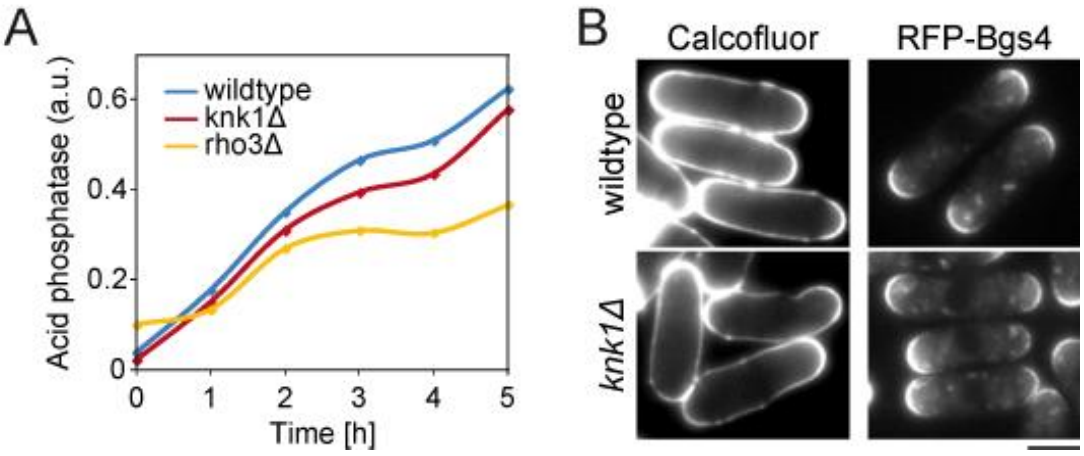

Supplemental Figure Legends

Figure S1. (A) Timelapse images of a *knk1Δ* cells by bright-field microscopy at 36°C. Arrows indicate direction of growth, yellow arrows upon initiation of growth, pink arrows after change of growth direction. Bar, 5µm. **(B)** Top, western blot of total cell extracts prepared from endogenous *knk1-GFP* or *knk1Δ nmt1-knk1-YFP* (*leu1* locus, under thiamine-repressible *nmt1* promoter) strains grown in minimal medium without thiamine. Western Blot was probed with anti-GFP antibody. Knk1 expression was detected after 18 to 20h after induction. Bottom, Percentage of kinked cells in *knk1Δ* or *knk1Δ nmt1-knk1-YFP* strains at indicated time points after induction of Knk1-YFP expression at 25°C. **(C)** Percentage of monopolar, bipolar and septated cells in wildtype and *knk1Δ* at 25°C using RFP-Bgs4 (glucan synthase localized to growing cell tips) [1]. Bars represent means from 3 independent experiments (n>300 cells per experiment). Error bars: s.d.

Figure S2. (A) MT cytoskeleton labeled with GFP-Atb2 and **(B)** actin with GFP-CHD (calponin-homology domain) under *nmt1* promoter in wildtype and *knk1Δ.* Recorded by spinning disk confocal and presented as maximum z-projection of 3D stacks. **(C)** Knk1-2xGFP localization in *mal3Δ* and *tea1Δ*; recorded as single medial z-section. **(D)** Tea1-GFP localization in wildtype and *knk1Δ*; recorded as single medial z-section. **(E)** Percentage of kinked and bent cells in wildtype and *knk1Δ* mutants at 25°C. Bars represent means from 3 independent experiments (n>300 cells per experiment). Error bars: s.d. Bars, 5µm.

Figure S3. (A) Left, Timelapse images of cell expressing Knk1-2xGFP and Rlc1-mCherry during cytokinesis; recorded as single medial z-sections. Right, Image constructed from a 3D stack. Bar, 1µm. **(B)** Percentage of kinked cells after 3h at 36°C. Bars represent means from 3 independent experiments (n>300 cells per experiment). Error bars: s.d. **(C)** Top, western blot of total cell extracts prepared from strains expressing respective Knk1-2xGFP construct. Western blot was probed with anti-GFP or TAT1 antibodies (tubulin as a loading control). Below, Relative amounts of Knk1 normalized to wildtype. Bars represent means from 3 independent experiments. Error bars: s.d.

Figure S4. (A) Left, Knk1 localization in wildtype and *wsp1Δ.* Images recorded as single medial z-sections. Bar, 5µm. Right, Knk1 intensities averaged over individual tips: wildtype (70.4±46.9 a.u.), *sla2Δ* (150.3±119.9, $p<10^{-8}$), and *wsp1Δ* (59.8±88.3, p=0.21). (n=100) **(B)** Top, western blot of total cell extracts prepared from *knk1-2xGFP* strains. Western blot was probed with anti-GFP or TAT1 antibodies (tubulin as a loading control). Below, Relative amounts of Knk1 normalized to wildtype. Bars represent means from 3 independent experiments. Error bars: s.d.

(C) Cells coexpressing Sla2-TagRFP (actin patch) and Knk1-2xGFP. Arrow highlights Sla2 patch moving inwards. Bottom, Line scan of individual cell (asterisk) of Sla2 and Knk1 fluorescence intensity along cell tip, averaged at each point over tip width. Bars, 5µm. **(D)** Top, Bar quantification of FM4-64 uptake measured as mean cytoplasmic intensity in wildtype, *knk1Δ* and *sla2Δ*. Bars represent means. Error bars: s.d. (n≥41). Bottom, images recorded at single medial z-sections. Bar, 5µm. **(E)** Sla2-GFP distribution in wildtype and *cdc42-L160S*. Images recorded as single medial z-sections. Bar, 5µm.

Figure S5. **(A)** Frequency spectrum of Knk1-2xGFP tip intensities analyzed by Fast Fourier Transform analysis using selected intervals (with periodic anti-correlated dynamics detected by eye) in *sla2Δ* (n=15, 0.074min^{-1}). **(B)** Timelapse images of Knk1-2xGFP in wildtype at 25°C. Images recorded as single medial z-sections at 1min intervals. Panel shows Knk1 distribution at timepoints corresponding to Linegraphs in (C). **(C)** Knk1-2xGFP tip intensities in wildtype at 1min intervals. **(D)** Frequency spectrum of Knk1-2xGFP tip intensities in wildtype (n=31). No clear periodic behavior can be detected. **(E)** CRIB-GFP distribution in wildtype, *knk1Δ* and *sla2Δ*. Images recorded as single z-section. Bars, 5µm.

Figure S6. (A) Acid phosphatase secretion to culture medium in logarithmic cultures of wildtype, *knk1Δ* and *rho3Δ* incubated at 36°C for 5h. *rho3Δ* is used a control as it has been reported to show lower levels of secretion [2]. **(B)** Calcofluor staining of the cell wall and RFP-Bgs4 distribution in wildtype and *knk1Δ*. No atypical accumulation of cell wall material in kinked cells was observed. **(C)** For3-3xGFP distribution in wildtype and *wsp1Δ* cells. Images recorded as single medial z-sections. Bar, 5µm. Cell tip used for magnification marked by yellow outline. Bar, 1µm. **(D)** Line scans of For3-3xGFP and Tea1-GFP fluorescence intensities along cell tips averaged for individual tips. p-Value measured for highlighted area (For3-3xGFP p=0.002 and Tea1-GFP p=0.84) (n=30).

Experimental Procedures

Strains and media

Standard fission yeast media and techniques were used as described [3]. Deletions and tagging were constructed by an established homologous recombination technique [4]. Strains used in this study are listed in Table S1.

Construction of Knk1 overexpressing and Knk1 mutants expressing strains

The *knk1* gene was overexpressed using the thiamine-repressible *nmt1* promoter [5] by integration of the pDUAL2 vector (RIKEN BioResource Center, [6]) into the *leu1-32* locus after digest with *NotI*.

Knk1N- and Knk1C-2xGFP strains were constructed by an established homologous recombination technique [4].

The wildtype Knk1 tagged to 2xGFP, *pknk1* promoter and *tknk1* terminator, were cloned into a pFA6a-based expression vector [7] to create pKS48 (pFa6a-*pknk1-knk1-2xGFP-tADH-kanMX6-tknk1*). Site-directed mutagenesis was carried out by using the QuickChange II XL Site-Directed Mutagenesis Kit (Stratagene). Primers used for mutagenesis are listed with the mutated codons underlined: G419A 5'- ATGCTTCTTTTTGCACCCCCTGGCACCGGC-3' (sense) and 5'-TGCCAGGGGGTGCAAAAAGAAGCATGCCTTGTACG-3' (antisense); D478A D479A 5'-CGTTATCTTTGTTGCAGCAATTGATTCCATTCTTTCCGC-3' (sense) and 5'-GCGGAAAGAATGGAATCAATTGCTGCAACAAAGATAACG-3' (antisense). All mutations were confirmed by DNA sequencing. Plasmids were digested with *SnaBI* and *XbaI* and integrated at *knk1* locus in a *knk1Δ* strain.

Protein Analysis

Protein sequence analysis and homology search were done using the standard tolos BLAST and CCD.

Microscopy

Generally, cells were grown exponentially in YE5S at 25°C. For starvation, *tea1Δ* cells were grown for 3d at 25°C to stationary phase and transferred to fresh medium 3h before imaging (Fig. 1A). *cdc25-22* (Fig. 1*B*), *orb6-25* (Fig. 1*A*) and *knk1Δ* (Fig. 1*A-C*, *E*, S1A and S3*B*) strains were incubated at 36°C for 3h or 7h, respectively, before imaging. *nmt1-GFP-CHD* strain (Fig. S2*B*) grown for 24h in EMM3S without thiamine before imaging.

Two microscopic set up were used. For DIC images (Fig. 1*A*, *B* and 2*C*), RFP-Bgs4 (Fig. S1*C*), FM4-64 staining (Fig. S4*D*), CRIB-GFP (Fig. S5*E*) and Calcofluor staining (Fig. S6*B*), we used a Leica DMRXA2 upright microscope (www.leica-microsystems.com) equipped with a 100X/1.4NA Plan Apochromat objective and a CoolSNAP HQ CCD camera (www.photometrics.com). In this case, 2µL of cells were mounted directly between slide and coverslip. Images were taken as single focal planes

For imaging Knk1-2xGFP (Fig. S2*C*, 3*D*, 4*A*-*C*, S4*A*, *C*), Sla2-GFP/TagRFP (Fig. S4*C*, *E*), GFP/mCherry-Atb2 (Fig. S2*A*, 4*A*), GFP-CHD (Fig. S2*B*) and Tea1-GFP (Fig. S2*D*) and all timelapse movies (Fig. S1*A*, 2*A*, 3*A*, S3*A*, 5*A*-*G*, S5*A*-*D*)), we used the Yokogawa spinning disc confocal head mounted on a Nikon Eclipse Ti inverted microscope (www.nikoninstruments.com), equipped with Nikon PlanApo 100X/1.45 NA objective lens, a PIFOC objective stepper and a Hamamatsu cooled back-thinned HQ2 CCD camera (Roper) as previously described [8]. Cells were mounted in PDMS chambers filled with 2% agarose YE5S or EMM3S and imaged at 25°C if not stated otherwise. Usually, single z-sections, except for GFP/mCherry-Atb2 6 planes spaced 0.8µm, were acquired. For 3D reconstruction of Rlc1-mCherry Knk1-2xGFP (Fig. S3*A*) 50 planes spaced 0.1µm were acquired of separating cells. Timelapse movies were taken at stated intervals. For measuring MT dynamics, GFP-atb2 was imaged at a 5s interval. Additional details of imaging conditions are provided for each figure in supplemental section. For measuring oscillations, Knk1-2xGFP and CRIB-GFP were imaged at a 1min interval.

Microtubule and actin depolymerization

Strains were grown to exponential phase at 25°C in YE5S and incubated for 10min on glass bottom dishes (WPI Fluorodish FD35-100) coated with lectin (0.1mg/mL; Sigma L1395) for 5min, then washed twice with YE5S medium. The dish was then centrifuged at 1500rpm for 1min. 2mL medium were injected and cells were imaged. Medium was exchanged for medium containing 50µg/mL Carbendazim (MBC, Sigma) or 100µM Latrunculin A (Sigma) in DMSO. Cells were incubated for 20min and then imaged. Finally, drug was removed, cells were washed three times and new medium was added. Cells were imaged up to 90min after wash out.

FM4-64 uptake

FM4-64 (SynaptoRed, Merck) was dissolved in water at a concentration of 1.64mM and added to the cells at a final concentration of 40µM. Cells were incubated on ice for 5min, washed once with 1mL ice-cold medium and resuspended in fresh medium before imaging.

Data Analysis

Images were acquired and processed with MetaMorph 7.7 (www.MolecularDevices.com).

DIC images were used to quantify percentage of bent and kinked cells (Fig. 1*C*, S1*B*, 2*B*, S2*E*, S3*B*) and measure angles (Fig.1*E*, 2*D*-*E*). RFP-Bgs4 staining was used to measure NETO (Fig. S1*C*) by visual inspection.

Tip intensities were measured via Linescan Analysis, values were averaged for each tip and corrected for background. Data for fluorescence intensities (Fig. 4C, S4A) and angles ((Fig. 1E, 2D, E) were plotted as box plots generated with Kaleidagraph 4.0 (www.synergy.com). Each box encloses 50% of the data with the median value displayed as a line. The top and bottom of each box mark the minimum and maximum values within the data set that fall within an acceptable range. Any value outside of this range, called an outlier, is displayed as an individual point. Statistical analyses of data were performed using the Student's t-test for comparison between means in Microsoft Excel 2010.

Quantification of oscillatory dynamics of Knk1-2xGFP and CRIB-GFP

Quantification of oscillatory dynamics of fluorescent proteins was performed using a Fast Fourier Transform algorithm (MATLAB, The MathWorks). Fluorescent signal at cell tips was averaged after background subtraction. FFT analysis was done on data normalized by their average values. Intervals of frequencies with higher amplitudes were fitted with a gaussian function using Matlab algorithms. Analysis was done on all cells or on subgroup of cells exhibiting oscillations. This subgroup of cells was identified by eye and confirmed by autocorrelation analysis. Opposite tips intensities cross-correlation was determined with Matlab algorithms.

Western Blotting

To analyze total levels of chromosomally tagged Knk1-2xGFP (Fig. S3*C*, S4*B*), cells were grown exponentially grown in YE5S at 25°C, or for Knk1-GFP (chromosomally tagged) and Knk1-YFP (expressed from *leu1* under *nmt1* promoter) (Fig. S1*B*), cells were grown in EMM3S without thiamine. Protein extracts were prepared in extraction buffer (PBS 2mM EDTA) containing protease inhibitor cocktail (Roche). By Western Blotting, relative amounts of Knk1 were determined using anti-GFP antibody (Roche) compared to tubulin as a loading control detected by TAT1 antibody, and anti-mouse IgG-peroxidase (Sigma) secondary antibody.

Acid phosphatase measurement

Acid phosphatase secretion was assayed as described [9]. Cells were grown to log phase in YE5S at 36°C, washed twice, and resuspended in fresh medium at 36°C. Aliquots were taken at the time of resuspension (t=0) and every hour for 5 h. For each time sample, 1 mL of culture was centrifuged, and 0.5 mL of the supernatant was added

to 0.5 mL of substrate solution (2 mMp-nitrophenyl phosphate, 0.1M sodium acetate, pH 4.0; prewarmed to 30°C. Reactions were incubated at 30°C for 5 min and stopped by the addition of 0.5 mL 1MNaOH. The absorbance at 405 nm was measured, using the t=0 sample as a blank control. Results were made relative to the number of cells [optical density

(OD) 405 nm/OD 600 nm] and considered arbitrary units of secreted AP.

Table S1. List of *S. pombe* strains used in this study.

Strain	*Genotype*	Source
	Figure 1	
AP240	*h- ade6-M210 ura4-D18 leu1-32*	lab collection
TP25	*h+ ade6-M210 leu1-32 orb6-25*	lab collection [10]
TP468	*h+ ade6-M210 leu1-32 ura4-D18 for3Δ::KanMX6*	lab collection [11]
TP715	*h+ ade6-M216 leu1-32 ura4-D18 sla2Δ ::KanMX6*	BIONEER deletion collection
AP657	*h+ ade6-M210 leu1-32 ura4-D18 his3-D1 mal3Δ::his3+*	lab collection [12]
AP2020	*h- ade6-M216 leu1-32 ura4-D18 mto1Δ::ura4+*	lab collection [13]
AP1684	*h- ade6-704 leu1-32 ura4-D18 tea1Δ::ura4+*	lab collection [14]
TP474	*h- ade6-M210 ura4-D18 leu1-32 knk1Δ::KanMX6*	This work
AP239	*h+ leu1-32 cdc25-22*	lab collection [15]
TP536	*h- ade6-M210 leu1-32 cdc25-22 knk1Δ::KanMX6*	This work
	Figure 2	
TP382	*h- leu1-32 ura4-D18 GFP-atb2::KanMX6*	lab collection
TP531	*h- ade6-M216 leu1-32 ura4-D18 knk1Δ::KanMX6 GFP-atb2::Nat^R*	This work
TP530	*h- ade6-M210 leu1-32 ura4-D18 tea1Δ::ura4+ knk1Δ::KanMX6*	This work
TP651	*h+ ade6-M216 leu1-32 ura4-D18 his3? mal3Δ::his3+ knk1Δ::KanMX6*	This work
TP2136	*h+ ade6-M216 leu1-32 ura4-D18 tea1Δ::ura4+ knk1Δ::KanMX6 mal3Δ::hph^R*	This work
TP614	*h- ade6-M216 leu1-32 ura4-D18 mto1Δ::KanMX6 knk1Δ::Nat^R*	This work
TP2173	*h+ ade6-M216 leu1-32 ura4-D18 mto1Δ::KanMX6 knk1Δ::Nat^R tea1Δ::ura4+*	This work
	Figure 3	
TP801	*h+ ade6-M216 leu1-32 ura4-D18 rlc1-mCherry::Nat^R knk1-2xGFP::KanMX6 mCherry-atb2::Hph^R*	This work
TP685	*h- ade6-M210 ura4-D18 leu1-32 knk1-2xGFP::KanMX6*	This work
TP1084	*h- ade6-M210 leu1-32 ura4-D18 knk1Δ:: pknk1-knk1N(1-380)-2xGFP-TADH::KanMX6-tknk1*	This work
TP1086	*h- ade6-M210leu1-32 ura4-D18 knk1Δ:: pknk1-knk1C(350-660)-2xGFP-TADH::KanMX6-tknk1*	This work
TP1747	*h- ade6-M210 leu1-32 ura4-D18 knk1Δ:: pknk1-knk1(G419)-2xGFP-TADH::KanMX6-tknk1*	This work
TP1832	*h- ade6-M210 leu1-32 ura4-D18 knk1Δ:: pknk1-knk1(D478A E479A)-2xGFP-TADH::KanMX6-tknk1*	This work
	Figure 4	

TP762	*h- ade6-M216 leu1-32 ura4-D18 mCherry-atb2::Hph^R knk1-2xGFP::KanMX6*	This work
AP1096	*h- ade6-M210 leu1-32 ura4-D18 Crn1-GFP ::KanMX6*	lab collection [16]
TP846	*h- ade6-M210 leu1-32 ura4-D18 for3Δ::Nat^R knk1-2xGFP::KanMX6*	This work
TP781	*h+ ade6-M210 leu1-32 ura4-D18 sla2Δ::Nat^R knk1-2xGFP::KanMX6*	This work
TP855	*h+ leu1-32 ura4-D18 myo1Δ::KanMX6 knk1-2xGFP::KanMX6*	This work
TP871	*h- leu1-32 ura4-D18 HA-cdc42-L160S::ura4+ knk1-2xGFP::KanMX6*	This work
TP1788	*h+ leu1-32 ura4-D18 sla2Δ::natR HA-cdc42-L160S::ura4+ knk1-2xGFP::KanMX6*	This work
	Figure 5/S5	
TP682	*h+ leu1-32 CRIB-GFP::ura4+ (ura4-294::shk1prom:ScGIC2:3GFP:Ura+)*	Pilar Perez [17]
TP713	*h- leu1-32 CRIB-GFP::ura4+ knk1Δ::Nat^R*	This work
TP1611	*h- leu1-32 CRIB-GFP::ura4+ sla2Δ::KanMX6*	This work
	Figure S1	
TP481	*h- ade6-M210 leu1-32 ura4-D18 knk1-GFP::KanMX6*	This work
TP623	*h- ade6-M216 ura4-D18 knk1Δ::Nat^R + leu1+::(pDUAL)nmt1-Knk1-YFP-FLAG-His6-TADH1*	This work, plasmid from RIKEN BioResource Center
TP469	*h- his3-D1 leu1-32 ura4-D18 pbgs4-RFP-bgs4::leu1+ bgs4Δ::ura4+*	[1]
TP534	*h- ade6-M216 leu1-32 ura4-D18 knk1Δ::KanMX6 pbgs4-RFP-bgs4::leu1+ bgs4Δ::ura4+*	This work
	Figure S2	
TP6	*h- ade6-M216 ura4-D18 pnmt41-GFP-CHD::leu1+*	lab collection [18]
TP622	*h- ade6-M216 leu1-32 ura4-D18 knk1Δ::Nat^R pnmt41-GFP-CHD::leu+*	This work
TP904	*h+ ade6-M210 leu1-32 ua4-D18 his3? mal3Δ::his3+ knk1-2xGFP::KanMX6*	This work
TP758	*h- ade6-M216 leu1-32 ura4-D18 tea1Δ::ura4+ knk1-2xGFP::KanMX6*	This work
TP10	*h+ ade6-M216 leu1-32 ura4-D18 tea1-GFP::KanMX6*	lab collection [14]
AP659	*h+ tip1Δ::KanMX6*	Lab collection [19]
TP2181	*h- ade6-M216 ura4-D18 leu1-32 tip1Δ::KanMX6 knk1Δ::Nat^R*	This work
TP2196	*h- ade6-M216 ura4-D18 leu1-32 tip1Δ::KanMX6 knk1Δ::Nat^R tea1Δ::ura4+*	This work
TP900	*h+ ade6-M210 ura4-D18 leu1-32 his3-D1 klp5Δ::ura4+ klp6Δ::his3+*	lab collection [20]
TP950	*h- ade6-M210 ura4-D18 leu1-32 his3-D1 klp5Δ::ura4+ klp6Δ::his3+ knk1Δ::KanMX6*	This work
	Figure S3	
TP760	*h- ade6-M216 ura4-D18 leu1-32 rlc1-mcherry::Nat^R knk1-2xGFP::KanMX6*	This work
	Figure S4	
TP2182	*h- leu1-32 ura4-D18 his3-D1? wsp1Δ::KanMX6 knk1-2xGFP::Hph^R*	This work
TP903	*h+ ade6-M210 leu1-32 ura4-D18 sla2-TagRFP::Nat^R knk1-*	This work

	2xGFP::KanMX6	
TP681	*h+ ade6-M210 leu1-32 ura4-D18 sla2-GFP ::KanMX6*	lab collection [21]
TP2110	*h- leu1-32 ura4-D18 cdc42-L160S::ura4+ sla2-GFP::KanMX6*	This work
	Figure S6	
TP721	*h+ ade6-M216 leu1-32 ura4-D18 rho3Δ::KanMX6*	BIONEER deletion collection

Table S2. Quantification of Knk1-2xGFP and CRIB-GFP dynamics in wildtype and indicated mutants.

strain	n_{total} (cells)	intervals (total)	$n_{selected}$	intervals (selected)	Cross Correlation		Frequency (min^{-1}), (Periodicity, min)	
					total	selected	total	selected
Knk1-2xGFP	31	57±6min	n.d.	n.d.	-0.16±0.25	n.d.	n.d.	n.d.
sla2Δ Knk1-2xGFP	25	54±8min	15	48±8min	-0.39±0.24	-0.45±0.2	0.072 (13.9min)	0.074 (13.5min)
cdc42-L160S Knk1-2xGFP	21	65±8min	12	51±10min	-0.30±0.31	-0.5±0.29	0.068 (14.8min)	0.076 (13min)
CRIB-GFP	21	49±8min	14	22±5min	-0.41±0.29	-0.71±0.15	n.d.	0.19 (5.3min)
knk1Δ CRIB-GFP	21	55±8min	13	28±8min	-0.46±0.21	-0.76±0.13	n.d.	0.21 (4.8min)
sla2Δ CRIB-GFP	21	67±7min	8	26±6min	-0.55±0.26	-0.67±0.2	n.d.	n.d.
Tea1-GFP	18	60min	n.d.	n.d.	0.04±0.34	n.d.	n.d.	n.d.

n.d. not determined (parameter could not be confidently measured/defined)

Table summing up parameters of oscillatory behavior at cell tips of Knk1-2xGFP, CRIB-GFP and Tea1-GFP presented in Figure 5. While Knk1-2xGFP and CRIB-GFP exhibit periodic, anti-correlated dynamics, Tea1 shows uncorrelated fluctuations. Values are presented as means ± s.d.

Supplemental References

1. Cortes, J.C., et al., *The novel fission yeast (1,3)beta-D-glucan synthase catalytic subunit Bgs4p is essential during both cytokinesis and polarized growth.* J Cell Sci, 2005. **118**(Pt 1): p. 157-74.
2. Wang, H., X. Tang, and M.K. Balasubramanian, *Rho3p regulates cell separation by modulating exocyst function in Schizosaccharomyces pombe.* Genetics, 2003. **164**(4): p. 1323-31.
3. Moreno, S., A. Klar, and P. Nurse, *Molecular genetic analysis of fission yeast Schizosaccharomyces pombe.* Methods Enzymol, 1991. **194**: p. 795-823.
4. Bahler, J., et al., *Heterologous modules for efficient and versatile PCR-based gene targeting in Schizosaccharomyces pombe.* Yeast, 1998. **14**(10): p. 943-51.
5. Maundrell, K., *nmt1 of fission yeast. A highly transcribed gene completely repressed by thiamine.* J Biol Chem, 1990. **265**(19): p. 10857-64.
6. Matsuyama, A., et al., *ORFeome cloning and global analysis of protein localization in the fission yeast Schizosaccharomyces pombe.* Nat Biotechnol, 2006. **24**(7): p. 841-7.
7. Wach, A., et al., *New heterologous modules for classical or PCR-based gene disruptions in Saccharomyces cerevisiae.* Yeast, 1994. **10**(13): p. 1793-808.
8. Tran, P.T., A. Paoletti, and F. Chang, *Imaging green fluorescent protein fusions in living fission yeast cells.* Methods, 2004. **33**(3): p. 220-5.
9. Wang, H., et al., *The multiprotein exocyst complex is essential for cell separation in Schizosaccharomyces pombe.* Mol Biol Cell, 2002. **13**(2): p. 515-29.
10. Verde, F., J. Mata, and P. Nurse, *Fission yeast cell morphogenesis: identification of new genes and analysis of their role during the cell cycle.* J Cell Biol, 1995. **131**(6 Pt 1): p. 1529-38.
11. Feierbach, B. and F. Chang, *Roles of the fission yeast formin for3p in cell polarity, actin cable formation and symmetric cell division.* Curr Biol, 2001. **11**(21): p. 1656-65.
12. Beinhauer, J.D., et al., *Mal3, the fission yeast homologue of the human APC-interacting protein EB-1 is required for microtubule integrity and the maintenance of cell form.* J Cell Biol, 1997. **139**(3): p. 717-28.
13. Sawin, K.E., P.C. Lourenco, and H.A. Snaith, *Microtubule nucleation at non-spindle pole body microtubule-organizing centers requires fission yeast centrosomin-related protein mod20p.* Curr Biol, 2004. **14**(9): p. 763-75.
14. Mata, J. and P. Nurse, *tea1 and the microtubular cytoskeleton are important for generating global spatial order within the fission yeast cell.* Cell, 1997. **89**(6): p. 939-49.
15. Fantes, P., *Epistatic gene interactions in the control of division in fission yeast.* Nature, 1979. **279**(5712): p. 428-30.
16. Basu, R. and F. Chang, *Characterization of dip1p reveals a switch in Arp2/3-dependent actin assembly for fission yeast endocytosis.* Curr Biol, 2011. **21**(11): p. 905-16.
17. Tatebe, H., et al., *Pom1 DYRK regulates localization of the Rga4 GAP to ensure bipolar activation of Cdc42 in fission yeast.* Curr Biol, 2008. **18**(5): p. 322-30.
18. Karagiannis, J., et al., *The nuclear kinase Lsk1p positively regulates the septation initiation network and promotes the successful completion of cytokinesis in response to*

perturbation of the actomyosin ring in Schizosaccharomyces pombe. Mol Biol Cell, 2005. **16**(1): p. 358-71.

19. Brunner, D. and P. Nurse, *CLIP170-like tip1p spatially organizes microtubular dynamics in fission yeast.* Cell, 2000. **102**(5): p. 695-704.
20. West, R.R., et al., *Two related kinesins, klp5+ and klp6+, foster microtubule disassembly and are required for meiosis in fission yeast.* Mol Biol Cell, 2001. **12**(12): p. 3919-32.
21. Castagnetti, S., R. Behrens, and P. Nurse, *End4/Sla2 is involved in establishment of a new growth zone in Schizosaccharomyces pombe.* J Cell Sci, 2005. **118**(Pt 9): p. 1843-50.

Discussion Part I –

MT-dependent nuclear congression in fission yeast

Distinct roles for minus end-directed motors in nuclear movements

Here, we demonstrate that two minus end-directed motors, the kinesin-14 Klp2 and dynein, are required to efficiently drive nuclear congression in fission yeast. To our knowledge, this is the first report of how two minus end-directed motors translocate nuclei by distinct mechanisms, that is to say that these two motors cannot replace each other functionally. In our model (Fig. 5 in results I), Klp2 localizes dominantly to plus ends and cross-links MTs emanating from the opposite SPB in an antiparallel manner. Dynein accumulates at SPBs and probably pulls on MTs nucleated by the mating partner.

Although this process has been intensively studied in budding yeast, our work provides a first detailed description of nuclear congression in live fission yeast cells. Major difficulties lie in the fact that fission yeast cells mate rather inefficiently and at random time points. Therefore, the development of a microfluidic-based system allowing incubation and imaging over long periods was crucial to carry out the presented study. Screens through all MT motors revealed that Klp2 and dynein are major force generators and alone are sufficient to drive nuclear congression. Single mutants show only a more or less strong delay, but a double mutant completely fails to bring nuclei together demonstrating that each gene becomes essential in the absence of the other. This situation is reminiscent, for instance, to mitosis in budding yeast, where two redundant mechanisms orient and position the spindle, first by depolymerizing MTs captured at the cortex and secondly, by cortically anchored dynein exerting forces on astral MTs. The observation that deletion of *klp2* causes a greater delay than *dhc1* indicates that Klp2 generates stronger forces than dynein. That may be explained, for example, by different protein quantities, and may not reflect differences in force production on a single molecule level.

Additionally, we also find that proper control of MT dynamics may enhance efficiency of nuclear congression as *tea2* deletion causes a delay of 10 to 15min in wildtype, *klp2Δ* and *dhc1Δ* zygotes. That seems obvious, as shorter MTs are less likely to meet and be cross-linked by Klp2 or to reach the opposite SPB and be caught by dynein. Furthermore, we show that movement of the nuclei towards each other, without reaching each other, in a *klp2Δ dhc1Δ* zygote are dampened upon *tea2* deletion (Fig. S2H-J in results I) suggesting that MTs extending towards the cortex also exert forces able to push nuclei, as shown for interphase cells to position the nucleus in the center (Tran et al., 2001). Thus, shorter MTs in *tea2Δ* and *tip1Δ* cells can therefore push

nuclei only smaller distances away the cortex. However, these motor-independent forces are clearly not sufficient to drive nuclear congression.

We propose that Klp2-dependent pulling forces move nuclei towards each other. Klp2 as a member of the kinesin-14 family contains two MT-binding domains, one in the motor domain and one additional in the tail, allowing to interact with two MTs at once and to cross-link them (Braun et al., 2009). This appears to be a conserved feature among kinesin-14s and related kinesins, as two distinct MT-binding sites have been also found in *Drosophila* Ncd (Karabay and Walker, 1999) and *Arabidopsis* KCBPs (kinesin-like calmodulin-binding proteins) (Narasimhulu and Reddy, 1998). In general, these kinesins including Klp2, Ncd and HSET localize to MT plus ends dependent on EB1 through an SxIP motif (Janson et al., 2007, Goshima et al., 2005, Braun et al., 2013). We confirm this localization pattern for Klp2 during meiosis. Regarding their role, kinesin-14s are implicated in MT sliding, for instance, to regulate spindle length in human (Cai et al., 2009) and to focus kinetochores fibers at the spindle poles in *Drosophila* (Goshima et al., 2005, Oladipo et al., 2007). It was believed for long time that Kar3 at MT plus tips also acts by cross-linking and sliding MT relative to each other (Rose, 1996) or by inducing depolymerization and connecting shrinking MT ends (Molk et al., 2006). A recent study now demonstrates a novel mechanism for Kar3 in nuclear congression, where SPB-bound Kar3 pulls on MTs laterally (Gibeaux et al., 2013). Whether Kar3 is capable of mediating interaction between MTs remains to be addressed, as, at least to our knowledge, it has not been investigated, whether Kar3 contains two MT-binding sites accounting for MT cross-linking.

On the other hand, Klp2 has been shown to stabilize interphase antiparallel MT bundles by sliding newly nucleated MTs towards minus ends concentrated in the overlap zone of the bundle (Carazo-Salas et al., 2005) (Janson et al., 2007). It is therefore likely that Klp2 generates pulling forces during nuclear congression in a similar manner; by sliding antiparallel MTs relative to each. This mechanism has been suggested to explain nuclei clustering after separation of the DNA and spindle breakdown, which occurs in mutants defective in septation (Mana-Capelli et al., 2012). Alternatively, Klp2 might cross-link shrinking plus tips and potentially induce depolymerization. This hypothesis has been favored until recently for budding yeast karyogamy, because no extensive overlap bridging the nuclei has been observed (Molk et al., 2006). Both, Kar3 and Klp2, appear to operate via such a mechanism during mitosis to facilitate

retrieval of lost chromosomes to spindle poles (Grishchuk and McIntosh, 2006, Tanaka et al., 2007, Gachet et al., 2008). The motor proteins localizes at kinetochores and transport chromosomes to SPBs by lateral translocation along MTs and by provoking shortening of kinetochores fibers. If Klp2 utilizes this mode of action during nuclear congression, MTs should be dominantly connected at plus tips. In our studies, despite a rather complex MT array in fission yeast karyogamy, where behavior of single MTs can be hardly monitored, it becomes apparent that a bright bundle between the two nuclei is formed suggesting that the first hypothesis of Klp2 sliding MTs relative to each might be the case. However, as possibly both mechanisms might be applied, it will be necessary to visualize MT with a high time resolution in fluorescence microscopy and maybe via other methods such as electron microscopy to analyze organization and dynamics of MTs prior to bundle formation and within the bundle. Finally, in comparison to budding yeast, where Kar3 is recruited to the SPB specifically during meiosis, we tested whether Klp2 may localize to SPBs in meiosis. Since in wildtype cells, plus tips extending throughout the entire zygote rendering it difficult to judge, whether Klp2 is also recruited to SPBs, we visualized Klp2 in *mal3Δ* cells, where Klp2 is largely absent from the short MTs (Mana-Capelli et al., 2012), but can be still found in one or more dots around the nucleus (Fig. S3A in results I). We believe that, even without Mal3, Klp2 might still bind to MTs with a very low affinity and then walk and accumulate at minus ends anchored at the NE at multiple iMTOCs in non-mating cells and at the SPB exclusively during meiotic prophase (Ding et al., 1998). However, at the moment, we cannot exclude that Klp2 may be recruited to SPBs, in addition to plus ends, where it might function to support nuclear congression. As the levels of Klp2 at the SPB are minor compared to its MT-bound pool, we speculate that Klp2 contributes to migration of nuclei dominantly at the MT plus ends.

Dynein is a large protein complex composed of two heavy chains (Dhc1) and several subunits and accessory proteins. The Dhc1 is meiotically upregulated and cannot be detected at specific cellular structures during the vegetative cell cycle (Yamamoto et al., 1999). In our own studies, we observed dynein first and foremost at the SPBs and telocentrosome in mating cells, but not in neighboring cells that had not initiated mating. Also, mRNA transcript of subunits of the dynein complex, including *dli1* and *ssm4*, are degraded during the vegetative cell cycle ensuring its activity exclusively during meiosis (Harigaya et al., 2006). The simultaneous

induction of expression of Dhc1 and other components to form and stabilize the dynein complex appears to coincide with initiation of karyogamy. We show that dynein starts to accumulate at SPBs about 30min prior to SPB fusion, approximately at the time of cell fusion, and increases in intensity during nuclear congression suggesting that pulling forces, specifically generated by dynein, may also amplify. This is consistent with the results obtained by measuring SPB dynamics showing that, specifically in wildtype and *klp2Δ* zygotes, where dynein contributes to force generation, nuclear movements appear to accelerate. Moreover, the levels of dynein further increase, when nuclear congression is delayed, like in *klp2Δ* zygotes, indicating that dynein levels might continuously rise even after completion of nuclear congression. That suggests a model, where dynein first localizes to the SPB and only if it is present in sufficient quantities also to MTs allowing the progression through horsetail movement. This behavior could be regulated by dynein itself possessing a higher affinity for SPB-specific components than for MTs or by presence of regulatory proteins such as dynactin enhancing affinity to MTs. Therefore, fission yeast karyogamy represents a good model illustrating how different subcellular localizations of dynein achieve diversity in function. Here, within a relative short period of time, dynein is recruited to the SPB driving nuclear congression, to telocentrosomes contributing to telomere clustering (Yoshida et al., 2013) and to MTs and the cortex promoting nuclear horsetail movement. In the future, it could be therefore interesting to decipher the molecular details of these mechanisms to get a clue on how dynein and different regulators are controlled in space and time.

Finally, we hypothesize that dynein anchored at the SPB may interact with MTs emanating from the SPB of the mating partner pulling the two nuclei together, as it has been now demonstrated for Kar3 by electron microscopy (Gibeaux et al., 2013).

One major question arising from the work presented here is why two redundant parallel mechanisms, both including a minus end-directed motor, exist to drive nuclear movements, in contrast to only a single kinesin-14 motor in budding yeast or only one dynein for most minus end-directed translocations in mammals. It is tempting to speculate that fission yeast stands evolutionarily in between these two systems. First, it maintained a role for kinesin-14, but transferred its place of action from the SPB to MT plus ends. Kar3 is anchored to the SPB halfbridge during meiosis via Spc72 (pericentrin-like) and Kar1 (Gibeaux et al., 2013). In fission

yeast, no Kar1 homologue based on sequence or function has been identified. Instead, Klp2 might have developed a novel function by acquiring a second MT-binding domain. In *dhc1Δ* zygotes, where nuclear congression solely depends on Klp2 lacking forces generated at the SPBs, this process proceeds only with a slight delay, until nuclear contact is established. Considering that light microscopy can resolve distances of 200nm and higher, then one could imagine that two nuclei "touching" each other, are in fact still separated by a space below 200nm. Interestingly, *dhc1Δ* zygotes seem to exhibit an extended time between nuclear contact and completion of nuclear fusion (Fig. S1D in results I) suggesting that motors bound to the SPB bring nuclei more efficiently together on the last "nanometers" than when bound to MT plus ends. On the other hand, motor proteins localized to plus ends may be more advantageous to cover larger distances. This hypothesis is supported by the size differences between budding yeast with 3-4nm in diameter and fission yeast with approximately 10nm in length.

In summary, one could imagine that fission yeast cells use dynein as a backup system that is not expressed throughout the whole cell cycle, only if needed, and facilitates, in particular, late stages of nuclear congression. Interestingly, about 50% of zygotes lacking dynein initiate nuclear congression immediately upon cell fusion (Fig. 2E in results I), while the remaining 50% exhibited an initial phase without directed nuclear migrations (Fig. 2F in results I). These observations suggest to us that dynein may support interactions between antiparallel MTs required for initiation of nuclear congression. Our preliminary data suggests that this specific role of dynein may become more important in mating cells with more complex geometries adopting S- or U-shape (Fig. S2G in results I). We hypothesize that in simpler geometries, like straight or L-shapes, plus ends might be more likely to meet and be cross-linked by Klp2, but the presence of a large motor complex at the SPB may help catching MTs from the mating partner, when Klp2 fails.

All together, the distinct properties as well as specific localization pattern of motor proteins allow differential roles for minus end-directed motors in the same process of nuclear positioning. To our knowledge, the study presented here might be the first report of two minus end-directed motors acting in concert. In mammals, most minus end-directed translocations of organelles including nuclei and vesicles are executed by dynein. Cooperation between kinesins, primarily plus end directed, and dynein in nuclear positioning has been reported for several

systems, such as interkinetic nuclear migrations during brain development (Tsai et al., 2010), in myotubes (Wilson and Holzbaur, 2012) and in *C. elegans (Fridolfsson and Starr, 2010),* and provide bi-directionality of nuclear movements. Hence, our work suggests that also collaborations of dynein with kinesin-14s in parallel pathways may increase efficiency and accuracy of nuclear positioning events.

Novel roles for dynein subunits and accessory proteins

Surprisingly, dynactin is dispensable for dynein-dependent nuclear congression in fission yeast. This is in sharp contrast to mammal system, where dynactin appears to be required for virtually all activities carried out by dynein (Kardon and Vale, 2009) (Vallee et al., 2012). It is proposed to increase processivity of dynein along MTs (King and Schroer, 2000). In fission yeast, dynactin and the intermediate chain Dic1 bridging dynein and dynactin (Vaughan and Vallee, 1995) are absolutely required for dynein localization to MTs, but not to SPBs (Niccoli et al., 2004) (Fujita et al., 2010). In this organism, it has not been investigated whether dynactin is required for dynein activity or only helps recruiting dynein. Therefore, at *status quo* it remains elusive why fission yeast dynein does not require dynactin for all its functions. For the future, it may be interesting to reveal the structural differences between the dynactin and dynein complexes in fission yeast and mammals to obtain a better understanding of how dynactin influences dynein in these systems.

On the other hand, we discovered that the light intermediate chain Dli1 is crucial for dynein function during nuclear congression and horsetail movement, as its deletion greatly reduces dynein levels at SPBs and MTs. In mammals, DLICs link dynein to specific cargos, in detail DLIC1 targets dynein to pericentrin, while DLIC2 to the polarity protein Par3. In *C. elegans,* Dli1 is required for mitosis and pronuclear migrations, but its depletion does not affect recruitment of dynein to different subcellular structures (Yoder and Han, 2001). In contrast, in *Drosophila*, lack of LIC leads to reduced protein levels of all components of the dynein complex (Mische et al., 2008) and in *Aspergillus,* it is essential for the assembly of the core dynein complex (Zhang et al., 2009). Our own data in fission yeast propose that Dli1 serves similar functions as in *Drosophila* and *Aspergillus,* as dynein appears globally affected and not only at specific structures in *dli1Δ* cells. Dli1 may do so by controlling the stabilization of Dhc1, by facilitating dimerization of Dhc1 or by mediating interaction with other proteins allowing its

recruitment to SPBs and MTs. Some aspects could be addressed by Western Blot and immuno-precipitation experiments to test whether Dhc1 protein levels or rate of dimerization are affected upon deletion of *dli1*. Possibly, it could also permit interaction with Dic1 or dynactin complex for MT and with an SPB component, such as Kms1 (KASH), for SPB localization. That would imply that Dli1 bridges dynein and MT or SPBs respectively and might localize to these structures even in the absence of dynein. Preliminary data suggest otherwise, as Dhc1 but not Dli1 alone bind weakly to SPBs, when ectopically expressed in vegetative cells (Figure 6.1) suggesting that Dhc1 possesses domains to interact with MTs and SPB. When co-expressed, dynein is detected at the SPB at higher levels and at a higher frequency and also Dli1 can now be found at the SPB suggesting that Dli1 enhances dynein-mediated SPB recruitment.

A comparative analysis of the LICs from different organisms may help to understand from where their diversity in regulating dynein activity originate.

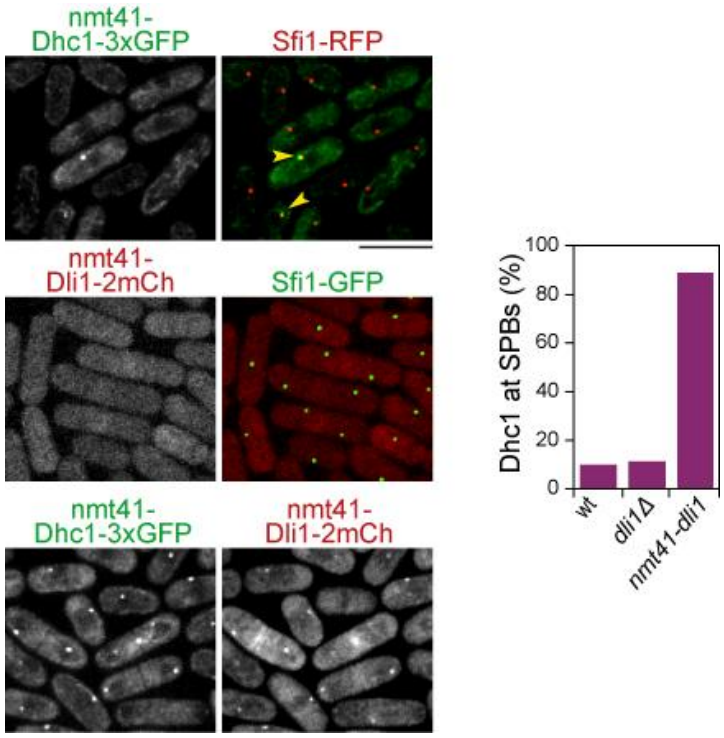

Figure 6.1. Supplemental results to Dli1 function in dynein regulation.

Left, ectopic expression of Dhc1-3xGFP or Dli1-2mCherry from the *nmt41* promoter (induced by removal of thiamine) in vegetative cells coexpressing Sfi1-RFP or –GFP respectively. Coexpression of Dhc1-3xGFP and Dli1-2mCherry in the same cells results in an increase of levels at SPBs of both proteins. Right, frequency of cells, in which Dhc1-3xGFP can be detected at SPBs. Bar, 5µm.

Discussion Part II –

A novel factor in cellular morphogenesis of fission yeast

A novel pathway maintain straight growth

The deletion of *knk1* causes a novel "kinked" shape phenotype in fission yeast. Knk1 localization to cell tips and the cell division site is consistent with a potential role for Knk1 in morphogenesis and more precisely in directing growth.

In particular, the rod-shaped fission yeast, a system that has been intensively studied regarding different aspects of polarization and growth, illustrates the role of MTs in positioning and maintaining growth zones, as MT-based defects lead to bent cells that grow in a polarized, but not straight manner. The *knk1Δ* phenotype resembles the bent cell shape of MT or *tea* mutants, as growth still occurs exclusively at the cell tips, but cells fail to maintain a linear long axis. Both morphological defects nevertheless can be distinguished. Bent cells are characterized by a continuous gradual deflection of the growth direction compared to kinks in *knk1Δ* cells, which appear to be caused by a unique event of growth deflection, and then growth follows this new altered direction. Also, the deflection of the growth direction at one time point is stronger in a kinked cells resulting in a sharp angle between cell tip and long axis. It should be noted that the kinked phenotype is, with approximately 10%, not very penetrant and kinks are therefore usually seen only at one cell pole. Rarely, cells exhibit kinks at both cell tips or two kinks at one cell pole, but both events can be enhanced in frequency when the growth phase is extended like in *cdc25-22* cells. That suggests that the formation of kinks is not necessarily a unique event, but its occurrence may be limited by the time spent growing or its detection by the angle of deflection. Kinks with smaller angles may be more difficult to be recognized. Furthermore, the example of a "kinking" cell, shown in Fig. S1A (in results II), demonstrates that both cell tips can potentially produce kinks prior to or after NETO. Once a kink has been established, polarity markers like Tea1 (Fig. S2D in results II, Figure 6.2A) localize in a symmetric manner around the cells tips. In the future, it will be interesting to monitor the localization of different polarity factors in time-lapse movies to analyze the temporal progression from deflection of growth to redistribution of polarity markers. This may also allow identifying upstream factors initiating the formation of a kink and whether this event can occur at any moment or is restricted to specific phases of the cell cycle. A major challenge will be the early detection of a kink and to timely relate this event to local shifts of polarity proteins.

Due to its phenotypic resemblance to MT mutants and the prediction based on sequence comparison that Knk1 may act as a MT-severing enzyme, we first tested whether Knk1 regulates organization or dynamics of the MT cytoskeleton. To date, no MT-severing enzymes have been identified in fission yeast, but one could imagine that, due to their involvement in initiating MT catastrophe, their absence might reduce catastrophe frequency, extend dwell time at the cortex and increase number of MTs per cell. For instance, the loss of fidgetin in human U2OS cells is characterized by an increase in number and length of astral MTs during mitosis (Mukherjee et al., 2012). However, no such alterations are observed in *knk1Δ* cells. Potentially, the defects caused by *knk1* deletion might be mild, and therefore difficult to detect. In fidgetin and other MT enzymes, interaction with MTs or, in the case of Vps4, the ESCRT complex is mediated by the N-terminal MIT domain. Knk1 shows a high conservation to this protein family in its AAA^+ domain, which is in general typical for AAA^+ ATPases, but lacked any sequence similarity in its N-terminal part. No MIT domain or any other motif known to bind to MTs can be detected in Knk1. Based on the lack of a MT-interacting domain and the absence of a MT-related phenotype in *knk1Δ* cells, we conclude that Knk1 does not control MT dynamics and, therefore, the predicted function as a MT-severing enzyme cannot be confirmed. In other words, the *knk1Δ* phenotype is not caused by an altered MT behavior.

MTs contribute to fission yeast morphogenesis by depositing the spatial cues Tea1 and Tea4 at the cell tips to maintain a straight axis. Deletion of *tea1* or *tea4* also results in a bent cell shape. In fact, it has been shown that Tea1 localizes in a dispersed or asymmetric pattern at the cell tips in some MT mutants causing the gradual deflection of growth. However, Tea1 localization in *knk1Δ* resembles wildtype cells (Figure 6.2A) and furthermore genetic interactions between *knk1* and *tea*, for example synergy or mimicking single mutants, cannot be detected, instead a double *tea1Δ knk1Δ* mutant is characterized by an addition of the *tea1Δ* and *knk1Δ* phenotypes. Inversely, Tea1 does not affect Knk1 localization. Similar observations are made, when genetic interactions of *knk1* with other components of the *tea* pathway are tested (Figure 6.2B) suggesting that none of these polarity factors are required to form kinks and their absence does not enhance the *knk1Δ* phenotype. Therefore, we conclude that Tea1 and Knk1 are recruited independently of each other and do not function in the same or in parallel pathways to control fission yeast morphogenesis.

Intriguingly, MT mutants show an aggravation of the *knk1Δ* phenotype, by increasing the frequency of kinks and the deflection angles. At first, this suggested to us that Knk1 and MTs might function in parallel pathways to control a specific aspect of morphogenesis and that MTs might have additional roles besides Tea1 deposition, for example the less understood Mal3/Moe1 pathway. But when *tea1* is deleted in a double *knk1Δ* MT mutant, kinks are detected at a similar frequency to a single *knk1Δ* mutant indicating that the aggravation is mediated by mispositioned Tea1, and not in a novel MT-dependent manner. It has been demonstrated that altered MT dynamicity renders cells highly susceptible to other perturbations of the cell shape and may unspecifically amplify any existing shape defects (Thadani et al., 2011). Therefore, we propose that there is no functional link between MTs and Knk1 and that they regulate different aspects of cellular morphogenesis and directed growth in fission yeast.

Next, we visualized the actin cytoskeleton in *knk1Δ* cells to test whether absence of Knk1 might induce alterations in actin structures. However, polarization, distribution and number of actin cables as well as actin patches appear undistinguishable from wildtype. In this study, we tested the role of Knk1 in exo- and endocytosis, the two major processes controlled and driven by the actin cytoskeleton, by assays to measure rate of uptake and secretion (Fig. S4D, S6A in results II). In summary, nor endo- nor exocytic activities reveal any abnormalities in *knk1Δ* cells suggesting that Knk1 might not be involved in these two membrane trafficking events remodeling the plasma membrane at the cell tips. Furthermore, distribution of actin patch marker Sla2, For3 nucleating actin cables and the exocyst subunit Sec8 is not altered in cells lacking Knk1 (Figure 6.2C). These assays and microscopic observations rely on a phenotype strong and penetrant enough to induce visible or measurable changes. Therefore, it may be necessary to measure dynamics of the actin cytoskeleton, like frequency and timing of invaginations, as well as the spatial and temporal regulation of the localization and dynamics of exo- or endocytic components more carefully in time-lapse movies with a high time resolution. Such studies may significantly benefit from an identification and characterization of potential substrates of Knk1 beforehand. At this point, we cannot rule out that Knk1 functions in certain steps of exo- or endocytosis redundantly to other proteins, but in wildtype cells it is not required for normal progression. Its role may not be essential for initiation, progression or completion of these processes and might have a rather regulatory effect or enhance efficiency.

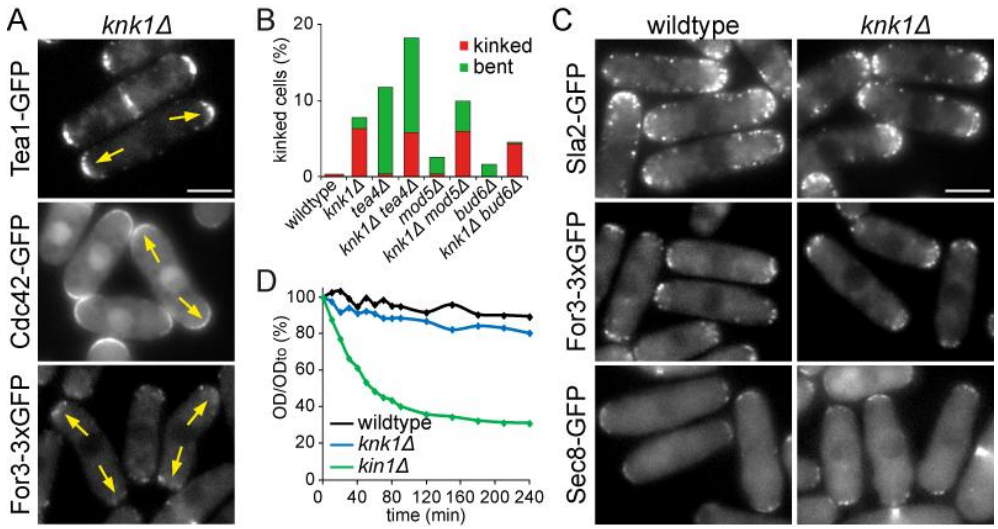

Figure 6.2. Supplemental results to Knk1 function.

(A) Symmetric distribution of polarity markers at straight and kinked cell tips. Yellow arrows indicate direction of growth. **(B)** Percentage of kinked and bent cells in wildtype and mutants at 25°C. **(C)** Cellular distribution of polarity and growth markers in wildtype in *knk1Δ* cells. **(D)** Zymolyase assay: cell number normalized to cell number at t_0 over time during treatment with cell wall digesting zymolyase. *kin1Δ* cells with defects in cell wall integrity serve as positive control. Bars, 5µm.

We then hypothesized that also alterations in the structure of the cell wall, either local weaknesses or swellings at the wrong places, might be able to deflect growth away from a straight direction. Interestingly, the morphological *knk1Δ* defect is reminiscent of the behavior of cells in an electrical field, where a local shift of cell wall synthesizing enzymes due to negative charges leads to an aberrant cell wall assembly as revealed by Calcofluor staining (Minc et al., 2009). However, neither an aberrant accumulations of the cell wall nor an asymmetric distribution of Bgs4 are detected in *knk1Δ* cells (Fig. S6B). As already mentioned, more subtle alterations might be difficult to detect. To test further for a potential involvement of Knk1 in cell wall synthesis, we analyzed whether the cell wall of *knk1Δ* cells is more sensitive to cell wall digesting enzymes such as zymolyase (Figure 6.2D). These assays usually reveal whether mutants display defects in controlling cell wall integrity. *knk1Δ* cells show no increased rate of cell lysis neither in absence nor presence of wall digesting enzymes. All together, these results suggest to us that kinks are not caused by an aberrant cell wall structure or assembly. Nevertheless, as the cell wall contains different components, a more thorough analysis of the cell wall might reveal abnormalities in thickness, frequency or distribution of specific components

that are not visualized by Calcofluor. Here, electron microscopic analyses have helped to discover alterations of mutant cell walls in the past.

In summary, we hypothesize that Knk1 regulates cell shape and direction of growth in a novel manner, implied by the unique *knk1Δ* shape defect. It appears that it is not required for function of most processes underlying morphogenesis such as endocytosis, exocytosis and cell wall synthesis. Furthermore, it is not involved in the organization or regulation of the dynamics of the cytoskeleton. Clearly, we cannot rule out that some assays are insensitive for subtle aberrations and, therefore, mild changes might have been overlooked due to technical difficulties. It remains open whether Knk1 might control proper distribution or turnover of these activities. To address this question, it will be necessary to identify interactors and substrates of Knk1, for example by Mass Spectrometry analysis or by analyzing genetic interactions in a double *knk1Δ* mutant screen. In a later chapter, I will discuss potential functions for Knk1 in maintaining a straight growth axis in fission yeast.

Regulation of the subcellular Knk1 localization

Knk1 is recruited to cell tips and the cell division site, which is typically observed for most polarity and growth factors. Thereby, it is dominantly detected at growing cell tips suggesting that its localization depends on the growth machinery. Additionally, the pattern along the cell tips is rather smooth indicating that Knk1 is not part of actin patches. Treatment with actin-depolymerizing LatA reveals that actin, but not MTs play a role in Knk1 recruitment to cell tips. Surprisingly, mutants lacking actin cables or with a reduced number of actin patches, exhibited Knk1 levels similar or higher compared to wildtype. We conclude that Knk1 does not bind directly to actin to localize to cell tips, but its localization might be regulated by actin-dependent processes. Consistently, in a *sla2Δ* mutant that is characterized by a reduced endocytic activity (Iwaki et al., 2004) Knk1 accumulates in the cell tips, similarly to known cargo proteins such as Syb1 (Basu and Chang, 2011). However, other endocytic mutants such as *myo1Δ* display normal Knk1 levels at the cell tips. That suggests that Knk1 does not constitute a cargo uptaken by endocytosis, but Sla2, independent of its role in endocytosis, might have a specific function in regulating Knk1 localization. This hypothesis is further supported by the observation that Knk1

levels are similarly increased in the *cdc42-L160S* mutant that, despite a reduction of actin cable assembly, mislocalization of the exocyst complex and inhibition of late steps in endosome recycling, exhibits no defects in endocytic uptake (Rincon et al., 2009, Estravis et al., 2011, Estravis et al., 2012). Taken together, Knk1 localization to cell tips is not regulated by endocytosis, but rather by another endocytosis-independent pathway including Sla2 and Cdc42.

Remarkably, the absence of Sla2 or reduced levels of active Cdc42 in the cell tips promote Knk1 accumulation suggesting that the interaction between Knk1 and Sla2/Cdc42 does not simply lead to recruitment of Knk1, but that these proteins negatively influence its attachment to cell tips. In fact, both mutants display lower levels of active Cdc42 at the cell tips relative to the cytoplasmic pool (Rincon et al., 2009) (Fig. S5E in results II), indicating that Knk1 localization correlates with inactivation of Cdc42. In future experiments, that could be addressed by using a constitutively active form of Cdc42, which should lower Knk1 levels, and a dominant-negative *cdc42* allele (Martin et al., 2007), that should result in enhanced Knk1 levels, if our hypothesis is correct.

It remains open whether Sla2 regulates Cdc42, or inversely, Cdc42 regulates Sla2 activity to, in turn, control Knk1 localization. At the moment, we favor the first hypothesis, as the *cdc42-L160S* allele does not cause endocytic defects. Alternatively, Cdc42 may not regulate overall activity or localization, but only certain functions of Sla2. Further implications of the Cdc42-Sla2 interaction will be discussed in a later chapter.

The results obtained by expressing mutant and truncated versions of Knk1 suggest that the N-terminus mediates localization to cell tips. A single Knk1 N-terminus might not exhibit high affinity to cell tips, but when several N-termini cooperate, for example by formation of a hexameric Knk1 complex induced by binding of ATP at the ATPase domains, Knk1 recruitment proceeds efficiently. Taken together, even though lacking *in vitro* characterization of *knk1* mutants, these results indicate that Knk1 probably works in a similar fashion to other AAA^+ proteins.

However, it remains mysterious how Knk1 binds to cell tips. No conserved domains are found within the N-terminal part, therefore we can only speculate with which cell tip-specific structures Knk1 may interact. Possibly, Knk1 might bind to other polarity proteins, but no such factors could be identified in this study. Alternatively, Knk1 might directly bind to membranes

via a yet unknown lipid-binding domain. That would imply that Knk1 localization might be dependent on distribution of certain lipids that are enriched in the cell tips. To date, the role and subcellular distribution of lipids is a rather unexplored field in fission yeast and not many tools are available to address these questions. When PIP2 levels are lowered by using the *ts* (temperature-sensitive) *its3-1* mutant allele for one hour at the restrictive temperature, cells undergo eventually cell lysis, but Knk1 can be detected at cell tips before cell lysis suggesting that PIP2 levels do not affect Knk1 recruitment (Figure 6.3). Once progress has been made in this field, it will be interesting to test the role of other lipids. These analyses of Knk1 and other proteins may widen our understanding of interactions between lipids and proteins and how cells locally control lipid composition.

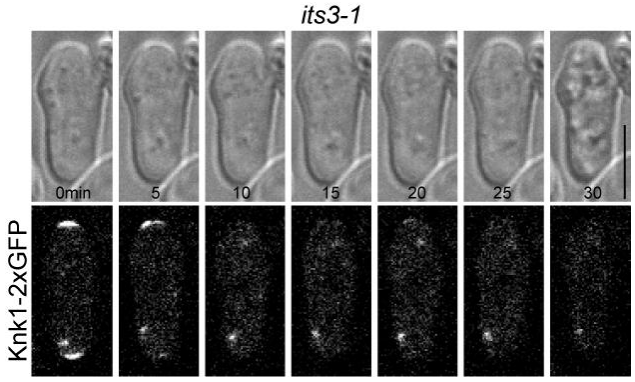

Figure 6.3. Supplemental results to regulation of Knk1 localization.

Knk1 localization in a *its3-1* mutant strains after 1h at 37°C. Images presented as maximum z-projection of 3D stacks. Bar, 5µm.

Oscillatory dynamics of Knk1

One remarkable feature of Knk1 is that it undergoes anti-correlated periodic oscillations between the two cell tips, at least in certain mutant backgrounds, *sla2Δ* and *cdc42-L160S*, where Knk1 levels are increased. In contrast, in wildtype cells, anti-correlated fluctuations with no clear uniform periodicity are observed. We imagine two explanations for this differential behavior of Knk1 in wildtype and mutant strains. First of all, the pool of cell tip-bound Knk1 is not always clearly distinguishable compared to cytoplasmic levels. Thus, it may be difficult to reliably distinguish the tip from the cytoplasmic signal and measurements of intensity fluctuations at cell tips may be artifactually influenced by fluctuations in the cytoplasm. Alternatively to technical

difficulties, an anti-correlated periodic oscillatory behavior might be induced by a mutant background, for example by limiting the amount of available Knk1 resulting in the competition of the two cell tips for Knk1. Sla2 and Cdc42 might do so, either by allowing more Knk1 to bind at one cell tip or by limiting regulatory factors that modify Knk1 to allow cell tip binding, as it has been proposed for Cdc42 and its GEFs (Das et al., 2012). More likely, first hypothesis may be true for Knk1, as both mutants show increased Knk1 levels at the cell tips. However, in both cases, this would lead to a depletion of the available pool of Knk1 and the second tip has to "wait" until new Knk1 molecules are free, for example due to the detachment of Knk1 from the first tip. Under wildtype conditions, such striking anti-correlated periodic oscillations might not be observed as regulatory proteins might usually be present in sufficient quantities or as the levels of Knk1 binding to cell tips might be strictly regulated, which means that the two cell tips do not compete for Knk1.

The existence of fluctuations, even though with no striking periodicity, and a cross-correlation coefficient of r = -0.16±0.25 indicating anti-correlation suggest that positive and negative feedback loops operate also in wildtype cells driving alternating cycles of Knk1 accumulation and detachment at the cell tips. The enhanced Knk1 levels in *sla2Δ* and *cdc42-L160S* cells indicate that Cdc42 and Sla2 might be part of the negative feedback mechanism. However, at this point, no further predictions can be made about the nature and the regulators of the feedback loops, as, in contrast to Cdc42, we lack an understanding of how Knk1 localization is controlled.

One question that we were not able to fully address derives from the observation that Cdc42 and Knk1 undergo oscillations at different periodicities, 5min for Cdc42 and ~15min for Knk1. At this moment, the oscillations for these two proteins cannot be reliably detected in the same genetic background. We propose that it may be interesting to visualize these proteins in the same cell in different colors to test for correlations between their oscillatory dynamics. Nonetheless, as, for example in *sla2Δ* cells, a periodicity for Knk1 at 15min can be detected, but none for Cdc42, that suggests the existence of at least two distinct oscillatory systems regulating different aspects of morphogenesis. Therefore, oscillatory properties might represent a commonly found feature to control cell shape.

One remarkable similarity between Knk1, Cdc42 and bacterial Min oscillatory systems is the involvement of an NTPase in each case. In bacteria, the ATP turnover at the ATPase MinD

drives the oscillations of the effector protein MinC that inhibits formation of the Z-ring at these sites (Lutkenhaus, 2007). MinD-ATP binds to the cell membrane, while ATP hydrolysis triggers release of MinD from the membrane. In the cytoplasm, ADP is exchanged for ATP, whereby the concentration of MinD-ATP raises dominantly at the new cell tip inducing a new cycle of MinC/D recruitment at this cell tip. Currently, it is not known whether turnover of GTP at Cdc42 is required to promote its own oscillations. Preliminary results of Knk1(D478A E479A), a Knk1 version with a mutagenized Walker B motif to inhibit ATP hydrolysis, suggest that Knk1 still undergoes oscillations at a similar periodicity like wildtype Knk1, when visualized in *sla2Δ* cells (Figure 6.4) indicating that ATP turnover is not crucial for oscillatory behavior. However, formal proof of a reduced ATPase activity of this Knk1 mutant, for example by *in vitro* experiments, has to be carried out. Future work on other NTPase involved in different cellular aspects may uncover that oscillatory dynamics may commonly utilized among this protein family, because either NTP turnover is an efficient mean to promote oscillations or functions carried out by NTPases are more accurately controlled by periodic phases of high and low NTPase activity.

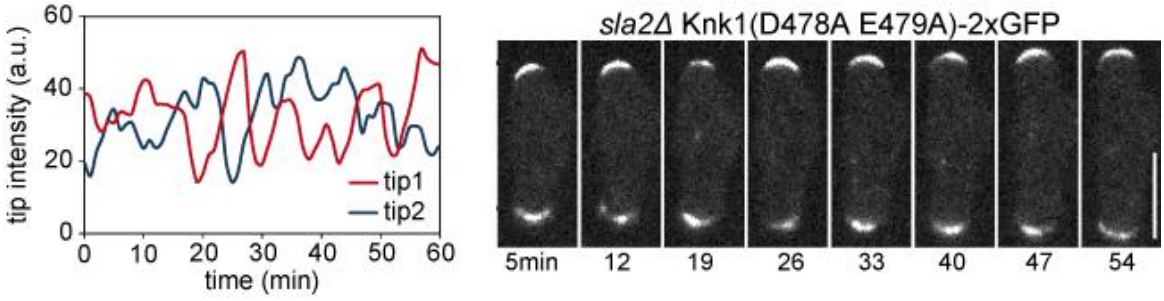

Figure 6.4. Supplemental results to oscillatory behavior of Knk1.

Time-lapse images and tip intensities of Knk1(D479A E479A)-2xGFP in a *sla2Δ* strain at 25°C. Images recorded as single medial z-sections showing Knk1 distribution. Bar, 5µm.

Finally, another open question that will be addressed in the future is whether oscillatory properties are required for the function of certain proteins. The Min system supporting proper localization of the cytokinetic Z-ring in bacteria shows oscillatory dynamics only in some bacteria. It appears that similar functions can be carried out by stably or periodically recruited proteins. Fission yeast Cdc42 oscillations are proposed to control transition from mono- to bipolar growth or to accurately control cell diameter (Das and Verde, 2013). Possibly, oscillations provide certain advantages, like flexibility or recycling of resources, to the cell, but

are not completely required. This point may represent a major direction for the studies of Knk1 as well as Cdc42.

Potential roles for Knk1 in directing growth

We hypothesize that Knk1 regulates cell shape in a yet unknown manner, without affecting progression of known processes underlying morphogenesis such as endocytosis, exocytosis and cell wall synthesis. As discussed above, we cannot rule out that some assays are insensitive for subtle aberrations and, therefore, mild changes might have been overlooked due to technical difficulties. It remains open whether Knk1 might control proper distribution or turnover of these activities. To address this question, it will be necessary to identify interactors and substrates of Knk1, for example by Mass Spectrometry analysis or by analyzing genetic interactions in a double *knk1Δ* mutant screen.

ATPases are implicated in various cellular processes, but in general act by remodeling substrate proteins and, thereby, help to refold, unfold, degrade or disassemble proteins and protein complexes. We propose to perform a Mass Spectrometry analysis using a Walker B-mutant version of Knk1 (Knk1D478A E479A) that binds ATP and allows hexamer formation, but blocks specifically ATP hydrolysis. In the past, such mutant proteins have helped to give clues about the function of AAA^+ proteins, as they act as "substrate traps" incapable of releasing substrate proteins (Hanson and Whiteheart, 2005). In subsequent studies, these insights may be used to test potential roles for Knk1 more promisingly.

Here, we can only speculate on how Knk1 maintains a straight growth axis, based on functions reported for AAA^+ proteins.

From budding yeast or *Aspergillus*, it is known that endo- and exocytosis must be spatially coordinated to maintain straight growth. Even though no studies have been carried out in fission yeast to address this subject, the rod-shaped cell form suggests that similar mechanisms are applied. Possibly, Knk1 could play a role in spatially regulating these processes. Then, absence of Knk1 might not influence the rate of exo- or endocytosis *per se*, but is required for initiation of endocytosis or fusion of secretory vesicle with the plasma membrane at the right places. This idea might be supported by the fact that many AAA^+ proteins are implicated in

membrane trafficking processes, by helping assembly or disassembly of protein complexes, like SNARE or ESCRT complexes, to prepare the structures involved more rapidly for the next event.

Other AAA^+ ATPases mediate the unfolding of proteins to remove them from intracellular structures or to prepare them for degradation by proteases. For instance, MT-severing enzymes pull at the C-terminal tails of tubulins leading to a partial unfolding and initiate MT catastrophe. Similarly, Knk1 might regulate the turnover of certain polarity factors at the cell tips. It is tempting to speculate that by periodically removing components of the growth machinery, Knk1 might prevent the amplification of random deflections in growth direction, otherwise stabilized by positive feedback loops reinforcing the growth machinery locally and resulting in the formation of kinks.

In both hypotheses, Knk1 regulates the distribution of certain activities and proteins, without affecting the process *per se*. We propose that cells depleted of *knk1* probably show a random asymmetry in specific morphological factors that eventually will redirect the growth machinery, as shown for cells in an electrical field.

New insights into fission yeast morphogenesis

The observation that a *cdc42* and a *sla2* mutant show a similar accumulation of Knk1 at cell tips, and that a double mutant only mimics the single *sla2Δ* mutant indicates that Cdc42 and Sla2 act together in the same pathway to control Knk1 localization and potentially other aspects of growth. Interestingly, this interaction might not be important to regulate endocytic activity.

The *cdc42* mutant used in this study displays no defects in endocytic uptake (Estravis et al., 2011). Therefore, in fission yeast, it remains unclear whether Cdc42, besides regulating most, if not all, process related to polarity, also coordinates endocytosis. The discovery that Orb2 regulates Myo1 activity (Attanapola et al., 2009) and that this kinase is a downstream effector of Cdc42 proposes such a link (Ottilie et al., 1995). However, future work will be required to test, whether Cdc42 is indeed important for endocytosis, as proposed in mammals, where WASp activated by Cdc42 stimulates Arp2/3-mediated actin polymerization to drive invagination (Ridley, 2006). In yeast, Wsp1 lacks the Cdc42 interaction domain (Chang and Martin, 2009), and, here, Cdc42 might impact on endocytosis through Myo1 and Orb2.

In this study, we propose a novel link between Cdc42 and the endocytic machinery that might regulate cellular functions independently of endocytosis. In budding yeast, the Cdc42 system is known to interact with the key endocytic proteins epsins that function cooperatively with Sla2 to couple plasma membrane and actin cytoskeleton dynamics in early steps of endocytosis (Aguilar et al., 2006). Mutants in the epsin ENTH (epsin N-terminal homology) domain display polarity defects due to decreased levels of active Cdc42 while endocytosis was unaffected. Since our study in fission yeast also suggests a link between the early endocytic adaptor protein Sla2 and Cdc42 in Knk1 localization, there may be a conserved connection between endocytic processes and Cdc42 pathway linking endocytosis and cell polarization machinery to regulate downstream growth factors.

In conclusion, our work provides further evidence that endocytosis and the Cdc42 system are coordinated also in fission yeast, suggesting that this link may be conserved. The molecular details of these interactions and their role are currently not understood, but will be probably addressed by future studies.

RÉSUMÉ

6. Introduction

6.1. Les mouvements nucléaires

6.1.1. Diversité des mouvements nucléaires chez les eucaryotes

Le noyau est souvent représenté schématiquement au centre des cellules, mais en réalité son emplacement est contrôlé par des mécanismes complexes qui servent à maintenir ou déplacer le noyau à une position précise. En général, les mouvements nucléaires observés pendant le développement de la plupart des eucaryotes dépendent des phases du cycle cellulaires ou de la différentiation cellulaire. La position du noyau est en effet cruciale pour des divers processus cellulaires comme la division cellulaire, la polarité, la motilité ou la reproduction sexuelle. A ce jour, des migrations nucléaires ont ainsi été observées dans de multiples types de cellules, de la levure à l'Homme.

Dans les cellules de la levure *Schizosaccharomyces pombe* qui se divisent par fission médiane, le noyau a une position centrale et définit la position du plan de division cellulaire (Tran et al., 2001). En revanche, les noyaux de la levure *Saccharomyces cerevisiae* sont placés de manière asymétrique avant la division (Huisman and Segal, 2005).

Chez les vertébrés, le développement du système nerveux est caractérisé par la migration interkinétique des noyaux, pendant laquelle les noyaux bougent sur l'axe apico-basal au cours du cycle cellulaire (Del Bene et al., 2008). Pendant la migration des cellules, le noyau se trouve proche de l'arrière pour ne pas perturber les processus opérant à l'avant de la cellule (Gomes et al., 2005, Dupin et al., 2009). Les myocytes contiennent des centaines de noyaux qui sont situés à équidistance, à la périphérie. Exceptionnellement, les noyaux se groupent sous la plaque motrice (Bruusgaard et al., 2003). De plus, il a été mis en évidence que des défauts de position des noyaux provoquent des maladies des muscles squelettiques et du système nerveux central (Razafsky et al., 2011). Enfin, les migrations nucléaires jouent un rôle important pendant de différentes phases de la reproduction sexuelle. En particulier, après la fertilisation, les pro-noyaux mâle et femelle s'assemblent et fusionnent au centre du zygote pour assurer la ségrégation fidèle de l'ADN zygotique lors des divisions suivantes (Reinsch and Gonczy, 1998). Tous ces exemples illustrent la nécessité de comprendre les mécanismes contrôlant les mouvements nucléaires.

6.1.2. Les mouvements nucléaires contrôlés par les microtubules

Le cytosquelette joue un rôle indispensable par générer la force nécessaire au déplacement du noyau. Il est connu que les trois éléments du cytosquelette, l'actine, les microtubules (MTs) et les filaments intermédiaires, sont utilisés seuls ou en combinaison par différents types de cellules, mais les MTs semblent jouer un rôle clef dans la plupart des organismes. Trois principaux modes de production de force ont été décrits – en tirant, en poussant ou par transport le long d'un filament du cytosquelette.

Deux classes de moteurs moléculaires qui utilisent les microtubules comme rails sont connues : la dynéine et les kinésines. Ces moteurs hydrolysent l'ATP dans leur domaine moteur globulaire liant les MTs, ce qui provoque des changements au niveau de la conformation moléculaire qui se traduisent par un déplacement de la protéine motrice par rapport au MT. D'autres domaines servent à contrôler l'oligomérisation, l'interaction avec d'autres protéines et la localisation sur différentes structures cellulaires. (Schliwa and Woehlke, 2003). Le déplacement de ces moteurs moléculaires se fait soit en direction du pôle plus du MT, pour la plupart des kinésines, ou moins dans le cas de la dynéine et de la famille des kinésines-14.

Les kinésines sont généralement composées de deux chaînes lourdes et, chez les métazoaires, deux chaînes légères (Vale, 2003). Le domaine moteur se trouve souvent proche de l'extrémité N-terminale. Dans ce cas, la kinésine se déplace en direction du pôle plus du microtubule. Les membres de la famille des kinésines-14 ont un domaine moteur à l'extrémité C-terminale et se déplacent en direction du pôle moins. Certains d'entre eux ont un deuxième domaine pour interagir avec les microtubules à l'extrémité N-terminale. Cela leur permet de lier deux microtubules en même temps. Es protéines motrices peuvent collaborer et ainsi mettre des MTs en fagots et induire le glissement de MTs antiparallèles les uns par rapport aux autres (Oladipo et al., 2007, Braun et al., 2009).

La dynéine est un complexe composé de deux chaînes lourdes (DHCs) qui sont responsables de l'activité motrice et de la liaison aux MTs (Sakakibara and Oiwa, 2011), et de multiples sous-unités accessoires, comme les chaînes intermédiaires (DICs), légères intermédiaires (DLICs) et légères (DLCs). De plus, la dynéine s'associe à des protéines qui contrôlent son activité. En particulier, le complexe dynactine est nécessaire pour quasiment toutes

les fonctions de la dynéine. Il contient aussi un domaine de liaison aux MTs et, quand il est associé à la dynéine, il améliore sa processivité et stimule sa motilité (King and Schroer, 2000).

Les MTs et leurs moteurs moléculaires jouent un rôle majeur dans la génération des forces nécessaires au déplacement des noyaux. En général, le noyau est attaché aux microtubules au niveau d'un MTOC comme le centrosome (Azimzadeh and Bornens, 2007). Les pôles plus des MTs sont dynamiques et polymérisent et dépolymérisent en permanence. Les MTs étant rigides, si un MT en polymérisation attaché au noyau entre un contact avec un objet rigide, par exemple le cortex, il peut transmettre une force de répulsion au noyau et l'éloigner de cet objet au fur et à mesure de sa croissance. Deuxièmement, des protéines motrices avec une motilité en direction du pôle moins, comme la dynéine, sont recrutées sur les sites où les MTs touchent le cortex et en interaction avec eux, elles peuvent tirer les MTs et le noyau qui est associé. Ce mécanisme est bien décrit chez la levure *Saccharomyces cerevisiae* qui l'utilise pour positionner l'appareil mitotique au cours entre la cellule mère et la cellule fille, est conservé de la levure jusqu'à l'Homme. Enfin, certains moteurs s'associent directement à l'enveloppe nucléaire et transportent le noyau le long des microtubules en direction du pôle plus ou moins. Ce type de mouvement apporte de la bidirectionnalité aux migrations nucléaires (Tsai et al., 2010).

6.1.3. La congression nucléaire chez la levure

Les deux levures *S. cerevisiae* et *S. pombe* sont très utiles pour les études des mécanismes contrôlant les mouvements nucléaires. Chez ces organismes, le noyau est associé aux MTs au niveau du SPB (spindle pôle body), l'équivalent du centrosome, et est positionné par les MTs.

En milieu pauvre en azote et en présence des deux types sexuels, les cellules haploïdes de *S. pombe* se conjuguent puis activent le programme méiotique pour produire des spores (Harigaya and Yamamoto, 2007). Deux cellules voisines s'allongent l'une vers l'autre par production d'une extension, le « shmoo », et fusionnent au site du contact. Cette étape est suivie par la karyogamie, pendant laquelle les deux noyaux s'approchent et fusionnent pour former un zygote diploïde qui entre en méiose. Les deux divisions méiotiques produisent quatre noyaux haploïdes encapsulés dans une paroi cellulaire spécialisée. Ces spores peuvent germer quand les conditions redeviennent plus favorables.

Deux mécanismes différents de positionnement du noyau ont été identifiés chez *S. pombe*. Premièrement, le positionnement central du noyau pendant l'interphase. Il dépend des MTs qui s'organisent en faisceaux linéaires antiparallèles associés à l'enveloppe nucléaire grâce à l'activité du complexe Mto1/Mto2 qui lie l'enveloppe nucléaire et les MTs et promeut leur nucléation, de la MAP Ase1 qui met les MTs nucléés en configuration antiparallèle et de la kinésine-14 Klp2 qui induit le glissement des MTs antiparallèles vers les pôles moins et rassemble ainsi les pôles moins de MTs au centre de la cellule (Carazo-Salas and Nurse, 2006, Daga et al., 2006 , Janson et al., 2005 , Janson et al., 2007 , Carazo-Salas et al., 2005). Cette organisation des MTs en faisceaux antiparallèles oriente les pôles plus des MTs vers le cortex, où, par polymérisation, ils produisent des forces repoussant le noyau. Un équilibre des forces exercées par les MTs en contact avec les deux extrémités de la cellule maintient le noyau au milieu (Tran et al., 2001).

Deuxièmement, la prophase méiotique chez *Schizosaccharomyces pombe* est caractérisée par une oscillation du noyau appelée « nuclear horsetail movement » au cours de laquelle le noyau migre d'un côté à l'autre côté du zygote pendant plusieurs heures (Chikashige et al., 1994). Ce mouvement est dirigé par la dynéine, accrochée au cortex qui tire les MTs attachés au noyau au niveau du SPB. Les chaînes intermédiaires et légères intermédiaires de la dynéine et la dynactine sont essentielles pour la localisation et la fonction de la dynéine pendant ce processus.

Lors de la conjugaison des cellules haploïdes, avant l'entrée en méiose, les noyaux des deux cellules associées se rapprochent pour pouvoir fusionner. Ce mouvement s'appelle la congression nucléaire. Chez *S. cerevisiae*, ce processus est contrôlé par la kinésine-14 Kar3 (Meluh and Rose, 1990, Molk et al., 2006). Kar3 se localise aux pôles plus de MTs. Après la fusion cellulaire, Kar3 réticule des MTs antiparallèles émanant des deux SPBs. Kar3 pourrait alors induire le glissement de MTs afin de tirer les noyaux l'un vers l'autre (Rose, 1996). Alternativement, Kar3 pourrait maintenir associés les pôles plus de MTs émanant des deux SPBs alors qu'ils dépolymérisent (Molk et al., 2006). Récemment, une nouvelle étude par microscopie électronique a mis en évidence que Kar3, associé au SPB, interagit latéralement avec les MTs émanant du SPB opposé (Gibeaux et al., 2013).

En revanche, la congression nucléaire a été peu étudiée chez *S. pombe*. Une seule étude, dans des zygotes déficients pour Klp2 ou de la dynéine, faite sur cellules fixées a révélé des défauts de fusion des noyaux suggérant que l'absence de Klp2 ou de la dynéine mène à un échec

de congression ou de fusion nucléaire (Troxell et al., 2001).Au cours de ma thèse, à l'aide d'imagerie à long terme basée sur la microfluidique, j'ai donc analysé les mécanismes moléculaires contrôlant la congression des noyaux dans les cellules vivantes de la levure *S. pombe*.

6.2. La morphogenèse cellulaire

6.2.1. Les facteurs clefs contrôlant la morphologie cellulaire chez les eucaryotes

La polarité cellulaire est caractérisée par une distribution asymétrique des composants ou structures cellulaires et peut déterminer la zone et l'orientation de la croissance cellulaire. La croissance polarisée contrôle principalement la forme d'une cellule. La morphologie cellulaire semble importante pour la fonction des cellules et pour la cohésion des tissus. En général, des signaux internes ou externes génèrent une asymétrie moléculaire dans les cellules. Ensuite, le cytosquelette et des mécanismes de rétrocontrôle positifs maintiennent cette asymétrie (Pruyne et al., 2004, St Johnston and Ahringer, 2010).

L'actine qui est contrôlée par les RhoGTPases est importante en particulier pour deux processus: l'exocytose et endocytose ou l'absorption (Heasman and Ridley, 2008, Perez and Rincon, 2010).

Les RhoGTPases, comme Cdc42, sont des régulateurs de la croissance et de la polarité. Quand elles lient le GTP, ces protéines sont actives et capables d'activer leurs effecteurs. Ensuite, elles hydrolysent le GTP et ne sont plus actives. Les protéines GAPs et GEFs, qui régulent l'activité de l'hydrolyse du GTP des RhoGTPases, contrôlent sa distribution spatiale.

L'exocytose est le processus permettant la fusion des vésicules de sécrétion avec la membrane plasmique et la sécrétion des protéines extracellulaires. Ces vésicules sont transportées le long des filaments d'actine qui sont polymérisés par les formines (Porat-Shliom et al., 2013). En plus, un réseau d'actine se forme autour des vésicules endocytique qui sont générées par l'invagination de la membrane lors de l'absorption des protéines et molécules extracellulaires ou membranaires. Un rôle important de l'endocytose est de maintenir la distribution asymétrique des protéines de polarité comme Cdc42 localisée au cortex (Marco et al., 2007). Pendant une première phase, la clathrine et les « endocytic coat factors » s'accumulent à la membrane. Un

facteur majeur de cette phase est Sla2/Hip1 qui se lie aux lipides (PIP2) et à l'actine et maintient la connexion entre ces deux structures. L'absence de Sla2 n'empêche pas la formation du puits ou la polymérisation de l'actine, mais l'actine n'est plus capable de faire progresser l'invagination (Kaksonen et al., 2003). Ensuite, le complexe de Arp2/3 et ses activateurs, par exemple Las17/WASp et myosine I, s'accumulent et stimulent la polymérisation de l'actine et l'internalisation de la vésicule. Enfin, des protéines qui pincent et fusionnent la membrane permettent la scission de la vésicule.

Finalement, les MTs jouent aussi un rôle dans la maintenance de la position de zones polarisées, mais ils ne sont pas nécessaire pour initier la polarité en tant que tel (Siegrist and Doe, 2007). En fait, chez *S. pombe* et dans les cellules migrantes, les MTs déposent des protéines de polarité au cortex qui elles-mêmes stimulent l'activité des composants favorisant la nucléation de l'actine, comme les formines, pour renforcer ces zones.

6.2.2. La morphogenèse chez *Schizosaccharomyces pombe*

La levure unicellulaire *Schizosaccharomyces pombe* est un système modèle reconnu pour l'étude la morphogenèse. Elle forme des cellules cylindriques par croissance linéaire polarisée de ses extrémités. L'identification de mutants ayant des formes anormales a permis d'identifier les gènes et voies principales de régulation de la morphogenèse de cet organisme. Comme chez d'autres organismes, le cytosquelette, composé de filaments d'actine et de microtubules, joue un rôle capital dans la morphogenèse et des modifications de l'un ou l'autre provoquent des changements caractéristiques de la forme cellulaire. Les mutations qui affectent le cytosquelette d'actine créent des cellules courtes et grosses. Les mutations perturbant les microtubules produisent des cellules courbes ou branchées parce que la croissance n'est plus focalisée aux extrémités.

Pendant l'interphase, l'actine forme deux types de structures distinctes qui se concentrent aux extrémités cellulaires et sont nécessaires pour la croissance (Kovar et al., 2011). Premièrement, les câbles d'actine servent de rails pour le transport des vésicules de sécrétion par la myosine V. De cette manière, du nouveau matériel qui permet d'agrandir la membrane plasmique et la paroi cellulaire est ajouté par sécrétion surtout aux extrémités de la cellule. Deuxièmement, des patches d'actine sont associés à l'activité endocytique.

En résumé, la GTPase Cdc42 est le régulateur principal de la polarisation et de la croissance, et elle est surtout active aux pôles cellulaires (Perez and Rincon, 2010). Si l'activité de Cdc42 n'est pas contrôlée, les cellules deviennent arrondies à cause d'une croissance isotropique, comme dans un mutant de *orb6* (Das et al., 2009). Récemment, il a été découvert que Cdc42 oscille périodiquement entre les deux extrémités de la cellule avec une périodicité de 5 minutes (Das et al., 2012), mais la fonction de cette oscillation n'est pas encore claire. Une hypothèse est qu'une protéine qui oscille pourrait contrôler certains aspects de la morphogenèse plus précisément qu'une protéine qui se lie de façon stable aux extrémités. Cdc42 active des protéines effectrices, surtout la formine For3 qui polymérise les câbles d'actine (Martin et al., 2007). Les cellules qui n'expriment pas *for3* deviennent plus courtes et plus larges, parce que leur croissance est moins polarisée.

Les défauts dans la voie d'endocytose, par exemple par la délétion de *sla2*, provoquent des modifications similaires de la forme de la cellule (Iwaki et al., 2004, Castagnetti et al., 2005).

Les MTs déterminent l'axe de croissance en définissant les extrémités comme sites de croissance en déposant des « landmark proteins » comme Tea1 qui contrôlent la linéarité de la croissance (Chang and Martin, 2009). Comme mentionné plus haut, pendant l'interphase, les MTs s'arrangent en 3-5 faisceaux de MTs orientés parallèlement à l'axe le plus long de la cellule. Les pôles moins de MTs se concentrent au centre de la cellule autour du noyau, et les pôles plus sont dynamiques et polymérisent vers les extrémités ou ils touchent le cortex pendant 50-80s avant de dépolymériser. Lors de son contact avec le cortex, Tea1, qui est transportée au pôle plus d'un MT polymérisant, est déposée sur le cortex où elle contribue à l'activation de For3 (Martin et al., 2005). Les cellules *tea1Δ* sont toujours polarisées, mais elles perdent leur axe linéaire de croissance et deviennent courbes. Ces altérations de la forme cellulaire sont observées aussi chez les mutants de MTs, qui sont incapables de déposer correctement Tea1. C'est le cas des cellules *mal3Δ,* l'homologue de EB1, qui produisent des MTs très courts qui ne sont pas capable d'arriver aux extrémités (Beinhauer et al., 1997, Busch and Brunner, 2004).

Dans cette étude, j'ai ainsi identifié une nouvelle protéine, Knk1, qui contrôle la forme des extrémités de la cellule et fonde une nouvelle classe de mutants impliqués dans la forme cellulaire. Une comparaison structurale révèle que Knk1 appartient à la famille des ATPases, conservée des bactéries à l'Homme, et participant à de nombreux processus cellulaires fondamentaux, comme la dégradation des protéines et le trafic membranaire (Hanson and

Whiteheart, 2005, Wendler et al., 2012). Malgré leurs fonctions diverses, elles partagent des mécanismes fonctionnels commun et forment des oligomères hexamèriques adoptant une configuration en anneau.

7. Résultats

7.1. La dynéine et une kinésine-14 contrôlent la congression nucléaire chez la levure *S. Pombe*

J'ai étudié les mécanismes contrôlant la congression des noyaux pendant la conjugaison de la levure *S. pombe.* A l'aide d'imagerie à long terme basée sur la microfluidique, j'ai mesuré la durée précise de la congression nucléaire qui est la période entre la fusion des cellules et la fusion des noyaux. Après avoir testé le rôle de tous les moteurs moléculaires des MTs (9 kinésines et une dynéine/Dhc1), j'ai démontré que deux moteurs, la dynéine et la kinésine-14 Klp2 contribuent à ce processus. En effet, la délétion d'un de ces deux moteurs provoque un délai de la congression des noyaux : les zygotes *klp2Δ* terminent la congression avec un délai de 20 minutes, et les zygotes *dhc1Δ* avec un délai moins fort de 5 minutes. Malgré ce délai, les noyaux finissent par se rapprocher et fusionner dans ces mutants simples. Mais dans un double mutant dans lequel les gènes de *klp2* et *dhc1* sont supprimés, les noyaux restent séparés. Ceci suggère que dans les cellules sauvages, ces deux moteurs se dirigeant vers les pôles moins des MTs participent à des voies parallèles promouvant la congression des noyaux.

De plus, j'ai découvert que la délétion de la kinésine *tea2* provoque aussi un délai de 13 minutes de la congression des noyaux, mais contrairement aux délétions de Klp2 et de la dynéine, la délétion de *tea2* n'est pas synergique avec celle de *dhc1* ou *klp2*. En fait, Tea2 joue un rôle dans le contrôle de la dynamique des MTs, puisque les cellules *tea2Δ* ont des MTs plus courts. Ainsi, une bonne dynamique des MTs facilite la congression nucléaire, mais n'est pas strictement requise pour le rapprochement des noyaux.

Une analyse détaillée de la dynamique des SPBs à l'aide d'imagerie à haute résolution temporale a révélée que la congression s'accélère dans les cellules sauvages ou *klp2Δ.* La dynéine contribue a cette accélération puisque la vitesse de congression est constante en absence

de dynéine. Ces résultats démontrent que Klp2 et la dynéine fonctionnent dans des voies distinctes.

J'ai ensuite étudié et comparé la localisation cellulaire de ces deux moteurs. Klp2 se localise surtout sur les MTs et au pôle plus des MTs sous contrôle de Mal3/EB1. La dynéine s'associe quant à elle aux SPBs. En fait, la dynéine est seulement observée dans les cellules qui sont en train de conjuguer, mais pas dans les cellules végétatives. La dynéine est détectée au niveau des SPBs dans 89.2% des cellules dans lesquelles les deux noyaux se rapprochent. Quand j'ai filmé les cellules pendant la congression des noyaux, j'ai découvert que la dynéine s'accumule au SPB pendant ce processus, à partir de 31.2 minutes (en moyenne) avant leur fusion de SPBs et augmente en niveau jusqu'à leur fusion de SPBs. Cette observation est en accord avec le résultat selon lequel la congression nucléaire dirigée par la dynéine s'accélère au cours du temps. De plus, si le temps de congression est allongé, par exemple dans les zygotes *klp2Δ*, le niveau de dynéine augmente encore plus pour atteindre, jusqu'à 1.6 fois plus au moment de la fusion de SPBs en comparaison avec des zygotes sauvages. Pour tester si la localisation de la dynéine au niveau du SPB est seulement un résultat de sa motilité vers les pôles moins des MTs, j'ai exprimé une version de dynéine sans domaine moteur. Cette protéine tronquée est toujours capable de se lier au SPB démontrant que la dynéine ne s'accumule pas au SPB par migration sur les MTs.

Les résultats présentés jusqu'à maintenant indiquent que la dynéine fonctionne au SPB en tirant sur les MTs émanant du SPB opposé. Ceci suggère que la dynéine opère différemment pour diriger le "horsetail movement" et la congression des noyaux. Pour vérifier cette hypothèse, j'ai analysé la congression des noyaux dans des zygotes qui n'expriment pas *num1* qui permet l'ancrage cortical de la dynéine et *ssm4*, un composant du complexe dynactine qui est requis pour l'association de dynéine aux MTs, mais pas au SPB. Remarquablement, dans les deux cas, la congression des noyaux n'est pas affectée, ce qui confirme notre hypothèse. En revanche, le niveau de dynéine au SPB dépend de la chaîne légère intermédiaire Dli1. En effet, dans les zygotes *dli1Δ*, la dynéine est absente du SPB et des MTs, et les noyaux se rapprochent avec un très grand délai de 100 minutes en absence de Klp2. Ceci montre que Dli1est requise pour la congression des noyaux et la bonne fonctionnement du complexe de dynéine localisé au SPB.

En résumé, la localisation différentielle des deux moteurs et leurs phénotypes différents suggèrent des rôles distincts pour tirer les noyaux l'un vers l'autre. Klp2 associée aux MTs

pourrait induire le glissement de MTs antiparallèles émanant des deux SPBs, alors que la dynéine localisée au SPB pourrait tirer sur des MTs émanant du SPB opposé.

7.2. L'AAA-ATPase oscillatoire Knk1 fonctionne dans une nouvelle voie de morphogenèse chez la levure *S. pombe*

Au cours d'un crible génétique visant à trouver de nouveaux mutants de forme chez S. pombe, j'ai identifié un nouveau gène, *knk1*, qui joue un rôle dans la maintenance de la croissance linéaire. En absence de Knk1, les cellules croissent toujours de manière polarisée, mais l'axe de croissance peut changer soudainement, ce qui provoque la formation d'un coude. Le défaut de forme provoqué par l'absence de Knk1 est nouveau puisqu'à notre connaissance, aucun mutant présentant de défaut similaire n'a été rapporté dans la littérature. Les coudes sont observés dans environ 10% des cellules *knk1Δ* et forment typiquement un angle moyen de 26.8° entre l'axe de la croissance à l'extrémité et l'axe long de la cellule. Pour comprendre comment le coude est produit, j'ai analysé l'organisation et la dynamique de MTs dans le mutant *knk1Δ*, mais elles sont similaires au sauvage indiquant que le coude n'est pas provoqué par les défauts dans la fonction de MTs. Le mutant *tea1Δ knk1Δ* génère des coudes à une fréquence et un angle similaire à ceux du mutant simple *knk1Δ*. Par contre, les défauts de morphologie sont plus graves dans un double mutant où Knk1 et les microtubules sont perturbés que dans les simples mutants correspondants suggérant que les MTs et Knk1 pourraient fonctionner dans les voies parallèles. Par exemple, 28.7% des cellules du mutant *mal3Δ knk1Δ* possèdent des coudes avec un angle moyen de 38.3°. Mais si *tea1* est également supprimé dans ce mutant, le phénotype ressemble toujours à celui du mutant simple *knk1Δ*. Ceci indique que, si la localisation de Tea1 est perturbée, par exemple en absence de Mal3, les défauts existants de la forme cellulaire peuvent être aggravés, mais ni les MTs ni Tea1 ne jouent un rôle pendant la génération d'un coude dans les cellules *knk1Δ*. En résumé, ceci indique que Knk1 participe à une nouvelle voie contrôlant la croissance polarisée.

J'ai ensuite observé la localisation de Knk1 en fusion avec deux copies de la GFP. Knk1 se localise aux extrémités cellulaires, ce qui est en accord avec un rôle dans la morphogenèse. Knk1 appartient à la famille des ATPases qui hydrolysent l'ATP et forment des oligomères hexamèriques adoptant une configuration en anneau. J'ai crée des versions mutantes de Knk1 par

troncation ou mutagenèse dirigée. Knk1N (N-terminus) se localise faiblement aux extrémités, ce qui n'est pas le cas pour Knk1C (C-terminus) qui contient le domaine ATPase. Ceci suggère que l'extrémité N-terminale permet l'association aux extrémités cellulaires, mais l'extrémité C-terminale la rend plus efficace, parce qu'elle permet la coopération de 6 molécules. De plus, la localisation du mutant Knk1(G419A), qui n'est plus capable de lier l'ATP nécessaire à l'oligomérisation, ressemble à celle de Knk1N. Mais le mutant Knk1(D478A E479A), qui forme des complexes hexamèriques malgré son incapacité à hydrolyser l'ATP, se localise à l'extrémité de la cellule avec un niveau similaire à celui de Knk1 sauvage. Ces résultats suggèrent collectivement que l'association à l'ATP, qui permet l'oligomérisation, mais pas son hydrolyse, est requise pour la localisation de Knk1.

Pour comprendre comment Knk1 s'accumule aux extrémités, j'ai testé la localisation de Knk1 dans quelques mutants ou conditions perturbant les MTs, par exemple par ajout de MBC, ou perturbant l'actine, par exemple par ajout de Latrunculin A ou en supprimant *for3* ou *sla2*. Ces expériences indiquent que les MTs et les câbles d'actine sont dispensables pour la localisation de Knk1, mais Sla2 contrôle le niveau de Knk1, puisque dans les cellules *sla2Δ,* dans lesquelles l'endocytose est perturbée, Knk1 s'accumule aux extrémités plus fortement. Des modifications similaires sont observées dans le mutant *cdc42-L160S*, qui n'a pas des défauts d'endocytose. En revanche, dans le mutant d'endocytose, *myo1*, les niveaux de Knk1 sont comparables aux niveaux sauvages. Ceci indique que le niveau de Knk1 est régulé par Sla2 et Cdc42 d'une manière indépendante de l'endocytose.

Enfin, j'ai découvert que Knk1 possède une propriété unique : elle oscille périodiquement entre les deux extrémités de la cellule dans les mutants *sla2* et *cdc42* avec une période de 14 minutes obtenu par transformée de Fourier rapide. Puisque Cdc42 oscille avec une période de 5 minutes, mes résultats proposent l'existence d'au moins deux systèmes oscillatoires séparés contribuant à la morphogenèse de *S. pombe*.

8. Conclusion

8.1. Congression nucléaire contrôlée par les microtubules chez *S. pombe*

L'étude présentée ici représente la première description détaillée de la congression des noyaux dans les cellules vivantes chez *S. pombe* et confirme les observations faites par Troxell et al. (2001). Cette étude indique que deux moteurs moléculaire des MTs, la dynéine et la kinésine-14 Klp2 contribuent à ce processus, chacun étant suffisant en absence de l'autre pour accomplir la congression. Mais un double mutant est incapable de tirer les noyaux l'un vers l'autre démontrant que les deux moteurs ont des fonctions redondantes pendant la congression nucléaire. De plus, j'ai decouvert que le contrôle correct des paramètres dynamiques de MTs favorise une congression efficace. Logiquement, des MTs plus courts ont une probabilité moindre d'interaction et génèrent des forces moins importantes. En tout cas, les forces produites indépendamment de l'activité de moteurs moléculaires ne suffisent pas pour accomplir la congression des noyaux.

La localisation différentielle des deux moteurs suggère des rôles distincts pour tirer les noyaux l'un vers l'autre. La dynéine s'associe aux SPBs. Son niveau au SPB dépend de la chaîne légère intermédiaire Dli1 qui pourrait potentiellement stabiliser le complexe dynéine et est requise pour la congression des noyaux, alors que la dynactine ne l'est pas. Klp2 se localise sur les MTs. Klp2 pourrait induire le glissement de MTs antiparallèles émanant des deux SPBs, alors que la dynéine localisée au SPB pourrait tirer sur des MTs émanant du SPB opposé.

A notre connaissance, l'étude présentée ici devrait être la première à mettre en évidence la coopération de deux moteurs moléculaires se dirigeant vers les pôles moins de MTs dans les migrations nucléaires.

8.2. Un nouveau facteur de morphogenèse chez *S. Pombe*

Dans un deuxième projet, j'ai caractérisé un nouveau facteur morphogénétique, l'AAA^+-ATPase Knk1, qui promeut la croissance linéaire chez *S. pombe*. L'absence de Knk1 provoque la formation d'un coude à proximité des extrémités cellulaires. Ce défaut de forme original ne résulte pas de défauts des MTs ou de localisation de Tea1, qui participent à la localisation de la

machinerie de croissance et à la linéarité de la croissance. Knk1 se localise aux extrémités de la cellule indépendamment des MTs et des câbles d'actine. Cette localisation requiert son N-terminus et est renforcée quand le domaine ATPase C-terminal lie l'ATP. La concentration de Knk1 aux extrémités est aussi contrôlée par Sla2 et Cdc42 indépendamment de l'endocytose. Enfin, Knk1 oscille périodiquement entre les deux extrémités de la cellule, de manière anti-corrélée, et indépendamment des oscillations de Cdc42, suggérant l'existence d'au moins deux systèmes oscillatoires séparés contribuant à la morphogenèse de *S. pombe*.

REFERENCES

ADAMES, N. R. & COOPER, J. A. 2000. Microtubule interactions with the cell cortex causing nuclear movements in Saccharomyces cerevisiae. *J Cell Biol,* 149**,** 863-74.

ADAMS, I. R. & KILMARTIN, J. V. 1999. Localization of core spindle pole body (SPB) components during SPB duplication in Saccharomyces cerevisiae. *J Cell Biol,* 145**,** 809-23.

AGUILAR, R. C., LONGHI, S. A., SHAW, J. D., YEH, L. Y., KIM, S., SCHON, A., FREIRE, E., HSU, A., MCCORMICK, W. K., WATSON, H. A. & WENDLAND, B. 2006. Epsin N-terminal homology domains perform an essential function regulating Cdc42 through binding Cdc42 GTPase-activating proteins. *Proc Natl Acad Sci U S A,* 103**,** 4116-21.

AKHMANOVA, A. & STEINMETZ, M. O. 2008. Tracking the ends: a dynamic protein network controls the fate of microtubule tips. *Nat Rev Mol Cell Biol,* 9**,** 309-22.

AKHMANOVA, A. & STEINMETZ, M. O. 2010. Microtubule +TIPs at a glance. *J Cell Sci,* 123**,** 3415-9.

AL-BASSAM, J. & CHANG, F. 2011. Regulation of microtubule dynamics by TOG-domain proteins XMAP215/Dis1 and CLASP. *Trends Cell Biol,* 21**,** 604-14.

AL-BASSAM, J., KIM, H., BROUHARD, G., VAN OIJEN, A., HARRISON, S. C. & CHANG, F. 2010. CLASP promotes microtubule rescue by recruiting tubulin dimers to the microtubule. *Dev Cell,* 19**,** 245-58.

AL-BASSAM, J., OZER, R. S., SAFER, D., HALPAIN, S. & MILLIGAN, R. A. 2002. MAP2 and tau bind longitudinally along the outer ridges of microtubule protofilaments. *J Cell Biol,* 157**,** 1187-96.

AL-BASSAM, J., VAN BREUGEL, M., HARRISON, S. C. & HYMAN, A. 2006. Stu2p binds tubulin and undergoes an open-to-closed conformational change. *J Cell Biol,* 172**,** 1009-22.

ALBERTS, A. S. 2001. Identification of a carboxyl-terminal diaphanous-related formin homology protein autoregulatory domain. *J Biol Chem,* 276**,** 2824-30.

ALBERTS, B. 2008. *Molecular biology of the cell,* New York, Garland Science.

ALLAN, V. & VALE, R. 1994. Movement of membrane tubules along microtubules in vitro: evidence for specialised sites of motor attachment. *J Cell Sci,* 107 (Pt 7)**,** 1885-97.

AMANN, K. J. & POLLARD, T. D. 2001. The Arp2/3 complex nucleates actin filament branches from the sides of pre-existing filaments. *Nat Cell Biol,* 3**,** 306-10.

AMOS, L. & KLUG, A. 1974. Arrangement of subunits in flagellar microtubules. *J Cell Sci,* 14**,** 523-49.

ANANTHANARAYANAN, V., SCHATTAT, M., VOGEL, S. K., KRULL, A., PAVIN, N. & TOLIC-NORRELYKKE, I. M. 2013. Dynein motion switches from diffusive to directed upon cortical anchoring. *Cell,* 153**,** 1526-36.

ANDERS, A. & SAWIN, K. E. 2011. Microtubule stabilization in vivo by nucleation-incompetent gamma-tubulin complex. *J Cell Sci,* 124**,** 1207-13.

ARASADA, R. & POLLARD, T. D. 2011. Distinct roles for F-BAR proteins Cdc15p and Bzz1p in actin polymerization at sites of endocytosis in fission yeast. *Curr Biol,* 21**,** 1450-9.

ARELLANO, M., NICCOLI, T. & NURSE, P. 2002. Tea3p is a cell end marker activating polarized growth in Schizosaccharomyces pombe. *Curr Biol,* 12**,** 751-6.

ARKOWITZ, R. A. & BASSILANA, M. 2011. Polarized growth in fungi: symmetry breaking and hyphal formation. *Semin Cell Dev Biol,* 22**,** 806-15.

ARNAL, I., HEICHETTE, C., DIAMANTOPOULOS, G. S. & CHRETIEN, D. 2004. CLIP-170/tubulin-curved oligomers coassemble at microtubule ends and promote rescues. *Curr Biol,* 14**,** 2086-95.

ATTANAPOLA, S. L., ALEXANDER, C. J. & MULVIHILL, D. P. 2009. Ste20-kinase-dependent TEDS-site phosphorylation modulates the dynamic localisation and endocytic function of the fission yeast class I myosin, Myo1. *J Cell Sci,* 122**,** 3856-61.

AZIMZADEH, J. & BORNENS, M. 2007. Structure and duplication of the centrosome. *J Cell Sci,* 120**,** 2139-42.

BAMBURG, J. R., MCGOUGH, A. & ONO, S. 1999. Putting a new twist on actin: ADF/cofilins modulate actin dynamics. *Trends Cell Biol,* 9**,** 364-70.

BASU, R. & CHANG, F. 2011. Characterization of dip1p reveals a switch in Arp2/3-dependent actin assembly for fission yeast endocytosis. *Curr Biol,* 21**,** 905-16.

BASU, R., MUNTEANU, E. L. & CHANG, F. 2014. Role of turgor pressure in endocytosis in fission yeast. *Mol Biol Cell,* 25**,** 679-87.

BAYE, L. M. & LINK, B. A. 2008. Nuclear migration during retinal development. *Brain Res,* 1192**,** 29-36.

BEINHAUER, J. D., HAGAN, I. M., HEGEMANN, J. H. & FLEIG, U. 1997. Mal3, the fission yeast homologue of the human APC-interacting protein EB-1 is required for microtubule integrity and the maintenance of cell form. *J Cell Biol,* 139**,** 717-28.

BELLION, A., BAUDOIN, J. P., ALVAREZ, C., BORNENS, M. & METIN, C. 2005. Nucleokinesis in tangentially migrating neurons comprises two alternating phases: forward migration of the Golgi/centrosome associated with centrosome splitting and myosin contraction at the rear. *J Neurosci,* 25**,** 5691-9.

BELMONT, L. D. & MITCHISON, T. J. 1996. Identification of a protein that interacts with tubulin dimers and increases the catastrophe rate of microtubules. *Cell,* 84**,** 623-31.

BENDEZU, F. O. & MARTIN, S. G. 2011. Actin cables and the exocyst form two independent morphogenesis pathways in the fission yeast. *Mol Biol Cell,* 22**,** 44-53.

BENDEZU, F. O. & MARTIN, S. G. 2012. Cdc42 oscillations in yeasts. *Sci Signal,* 5**,** pe53.

BENDEZU, F. O. & MARTIN, S. G. 2013. Cdc42 explores the cell periphery for mate selection in fission yeast. *Curr Biol,* 23**,** 42-7.

BENDEZU, F. O., VINCENZETTI, V. & MARTIN, S. G. 2012. Fission yeast Sec3 and Exo70 are transported on actin cables and localize the exocyst complex to cell poles. *PLoS One,* 7**,** e40248.

BERLIN, V., STYLES, C. A. & FINK, G. R. 1990. BIK1, a protein required for microtubule function during mating and mitosis in Saccharomyces cerevisiae, colocalizes with tubulin. *J Cell Biol,* 111**,** 2573-86.

BETTENCOURT-DIAS, M. & GLOVER, D. M. 2007. Centrosome biogenesis and function: centrosomics brings new understanding. *Nat Rev Mol Cell Biol,* 8**,** 451-63.

BOETTNER, D. R., CHI, R. J. & LEMMON, S. K. 2012. Lessons from yeast for clathrin-mediated endocytosis. *Nat Cell Biol,* 14**,** 2-10.

BOUISSOU, A., VEROLLET, C., SOUSA, A., SAMPAIO, P., WRIGHT, M., SUNKEL, C. E., MERDES, A. & RAYNAUD-MESSINA, B. 2009. {gamma}-Tubulin ring complexes regulate microtubule plus end dynamics. *J Cell Biol,* 187**,** 327-34.

BRATMAN, S. V. & CHANG, F. 2007. Stabilization of overlapping microtubules by fission yeast CLASP. *Dev Cell,* 13**,** 812-27.

BRAUN, M., DRUMMOND, D. R., CROSS, R. A. & MCAINSH, A. D. 2009. The kinesin-14 Klp2 organizes microtubules into parallel bundles by an ATP-dependent sorting mechanism. *Nat Cell Biol,* 11**,** 724-30.

BRAUN, M., LANSKY, Z., BAJER, S., FINK, G., KASPRZAK, A. A. & DIEZ, S. 2013. The human kinesin-14 HSET tracks the tips of growing microtubules in vitro. *Cytoskeleton (Hoboken),* 70**,** 515-21.

BRAZER, S. C., WILLIAMS, H. P., CHAPPELL, T. G. & CANDE, W. Z. 2000. A fission yeast kinesin affects Golgi membrane recycling. *Yeast,* 16**,** 149-66.

BRODERICK, M. J. & WINDER, S. J. 2002. Towards a complete atomic structure of spectrin family proteins. *J Struct Biol,* 137**,** 184-93.

BROUHARD, G. J., STEAR, J. H., NOETZEL, T. L., AL-BASSAM, J., KINOSHITA, K., HARRISON, S. C., HOWARD, J. & HYMAN, A. A. 2008. XMAP215 is a processive microtubule polymerase. *Cell,* 132**,** 79-88.

BROWNING, H., HACKNEY, D. D. & NURSE, P. 2003. Targeted movement of cell end factors in fission yeast. *Nat Cell Biol,* 5**,** 812-8.

BROWNING, H., HAYLES, J., MATA, J., AVELINE, L., NURSE, P. & MCINTOSH, J. R. 2000. Tea2p is a kinesin-like protein required to generate polarized growth in fission yeast. *J Cell Biol,* 151**,** 15-28.

BRUNNER, D. & NURSE, P. 2000. CLIP170-like tip1p spatially organizes microtubular dynamics in fission yeast. *Cell,* 102**,** 695-704.

BRUUSGAARD, J. C., LIESTOL, K., EKMARK, M., KOLLSTAD, K. & GUNDERSEN, K. 2003. Number and spatial distribution of nuclei in the muscle fibres of normal mice studied in vivo. *J Physiol,* 551**,** 467-78.

BULLOCK, S. L. & ISH-HOROWICZ, D. 2001. Conserved signals and machinery for RNA transport in Drosophila oogenesis and embryogenesis. *Nature,* 414**,** 611-6.

BURAKOV, A., NADEZHDINA, E., SLEPCHENKO, B. & RODIONOV, V. 2003. Centrosome positioning in interphase cells. *J Cell Biol,* 162**,** 963-9.

BURGESS, S. A., WALKER, M. L., SAKAKIBARA, H., KNIGHT, P. J. & OIWA, K. 2003. Dynein structure and power stroke. *Nature,* 421**,** 715-8.

BURKE, B. & ROUX, K. J. 2009. Nuclei take a position: managing nuclear location. *Dev Cell,* 17**,** 587-97.

BURNS, R. G. 1991. Alpha-, beta-, and gamma-tubulins: sequence comparisons and structural constraints. *Cell Motil Cytoskeleton,* 20**,** 181-9.

BUSCH, K. E. & BRUNNER, D. 2004. The microtubule plus end-tracking proteins mal3p and tip1p cooperate for cell-end targeting of interphase microtubules. *Curr Biol,* 14**,** 548-59.

BUSCH, K. E., HAYLES, J., NURSE, P. & BRUNNER, D. 2004. Tea2p kinesin is involved in spatial microtubule organization by transporting tip1p on microtubules. *Dev Cell,* 6**,** 831-43.

BUSSON, S., DUJARDIN, D., MOREAU, A., DOMPIERRE, J. & DE MEY, J. R. 1998. Dynein and dynactin are localized to astral microtubules and at cortical sites in mitotic epithelial cells. *Curr Biol,* 8**,** 541-4.

CADOT, B., GACHE, V., VASYUTINA, E., FALCONE, S., BIRCHMEIER, C. & GOMES, E. R. 2012. Nuclear movement during myotube formation is microtubule and dynein dependent and is regulated by Cdc42, Par6 and Par3. *EMBO Rep,* 13**,** 741-9.

CAI, S., WEAVER, L. N., EMS-MCCLUNG, S. C. & WALCZAK, C. E. 2009. Kinesin-14 family proteins HSET/XCTK2 control spindle length by cross-linking and sliding microtubules. *Mol Biol Cell,* 20**,** 1348-59.

CALLAN, H. G. & TOMLIN, S. G. 1950. Experimental studies on amphibian oocyte nuclei. I. Investigation of the structure of the nuclear membrane by means of the electron microscope. *Proc R Soc Lond B Biol Sci,* 137**,** 367-78.

CAMPELLONE, K. G. & WELCH, M. D. 2010. A nucleator arms race: cellular control of actin assembly. *Nat Rev Mol Cell Biol,* 11**,** 237-51.

CARAZO-SALAS, R. E., ANTONY, C. & NURSE, P. 2005. The kinesin Klp2 mediates polarization of interphase microtubules in fission yeast. *Science,* 309**,** 297-300.

CARAZO-SALAS, R. E. & NURSE, P. 2006. Self-organization of interphase microtubule arrays in fission yeast. *Nat Cell Biol,* 8**,** 1102-7.

CASE, R. B., PIERCE, D. W., HOM-BOOHER, N., HART, C. L. & VALE, R. D. 1997. The directional preference of kinesin motors is specified by an element outside of the motor catalytic domain. *Cell,* 90**,** 959-66.

CASSIMERIS, L. & SPITTLE, C. 2001. Regulation of microtubule-associated proteins. *Int Rev Cytol,* 210**,** 163-226.

CASTAGNETTI, S., BEHRENS, R. & NURSE, P. 2005. End4/Sla2 is involved in establishment of a new growth zone in Schizosaccharomyces pombe. *J Cell Sci,* 118**,** 1843-50.

CHANG-JIE, J. & SONOBE, S. 1993. Identification and preliminary characterization of a 65 kDa higher-plant microtubule-associated protein. *J Cell Sci,* 105 (Pt 4)**,** 891-901.

CHANG, F., DRUBIN, D. & NURSE, P. 1997. cdc12p, a protein required for cytokinesis in fission yeast, is a component of the cell division ring and interacts with profilin. *J Cell Biol,* 137**,** 169-82.

CHANG, F. & MARTIN, S. G. 2009. Shaping fission yeast with microtubules. *Cold Spring Harb Perspect Biol,* 1**,** a001347.

CHANG, F. & NURSE, P. 1996. How fission yeast fission in the middle. *Cell,* 84**,** 191-4.

CHEN, C. R., CHEN, J. & CHANG, E. C. 2000. A conserved interaction between Moe1 and Mal3 is important for proper spindle formation in Schizosaccharomyces pombe. *Mol Biol Cell,* 11**,** 4067-77.

CHEN, C. R., LI, Y. C., CHEN, J., HOU, M. C., PAPADAKI, P. & CHANG, E. C. 1999. Moe1, a conserved protein in Schizosaccharomyces pombe, interacts with a Ras effector, Scd1, to affect proper spindle formation. *Proc Natl Acad Sci U S A,* 96**,** 517-22.

CHEN, T. J., GEHLER, S., SHAW, A. E., BAMBURG, J. R. & LETOURNEAU, P. C. 2006. Cdc42 participates in the regulation of ADF/cofilin and retinal growth cone filopodia by brain derived neurotrophic factor. *J Neurobiol,* 66**,** 103-14.

CHHABRA, E. S. & HIGGS, H. N. 2007. The many faces of actin: matching assembly factors with cellular structures. *Nat Cell Biol,* 9**,** 1110-21.

CHIKASHIGE, Y., DING, D. Q., FUNABIKI, H., HARAGUCHI, T., MASHIKO, S., YANAGIDA, M. & HIRAOKA, Y. 1994. Telomere-led premeiotic chromosome movement in fission yeast. *Science,* 264**,** 270-3.

CHIKASHIGE, Y., TSUTSUMI, C., YAMANE, M., OKAMASA, K., HARAGUCHI, T. & HIRAOKA, Y. 2006. Meiotic proteins bqt1 and bqt2 tether telomeres to form the bouquet arrangement of chromosomes. *Cell,* 125**,** 59-69.

CHOW, K. H., FACTOR, R. E. & ULLMAN, K. S. 2012. The nuclear envelope environment and its cancer connections. *Nat Rev Cancer,* 12**,** 196-209.

COLL, P. M., RINCON, S. A., IZQUIERDO, R. A. & PEREZ, P. 2007. Hob3p, the fission yeast ortholog of human BIN3, localizes Cdc42p to the division site and regulates cytokinesis. *EMBO J,* 26**,** 1865-77.

COURTHEOUX, T., GAY, G., REYES, C., GOLDSTONE, S., GACHET, Y. & TOURNIER, S. 2007. Dynein participates in chromosome segregation in fission yeast. *Biol Cell,* 99**,** 627-37.

COY, D. L., HANCOCK, W. O., WAGENBACH, M. & HOWARD, J. 1999. Kinesin's tail domain is an inhibitory regulator of the motor domain. *Nat Cell Biol,* 1**,** 288-92.

CRISP, M., LIU, Q., ROUX, K., RATTNER, J. B., SHANAHAN, C., BURKE, B., STAHL, P. D. & HODZIC, D. 2006. Coupling of the nucleus and cytoplasm: role of the LINC complex. *J Cell Biol,* 172**,** 41-53.

CROSS, R. A. 2010. Kinesin-14: the roots of reversal. *BMC Biol,* 8**,** 107.

CULVER-HANLON, T. L., LEX, S. A., STEPHENS, A. D., QUINTYNE, N. J. & KING, S. J. 2006. A microtubule-binding domain in dynactin increases dynein processivity by skating along microtubules. *Nat Cell Biol,* 8**,** 264-70.

DAGA, R. R., LEE, K. G., BRATMAN, S., SALAS-PINO, S. & CHANG, F. 2006. Self-organization of microtubule bundles in anucleate fission yeast cells. *Nat Cell Biol,* 8**,** 1108-13.

DAMMERMANN, A., CIPAK, L. & GREGAN, J. 2012. Microtubule organization: a pericentriolar material-like structure in yeast meiosis. *Curr Biol,* 22**,** R229-31.

DAS, M., DRAKE, T., WILEY, D. J., BUCHWALD, P., VAVYLONIS, D. & VERDE, F. 2012. Oscillatory dynamics of Cdc42 GTPase in the control of polarized growth. *Science,* 337**,** 239-43.

DAS, M. & VERDE, F. 2013. Role of Cdc42 dynamics in the control of fission yeast cell polarization. *Biochem Soc Trans,* 41**,** 1745-9.

DAS, M., WILEY, D. J., CHEN, X., SHAH, K. & VERDE, F. 2009. The conserved NDR kinase Orb6 controls polarized cell growth by spatial regulation of the small GTPase Cdc42. *Curr Biol,* 19**,** 1314-9.

DAS, M., WILEY, D. J., MEDINA, S., VINCENT, H. A., LARREA, M., ORIOLO, A. & VERDE, F. 2007. Regulation of cell diameter, For3p localization, and cell symmetry by fission yeast Rho-GAP Rga4p. *Mol Biol Cell,* 18**,** 2090-101.

DECASTRO, M. J., HO, C. H. & STEWART, R. J. 1999. Motility of dimeric ncd on a metal-chelating surfactant: evidence that ncd is not processive. *Biochemistry,* 38**,** 5076-81.

DEHMELT, L. & HALPAIN, S. 2005. The MAP2/Tau family of microtubule-associated proteins. *Genome Biol,* 6**,** 204.

DEL BENE, F., WEHMAN, A. M., LINK, B. A. & BAIER, H. 2008. Regulation of neurogenesis by interkinetic nuclear migration through an apical-basal notch gradient. *Cell,* 134**,** 1055-65.

DESAI, A. & MITCHISON, T. J. 1997. Microtubule polymerization dynamics. *Annu Rev Cell Dev Biol,* 13**,** 83-117.

DIMITROV, A., QUESNOIT, M., MOUTEL, S., CANTALOUBE, I., POUS, C. & PEREZ, F. 2008. Detection of GTP-tubulin conformation in vivo reveals a role for GTP remnants in microtubule rescues. *Science,* 322**,** 1353-6.

DING, D. Q., CHIKASHIGE, Y., HARAGUCHI, T. & HIRAOKA, Y. 1998. Oscillatory nuclear movement in fission yeast meiotic prophase is driven by astral microtubules, as revealed by continuous observation of chromosomes and microtubules in living cells. *J Cell Sci,* 111 (Pt 6)**,** 701-12.

DING, D. Q., YAMAMOTO, A., HARAGUCHI, T. & HIRAOKA, Y. 2004. Dynamics of homologous chromosome pairing during meiotic prophase in fission yeast. *Dev Cell,* 6**,** 329-41.

DING, R., WEST, R. R., MORPHEW, D. M., OAKLEY, B. R. & MCINTOSH, J. R. 1997. The spindle pole body of Schizosaccharomyces pombe enters and leaves the nuclear envelope as the cell cycle proceeds. *Mol Biol Cell,* 8**,** 1461-79.

DING, X., XU, R., YU, J., XU, T., ZHUANG, Y. & HAN, M. 2007. SUN1 is required for telomere attachment to nuclear envelope and gametogenesis in mice. *Dev Cell,* 12**,** 863-72.

DONG, Y., PRUYNE, D. & BRETSCHER, A. 2003. Formin-dependent actin assembly is regulated by distinct modes of Rho signaling in yeast. *J Cell Biol,* 161**,** 1081-92.

DOWNING, K. H. & NOGALES, E. 1998. Tubulin and microtubule structure. *Curr Opin Cell Biol,* 10**,** 16-22.

DRECHSEL, D. N. & KIRSCHNER, M. W. 1994. The minimum GTP cap required to stabilize microtubules. *Curr Biol,* 4**,** 1053-61.

DRUMMOND, D. R. & CROSS, R. A. 2000. Dynamics of interphase microtubules in Schizosaccharomyces pombe. *Curr Biol,* 10**,** 766-75.

DUJARDIN, D. L. & VALLEE, R. B. 2002. Dynein at the cortex. *Curr Opin Cell Biol,* 14**,** 44-9.

DUPIN, I., CAMAND, E. & ETIENNE-MANNEVILLE, S. 2009. Classical cadherins control nucleus and centrosome position and cell polarity. *J Cell Biol,* 185**,** 779-86.

DUPIN, I. & ETIENNE-MANNEVILLE, S. 2011. Nuclear positioning: mechanisms and functions. *Int J Biochem Cell Biol,* 43**,** 1698-707.

EGELMAN, E. H., FRANCIS, N. & DEROSIER, D. J. 1982. F-actin is a helix with a random variable twist. *Nature,* 298**,** 131-5.

ENDOW, S. A. & WALIGORA, K. W. 1998. Determinants of kinesin motor polarity. *Science,* 281**,** 1200-2.

ESTRAVIS, M., RINCON, S. & PEREZ, P. 2012. Cdc42 regulation of polarized traffic in fission yeast. *Commun Integr Biol,* 5**,** 370-3.

ESTRAVIS, M., RINCON, S. A., SANTOS, B. & PEREZ, P. 2011. Cdc42 regulates multiple membrane traffic events in fission yeast. *Traffic,* 12**,** 1744-58.

EVANS, L., MITCHISON, T. & KIRSCHNER, M. 1985. Influence of the centrosome on the structure of nucleated microtubules. *J Cell Biol,* 100**,** 1185-91.

FAWCETT, D. W. 1966. On the occurrence of a fibrous lamina on the inner aspect of the nuclear envelope in certain cells of vertebrates. *Am J Anat,* 119**,** 129-45.

FEIERBACH, B. & CHANG, F. 2001. Roles of the fission yeast formin for3p in cell polarity, actin cable formation and symmetric cell division. *Curr Biol,* 11**,** 1656-65.

FEIERBACH, B., VERDE, F. & CHANG, F. 2004. Regulation of a formin complex by the microtubule plus end protein tea1p. *J Cell Biol,* 165**,** 697-707.

FELDHERR, C. M., KALLENBACH, E. & SCHULTZ, N. 1984. Movement of a karyophilic protein through the nuclear pores of oocytes. *J Cell Biol,* 99**,** 2216-22.

FINK, G., HAJDO, L., SKOWRONEK, K. J., REUTHER, C., KASPRZAK, A. A. & DIEZ, S. 2009. The mitotic kinesin-14 Ncd drives directional microtubule-microtubule sliding. *Nat Cell Biol,* 11**,** 717-23.

FISCHER, R. & TIMBERLAKE, W. E. 1995. Aspergillus nidulans apsA (anucleate primary sterigmata) encodes a coiled-coil protein required for nuclear positioning and completion of asexual development. *J Cell Biol,* 128**,** 485-98.

FISCHER, R., ZEKERT, N. & TAKESHITA, N. 2008. Polarized growth in fungi--interplay between the cytoskeleton, positional markers and membrane domains. *Mol Microbiol,* 68**,** 813-26.

FOE, V. E. & ALBERTS, B. M. 1983. Studies of nuclear and cytoplasmic behaviour during the five mitotic cycles that precede gastrulation in Drosophila embryogenesis. *J Cell Sci,* 61**,** 31-70.

FOLKER, E. S., SCHULMAN, V. K. & BAYLIES, M. K. 2014. Translocating myonuclei have distinct leading and lagging edges that require kinesin and dynein. *Development,* 141**,** 355-66.

FONG, C. S., SATO, M. & TODA, T. 2010. Fission yeast Pcp1 links polo kinase-mediated mitotic entry to gamma-tubulin-dependent spindle formation. *EMBO J,* 29**,** 120-30.

FOSTER, K. A. & GILBERT, S. P. 2000. Kinetic studies of dimeric Ncd: evidence that Ncd is not processive. *Biochemistry,* 39**,** 1784-91.

FRIDOLFSSON, H. N., LY, N., MEYERZON, M. & STARR, D. A. 2010. UNC-83 coordinates kinesin-1 and dynein activities at the nuclear envelope during nuclear migration. *Dev Biol,* 338**,** 237-50.

FRIDOLFSSON, H. N. & STARR, D. A. 2010. Kinesin-1 and dynein at the nuclear envelope mediate the bidirectional migrations of nuclei. *J Cell Biol,* 191**,** 115-28.

FU, C., WARD, J. J., LOIODICE, I., VELVE-CASQUILLAS, G., NEDELEC, F. J. & TRAN, P. T. 2009. Phospho-regulated interaction between kinesin-6 Klp9p and microtubule bundler Ase1p promotes spindle elongation. *Dev Cell,* 17**,** 257-67.

FUJITA, I., YAMASHITA, A. & YAMAMOTO, M. 2010. Contribution of dynein light intermediate and intermediate chains to subcellular localization of the dynein-dynactin motor complex in Schizosaccharomyces pombe. *Genes Cells,* 15**,** 359-72.

FUNABIKI, H., HAGAN, I., UZAWA, S. & YANAGIDA, M. 1993. Cell cycle-dependent specific positioning and clustering of centromeres and telomeres in fission yeast. *J Cell Biol,* 121**,** 961-76.

FUNAYA, C., SAMARASINGHE, S., PRUGGNALLER, S., OHTA, M., CONNOLLY, Y., MULLER, J., MURAKAMI, H., GRALLERT, A., YAMAMOTO, M., SMITH, D., ANTONY, C. & TANAKA, K. 2012. Transient structure associated with the spindle pole body directs meiotic microtubule reorganization in S. pombe. *Curr Biol,* 22**,** 562-74.

GACHET, Y. & HYAMS, J. S. 2005. Endocytosis in fission yeast is spatially associated with the actin cytoskeleton during polarised cell growth and cytokinesis. *J Cell Sci,* 118**,** 4231-42.

GACHET, Y., REYES, C., COURTHEOUX, T., GOLDSTONE, S., GAY, G., SERRURIER, C. & TOURNIER, S. 2008. Sister kinetochore recapture in fission yeast occurs by two distinct mechanisms, both requiring Dam1 and Klp2. *Mol Biol Cell,* 19**,** 1646-62.

GALL, J. G. 1967. Octagonal nuclear pores. *J Cell Biol,* 32**,** 391-9.

GAMBLIN, T. C., NACHMANOFF, K., HALPAIN, S. & WILLIAMS, R. C., JR. 1996. Recombinant microtubule-associated protein 2c reduces the dynamic instability of individual microtubules. *Biochemistry,* 35**,** 12576-86.

GARCIA, M. A., KOONRUGSA, N. & TODA, T. 2002. Two kinesin-like Kin I family proteins in fission yeast regulate the establishment of metaphase and the onset of anaphase A. *Curr Biol,* 12**,** 610-21.

GARCIA, P., TAJADURA, V., GARCIA, I. & SANCHEZ, Y. 2006. Role of Rho GTPases and Rho-GEFs in the regulation of cell shape and integrity in fission yeast. *Yeast,* 23**,** 1031-43.

GARD, D. L. & KIRSCHNER, M. W. 1987. A microtubule-associated protein from Xenopus eggs that specifically promotes assembly at the plus-end. *J Cell Biol,* 105**,** 2203-15.

GEE, M. A., HEUSER, J. E. & VALLEE, R. B. 1997. An extended microtubule-binding structure within the dynein motor domain. *Nature,* 390**,** 636-9.

GENNERICH, A., CARTER, A. P., RECK-PETERSON, S. L. & VALE, R. D. 2007. Force-induced bidirectional stepping of cytoplasmic dynein. *Cell,* 131**,** 952-65.

GENNERICH, A. & VALE, R. D. 2009. Walking the walk: how kinesin and dynein coordinate their steps. *Curr Opin Cell Biol,* 21**,** 59-67.

GERACE, L. & BURKE, B. 1988. Functional organization of the nuclear envelope. *Annu Rev Cell Biol,* 4**,** 335-74.

GIBBONS, I. R., GARBARINO, J. E., TAN, C. E., RECK-PETERSON, S. L., VALE, R. D. & CARTER, A. P. 2005. The affinity of the dynein microtubule-binding domain is modulated by the conformation of its coiled-coil stalk. *J Biol Chem,* 280**,** 23960-5.

GIBEAUX, R., POLITI, A. Z., NEDELEC, F., ANTONY, C. & KNOP, M. 2013. Spindle pole body-anchored Kar3 drives the nucleus along microtubules from another nucleus in preparation for nuclear fusion during yeast karyogamy. *Genes Dev,* 27**,** 335-49.

GIDDINGS, T. H., JR., O'TOOLE, E. T., MORPHEW, M., MASTRONARDE, D. N., MCINTOSH, J. R. & WINEY, M. 2001. Using rapid freeze and freeze-substitution for the preparation of yeast cells for electron microscopy and three-dimensional analysis. *Methods Cell Biol,* 67**,** 27-42.

GOMES, E. R., JANI, S. & GUNDERSEN, G. G. 2005. Nuclear movement regulated by Cdc42, MRCK, myosin, and actin flow establishes MTOC polarization in migrating cells. *Cell,* 121**,** 451-63.

GOSHIMA, G., NEDELEC, F. & VALE, R. D. 2005a. Mechanisms for focusing mitotic spindle poles by minus end-directed motor proteins. *J Cell Biol,* 171**,** 229-40.

GOSHIMA, G., WOLLMAN, R., STUURMAN, N., SCHOLEY, J. M. & VALE, R. D. 2005b. Length control of the metaphase spindle. *Curr Biol,* 15**,** 1979-88.

GRADY, R. M., STARR, D. A., ACKERMAN, G. L., SANES, J. R. & HAN, M. 2005. Syne proteins anchor muscle nuclei at the neuromuscular junction. *Proc Natl Acad Sci U S A,* 102**,** 4359-64.

GRIFFIS, E. R., STUURMAN, N. & VALE, R. D. 2007. Spindly, a novel protein essential for silencing the spindle assembly checkpoint, recruits dynein to the kinetochore. *J Cell Biol,* 177**,** 1005-15.

GRISHCHUK, E. L. & MCINTOSH, J. R. 2006. Microtubule depolymerization can drive poleward chromosome motion in fission yeast. *EMBO J,* 25**,** 4888-96.

GRISHCHUK, E. L., SPIRIDONOV, I. S. & MCINTOSH, J. R. 2007. Mitotic chromosome biorientation in fission yeast is enhanced by dynein and a minus-end-directed, kinesin-like protein. *Mol Biol Cell,* 18**,** 2216-25.

GROSSMAN, E., MEDALIA, O. & ZWERGER, M. 2012. Functional architecture of the nuclear pore complex. *Annu Rev Biophys,* 41**,** 557-84.

GRUENBAUM, Y., MARGALIT, A., GOLDMAN, R. D., SHUMAKER, D. K. & WILSON, K. L. 2005. The nuclear lamina comes of age. *Nat Rev Mol Cell Biol,* 6**,** 21-31.

GUNAWARDANE, R. N., MARTIN, O. C., CAO, K., ZHANG, L., DEJ, K., IWAMATSU, A. & ZHENG, Y. 2000. Characterization and reconstitution of Drosophila gamma-tubulin ring complex subunits. *J Cell Biol,* 151**,** 1513-24.

GUNDERSEN, G. G. & WORMAN, H. J. 2013. Nuclear positioning. *Cell,* 152**,** 1376-89.

GUPTA, S. & MCCOLLUM, D. 2011. Crosstalk between NDR kinase pathways coordinates cell cycle dependent actin rearrangements. *Cell Div,* 6**,** 19.

HABURA, A., TIKHONENKO, I., CHISHOLM, R. L. & KOONCE, M. P. 1999. Interaction mapping of a dynein heavy chain. Identification of dimerization and intermediate-chain binding domains. *J Biol Chem,* 274**,** 15447-53.

HACKNEY, D. D. 1995. Highly processive microtubule-stimulated ATP hydrolysis by dimeric kinesin head domains. *Nature,* 377**,** 448-50.

HAGAN, I. & YANAGIDA, M. 1992. Kinesin-related cut7 protein associates with mitotic and meiotic spindles in fission yeast. *Nature,* 356**,** 74-6.

HAGAN, I. M. 1998. The fission yeast microtubule cytoskeleton. *J Cell Sci,* 111 (Pt 12)**,** 1603-12.

HANCOCK, W. O. & HOWARD, J. 1998. Processivity of the motor protein kinesin requires two heads. *J Cell Biol,* 140**,** 1395-405.

HANSON, P. I. & WHITEHEART, S. W. 2005. AAA+ proteins: have engine, will work. *Nat Rev Mol Cell Biol,* 6**,** 519-29.

HANUKOGLU, I. & FUCHS, E. 1983. The cDNA sequence of a Type II cytoskeletal keratin reveals constant and variable structural domains among keratins. *Cell,* 33**,** 915-24.

HAQUE, F., LLOYD, D. J., SMALLWOOD, D. T., DENT, C. L., SHANAHAN, C. M., FRY, A. M., TREMBATH, R. C. & SHACKLETON, S. 2006. SUN1 interacts with nuclear lamin A and cytoplasmic nesprins to provide a physical connection between the nuclear lamina and the cytoskeleton. *Mol Cell Biol,* 26**,** 3738-51.

HARIGAYA, Y., TANAKA, H., YAMANAKA, S., TANAKA, K., WATANABE, Y., TSUTSUMI, C., CHIKASHIGE, Y., HIRAOKA, Y., YAMASHITA, A. & YAMAMOTO, M. 2006. Selective elimination of messenger RNA prevents an incidence of untimely meiosis. *Nature,* 442**,** 45-50.

HARIGAYA, Y. & YAMAMOTO, M. 2007. Molecular mechanisms underlying the mitosis-meiosis decision. *Chromosome Res,* 15**,** 523-37.

HARTMAN, M. A. & SPUDICH, J. A. 2012. The myosin superfamily at a glance. *J Cell Sci,* 125**,** 1627-32.

HAYLES, J. & NURSE, P. 2001. A journey into space. *Nat Rev Mol Cell Biol,* 2**,** 647-56.

HE, B. & GUO, W. 2009. The exocyst complex in polarized exocytosis. *Curr Opin Cell Biol,* 21**,** 537-42.

HEASMAN, S. J. & RIDLEY, A. J. 2008. Mammalian Rho GTPases: new insights into their functions from in vivo studies. *Nat Rev Mol Cell Biol,* 9**,** 690-701.

HELFAND, B. T., CHANG, L. & GOLDMAN, R. D. 2004. Intermediate filaments are dynamic and motile elements of cellular architecture. *J Cell Sci,* 117**,** 133-41.

HERRMANN, H. & AEBI, U. 2004. Intermediate filaments: molecular structure, assembly mechanism, and integration into functionally distinct intracellular Scaffolds. *Annu Rev Biochem,* 73**,** 749-89.

HERRMANN, H., BAR, H., KREPLAK, L., STRELKOV, S. V. & AEBI, U. 2007. Intermediate filaments: from cell architecture to nanomechanics. *Nat Rev Mol Cell Biol,* 8**,** 562-73.

HIROKAWA, N., NODA, Y., TANAKA, Y. & NIWA, S. 2009. Kinesin superfamily motor proteins and intracellular transport. *Nat Rev Mol Cell Biol,* 10**,** 682-96.

HIROKAWA, N., PFISTER, K. K., YORIFUJI, H., WAGNER, M. C., BRADY, S. T. & BLOOM, G. S. 1989. Submolecular domains of bovine brain kinesin identified by electron microscopy and monoclonal antibody decoration. *Cell,* 56**,** 867-78.

HOLLERAN, E. A., LIGON, L. A., TOKITO, M., STANKEWICH, M. C., MORROW, J. S. & HOLZBAUR, E. L. 2001. beta III spectrin binds to the Arp1 subunit of dynactin. *J Biol Chem,* 276**,** 36598-605.

HOLMES, K. C. 2009. Structural biology: actin in a twist. *Nature,* 457**,** 389-90.

HONNAPPA, S., GOUVEIA, S. M., WEISBRICH, A., DAMBERGER, F. F., BHAVESH, N. S., JAWHARI, H., GRIGORIEV, I., VAN RIJSSEL, F. J., BUEY, R. M., LAWERA, A., JELESAROV, I., WINKLER, F. K., WUTHRICH, K., AKHMANOVA, A. & STEINMETZ, M. O. 2009. An EB1-binding motif acts as a microtubule tip localization signal. *Cell,* 138**,** 366-76.

HONNAPPA, S., OKHRIMENKO, O., JAUSSI, R., JAWHARI, H., JELESAROV, I., WINKLER, F. K. & STEINMETZ, M. O. 2006. Key interaction modes of dynamic +TIP networks. *Mol Cell,* 23**,** 663-71.

HOU, H., ZHOU, Z., WANG, Y., WANG, J., KALLGREN, S. P., KURCHUK, T., MILLER, E. A., CHANG, F. & JIA, S. 2012. Csi1 links centromeres to the nuclear envelope for centromere clustering. *J Cell Biol,* 199**,** 735-44.

HOWARD, J. & HYMAN, A. A. 2007. Microtubule polymerases and depolymerases. *Curr Opin Cell Biol,* 19**,** 31-5.

HOWELL, A. S., JIN, M., WU, C. F., ZYLA, T. R., ELSTON, T. C. & LEW, D. J. 2012. Negative feedback enhances robustness in the yeast polarity establishment circuit. *Cell,* 149**,** 322-33.

HSU, S. C., TING, A. E., HAZUKA, C. D., DAVANGER, S., KENNY, J. W., KEE, Y. & SCHELLER, R. H. 1996. The mammalian brain rsec6/8 complex. *Neuron,* 17**,** 1209-19.

HUISMAN, S. M. & SEGAL, M. 2005. Cortical capture of microtubules and spindle polarity in budding yeast - where's the catch? *J Cell Sci,* 118**,** 463-71.

HWANG, E., KUSCH, J., BARRAL, Y. & HUFFAKER, T. C. 2003. Spindle orientation in Saccharomyces cerevisiae depends on the transport of microtubule ends along polarized actin cables. *J Cell Biol,* 161**,** 483-8.

ICHIHARA, K., KITAZAWA, H., IGUCHI, Y., HOTANI, H. & ITOH, T. J. 2001. Visualization of the stop of microtubule depolymerization that occurs at the high-density region of microtubule-associated protein 2 (MAP2). *J Mol Biol,* 312**,** 107-18.

ISHIGURO, J. 1998. Genetic control of fission yeast cell wall synthesis: the genes involved in wall biogenesis and their interactions in Schizosaccharomyces pombe. *Genes Genet Syst,* 73**,** 181-91.

IWAKI, T., TANAKA, N., TAKAGI, H., GIGA-HAMA, Y. & TAKEGAWA, K. 2004. Characterization of end4+, a gene required for endocytosis in Schizosaccharomyces pombe. *Yeast,* 21**,** 867-81.

JANKE, C. & BULINSKI, J. C. 2011. Post-translational regulation of the microtubule cytoskeleton: mechanisms and functions. *Nat Rev Mol Cell Biol,* 12**,** 773-86.

JANSON, M. E., LOUGHLIN, R., LOIODICE, I., FU, C., BRUNNER, D., NEDELEC, F. J. & TRAN, P. T. 2007. Crosslinkers and motors organize dynamic microtubules to form stable bipolar arrays in fission yeast. *Cell,* 128**,** 357-68.

JANSON, M. E., SETTY, T. G., PAOLETTI, A. & TRAN, P. T. 2005. Efficient formation of bipolar microtubule bundles requires microtubule-bound gamma-tubulin complexes. *J Cell Biol,* 169**,** 297-308.

JASPERSEN, S. L. & GHOSH, S. 2012. Nuclear envelope insertion of spindle pole bodies and nuclear pore complexes. *Nucleus,* 3**,** 226-36.

JASPERSEN, S. L. & WINEY, M. 2004. The budding yeast spindle pole body: structure, duplication, and function. *Annu Rev Cell Dev Biol,* 20**,** 1-28.

JEONG, J. W., RHEE, D. K., CHO, S. Y., HAE, K. L., KIM, D. U., WON, M. & KIM, H. B. 2002. Cloning and characterization of the kinesin-related protein, Krp1p, in Schizosaccharomyces pombe. *Mol Cells,* 13**,** 389-98.

JI, J. Y., LEE, R. T., VERGNES, L., FONG, L. G., STEWART, C. L., REUE, K., YOUNG, S. G., ZHANG, Q., SHANAHAN, C. M. & LAMMERDING, J. 2007. Cell nuclei spin in the absence of lamin b1. *J Biol Chem,* 282**,** 20015-26.

JOURDAIN, L., CURMI, P., SOBEL, A., PANTALONI, D. & CARLIER, M. F. 1997. Stathmin: a tubulin-sequestering protein which forms a ternary T2S complex with two tubulin molecules. *Biochemistry,* 36**,** 10817-21.

KABSCH, W. & VANDEKERCKHOVE, J. 1992. Structure and function of actin. *Annu Rev Biophys Biomol Struct,* 21**,** 49-76.

KAKSONEN, M., SUN, Y. & DRUBIN, D. G. 2003. A pathway for association of receptors, adaptors, and actin during endocytic internalization. *Cell,* 115**,** 475-87.

KAKSONEN, M., TORET, C. P. & DRUBIN, D. G. 2006. Harnessing actin dynamics for clathrin-mediated endocytosis. *Nat Rev Mol Cell Biol,* 7**,** 404-14.

KARABAY, A. & WALKER, R. A. 1999. Identification of microtubule binding sites in the Ncd tail domain. *Biochemistry,* 38**,** 1838-49.

KARDON, J. R., RECK-PETERSON, S. L. & VALE, R. D. 2009. Regulation of the processivity and intracellular localization of Saccharomyces cerevisiae dynein by dynactin. *Proc Natl Acad Sci U S A,* 106**,** 5669-74.

KARDON, J. R. & VALE, R. D. 2009. Regulators of the cytoplasmic dynein motor. *Nat Rev Mol Cell Biol,* 10**,** 854-65.

KASEDA, K., HIGUCHI, H. & HIROSE, K. 2003. Alternate fast and slow stepping of a heterodimeric kinesin molecule. *Nat Cell Biol,* 5**,** 1079-82.

KAWAMURA, E. & WASTENEYS, G. O. 2008. MOR1, the Arabidopsis thaliana homologue of Xenopus MAP215, promotes rapid growth and shrinkage, and suppresses the pausing of microtubules in vivo. *J Cell Sci,* 121**,** 4114-23.

KIKKAWA, M., ISHIKAWA, T., NAKATA, T., WAKABAYASHI, T. & HIROKAWA, N. 1994. Direct visualization of the microtubule lattice seam both in vitro and in vivo. *J Cell Biol,* 127**,** 1965-71.

KING, S. J. & SCHROER, T. A. 2000. Dynactin increases the processivity of the cytoplasmic dynein motor. *Nat Cell Biol,* 2**,** 20-4.

KINOSHITA, K., NOETZEL, T. L., ARNAL, I., DRECHSEL, D. N. & HYMAN, A. A. 2006. Global and local control of microtubule destabilization promoted by a catastrophe kinesin MCAK/XKCM1. *J Muscle Res Cell Motil,* 27**,** 107-14.

KNOP, M. & SCHIEBEL, E. 1997. Spc98p and Spc97p of the yeast gamma-tubulin complex mediate binding to the spindle pole body via their interaction with Spc110p. *EMBO J,* 16**,** 6985-95.

KOLLMAN, J. M., MERDES, A., MOUREY, L. & AGARD, D. A. 2011. Microtubule nucleation by gamma-tubulin complexes. *Nat Rev Mol Cell Biol,* 12**,** 709-21.

KOLLMAN, J. M., POLKA, J. K., ZELTER, A., DAVIS, T. N. & AGARD, D. A. 2010. Microtubule nucleating gamma-TuSC assembles structures with 13-fold microtubule-like symmetry. *Nature,* 466**,** 879-82.

KOLLMAN, J. M., ZELTER, A., MULLER, E. G., FOX, B., RICE, L. M., DAVIS, T. N. & AGARD, D. A. 2008. The structure of the gamma-tubulin small complex: implications of its architecture and flexibility for microtubule nucleation. *Mol Biol Cell,* 19**,** 207-15.

KON, T., IMAMULA, K., ROBERTS, A. J., OHKURA, R., KNIGHT, P. J., GIBBONS, I. R., BURGESS, S. A. & SUTOH, K. 2009. Helix sliding in the stalk coiled coil of dynein couples ATPase and microtubule binding. *Nat Struct Mol Biol,* 16**,** 325-33.

KORINEK, W. S., COPELAND, M. J., CHAUDHURI, A. & CHANT, J. 2000. Molecular linkage underlying microtubule orientation toward cortical sites in yeast. *Science,* 287**,** 2257-9.

KOVAR, D. R., SIROTKIN, V. & LORD, M. 2011. Three's company: the fission yeast actin cytoskeleton. *Trends Cell Biol,* 21**,** 177-87.

KOYANO, T., KUME, K., KONISHI, M., TODA, T. & HIRATA, D. 2010. Search for kinases related to transition of growth polarity in fission yeast. *Biosci Biotechnol Biochem,* 74**,** 1129-33.

KRENDEL, M. & MOOSEKER, M. S. 2005. Myosins: tails (and heads) of functional diversity. *Physiology (Bethesda),* 20**,** 239-51.

KUHN, S. & GEYER, M. 2014. Formins as effector proteins of Rho GTPases. *Small GTPases,* 5.

KURIYAMA, R. & BORISY, G. G. 1981. Centriole cycle in Chinese hamster ovary cells as determined by whole-mount electron microscopy. *J Cell Biol,* 91**,** 814-21.

LAAN, L., PAVIN, N., HUSSON, J., ROMET-LEMONNE, G., VAN DUIJN, M., LOPEZ, M. P., VALE, R. D., JULICHER, F., RECK-PETERSON, S. L. & DOGTEROM, M. 2012. Cortical dynein controls microtubule dynamics to generate pulling forces that position microtubule asters. *Cell,* 148**,** 502-14.

LAMBERT DE ROUVROIT, C. & GOFFINET, A. M. 2001. Neuronal migration. *Mech Dev,* 105**,** 47-56.

LAPPALAINEN, P. & DRUBIN, D. G. 1997. Cofilin promotes rapid actin filament turnover in vivo. *Nature,* 388**,** 78-82.

LAPPALAINEN, P., KESSELS, M. M., COPE, M. J. & DRUBIN, D. G. 1998. The ADF homology (ADF-H) domain: a highly exploited actin-binding module. *Mol Biol Cell,* 9**,** 1951-9.

LAWRENCE, C. J., DAWE, R. K., CHRISTIE, K. R., CLEVELAND, D. W., DAWSON, S. C., ENDOW, S. A., GOLDSTEIN, L. S., GOODSON, H. V., HIROKAWA, N., HOWARD, J., MALMBERG, R. L., MCINTOSH, J. R., MIKI, H., MITCHISON, T. J., OKADA, Y., REDDY, A. S., SAXTON, W. M., SCHLIWA, M., SCHOLEY, J. M., VALE, R. D., WALCZAK, C. E. & WORDEMAN, L. 2004. A standardized kinesin nomenclature. *J Cell Biol,* 167**,** 19-22.

LEE, K. K., STARR, D., COHEN, M., LIU, J., HAN, M., WILSON, K. L. & GRUENBAUM, Y. 2002. Lamin-dependent localization of UNC-84, a protein required for nuclear migration in Caenorhabditis elegans. *Mol Biol Cell,* 13**,** 892-901.

LEE, W. L., BEZANILLA, M. & POLLARD, T. D. 2000. Fission yeast myosin-I, Myo1p, stimulates actin assembly by Arp2/3 complex and shares functions with WASp. *J Cell Biol,* 151**,** 789-800.

LEE, W. L., OBERLE, J. R. & COOPER, J. A. 2003. The role of the lissencephaly protein Pac1 during nuclear migration in budding yeast. *J Cell Biol,* 160**,** 355-64.

LEFEVRE, J., CHERNOV, K. G., JOSHI, V., DELGA, S., TOMA, F., PASTRE, D., CURMI, P. A. & SAVARIN, P. 2011. The C terminus of tubulin, a versatile partner for cationic molecules: binding of Tau, polyamines, and calcium. *J Biol Chem,* 286**,** 3065-78.

LEWIS, S. A., WANG, D. H. & COWAN, N. J. 1988. Microtubule-associated protein MAP2 shares a microtubule binding motif with tau protein. *Science,* 242**,** 936-9.

LI, R. & GUNDERSEN, G. G. 2008. Beyond polymer polarity: how the cytoskeleton builds a polarized cell. *Nat Rev Mol Cell Biol,* 9**,** 860-73.

LI, Y., YU, W., LIANG, Y. & ZHU, X. 2007. Kinetochore dynein generates a poleward pulling force to facilitate congression and full chromosome alignment. *Cell Res,* 17**,** 701-12.

LOIODICE, I., STAUB, J., SETTY, T. G., NGUYEN, N. P., PAOLETTI, A. & TRAN, P. T. 2005. Ase1p organizes antiparallel microtubule arrays during interphase and mitosis in fission yeast. *Mol Biol Cell,* 16**,** 1756-68.

LU, J. & POLLARD, T. D. 2001. Profilin binding to poly-L-proline and actin monomers along with ability to catalyze actin nucleotide exchange is required for viability of fission yeast. *Mol Biol Cell,* 12**,** 1161-75.

LUDERS, J. & STEARNS, T. 2007. Microtubule-organizing centres: a re-evaluation. *Nat Rev Mol Cell Biol,* 8**,** 161-7.

LUTKENHAUS, J. 2007. Assembly dynamics of the bacterial MinCDE system and spatial regulation of the Z ring. *Annu Rev Biochem,* 76**,** 539-62.

LUXTON, G. W., GOMES, E. R., FOLKER, E. S., VINTINNER, E. & GUNDERSEN, G. G. 2010. Linear arrays of nuclear envelope proteins harness retrograde actin flow for nuclear movement. *Science,* 329**,** 956-9.

LUXTON, G. W. & GUNDERSEN, G. G. 2011. Orientation and function of the nuclear-centrosomal axis during cell migration. *Curr Opin Cell Biol,* 23**,** 579-88.

LYNCH, E. M., GROOCOCK, L. M., BOREK, W. E. & SAWIN, K. E. 2014. Activation of the gamma-tubulin complex by the Mto1/2 complex. *Curr Biol,* 24**,** 896-903.

MACHESKY, L. M., ATKINSON, S. J., AMPE, C., VANDEKERCKHOVE, J. & POLLARD, T. D. 1994. Purification of a cortical complex containing two unconventional actins from Acanthamoeba by affinity chromatography on profilin-agarose. *J Cell Biol,* 127**,** 107-15.

MACHESKY, L. M. & INSALL, R. H. 1998. Scar1 and the related Wiskott-Aldrich syndrome protein, WASP, regulate the actin cytoskeleton through the Arp2/3 complex. *Curr Biol,* 8**,** 1347-56.

MACHESKY, L. M., MULLINS, R. D., HIGGS, H. N., KAISER, D. A., BLANCHOIN, L., MAY, R. C., HALL, M. E. & POLLARD, T. D. 1999. Scar, a WASp-related protein, activates nucleation of actin filaments by the Arp2/3 complex. *Proc Natl Acad Sci U S A,* 96**,** 3739-44.

MADDOX, P. S., STEMPLE, J. K., SATTERWHITE, L., SALMON, E. D. & BLOOM, K. 2003. The minus end-directed motor Kar3 is required for coupling dynamic microtubule plus ends to the cortical shmoo tip in budding yeast. *Curr Biol,* 13**,** 1423-8.

MALONE, C. J., FIXSEN, W. D., HORVITZ, H. R. & HAN, M. 1999. UNC-84 localizes to the nuclear envelope and is required for nuclear migration and anchoring during C. elegans development. *Development,* 126**,** 3171-81.

MALONE, C. J., MISNER, L., LE BOT, N., TSAI, M. C., CAMPBELL, J. M., AHRINGER, J. & WHITE, J. G. 2003. The C. elegans hook protein, ZYG-12, mediates the essential attachment between the centrosome and nucleus. *Cell,* 115**,** 825-36.

MANA-CAPELLI, S., MCLEAN, J. R., CHEN, C. T., GOULD, K. L. & MCCOLLUM, D. 2012. The kinesin-14 Klp2 is negatively regulated by the SIN for proper spindle elongation and telophase nuclear positioning. *Mol Biol Cell,* 23**,** 4592-600.

MANDELKOW, E. M., SCHULTHEISS, R., RAPP, R., MULLER, M. & MANDELKOW, E. 1986. On the surface lattice of microtubules: helix starts, protofilament number, seam, and handedness. *J Cell Biol,* 102**,** 1067-73.

MARCO, E., WEDLICH-SOLDNER, R., LI, R., ALTSCHULER, S. J. & WU, L. F. 2007. Endocytosis optimizes the dynamic localization of membrane proteins that regulate cortical polarity. *Cell,* 129**,** 411-22.

MARTIN, S. G., MCDONALD, W. H., YATES, J. R., 3RD & CHANG, F. 2005. Tea4p links microtubule plus ends with the formin for3p in the establishment of cell polarity. *Dev Cell,* 8**,** 479-91.

MARTIN, S. G., RINCON, S. A., BASU, R., PEREZ, P. & CHANG, F. 2007. Regulation of the formin for3p by cdc42p and bud6p. *Mol Biol Cell,* 18**,** 4155-67.

MARX, A., MULLER, J. & MANDELKOW, E. 2005. The structure of microtubule motor proteins. *Adv Protein Chem,* 71**,** 299-344.

MATA, J. & NURSE, P. 1997. tea1 and the microtubular cytoskeleton are important for generating global spatial order within the fission yeast cell. *Cell,* 89**,** 939-49.

MATULIENE, J., ESSNER, R., RYU, J., HAMAGUCHI, Y., BAAS, P. W., HARAGUCHI, T., HIRAOKA, Y. & KURIYAMA, R. 1999. Function of a minus-end-directed kinesin-like motor protein in mammalian cells. *J Cell Sci,* 112 (Pt 22)**,** 4041-50.

MAZUMDAR, A. & MAZUMDAR, M. 2002. How one becomes many: blastoderm cellularization in Drosophila melanogaster. *Bioessays,* 24**,** 1012-22.

MCGEE, M. D., RILLO, R., ANDERSON, A. S. & STARR, D. A. 2006. UNC-83 IS a KASH protein required for nuclear migration and is recruited to the outer nuclear membrane by a physical interaction with the SUN protein UNC-84. *Mol Biol Cell,* 17**,** 1790-801.

MELUH, P. B. & ROSE, M. D. 1990. KAR3, a kinesin-related gene required for yeast nuclear fusion. *Cell,* 60**,** 1029-41.

MESNGON, M. T., TARRICONE, C., HEBBAR, S., GUILLOTTE, A. M., SCHMITT, E. W., LANIER, L., MUSACCHIO, A., KING, S. J. & SMITH, D. S. 2006. Regulation of cytoplasmic dynein ATPase by Lis1. *J Neurosci,* 26**,** 2132-9.

METTLEN, M., PUCADYIL, T., RAMACHANDRAN, R. & SCHMID, S. L. 2009. Dissecting dynamin's role in clathrin-mediated endocytosis. *Biochem Soc Trans,* 37**,** 1022-6.

METZGER, T., GACHE, V., XU, M., CADOT, B., FOLKER, E. S., RICHARDSON, B. E., GOMES, E. R. & BAYLIES, M. K. 2012. MAP and kinesin-dependent nuclear positioning is required for skeletal muscle function. *Nature,* 484**,** 120-4.

MIKI, H., SETOU, M., KANESHIRO, K. & HIROKAWA, N. 2001. All kinesin superfamily protein, KIF, genes in mouse and human. *Proc Natl Acad Sci U S A,* 98**,** 7004-11.

MILLER, R. K., MATHEOS, D. & ROSE, M. D. 1999. The cortical localization of the microtubule orientation protein, Kar9p, is dependent upon actin and proteins required for polarization. *J Cell Biol,* 144**,** 963-75.

MILLER, R. K. & ROSE, M. D. 1998. Kar9p is a novel cortical protein required for cytoplasmic microtubule orientation in yeast. *J Cell Biol,* 140**,** 377-90.

MIMORI-KIYOSUE, Y., GRIGORIEV, I., SASAKI, H., MATSUI, C., AKHMANOVA, A., TSUKITA, S. & VOROBJEV, I. 2006. Mammalian CLASPs are required for mitotic spindle organization and kinetochore alignment. *Genes Cells,* 11**,** 845-57.

MIMORI-KIYOSUE, Y., SHIINA, N. & TSUKITA, S. 2000. The dynamic behavior of the APC-binding protein EB1 on the distal ends of microtubules. *Curr Biol,* 10**,** 865-8.

MINC, N., BOUDAOUD, A. & CHANG, F. 2009a. Mechanical forces of fission yeast growth. *Curr Biol,* 19**,** 1096-101.

MINC, N., BRATMAN, S. V., BASU, R. & CHANG, F. 2009b. Establishing new sites of polarization by microtubules. *Curr Biol,* 19**,** 83-94.

MINC, N. & CHANG, F. 2010. Electrical control of cell polarization in the fission yeast Schizosaccharomyces pombe. *Curr Biol,* 20**,** 710-6.

MISCHE, S., HE, Y., MA, L., LI, M., SERR, M. & HAYS, T. S. 2008. Dynein light intermediate chain: an essential subunit that contributes to spindle checkpoint inactivation. *Mol Biol Cell,* 19**,** 4918-29.

MISHRA, M., HUANG, J. & BALASUBRAMANIAN, M. K. 2014. The yeast actin cytoskeleton. *FEMS Microbiol Rev,* 38**,** 213-27.

MITCHISON, J. M. & NURSE, P. 1985. Growth in cell length in the fission yeast Schizosaccharomyces pombe. *J Cell Sci,* 75**,** 357-76.

MITCHISON, T. & KIRSCHNER, M. 1984. Dynamic instability of microtubule growth. *Nature,* 312**,** 237-42.

MITCHISON, T. J. 1993. Localization of an exchangeable GTP binding site at the plus end of microtubules. *Science,* 261**,** 1044-7.

MOCKRIN, S. C. & KORN, E. D. 1980. Acanthamoeba profilin interacts with G-actin to increase the rate of exchange of actin-bound adenosine 5'-triphosphate. *Biochemistry,* 19**,** 5359-62.

MOLK, J. N. & BLOOM, K. 2006. Microtubule dynamics in the budding yeast mating pathway. *J Cell Sci,* 119**,** 3485-90.

MOLK, J. N., SALMON, E. D. & BLOOM, K. 2006. Nuclear congression is driven by cytoplasmic microtubule plus end interactions in S. cerevisiae. *J Cell Biol,* 172**,** 27-39.

MORITZ, M., BRAUNFELD, M. B., GUENEBAUT, V., HEUSER, J. & AGARD, D. A. 2000. Structure of the gamma-tubulin ring complex: a template for microtubule nucleation. *Nat Cell Biol,* 2**,** 365-70.

MORITZ, M., BRAUNFELD, M. B., SEDAT, J. W., ALBERTS, B. & AGARD, D. A. 1995. Microtubule nucleation by gamma-tubulin-containing rings in the centrosome. *Nature,* 378**,** 638-40.

MOSELEY, J. B. & GOODE, B. L. 2006. The yeast actin cytoskeleton: from cellular function to biochemical mechanism. *Microbiol Mol Biol Rev,* 70**,** 605-45.

MOSELEY, J. B., MAYEUX, A., PAOLETTI, A. & NURSE, P. 2009. A spatial gradient coordinates cell size and mitotic entry in fission yeast. *Nature,* 459**,** 857-60.

MOTEGI, F., ARAI, R. & MABUCHI, I. 2001. Identification of two type V myosins in fission yeast, one of which functions in polarized cell growth and moves rapidly in the cell. *Mol Biol Cell,* 12**,** 1367-80.

MUKHERJEE, S., DIAZ VALENCIA, J. D., STEWMAN, S., METZ, J., MONNIER, S., RATH, U., ASENJO, A. B., CHARAFEDDINE, R. A., SOSA, H. J., ROSS, J. L., MA, A. & SHARP, D. J. 2012. Human Fidgetin is a microtubule severing the enzyme and minus-end depolymerase that regulates mitosis. *Cell Cycle,* 11**,** 2359-66.

NAKANO, K., TOYA, M., YONEDA, A., ASAMI, Y., YAMASHITA, A., KAMASAWA, N., OSUMI, M. & YAMAMOTO, M. 2011. Pob1 ensures cylindrical cell shape by coupling two distinct rho signaling events during secretory vesicle targeting. *Traffic,* 12**,** 726-39.

NARASIMHULU, S. B. & REDDY, A. S. 1998. Characterization of microtubule binding domains in the Arabidopsis kinesin-like calmodulin binding protein. *Plant Cell,* 10**,** 957-65.

NELSON, W. J. 2003. Adaptation of core mechanisms to generate cell polarity. *Nature,* 422**,** 766-74.

NEUWALD, A. F., ARAVIND, L., SPOUGE, J. L. & KOONIN, E. V. 1999. AAA+: A class of chaperone-like ATPases associated with the assembly, operation, and disassembly of protein complexes. *Genome Res,* 9**,** 27-43.

NGUYEN-NGOC, T., AFSHAR, K. & GONCZY, P. 2007. Coupling of cortical dynein and G alpha proteins mediates spindle positioning in Caenorhabditis elegans. *Nat Cell Biol,* 9**,** 1294-302.

NICCOLI, T., YAMASHITA, A., NURSE, P. & YAMAMOTO, M. 2004. The p150-Glued Ssm4p regulates microtubular dynamics and nuclear movement in fission yeast. *J Cell Sci,* 117**,** 5543-56.

NOGALES, E. & WANG, H. W. 2006. Structural mechanisms underlying nucleotide-dependent self-assembly of tubulin and its relatives. *Curr Opin Struct Biol,* 16**,** 221-9.

NOGALES, E., WHITTAKER, M., MILLIGAN, R. A. & DOWNING, K. H. 1999. High-resolution model of the microtubule. *Cell,* 96**,** 79-88.

NOGALES, E., WOLF, S. G. & DOWNING, K. H. 1998. Structure of the alpha beta tubulin dimer by electron crystallography. *Nature,* 391**,** 199-203.

NURNBERG, A., KITZING, T. & GROSSE, R. 2011. Nucleating actin for invasion. *Nat Rev Cancer,* 11**,** 177-87.

OAKLEY, C. E. & OAKLEY, B. R. 1989. Identification of gamma-tubulin, a new member of the tubulin superfamily encoded by mipA gene of Aspergillus nidulans. *Nature,* 338**,** 662-4.

OGURA, T. & WILKINSON, A. J. 2001. AAA+ superfamily ATPases: common structure--diverse function. *Genes Cells,* 6**,** 575-97.

OHTA, M., SATO, M. & YAMAMOTO, M. 2012. Spindle pole body components are reorganized during fission yeast meiosis. *Mol Biol Cell,* 23**,** 1799-811.

OHTAKA, A., SAITO, T. T., OKUZAKI, D. & NOJIMA, H. 2007. Meiosis specific coiled-coil proteins in Shizosaccharomyces pombe. *Cell Div,* 2**,** 14.

OKADA, Y. & HIROKAWA, N. 2000. Mechanism of the single-headed processivity: diffusional anchoring between the K-loop of kinesin and the C terminus of tubulin. *Proc Natl Acad Sci U S A,* 97**,** 640-5.

OLADIPO, A., COWAN, A. & RODIONOV, V. 2007. Microtubule motor Ncd induces sliding of microtubules in vivo. *Mol Biol Cell,* 18**,** 3601-6.

OLMSTED, Z. T., RIEHLMAN, T. D., BRANCA, C. N., COLLIVER, A. G., CRUZ, L. O. & PALUH, J. L. 2013. Kinesin-14 Pkl1 targets gamma-tubulin for release from the gamma-tubulin ring complex (gamma-TuRC). *Cell Cycle,* 12**,** 842-8.

OTTILIE, S., MILLER, P. J., JOHNSON, D. I., CREASY, C. L., SELLS, M. A., BAGRODIA, S., FORSBURG, S. L. & CHERNOFF, J. 1995. Fission yeast pak1+ encodes a protein kinase that interacts with Cdc42p and is involved in the control of cell polarity and mating. *EMBO J,* 14**,** 5908-19.

PAINTRAND, M., MOUDJOU, M., DELACROIX, H. & BORNENS, M. 1992. Centrosome organization and centriole architecture: their sensitivity to divalent cations. *J Struct Biol,* 108**,** 107-28.

PALMER, R. E., SULLIVAN, D. S., HUFFAKER, T. & KOSHLAND, D. 1992. Role of astral microtubules and actin in spindle orientation and migration in the budding yeast, Saccharomyces cerevisiae. *J Cell Biol,* 119**,** 583-93.

PARNAIK, V. K. 2008. Role of nuclear lamins in nuclear organization, cellular signaling, and inherited diseases. *Int Rev Cell Mol Biol,* 266**,** 157-206.

PASCHAL, B. M., SHPETNER, H. S. & VALLEE, R. B. 1987. MAP 1C is a microtubule-activated ATPase which translocates microtubules in vitro and has dynein-like properties. *J Cell Biol,* 105**,** 1273-82.

PEARSON, C. G. & BLOOM, K. 2004. Dynamic microtubules lead the way for spindle positioning. *Nat Rev Mol Cell Biol,* 5**,** 481-92.

PELHAM, R. J., JR. & CHANG, F. 2001. Role of actin polymerization and actin cables in actin-patch movement in Schizosaccharomyces pombe. *Nat Cell Biol,* 3**,** 235-44.

PENG, J., WALLAR, B. J., FLANDERS, A., SWIATEK, P. J. & ALBERTS, A. S. 2003. Disruption of the Diaphanous-related formin Drf1 gene encoding mDia1 reveals a role for Drf3 as an effector for Cdc42. *Curr Biol,* 13**,** 534-45.

PEREZ, F., DIAMANTOPOULOS, G. S., STALDER, R. & KREIS, T. E. 1999. CLIP-170 highlights growing microtubule ends in vivo. *Cell,* 96**,** 517-27.

PEREZ, P. & RINCON, S. A. 2010. Rho GTPases: regulation of cell polarity and growth in yeasts. *Biochem J,* 426**,** 243-53.

PERIS, L., THERY, M., FAURE, J., SAOUDI, Y., LAFANECHERE, L., CHILTON, J. K., GORDON-WEEKS, P., GALJART, N., BORNENS, M., WORDEMAN, L., WEHLAND, J., ANDRIEUX, A. & JOB, D. 2006. Tubulin tyrosination is a major factor affecting the recruitment of CAP-Gly proteins at microtubule plus ends. *J Cell Biol,* 174**,** 839-49.

PIEL, M., MEYER, P., KHODJAKOV, A., RIEDER, C. L. & BORNENS, M. 2000. The respective contributions of the mother and daughter centrioles to centrosome activity and behavior in vertebrate cells. *J Cell Biol,* 149**,** 317-30.

POLAKOVA, S., BENKO, Z., ZHANG, L. & GREGAN, J. 2014. Mal3, the Schizosaccharomyces pombe homolog of EB1, is required for karyogamy and for promoting oscillatory nuclear movement during meiosis. *Cell Cycle,* 13**,** 72-7.

POLLARD, T. D. 2007. Regulation of actin filament assembly by Arp2/3 complex and formins. *Annu Rev Biophys Biomol Struct,* 36**,** 451-77.

POLLARD, T. D., BLANCHOIN, L. & MULLINS, R. D. 2000. Molecular mechanisms controlling actin filament dynamics in nonmuscle cells. *Annu Rev Biophys Biomol Struct,* 29**,** 545-76.

POLLARD, T. D. & BORISY, G. G. 2003. Cellular motility driven by assembly and disassembly of actin filaments. *Cell,* 112**,** 453-65.

POLLARD, T. D. & COOPER, J. A. 2009. Actin, a central player in cell shape and movement. *Science,* 326**,** 1208-12.

PORAT-SHLIOM, N., MILBERG, O., MASEDUNSKAS, A. & WEIGERT, R. 2013. Multiple roles for the actin cytoskeleton during regulated exocytosis. *Cell Mol Life Sci,* 70**,** 2099-121.

PROCTOR, S. A., MINC, N., BOUDAOUD, A. & CHANG, F. 2012. Contributions of turgor pressure, the contractile ring, and septum assembly to forces in cytokinesis in fission yeast. *Curr Biol,* 22**,** 1601-8.

PRUYNE, D., EVANGELISTA, M., YANG, C., BI, E., ZIGMOND, S., BRETSCHER, A. & BOONE, C. 2002. Role of formins in actin assembly: nucleation and barbed-end association. *Science,* 297**,** 612-5.

PRUYNE, D., LEGESSE-MILLER, A., GAO, L., DONG, Y. & BRETSCHER, A. 2004. Mechanisms of polarized growth and organelle segregation in yeast. *Annu Rev Cell Dev Biol,* 20**,** 559-91.

PUCKELWARTZ, M. J., KESSLER, E., ZHANG, Y., HODZIC, D., RANDLES, K. N., MORRIS, G., EARLEY, J. U., HADHAZY, M., HOLASKA, J. M., MEWBORN, S. K., PYTEL, P. & MCNALLY, E. M. 2009. Disruption of nesprin-1 produces an Emery Dreifuss muscular dystrophy-like phenotype in mice. *Hum Mol Genet,* 18**,** 607-20.

PUROHIT, A., TYNAN, S. H., VALLEE, R. & DOXSEY, S. J. 1999. Direct interaction of pericentrin with cytoplasmic dynein light intermediate chain contributes to mitotic spindle organization. *J Cell Biol,* 147**,** 481-92.

RALSTON, E., LU, Z., BISCOCHO, N., SOUMAKA, E., MAVROIDIS, M., PRATS, C., LOMO, T., CAPETANAKI, Y. & PLOUG, T. 2006. Blood vessels and desmin control the positioning of nuclei in skeletal muscle fibers. *J Cell Physiol,* 209**,** 874-82.

RAZAFSKY, D. & HODZIC, D. 2009. Bringing KASH under the SUN: the many faces of nucleo-cytoskeletal connections. *J Cell Biol,* 186**,** 461-72.

RAZAFSKY, D., ZANG, S. & HODZIC, D. 2011. UnLINCing the nuclear envelope: towards an understanding of the physiological significance of nuclear positioning. *Biochem Soc Trans,* 39**,** 1790-4.

RECK-PETERSON, S. L. & VALE, R. D. 2004. Molecular dissection of the roles of nucleotide binding and hydrolysis in dynein's AAA domains in Saccharomyces cerevisiae. *Proc Natl Acad Sci U S A,* 101**,** 1491-5.

RECK-PETERSON, S. L., YILDIZ, A., CARTER, A. P., GENNERICH, A., ZHANG, N. & VALE, R. D. 2006. Single-molecule analysis of dynein processivity and stepping behavior. *Cell,* 126**,** 335-48.

REINSCH, S. & GONCZY, P. 1998. Mechanisms of nuclear positioning. *J Cell Sci,* 111 (Pt 16)**,** 2283-95.

REINSCH, S. & KARSENTI, E. 1997. Movement of nuclei along microtubules in Xenopus egg extracts. *Curr Biol,* 7**,** 211-4.

RHEE, D. K., CHO, B. A. & KIM, H. B. 2005. ATP-binding motifs play key roles in Krp1p, kinesin-related protein 1, function for bi-polar growth control in fission yeast. *Biochem Biophys Res Commun,* 331**,** 658-68.

RICE, S., LIN, A. W., SAFER, D., HART, C. L., NABER, N., CARRAGHER, B. O., CAIN, S. M., PECHATNIKOVA, E., WILSON-KUBALEK, E. M., WHITTAKER, M., PATE, E., COOKE, R., TAYLOR, E. W., MILLIGAN, R. A. & VALE, R. D. 1999. A structural change in the kinesin motor protein that drives motility. *Nature,* 402**,** 778-84.

RIDLEY, A. J. 2006. Rho GTPases and actin dynamics in membrane protrusions and vesicle trafficking. *Trends Cell Biol,* 16**,** 522-9.

RINCON, S. A., ESTRAVIS, M. & PEREZ, P. 2014. Cdc42 regulates polarized growth and cell integrity in fission yeast. *Biochem Soc Trans,* 42**,** 201-5.

RINCON, S. A., SANTOS, B. & PEREZ, P. 2006. Fission yeast Rho5p GTPase is a functional paralogue of Rho1p that plays a role in survival of spores and stationary-phase cells. *Eukaryot Cell,* 5**,** 435-46.

RINCON, S. A., YE, Y., VILLAR-TAJADURA, M. A., SANTOS, B., MARTIN, S. G. & PEREZ, P. 2009. Pob1 participates in the Cdc42 regulation of fission yeast actin cytoskeleton. *Mol Biol Cell,* 20**,** 4390-9.

ROBINSON, D. N. & COOLEY, L. 1997. Genetic analysis of the actin cytoskeleton in the Drosophila ovary. *Annu Rev Cell Dev Biol,* 13**,** 147-70.

RODIONOV, V. I., GYOEVA, F. K., KASHINA, A. S., KUZNETSOV, S. A. & GELFAND, V. I. 1990. Microtubule-associated proteins and microtubule-based translocators have different binding sites on tubulin molecule. *J Biol Chem,* 265**,** 5702-7.

RODRIGUEZ, A. S., BATAC, J., KILLILEA, A. N., FILOPEI, J., SIMEONOV, D. R., LIN, I. & PALUH, J. L. 2008. Protein complexes at the microtubule organizing center regulate bipolar spindle assembly. *Cell Cycle,* 7**,** 1246-53.

ROHATGI, R., MA, L., MIKI, H., LOPEZ, M., KIRCHHAUSEN, T., TAKENAWA, T. & KIRSCHNER, M. W. 1999. The interaction between N-WASP and the Arp2/3 complex links Cdc42-dependent signals to actin assembly. *Cell,* 97**,** 221-31.

ROLL-MECAK, A. & MCNALLY, F. J. 2010. Microtubule-severing enzymes. *Curr Opin Cell Biol,* 22**,** 96-103.

ROLL-MECAK, A. & VALE, R. D. 2008. Structural basis of microtubule severing by the hereditary spastic paraplegia protein spastin. *Nature,* 451**,** 363-7.

ROMERO, S., LE CLAINCHE, C., DIDRY, D., EGILE, C., PANTALONI, D. & CARLIER, M. F. 2004. Formin is a processive motor that requires profilin to accelerate actin assembly and associated ATP hydrolysis. *Cell,* 119**,** 419-29.

ROSE, M. D. 1996. Nuclear fusion in the yeast Saccharomyces cerevisiae. *Annu Rev Cell Dev Biol,* 12**,** 663-95.

SABLIN, E. P. 2000. Kinesins and microtubules: their structures and motor mechanisms. *Curr Opin Cell Biol,* 12**,** 35-41.

SABLIN, E. P., CASE, R. B., DAI, S. C., HART, C. L., RUBY, A., VALE, R. D. & FLETTERICK, R. J. 1998. Direction determination in the minus-end-directed kinesin motor ncd. *Nature,* 395**,** 813-6.

SAITO, T. T., OKUZAKI, D. & NOJIMA, H. 2006. Mcp5, a meiotic cell cortex protein, is required for nuclear movement mediated by dynein and microtubules in fission yeast. *J Cell Biol,* 173**,** 27-33.

SAITO, T. T., TOUGAN, T., OKUZAKI, D., KASAMA, T. & NOJIMA, H. 2005. Mcp6, a meiosis-specific coiled-coil protein of Schizosaccharomyces pombe, localizes to the spindle pole body and is required for horsetail movement and recombination. *J Cell Sci,* 118**,** 447-59.

SAKAKIBARA, H. & OIWA, K. 2011. Molecular organization and force-generating mechanism of dynein. *FEBS J,* 278**,** 2964-79.

SALBREUX, G., CHARRAS, G. & PALUCH, E. 2012. Actin cortex mechanics and cellular morphogenesis. *Trends Cell Biol,* 22**,** 536-45.

SAMSO, M., RADERMACHER, M., FRANK, J. & KOONCE, M. P. 1998. Structural characterization of a dynein motor domain. *J Mol Biol,* 276**,** 927-37.

SAWIN, K. E., LOURENCO, P. C. & SNAITH, H. A. 2004. Microtubule nucleation at non-spindle pole body microtubule-organizing centers requires fission yeast centrosomin-related protein mod20p. *Curr Biol,* 14**,** 763-75.

SAWIN, K. E. & SNAITH, H. A. 2004. Role of microtubules and tea1p in establishment and maintenance of fission yeast cell polarity. *J Cell Sci,* 117**,** 689-700.

SAWIN, K. E. & TRAN, P. T. 2006. Cytoplasmic microtubule organization in fission yeast. *Yeast,* 23**,** 1001-14.

SCHLIWA, M. & WOEHLKE, G. 2003. Molecular motors. *Nature,* 422**,** 759-65.

SCHMORANZER, J., FAWCETT, J. P., SEGURA, M., TAN, S., VALLEE, R. B., PAWSON, T. & GUNDERSEN, G. G. 2009. Par3 and dynein associate to regulate local microtubule dynamics and centrosome orientation during migration. *Curr Biol,* 19**,** 1065-74.

SCHNEIDER, M., LU, W., NEUMANN, S., BRACHNER, A., GOTZMANN, J., NOEGEL, A. A. & KARAKESISOGLOU, I. 2011. Molecular mechanisms of centrosome and cytoskeleton anchorage at the nuclear envelope. *Cell Mol Life Sci,* 68**,** 1593-610.

SCHNITZER, M. J. & BLOCK, S. M. 1997. Kinesin hydrolyses one ATP per 8-nm step. *Nature,* 388**,** 386-90.

SCHROER, T. A. & SHEETZ, M. P. 1991. Two activators of microtubule-based vesicle transport. *J Cell Biol,* 115**,** 1309-18.

SCHUYLER, S. C., LIU, J. Y. & PELLMAN, D. 2003. The molecular function of Ase1p: evidence for a MAP-dependent midzone-specific spindle matrix. Microtubule-associated proteins. *J Cell Biol,* 160**,** 517-28.

SELVE, N. & WEGNER, A. 1986. Rate of treadmilling of actin filaments in vitro. *J Mol Biol,* 187**,** 627-31.

SHAW, B. D., CHUNG, D. W., WANG, C. L., QUINTANILLA, L. A. & UPADHYAY, S. 2011. A role for endocytic recycling in hyphal growth. *Fungal Biol,* 115**,** 541-6.

SHIMA, T., IMAMULA, K., KON, T., OHKURA, R. & SUTOH, K. 2006. Head-head coordination is required for the processive motion of cytoplasmic dynein, an AAA+ molecular motor. *J Struct Biol,* 156**,** 182-9.

SHU, T., AYALA, R., NGUYEN, M. D., XIE, Z., GLEESON, J. G. & TSAI, L. H. 2004. Ndel1 operates in a common pathway with LIS1 and cytoplasmic dynein to regulate cortical neuronal positioning. *Neuron,* 44**,** 263-77.

SIEGRIST, S. E. & DOE, C. Q. 2007. Microtubule-induced cortical cell polarity. *Genes Dev,* 21**,** 483-96.

SIPICZKI, M. 2007. Splitting of the fission yeast septum. *FEMS Yeast Res,* 7**,** 761-70.

SIROTKIN, V., BERRO, J., MACMILLAN, K., ZHAO, L. & POLLARD, T. D. 2010. Quantitative analysis of the mechanism of endocytic actin patch assembly and disassembly in fission yeast. *Mol Biol Cell,* 21**,** 2894-904.

SIVARAM, M. V., SAPORITA, J. A., FURGASON, M. L., BOETTCHER, A. J. & MUNSON, M. 2005. Dimerization of the exocyst protein Sec6p and its interaction with the t-SNARE Sec9p. *Biochemistry,* 44**,** 6302-11.

SNAITH, H. A., SAMEJIMA, I. & SAWIN, K. E. 2005. Multistep and multimode cortical anchoring of tea1p at cell tips in fission yeast. *EMBO J,* 24**,** 3690-9.

SONNINO, S. & PRINETTI, A. 2013. Membrane domains and the "lipid raft" concept. *Curr Med Chem,* 20**,** 4-21.

SPROUL, L. R., ANDERSON, D. J., MACKEY, A. T., SAUNDERS, W. S. & GILBERT, S. P. 2005. Cik1 targets the minus-end kinesin depolymerase kar3 to microtubule plus ends. *Curr Biol,* 15**,** 1420-7.

ST JOHNSTON, D. & AHRINGER, J. 2010. Cell polarity in eggs and epithelia: parallels and diversity. *Cell,* 141**,** 757-74.

STARR, D. A. 2007. Communication between the cytoskeleton and the nuclear envelope to position the nucleus. *Mol Biosyst,* 3**,** 583-9.

STARR, D. A. 2009. A nuclear-envelope bridge positions nuclei and moves chromosomes. *J Cell Sci,* 122**,** 577-86.

STARR, D. A. & FRIDOLFSSON, H. N. 2010. Interactions between nuclei and the cytoskeleton are mediated by SUN-KASH nuclear-envelope bridges. *Annu Rev Cell Dev Biol,* 26**,** 421-44.

STARR, D. A. & HAN, M. 2005. A genetic approach to study the role of nuclear envelope components in nuclear positioning. *Novartis Found Symp,* 264**,** 208-19; discussion 219-230.

STARR, D. A., HERMANN, G. J., MALONE, C. J., FIXSEN, W., PRIESS, J. R., HORVITZ, H. R. & HAN, M. 2001. unc-83 encodes a novel component of the nuclear envelope and is essential for proper nuclear migration. *Development,* 128**,** 5039-50.

STEINMETZ, M. O. 2007. Structure and thermodynamics of the tubulin-stathmin interaction. *J Struct Biol,* 158**,** 137-47.

STRADAL, T., KRANEWITTER, W., WINDER, S. J. & GIMONA, M. 1998. CH domains revisited. *FEBS Lett,* 431**,** 134-7.

STRADAL, T. E., ROTTNER, K., DISANZA, A., CONFALONIERI, S., INNOCENTI, M. & SCITA, G. 2004. Regulation of actin dynamics by WASP and WAVE family proteins. *Trends Cell Biol,* 14**,** 303-11.

STRAUB, F. B. & FEUER, G. 1989. Adenosinetriphosphate. The functional group of actin. 1950. *Biochim Biophys Acta,* 1000**,** 180-95.

STRELKOV, S. V., HERRMANN, H. & AEBI, U. 2003. Molecular architecture of intermediate filaments. *Bioessays,* 25**,** 243-51.

SUDHOF, T. C. & ROTHMAN, J. E. 2009. Membrane fusion: grappling with SNARE and SM proteins. *Science,* 323**,** 474-7.

SUN, H. Q., YAMAMOTO, M., MEJILLANO, M. & YIN, H. L. 1999. Gelsolin, a multifunctional actin regulatory protein. *J Biol Chem,* 274**,** 33179-82.

SVOBODA, K., SCHMIDT, C. F., SCHNAPP, B. J. & BLOCK, S. M. 1993. Direct observation of kinesin stepping by optical trapping interferometry. *Nature,* 365**,** 721-7.

TAHERI-TALESH, N., HORIO, T., ARAUJO-BAZAN, L., DOU, X., ESPESO, E. A., PENALVA, M. A., OSMANI, S. A. & OAKLEY, B. R. 2008. The tip growth apparatus of Aspergillus nidulans. *Mol Biol Cell,* 19**,** 1439-49.

TALLADA, V. A., TANAKA, K., YANAGIDA, M. & HAGAN, I. M. 2009. The S. pombe mitotic regulator Cut12 promotes spindle pole body activation and integration into the nuclear envelope. *J Cell Biol,* 185**,** 875-88.

TAN, S. C., SCHERER, J. & VALLEE, R. B. 2011. Recruitment of dynein to late endosomes and lysosomes through light intermediate chains. *Mol Biol Cell,* 22**,** 467-77.

TANAKA, K., KITAMURA, E., KITAMURA, Y. & TANAKA, T. U. 2007. Molecular mechanisms of microtubule-dependent kinetochore transport toward spindle poles. *J Cell Biol,* 178**,** 269-81.

TANAKA, K., KOHDA, T., YAMASHITA, A., NONAKA, N. & YAMAMOTO, M. 2005. Hrs1p/Mcp6p on the meiotic SPB organizes astral microtubule arrays for oscillatory nuclear movement. *Curr Biol,* 15**,** 1479-86.

TANAKA, T., SERNEO, F. F., HIGGINS, C., GAMBELLO, M. J., WYNSHAW-BORIS, A. & GLEESON, J. G. 2004. Lis1 and doublecortin function with dynein to mediate coupling of the nucleus to the centrosome in neuronal migration. *J Cell Biol,* 165**,** 709-21.

TAPLEY, E. C. & STARR, D. A. 2013. Connecting the nucleus to the cytoskeleton by SUN-KASH bridges across the nuclear envelope. *Curr Opin Cell Biol,* 25**,** 57-62.

TEIXIDO-TRAVESA, N., ROIG, J. & LUDERS, J. 2012. The where, when and how of microtubule nucleation - one ring to rule them all. *J Cell Sci,* 125**,** 4445-56.

TERENNA, C. R., MAKUSHOK, T., VELVE-CASQUILLAS, G., BAIGL, D., CHEN, Y., BORNENS, M., PAOLETTI, A., PIEL, M. & TRAN, P. T. 2008. Physical mechanisms redirecting cell polarity and cell shape in fission yeast. *Curr Biol,* 18**,** 1748-53.

TERRY, L. J., SHOWS, E. B. & WENTE, S. R. 2007. Crossing the nuclear envelope: hierarchical regulation of nucleocytoplasmic transport. *Science,* 318**,** 1412-6.

THADANI, R., HUANG, D. & OLIFERENKO, S. 2011. Robust polarity specification operates above a threshold of microtubule dynamicity. *Cytoskeleton (Hoboken),* 68**,** 290-9.

TIRNAUER, J. S., GREGO, S., SALMON, E. D. & MITCHISON, T. J. 2002. EB1-microtubule interactions in Xenopus egg extracts: role of EB1 in microtubule stabilization and mechanisms of targeting to microtubules. *Mol Biol Cell,* 13**,** 3614-26.

TISCHER, C., BRUNNER, D. & DOGTEROM, M. 2009. Force- and kinesin-8-dependent effects in the spatial regulation of fission yeast microtubule dynamics. *Mol Syst Biol,* 5**,** 250.

TOBA, S., WATANABE, T. M., YAMAGUCHI-OKIMOTO, L., TOYOSHIMA, Y. Y. & HIGUCHI, H. 2006. Overlapping hand-over-hand mechanism of single molecular motility of cytoplasmic dynein. *Proc Natl Acad Sci U S A,* 103**,** 5741-5.

TOYA, M., SATO, M., HASELMANN, U., ASAKAWA, K., BRUNNER, D., ANTONY, C. & TODA, T. 2007. Gamma-tubulin complex-mediated anchoring of spindle microtubules to spindle-pole bodies requires Msd1 in fission yeast. *Nat Cell Biol,* 9**,** 646-53.

TRAN, P. T., MADDOX, P., CHANG, F. & INOUE, S. 1999. Dynamic confocal imaging of interphase and mitotic microtubules in the fission yeast, S. pombe. *Biol Bull,* 197**,** 262-3.

TRAN, P. T., MARSH, L., DOYE, V., INOUE, S. & CHANG, F. 2001. A mechanism for nuclear positioning in fission yeast based on microtubule pushing. *J Cell Biol,* 153**,** 397-411.

TROXELL, C. L., SWEEZY, M. A., WEST, R. R., REED, K. D., CARSON, B. D., PIDOUX, A. L., CANDE, W. Z. & MCINTOSH, J. R. 2001. pkl1(+)and klp2(+): Two kinesins of the Kar3 subfamily in fission yeast perform different functions in both mitosis and meiosis. *Mol Biol Cell,* 12**,** 3476-88.

TSAI, J. W., BREMNER, K. H. & VALLEE, R. B. 2007. Dual subcellular roles for LIS1 and dynein in radial neuronal migration in live brain tissue. *Nat Neurosci,* 10**,** 970-9.

TSAI, J. W., LIAN, W. N., KEMAL, S., KRIEGSTEIN, A. R. & VALLEE, R. B. 2010. Kinesin 3 and cytoplasmic dynein mediate interkinetic nuclear migration in neural stem cells. *Nat Neurosci,* 13**,** 1463-71.

TYNAN, S. H., GEE, M. A. & VALLEE, R. B. 2000a. Distinct but overlapping sites within the cytoplasmic dynein heavy chain for dimerization and for intermediate chain and light intermediate chain binding. *J Biol Chem,* 275**,** 32769-74.

TYNAN, S. H., PUROHIT, A., DOXSEY, S. J. & VALLEE, R. B. 2000b. Light intermediate chain 1 defines a functional subfraction of cytoplasmic dynein which binds to pericentrin. *J Biol Chem,* 275**,** 32763-8.

VADUVA, G., MARTIN, N. C. & HOPPER, A. K. 1997. Actin-binding verprolin is a polarity development protein required for the morphogenesis and function of the yeast actin cytoskeleton. *J Cell Biol,* 139**,** 1821-33.

VAJJHALA, P. R., NGUYEN, C. H., LANDSBERG, M. J., KISTLER, C., GAN, A. L., KING, G. F., HANKAMER, B. & MUNN, A. L. 2008. The Vps4 C-terminal helix is a critical determinant for assembly and ATPase activity and has elements conserved in other members of the meiotic clade of AAA ATPases. *FEBS J,* 275**,** 1427-49.

VALDEZ-TAUBAS, J. & PELHAM, H. R. 2003. Slow diffusion of proteins in the yeast plasma membrane allows polarity to be maintained by endocytic cycling. *Curr Biol,* 13**,** 1636-40.

VALE, R. D. 2003. The molecular motor toolbox for intracellular transport. *Cell,* 112**,** 467-80.

VALE, R. D., FUNATSU, T., PIERCE, D. W., ROMBERG, L., HARADA, Y. & YANAGIDA, T. 1996. Direct observation of single kinesin molecules moving along microtubules. *Nature,* 380**,** 451-3.

VALLEE, R. B. & HOOK, P. 2003. Molecular motors: A magnificent machine. *Nature,* 421**,** 701-2.

VALLEE, R. B., MCKENNEY, R. J. & ORI-MCKENNEY, K. M. 2012. Multiple modes of cytoplasmic dynein regulation. *Nat Cell Biol,* 14**,** 224-30.

VAN DER VAART, B., AKHMANOVA, A. & STRAUBE, A. 2009. Regulation of microtubule dynamic instability. *Biochem Soc Trans,* 37**,** 1007-13.

VAUGHAN, K. T. & VALLEE, R. B. 1995. Cytoplasmic dynein binds dynactin through a direct interaction between the intermediate chains and p150Glued. *J Cell Biol,* 131**,** 1507-16.

VAUGHAN, P. S., MIURA, P., HENDERSON, M., BYRNE, B. & VAUGHAN, K. T. 2002. A role for regulated binding of p150(Glued) to microtubule plus ends in organelle transport. *J Cell Biol,* 158**,** 305-19.

VEITH, D., SCHERR, N., EFIMOV, V. P. & FISCHER, R. 2005. Role of the spindle-pole-body protein ApsB and the cortex protein ApsA in microtubule organization and nuclear migration in Aspergillus nidulans. *J Cell Sci,* 118**,** 3705-16.

VELVE-CASQUILLAS, G., LE BERRE, M., PIEL, M. & TRAN, P. T. 2010. Microfluidic tools for cell biological research. *Nano Today,* 5**,** 28-47.

VERDE, F., MATA, J. & NURSE, P. 1995. Fission yeast cell morphogenesis: identification of new genes and analysis of their role during the cell cycle. *J Cell Biol,* 131**,** 1529-38.

VOGEL, S. K., PAVIN, N., MAGHELLI, N., JULICHER, F. & TOLIC-NORRELYKKE, I. M. 2009. Self-organization of dynein motors generates meiotic nuclear oscillations. *PLoS Biol,* 7**,** e1000087.

WACHTLER, V. & BALASUBRAMANIAN, M. K. 2006. Yeast lipid rafts?--an emerging view. *Trends Cell Biol,* 16**,** 1-4.

WACHTLER, V., RAJAGOPALAN, S. & BALASUBRAMANIAN, M. K. 2003. Sterol-rich plasma membrane domains in the fission yeast Schizosaccharomyces pombe. *J Cell Sci,* 116**,** 867-74.

WALCZAK, C. E. & SHAW, S. L. 2010. A MAP for bundling microtubules. *Cell,* 142**,** 364-7.

WALKER, R. A., O'BRIEN, E. T., PRYER, N. K., SOBOEIRO, M. F., VOTER, W. A., ERICKSON, H. P. & SALMON, E. D. 1988. Dynamic instability of individual microtubules analyzed by video light microscopy: rate constants and transition frequencies. *J Cell Biol,* 107**,** 1437-48.

WANG, C. L. & COLUCCIO, L. M. 2010. New insights into the regulation of the actin cytoskeleton by tropomyosin. *Int Rev Cell Mol Biol,* 281**,** 91-128.

WANG, H., TANG, X., LIU, J., TRAUTMANN, S., BALASUNDARAM, D., MCCOLLUM, D. & BALASUBRAMANIAN, M. K. 2002. The multiprotein exocyst complex is essential for cell separation in Schizosaccharomyces pombe. *Mol Biol Cell,* 13**,** 515-29.

WEDLICH-SOLDNER, R., WAI, S. C., SCHMIDT, T. & LI, R. 2004. Robust cell polarity is a dynamic state established by coupling transport and GTPase signaling. *J Cell Biol,* 166**,** 889-900.

WEINBERG, J. & DRUBIN, D. G. 2012. Clathrin-mediated endocytosis in budding yeast. *Trends Cell Biol,* 22**,** 1-13.

WELCH, M. D. & MULLINS, R. D. 2002. Cellular control of actin nucleation. *Annu Rev Cell Dev Biol,* 18**,** 247-88.

WENDLER, P., CINIAWSKY, S., KOCK, M. & KUBE, S. 2012. Structure and function of the AAA+ nucleotide binding pocket. *Biochim Biophys Acta,* 1823**,** 2-14.

WENDT, T. G., VOLKMANN, N., SKINIOTIS, G., GOLDIE, K. N., MULLER, J., MANDELKOW, E. & HOENGER, A. 2002. Microscopic evidence for a minus-end-directed power stroke in the kinesin motor ncd. *EMBO J,* 21**,** 5969-78.

WEST, R. R., MALMSTROM, T., TROXELL, C. L. & MCINTOSH, J. R. 2001. Two related kinesins, klp5+ and klp6+, foster microtubule disassembly and are required for meiosis in fission yeast. *Mol Biol Cell,* 12**,** 3919-32.

WHITE, S. R. & LAURING, B. 2007. AAA+ ATPases: achieving diversity of function with conserved machinery. *Traffic,* 8**,** 1657-67.

WIESE, C. & ZHENG, Y. 2000. A new function for the gamma-tubulin ring complex as a microtubule minus-end cap. *Nat Cell Biol,* 2**,** 358-64.

WILLINS, D. A., LIU, B., XIANG, X. & MORRIS, N. R. 1997. Mutations in the heavy chain of cytoplasmic dynein suppress the nudF nuclear migration mutation of Aspergillus nidulans. *Mol Gen Genet,* 255**,** 194-200.

WILSON, M. H. & HOLZBAUR, E. L. 2012. Opposing microtubule motors drive robust nuclear dynamics in developing muscle cells. *J Cell Sci,* 125**,** 4158-69.

WIN, T. Z., GACHET, Y., MULVIHILL, D. P., MAY, K. M. & HYAMS, J. S. 2001. Two type V myosins with non-overlapping functions in the fission yeast Schizosaccharomyces pombe: Myo52 is concerned with growth polarity and cytokinesis, Myo51 is a component of the cytokinetic actin ring. *J Cell Sci,* 114**,** 69-79.

WOOD, V., GWILLIAM, R., RAJANDREAM, M. A., LYNE, M., LYNE, R., STEWART, A., SGOUROS, J., PEAT, N., HAYLES, J., BAKER, S., BASHAM, D., BOWMAN, S., BROOKS, K., BROWN, D., BROWN, S., CHILLINGWORTH, T., CHURCHER, C., COLLINS, M., CONNOR, R., CRONIN, A., DAVIS, P., FELTWELL, T., FRASER, A., GENTLES, S., GOBLE,

A., HAMLIN, N., HARRIS, D., HIDALGO, J., HODGSON, G., HOLROYD, S., HORNSBY, T., HOWARTH, S., HUCKLE, E. J., HUNT, S., JAGELS, K., JAMES, K., JONES, L., JONES, M., LEATHER, S., MCDONALD, S., MCLEAN, J., MOONEY, P., MOULE, S., MUNGALL, K., MURPHY, L., NIBLETT, D., ODELL, C., OLIVER, K., O'NEIL, S., PEARSON, D., QUAIL, M. A., RABBINOWITSCH, E., RUTHERFORD, K., RUTTER, S., SAUNDERS, D., SEEGER, K., SHARP, S., SKELTON, J., SIMMONDS, M., SQUARES, R., SQUARES, S., STEVENS, K., TAYLOR, K., TAYLOR, R. G., TIVEY, A., WALSH, S., WARREN, T., WHITEHEAD, S., WOODWARD, J., VOLCKAERT, G., AERT, R., ROBBEN, J., GRYMONPREZ, B., WELTJENS, I., VANSTREELS, E., RIEGER, M., SCHAFER, M., MULLER-AUER, S., GABEL, C., FUCHS, M., DUSTERHOFT, A., FRITZC, C., HOLZER, E., MOESTL, D., HILBERT, H., BORZYM, K., LANGER, I., BECK, A., LEHRACH, H., REINHARDT, R., POHL, T. M., EGER, P., ZIMMERMANN, W., WEDLER, H., WAMBUTT, R., PURNELLE, B., GOFFEAU, A., CADIEU, E., DREANO, S., GLOUX, S., et al. 2002. The genome sequence of Schizosaccharomyces pombe. *Nature,* 415**,** 871-80.

XIANG, X. & FISCHER, R. 2004. Nuclear migration and positioning in filamentous fungi. *Fungal Genet Biol,* 41**,** 411-9.

XIANG, X., HAN, G., WINKELMANN, D. A., ZUO, W. & MORRIS, N. R. 2000. Dynamics of cytoplasmic dynein in living cells and the effect of a mutation in the dynactin complex actin-related protein Arp1. *Curr Biol,* 10**,** 603-6.

XIANG, X., OSMANI, A. H., OSMANI, S. A., XIN, M. & MORRIS, N. R. 1995. NudF, a nuclear migration gene in Aspergillus nidulans, is similar to the human LIS-1 gene required for neuronal migration. *Mol Biol Cell,* 6**,** 297-310.

XU, Y., MOSELEY, J. B., SAGOT, I., POY, F., PELLMAN, D., GOODE, B. L. & ECK, M. J. 2004. Crystal structures of a Formin Homology-2 domain reveal a tethered dimer architecture. *Cell,* 116**,** 711-23.

YAMAMOTO, A. & HIRAOKA, Y. 2003. Cytoplasmic dynein in fungi: insights from nuclear migration. *J Cell Sci,* 116**,** 4501-12.

YAMAMOTO, A., TSUTSUMI, C., KOJIMA, H., OIWA, K. & HIRAOKA, Y. 2001. Dynamic behavior of microtubules during dynein-dependent nuclear migrations of meiotic prophase in fission yeast. *Mol Biol Cell,* 12**,** 3933-46.

YAMAMOTO, A., WEST, R. R., MCINTOSH, J. R. & HIRAOKA, Y. 1999. A cytoplasmic dynein heavy chain is required for oscillatory nuclear movement of meiotic prophase and efficient meiotic recombination in fission yeast. *J Cell Biol,* 145**,** 1233-49.

YAMASHITA, A., FUJITA, Y. & YAMAMOTO, M. 2013. Proper microtubule structure is vital for timely progression through meiosis in fission yeast. *PLoS One,* 8**,** e65082.

YAMASHITA, A. & YAMAMOTO, M. 2006. Fission yeast Num1p is a cortical factor anchoring dynein and is essential for the horse-tail nuclear movement during meiotic prophase. *Genetics,* 173**,** 1187-96.

YILDIZ, A., TOMISHIGE, M., VALE, R. D. & SELVIN, P. R. 2004. Kinesin walks hand-over-hand. *Science,* 303**,** 676-8.

YIN, H., PRUYNE, D., HUFFAKER, T. C. & BRETSCHER, A. 2000. Myosin V orientates the mitotic spindle in yeast. *Nature,* 406**,** 1013-5.

YODER, J. H. & HAN, M. 2001. Cytoplasmic dynein light intermediate chain is required for discrete aspects of mitosis in Caenorhabditis elegans. *Mol Biol Cell,* 12**,** 2921-33.

YOSHIDA, M., KATSUYAMA, S., TATEHO, K., NAKAMURA, H., MIYOSHI, J., OHBA, T., MATSUHARA, H., MIKI, F., OKAZAKI, K., HARAGUCHI, T., NIWA, O., HIRAOKA, Y. & YAMAMOTO, A. 2013. Microtubule-organizing center formation at telomeres induces meiotic telomere clustering. *J Cell Biol,* 200**,** 385-95.

YUN, M., BRONNER, C. E., PARK, C. G., CHA, S. S., PARK, H. W. & ENDOW, S. A. 2003. Rotation of the stalk/neck and one head in a new crystal structure of the kinesin motor protein, Ncd. *EMBO J,* 22**,** 5382-9.

ZAICHICK, S. V., METODIEV, M. V., NELSON, S. A., DURBROVSKYI, O., DRAPER, E., COOPER, J. A. & STONE, D. E. 2009. The mating-specific Galpha interacts with a kinesin-14 and regulates pheromone-induced nuclear migration in budding yeast. *Mol Biol Cell,* 20**,** 2820-30.

ZHANG, J., LI, S., MUSA, S., ZHOU, H. & XIANG, X. 2009a. Dynein light intermediate chain in Aspergillus nidulans is essential for the interaction between heavy and intermediate chains. *J Biol Chem,* 284**,** 34760-8.

ZHANG, X., LEI, K., YUAN, X., WU, X., ZHUANG, Y., XU, T., XU, R. & HAN, M. 2009b. SUN1/2 and Syne/Nesprin-1/2 complexes connect centrosome to the nucleus during neurogenesis and neuronal migration in mice. *Neuron,* 64**,** 173-87.

ZHANG, X., XU, R., ZHU, B., YANG, X., DING, X., DUAN, S., XU, T., ZHUANG, Y. & HAN, M. 2007. Syne-1 and Syne-2 play crucial roles in myonuclear anchorage and motor neuron innervation. *Development,* 134**,** 901-8.

ZHENG, Y., WONG, M. L., ALBERTS, B. & MITCHISON, T. 1995. Nucleation of microtubule assembly by a gamma-tubulin-containing ring complex. *Nature,* 378**,** 578-83.

ZHU, C., ZHAO, J., BIBIKOVA, M., LEVERSON, J. D., BOSSY-WETZEL, E., FAN, J. B., ABRAHAM, R. T. & JIANG, W. 2005. Functional analysis of human microtubule-based motor proteins, the kinesins and dyneins, in mitosis/cytokinesis using RNA interference. *Mol Biol Cell,* 16**,** 3187-99.

ZIMMERMAN, W. C., SILLIBOURNE, J., ROSA, J. & DOXSEY, S. J. 2004. Mitosis-specific anchoring of gamma tubulin complexes by pericentrin controls spindle organization and mitotic entry. *Mol Biol Cell,* 15**,** 3642-57.

ANNEXE

Scheffler K, Tran PT.

Motor proteins: kinesin can replace myosin. Curr Biol. 2012 Jan 24;22(2).

(Comment on: Lo Presti L, Martin SG. Shaping fission yeast cells by rerouting actin-based transport on microtubules. Curr Biol. 2011 Dec 20;21(24).)

Current Biology Vol 22 No 2
R54

diverse functions. Indeed, the geometry of fission yeast may be ideal, and unique, for precisely this type of chimeric analysis. However, given the multiple and overlapping roles of the actin and microtubule cytoskeleton in complex cellular processes, such as cell polarity and cell shape, the chimeric analysis presented by Lo Presti and Martin [6] can help to simplify the different pathways even further. By eliminating one pathway, future research can focus on the molecular dissection of one pathway without compounding effects from another overlapping pathway.

References

1. Li, R., and Gundersen, G.G. (2008). Beyond polymer polarity: how the cytoskeleton builds a polarized cell. Nat. Rev. Mol. Cell Biol. *9*, 860–873.
2. Rodriguez, O.C., Schaefer, A.W., Mandato, C.A., Forscher, P., Bement, W.M., and Waterman-Storer, C.M. (2003). Conserved microtubule-actin interactions in cell movement and morphogenesis. Nat. Cell Biol. *5*, 599–609.
3. Siegrist, S.E., and Doe, C.Q. (2007). Microtubule-induced cortical cell polarity. Genes Dev. *21*, 483–496.
4. Brown, S.S. (1999). Cooperation between microtubule- and actin-based motor proteins. Annu. Rev. Cell Dev. Biol. *15*, 63–80.
5. Ross, J.L., Ali, M.Y., and Warshaw, D.M. (2008). Cargo transport: molecular motors navigate a complex cytoskeleton. Curr. Opin. Cell Biol. *20*, 41–47.
6. Lo Presti, L., and Martin, S.G. (2011). Shaping fission yeast cells by rerouting actin-based transport on microtubules. Curr. Biol. *21*, 2064–2069.
7. Chang, F., and Martin, S.G. (2009). Shaping fission yeast with microtubules. Cold Spring Harb. Perspect. Biol. *1*, a001347.
8. Martin, S.G. (2009). Microtubule-dependent cell morphogenesis in the fission yeast. Trends Cell Biol. *19*, 447–454.
9. Piel, M., and Tran, P.T. (2009). Cell shape and cell division in fission yeast. Curr. Biol. *19*, R823–R827.
10. Bendezu, F.O., and Martin, S.G. (2011). Actin cables and the exocyst form two independent morphogenesis pathways in the fission yeast. Mol. Biol. Cell *22*, 44–53.
11. Nakano, K., Toya, M., Yonada, A., Asami, Y., Yamashita, A., Kamasawa, N., Osumi, M., and Yamamoto, M. (2011). Pob1 ensures cylindrical cell shape by coupling two distinct rho signaling events during secretory vesicle targeting. Traffic *12*, 726–739.
12. Snaith, H.A., Thompson, J., Yates, J.R., 3rd, and Sawin, K.E. (2011). Characterization of Mug33 reveals complementary roles for actin cable-dependent transport and exocyst regulators in fission yeast exocytosis. J. Cell Sci. *124*, 2187–2199.
13. Feierbach, B., Verde, F., and Chang, F. (2004). Regulation of a formin complex by the microtubule plus end protein tea1p. J. Cell Biol. *165*, 697–707.

[1]Institut Curie, CNRS-UMR144, Paris 75005, France. [2]Cell and Developmental Biology, University of Pennsylvania, Philadelphia, PA 19104, USA.
*E-mail: tranp@mail.med.upenn.edu

DOI: 10.1016/j.cub.2011.12.007

Epigenetic Inheritance: What News for Evolution?

Whether epigenetic variation is important in adaptive evolution has been contentious. Two recent studies in *Arabidopsis thaliana* significantly add to our understanding of genome-wide variation and stability of an epigenetic mark, and thus help pave the path for realistically incorporating epigenetics into evolutionary theory.

Ben Hunter, Jesse D. Hollister, and Kirsten Bomblies

Epigenetic marks such as cytosine methylation or histone modifications can be very dynamic and can alter gene expression in response to environmental and developmental cues without changes in DNA sequence; in some cases epigenetic changes can be heritable through meiosis [1,2]. This has spurred interest — and heated debates — about whether epigenetic variation may play a significant role in adaptive evolution [3–6]. The need to formally consider epialleles in population genetics and evolutionary theory has been emphasized (e.g., [6,7]); however, more empirical data are necessary to parameterize models and assess the actual impacts of epigenetic variation on adaptive phenotypes (e.g., [3,8]).

Two recent studies in *Arabidopsis thaliana* have quantified spontaneous genome-wide methylation variation, and are a significant step forward in quantifying epigenetic change [9,10]. Both studies capitalized on a very useful resource: a set of well-characterized mutation accumulation lines propagated from one homozygous ancestor (Figure 1) [11]. This allows quantification of the rate and accumulation of differences in the absence of natural selection. Such lines exist for numerous species, which will allow for extensive comparative work [12]. In the *A. thaliana* studies two individuals each from five [9] and ten [10] 31^{st} generation lines were assayed for genome-wide cytosine methylation patterns and compared to lines that had been propagated for only three generations from the common ancestor (Figure 1). These lines have also been used to quantify the base mutation rate [13] as well as phenotypic divergence [11].

Both *A. thaliana* studies concluded that, in general, cytosine methylation is remarkably stable over the 64 generations that separate the most divergent lines (Figure 1). But at some loci it does vary: in the two studies 1.6% [9] and 6.4% [10] of methylated cytosines differed in methylation state among lines. This gives epimutation rate estimates orders of magnitude higher than the DNA base mutation rate. Consistent with patterns previously reported for variation among natural *A. thaliana* strains [14], variable CG-methylation sites were preferentially located in gene regions, while the methylation states of transposons and repeat regions were mostly stably inherited. Variation in non-CG methylation is comparatively rare, but showed the opposite pattern, being more variable in transposons and intergenic regions [9].

What does spontaneous variation imply for the potential for epigenetic change to play an important role in evolution? First, consider the genome-wide variation in stability of methylation states. Among the variable sites identified in these *A. thaliana* genome scans, a large proportion changed state in multiple independent lines, suggesting that some sites are indeed 'hotspots' for epigenetic change [9,10], and rates of reversion are appreciable [10]. It has been known

as neurons or melanocytes, utilize both cytoskeletal systems for the correct targeting of factors to polarized zones: long-range transport depends largely on microtubule tracks and shorter tracks are covered by actin filaments [4,5]. The transport of specific cargos along the cytoskeleton is mediated by motor proteins: actin-based myosin motors or microtubule-based kinesin or dynein motors. To date, these motors and their specific tracks have not been shown to be interchangeable. In a recent issue of *Current Biology*, Lo Presti and Martin [6] demonstrate that one cytoskeletal system can substitute for the other.

In the rod-shaped fission yeast *Schizosaccharomyces pombe*, polarized cell growth is organized by the actin cytoskeleton [7,8]. The formin For3p nucleates actin cables from the cell tips, which then act as tracks for Myo52p-dependent (myosin V) delivery of secretory vesicles to the cell tips. The cell tips are active polarized growth sites where new cell membrane and cell wall material are incorporated. Microtubules are not essential in polarized cell growth *per se*, but instead contribute to the initial establishment of growth sites and the direction of growth by depositing positional markers at cell tips [8,9]. Microtubules grow out from the cell center and their plus ends make dynamic contacts with the cell tips. The kinesin-7 Tea2p is thought to carry a complex consisting of the positional markers Tea1p and Tea4p on the microtubule track toward the cell tip, where the Tea1p–Tea4p complex is subsequently deposited and anchored to the membrane-bound receptor Mod5p. The Tea1p–Tea4p complex, now anchored at the cell tips, can activate For3p to nucleate and assemble actin cables. In this context, a series of events leads ultimately to polarized cell growth: microtubules → Tea2p-mediated transport of Tea1p–Tea4p complex → cell tip → formin For3p activation → actin cable formation → Myo52p-mediated vesicle transport → cell tip → polarized cell growth (Figure 1).

Lo Presti and Martin [6] showed that they can bypass important steps in this pathway, including actin cable formation and myosin-V-dependent vesicle transport, and still maintain polarized cell growth at cell tips. They engineered a chimera composed of the motor domain of the kinesin Tea2p and the cargo-binding domain of the myosin Myo52p. This chimera can bind Myo52p-specific cargo receptors, such as the Rab11-family GTPase Ypt3p, and deliver cargo to the cell tips using microtubules in a Tea2p-dependent manner, effectively re-routing vesicle transport from the actin cables to the microtubules (Figure 1).

Polarized secretion in fission yeast is regulated by two parallel and complementary pathways: actin-based For3p- and Myo52p-dependent transport of vesicles to cell tips; and the actin-independent exocyst complex, which tethers vesicles to the cell tips [10–12]. When either one of the two mechanisms is disrupted, cells still grow in a polarized manner but with a slightly defective shape. However, when both mechanisms are disrupted, cells exhibit a complete loss of polarized cell growth. The chimera not only restores polarized growth in either *Δfor3* or *Δmyo52* cells, but also in the double mutant *Δfor3-Δexo70*, which lacks both actin cables and a functional exocyst complex. This indicates that, regardless of the mode of delivery, whether by microtubule or by actin tracks, polarized growth is maintained as long as secretory vesicles are targeted to the cell tips.

Cell shape in fission yeast is also organized by the microtubule cytoskeleton [8,9]. As mentioned, microtubule plus ends deliver the Tea1p–Tea4p polarity marker complex to the cell tips. In the absence of these markers or when microtubules fail to deliver them to the cell tips, straight fission yeast cells grow into bent or branched shapes [8,9]. However, bent or branched growth requires actin cables, i.e. For3p. A *Δtea1 Δfor3* double mutant exhibits oval or round shape defects, but not bent or branched shape defects [13]. Lo Presti and Martin [6] showed that the chimera also rescued these shape defects. In the *Δtea4 Δmyo52* double mutant, where cells are misshapen into oval or round cells, the chimera restored cell shape to normal. Intriguingly, mutant cells expressing the chimera also have thinner and more pointed cell tips compared with wild-type cells. One explanation offered is that the contact area between the cell tips and the respective cytoskeletal filaments dictates the width of cells by defining the zone of vesicle delivery. In fission yeast, microtubules contact the hemispherical cell tips for 1 to 2 minutes, during which time they keep growing, which eventually brings the microtubule plus ends to the geometrical middle of the cell tip, resulting in an enhanced accumulation of cargos at that site. In contrast, actin cables emanate from a much larger zone around the cell tip and can thus deliver cargos to a broader area.

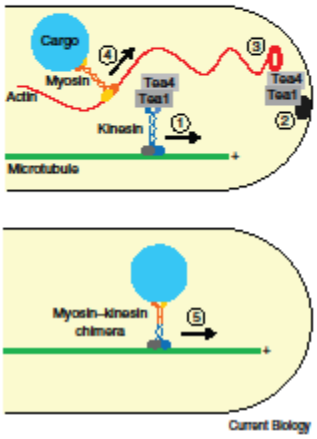

Figure 1. Fission yeast uses both the microtubule and actin cytoskeleton to establish and maintain cell polarity and cell shape.

The simplified sequence of events is: (1) the kinesin Tea2p carries the polarity marker Tea1p–Tea4p complex on microtubule tracks toward the cell tip; (2) Tea1p–Tea4p is anchored at the cell tip; (3) Tea4p activates the formin For3p to nucleate actin cables; and (4) myosinV Myo52p carries cargo on actin tracks toward the cell tip for polarized cell growth. Lo Presti and Martin [6] show that they can bypass the role of the actin cytoskeleton by creating a chimera of kinesin head and myosin tail. The chimera moves on microtubules but carries the proper cargo to the cell tips (5). The chimera can rescue cell polarity and cell shape in mutant cells.

In summary, this interesting study of Lo Presti and Martin [6] shows that microtubules can substitute for actin cables in cellular functions such as cargo transport and its subsequent effect on cell polarity and cell shape. It should be noted that the chimera cannot rescue all phenotypes conferred by the mutations studied. This is not unexpected, as each cytoskeletal element has evolved separately to perform pleiotropic and

Current Biology Vol 22 No 2
R54

diverse functions. Indeed, the geometry of fission yeast may be ideal, and unique, for precisely this type of chimeric analysis. However, given the multiple and overlapping roles of the actin and microtubule cytoskeleton in complex cellular processes, such as cell polarity and cell shape, the chimeric analysis presented by Lo Presti and Martin [6] can help to simplify the different pathways even further. By eliminating one pathway, future research can focus on the molecular dissection of one pathway without compounding effects from another overlapping pathway.

References

1. Li, R., and Gundersen, G.G. (2008). Beyond polymer polarity: how the cytoskeleton builds a polarized cell. Nat. Rev. Mol. Cell Biol. 9, 860–873.
2. Rodriguez, O.C., Schaefer, A.W., Mandato, C.A., Forscher, P., Bement, W.M., and Waterman-Storer, C.M. (2003). Conserved microtubule-actin interactions in cell movement and morphogenesis. Nat. Cell Biol. 5, 599–609.
3. Siegrist, S.E., and Doe, C.Q. (2007). Microtubule-induced cortical cell polarity. Genes Dev. 21, 483–496.
4. Brown, S.S. (1999). Cooperation between microtubule- and actin-based motor proteins. Annu. Rev. Cell Dev. Biol. 15, 63–80.
5. Ross, J.L., Ali, M.Y., and Warshaw, D.M. (2008). Cargo transport: molecular motors navigate a complex cytoskeleton. Curr. Opin. Cell Biol. 20, 41–47.
6. Lo Presti, L., and Martin, S.G. (2011). Shaping fission yeast cells by rerouting actin-based transport on microtubules. Curr. Biol. 21, 2064–2069.
7. Chang, F., and Martin, S.G. (2009). Shaping fission yeast with microtubules. Cold Spring Harb. Perspect. Biol. 1, a001347.
8. Martin, S.G. (2009). Microtubule-dependent cell morphogenesis in the fission yeast. Trends Cell Biol. 19, 447–454.
9. Pal, M., and Tran, P.T. (2009). Cell shape and cell division in fission yeast. Curr. Biol. 19, R823–R827.
10. Bendezu, F.O., and Martin, S.G. (2011). Actin cables and the exocyst form two independent morphogenesis pathways in the fission yeast. Mol. Biol. Cell 22, 44–53.
11. Nakano, K., Toya, M., Yonesda, A., Asami, Y., Yamashita, A., Kamasawa, N., Osumi, M., and Yamamoto, M. (2011). Pob1 ensures cylindrical cell shape by coupling two distinct rho signaling events during secretory vesicle targeting. Traffic 12, 726–739.
12. Snaith, H.A., Thompson, J., Yates, J.R., 3rd, and Sawin, K.E. (2011). Characterization of Mug33 reveals complementary roles for actin cable-dependent transport and exocyst regulators in fission yeast exocytosis. J. Cell Sci. 124, 2187–2199.
13. Feierbach, B., Verde, F., and Chang, F. (2004). Regulation of a formin complex by the microtubule plus end protein tea4p. J. Cell Biol. 165, 697–707.

[1]Institut Curie, CNRS-UMR144, Paris 75005, France. [2]Cell and Developmental Biology, University of Pennsylvania, Philadelphia, PA 19104, USA.
*E-mail: tranp@mail.med.upenn.edu

DOI: 10.1016/j.cub.2011.12.007

Epigenetic Inheritance: What News for Evolution?

Whether epigenetic variation is important in adaptive evolution has been contentious. Two recent studies in *Arabidopsis thaliana* significantly add to our understanding of genome-wide variation and stability of an epigenetic mark, and thus help pave the path for realistically incorporating epigenetics into evolutionary theory.

Ben Hunter, Jesse D. Hollister, and Kirsten Bomblies

Epigenetic marks such as cytosine methylation or histone modifications can be very dynamic and can alter gene expression in response to environmental and developmental cues without changes in DNA sequence; in some cases epigenetic changes can be heritable through meiosis [1,2]. This has spurred interest — and heated debates — about whether epigenetic variation may play a significant role in adaptive evolution [3–6]. The need to formally consider epialleles in population genetics and evolutionary theory has been emphasized (e.g., [6,7]); however, more empirical data are necessary to parameterize models and assess the actual impacts of epigenetic variation on adaptive phenotypes (e.g., [3,8]).

Two recent studies in *Arabidopsis thaliana* have quantified spontaneous genome-wide methylation variation, and are a significant step forward in quantifying epigenetic change [9,10]. Both studies capitalized on a very useful resource: a set of well-characterized mutation accumulation lines propagated from one homozygous ancestor (Figure 1) [11]. This allows quantification of the rate and accumulation of differences in the absence of natural selection. Such lines exist for numerous species, which will allow for extensive comparative work [12]. In the *A. thaliana* studies two individuals each from five [9] and ten [10] 31st generation lines were assayed for genome-wide cytosine methylation patterns and compared to lines that had been propagated for only three generations from the common ancestor (Figure 1). These lines have also been used to quantify the base mutation rate [13] as well as phenotypic divergence [11].

Both *A. thaliana* studies concluded that, in general, cytosine methylation is remarkably stable over the 64 generations that separate the most divergent lines (Figure 1). But at some loci it does vary: in the two studies 1.6% [9] and 6.4% [10] of methylated cytosines differed in methylation state among lines. This gives epimutation rate estimates orders of magnitude higher than the DNA base mutation rate. Consistent with patterns previously reported for variation among natural *A. thaliana* strains [14], variable CG-methylation sites were preferentially located in gene regions, while the methylation states of transposons and repeat regions were mostly stably inherited. Variation in non-CG methylation is comparatively rare, but showed the opposite pattern, being more variable in transposons and intergenic regions [9].

What does spontaneous variation imply for the potential for epigenetic change to play an important role in evolution? First, consider the genome-wide variation in stability of methylation states. Among the variable sites identified in these *A. thaliana* genome scans, a large proportion changed state in multiple independent lines, suggesting that some sites are indeed 'hotspots' for epigenetic change [9,10], and rates of reversion are appreciable [10]. It has been known